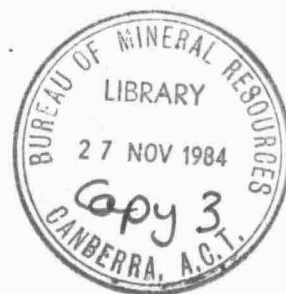


1984/22
43

BMR PUBLICATIONS COMPACTUS
(LENDING SECTION)



BUREAU OF MINERAL RESOURCES, GEOLOGY AND GEOPHYSICS

Record No. 1984/22

RECORD

GRANULITE-GNEISS TERRAINS OF THE
SOUTHWESTERN ARUNTA BLOCK, CENTRAL
AUSTRALIA: GLEN HELEN, NARWIETOOMA
AND ANBURLA 1:100 000 SHEET AREAS

A.Y. Glikson

Bureau of Mineral Resources, Geology and Geophysics
Canberra, A.C.T., Australia

Record No. 1984/22

GRANULITE-GNEISS TERRAINS OF THE
SOUTHWESTERN ARUNTA BLOCK, CENTRAL
AUSTRALIA: GLEN HELEN, NARWIETOOMA
AND ANBURLA 1:100 000 SHEET AREAS

A.Y. Glikson

Bureau of Mineral Resources, Geology and Geophysics
Canberra, A.C.T., Australia

LIST OF CONTENTS

Summary	7
I. INTRODUCTION	
[1] regional setting	10
[2] aims and methods of investigation	12
II. THE NORTHERN GRANULITE BLOCK	
[1] Mt Hay mafic granulite-anorthosite belt	15
[2] Mt Chapple intermediate granulite belt	19
[3] Redbank Hill porphyroblastic gneiss belt	22
[4] Mt Zeil felsic-intermediate granulite belt	26
[5] phase compositions	29
[6] precursors of the granulites	33
III. GEOCHEMISTRY OF MT HAY GRANULITES AND GNEISSES	
[1] mafic granulites	36
[2] anorthosites	37
[3] calc-granulites	38
[4] felsic granulites and gneisses	39
IV. THE SOUTHERN MIGMATITE-GNEISS-GRANITE BLOCK	
[1] Derwent Paragneiss	43
[2] Dashwood Migmatite	45
[3] Teapot Granite	47
[4] basic intrusions	
(a) gabbro stocks south of Mt Zeil	48
(b) basic dykes	50
(5) Heavitree Quartzite	51

V. REDBANK-MT ZEIL THRUST ZONE (RTZ)

000011[1]	general outline of the RTZ	1.52
[2]	the RTZ south of Redbank Hill	54
[3]	the RTZ in the Mt Zeil area	56
[4]	page relationships	59

VI. PRESSURE-TEMPERATURE ESTIMATES

Fig 1	hydrogeothermometers	2.1	62
[2]	geobarometers		64
Fig 3	Mt. Hay belt	2.1	66
[4]	Mt Chapple belt	2.1	68
Fig 5	Redbank Hill	4.1	70
[6]	Mt Zeil belt	5.1	71
[7]	the southern block	5.1	71

VII. IMPLICATIONS FOR CRUSTAL STRUCTURE AND EVOLUTION

[1]	geophysical-geological correlations	75
[2]	evolution of the northern granulite block	78
[3]	evolution of the southern migmatite-gneiss-granite terrain	83
[4]	summary and conclusions	87

REFERENCES

REFERENCES

LIST OF FIGURES

- I.1 - LANDSAT imagery of part of the HERMANNSBURG 1:250000 sheet area, central Australia
- I.2 - geological sketch map of the HERMANNSBURG 1:250000 sheet, showing position of Fig. I.1, and a schematic N-S cross section portraying the relations between major rock units.
- II.1 - Mt Hay and Mt Chapple basic granulite outcrops and microphotographs
- II.2 - stereographic plots of structural data: Mt Hay belt
- II.3 - Mt Hay anorthosite outcrops
- II.4 - stereographic plots of structural data: Mt Chapple
- II.5 - Redbank Hill outcrops and microphotographs
- II.6 - stereographic plots of structural data: Redbank Hill
- II.7 - Mt Zeil granulite outcrops
- II.8 - stereographic plots of structural data: Mt Zeil belt
- II.9 - ACF ternary diagrams of northern block granulites/ gneiss mineral compositions
- II.10 - pyroxene compositions according to the Di-Hd-En-Fs scheme
- II.11 - Amphibole compositions according to the Ed-Pg-Tr-Ts scheme
- II.12 - Mineral phase - whole rock chemical relations
- III.1 - mantle-normalised lithophile element abundances in Mt Hay granulites and gneisses
- III.2 - chondrite-normalised ferromagnesian and refractory element abundances in Mt Hay granulites and gneisses
- III.3 - CaO-SiO_2 and MgO-SiO_2 plots for Mt Hay granulite and gneiss data
- IV.1 - Derwent Gneiss and Dashwood Migmatite outcrops
- IV.2 - Teapot Granite outcrops
- IV.3 - ACF ternary diagrams of southern block mineral assemblages

- V.1 - aerial photograph of part of the Redbank-Mt Zeil Thrust Zone (RTZ) in the Mt Zeil area
- V.2 - Redbank-Mt Zeil Thrust Zone (RTZ) outcrops
- V.3 - microphotographs of RTZ rocks
- VI.1 - PT equilibrium loci of Mt Hay granulites
- VI.2 - PT equilibrium loci of Mt Hay felsic gneiss and granulite
- VI.3 - PT equilibrium loci of Mt Chapple garnet-two pyroxene granulite S-188
- VI.4 - PT equilibrium loci of Mt Chapple garnet-two pyroxene granulite S-194
- VI.5 - PT equilibrium loci of Mt Chapple garnet-sillimanite gneiss
- VI.6 - PT equilibrium loci of Redbank Hill granulites and porphyroblastic gneisses
- VI.7 - PT equilibrium relations of Mt Zeil garnet-sillimanite gneiss
- VII.1 - radiometric anomaly map of the northern part of HERMANNSBURG 1:250 000 sheet
- VII.2 - Bouguer gravity anomaly map of the northern part of the HERMANNSBURG 1:250 000 sheet
- VII.3 - aeromagnetic anomaly map of the northern part of the HERMANNSBURG 1:250000 sheet
- VII.4 - stereographic plots of poles to banding and of lineations; northern granulite block

LIST OF TABLES

- II.1-4 - microprobe analyses of selected mineral assemblages from the northern block in the ANBURLA, NARWIETOOMA and GLEN HELEN 1:100 000 Sheet areas (in microfiche)
- II.5 - compositional indices of pyroxenes
- II.6 - compositional indices of amphiboles
- II.7 - compositional indices of biotites
- II.8 - compositional indices of garnets
- III.1 - chemical analyses of granulites and gneisses from the Mt Hay belt
- III.2 - major element comparisons between Mt Hay granulites and average sedimentary compositions
- IV.1-3 - microprobe analyses of selected mineral analyses from the southern block, GLEN HELEN 1:100 000 Sheet area (in microfiche)
- VII.1 - Isotopic age data for the southwestern Arunta Block

SUMMARY

The results of a regional survey of the southwestern part of the Arunta complex, within the GLEN HELEN, NARWIETOOMA and ANBURLA 1:100 000 Sheet areas, central Australia, are reported. The terrain includes two major blocks adjoining the Redbank-Mt Zeil Thrust Zone (RTZ), a major ca 600 km long EW lineament. The northern block consists of mafic granulites, high-Mg LIL (large ion lithophile) and siderophile element-depleted granulites, anorthosites, garnet-two pyroxene granulites, and felsic to intermediate granulites and gneisses. The latter range from mm-scale lit-par-lit injection gneiss to km-size bodies to entire belts including remnant mafic granulites. Differentiation from orthopyroxene-plagioclase gneiss to garnet-biotite-K feldspar gneiss is generally positively related to the size of the felsic gneiss units intercalated with the granulites. The Mt Hay, Mt Chapple, Redbank Hill and Mt Zeil granulite-gneiss belts display an increase in the felsic/mafic rock ratio in this order - as reflected on radiometric maps. The Redbank Hill belt is dominated by large-feldspar glomeroblastic and porphyroblastic gneisses containing basic granulite relics, possibly reflecting an early phase the RTZ. The southern block consists of amphibolite facies quartzofeldspathic paragneiss and amphibolite intruded by orthogneiss, migmatite and granite which stand out as significant radiometric anomalies. The RTZ is marked by cataclastic gneiss, flaser gneiss, phyllonite, mylonite and ultramylonite, forming a single or bifurcating and branching zone from a few hundred metres to several km wide. The RTZ dips at angles as low as 40-30° northwards and include relict kernels of basic granulite. Effects of thrusting and shearing are widespread throughout the northern and particularly the southern blocks. Structural trends within granulite/gneiss of the northern block are subparallel to the RTZ. The principal tectonic fabric in this block is a steep NE plunging axial lineation defining isoclinal folds whose limbs strike WNW and dip steeply northward, i.e. steeper than the RTZ. Protoliths

of the basic granulites are interpreted in terms of deep seated intrusions or an infracrustal basic layer emplaced at ca 2.0 b.y., if coeval in age with Strangways Range granulites. The marked depletion of high-Mg (12% MgO) granulites in alkali elements (K, Rb, Ba), incompatible elements (P, Zr, Nb, Y, Ce, La) and siderophile elements (Ti, V, Cr, Cu, Zn) may suggest a cumulate and/or residual nature, consistent with the association of anorthosites and the apparent lack or scarcity of sedimentary material. Minor calc-granulites are interpreted as metamorphosed calcareous segregations. Garnet-sillimanite gneisses represent either meta-pelites or metamorphosed or hydrated quartzofeldspathic orthogneisses. PT estimates are consistent with a vertically zoned crustal model, suggesting generally greater equilibration depth for basic granulites. An electron probe study of granulites and gneisses from the northern block indicates equilibration of two-pyroxene granulites at ca 900°C and 6.5 kb, garnet-two pyroxene granulites at ca 680-770°C and 7.3-8.1 kb, felsic bands in mafic granulite at 670°C and 5.9 kb, sillimanite-garnet gneiss at ca 670°C and 8.8 kb and Redbank Hill porphyroblastic gneiss at ca 640°C and 6.4 kb. Metamorphism of the basic granulites occurred under average geotherms in the 30-50°C/km range whereas that of felsic gneisses in the 25-40°C/km range, which can be interpreted either in terms of polymetamorphism or protracted long term metamorphism under a waning geothermal gradient. Biotite is often the youngest phase in the granulites, and may signify partial hydration and K-introduction associated with anatexis. Harker variation diagrams support an igneous link between basic granulites and felsic gneiss components. The inferred sequence of major events, pending further isotopic studies, comprises the following principal stages: [1] ca 2.0 b.y. ago - emplacement of basic anorthositic protoliths; [2] 2.0-1.8 b.y. ago - granulite facies metamorphism culminated by hydration, anatexis, segregation and injection of felsic to intermediate magma fractions and consequent ascent of differentiated granitic bodies into higher crustal levels. D1 and D2 deformation, signify synmagmatic and postmagmatic deformations; [3] 1.6 b.y.

geothermal event recorded in the paragneisses of the southern block; [4] ca 1.0 b.y. ago and younger - major tectonothermal event probably associated with movements along the RTZ and imprinted both on the northern and the southern blocks, superposed on D3 flexures and denoted as D4. This sequence is considered as a partial record, and further studies are likely to unravel a more complex history for this terrain. In so far as the M¹ Hay type basic granulites represent an infracrustal basic layer and its anatectic derivatives, persistence of such rocks with depth beneath the Burt Plain and the +50 mg1 Papunya gravity 'high' would account for the origin of this anomaly.

I. INTRODUCTION

[1] regional setting

The southwestern part of the Precambrian Arunta Block, central Australia, consists of several latitudinal zones separated by major lineaments. In the HERMANNSBURG 1:250 000 Sheet area they include from north to south: (1) major massifs of granulite and granulite facies gneiss including the Mt Hay, Mt Chapple, Redbank Hill and Mt Zeil belts; (2) the Redbank-Mt Zeil thrust zone (RTZ) along which the granulites are thrust southward over paragneiss, orthogneiss, migmatite and granite; (3) metamorphic sequences of the Chewings Range, including quartzites which form the spine of this range, intruded by the Teapot Granite, banded gneiss and migmatites; (4) a major unconformity at the base of the late Proterozoic Heavitree Quartzite and major thrust faults (Ormiston thrust and Mt Sonder-Mt Razorback thrust) along which the gneiss-migmatite-granite units are thrust southward over the Heavitree Quartzite (Figs I.1-2).

The present survey was concerned with the granulite belts, the RTZ, and part of the gneiss-migmatite-granite terrain south of the RTZ, within the ANBURLA (5551), NARWIETOOMA (5451) and GLEN HELEN (5351) 1:100 000 Sheet areas, forming the southern part of the HERMANNSBURG 1:250 000 Sheet. The terrain under consideration covers a rectangular EW elongated area whose dimensions are approximately 135 km EW and 25 km NS. Mt Hay (1249 m), Mt Chapple (1167 m) and Redbank Hill form isolated EW elongated massifs fringing the southern part of the Burt Plain. The Mt Zeil granulites form a prominent range capped by Mt Zeil (1511 m), morphologically contiguous with, although higher than, the basement terrain NW of the Chewings Range (Mt Giles - 1284 m) (Fig.1.2), Ormiston Pound, Mt Sonder (1347 m) and Mt Razorback (1232 m). The Redbank - Mt Zeil thrust zone forms the northern limit of the gneiss-migmatite terrain north

of the Chewings Range, and within HERMANNSBURG, is expressed as a linear escarpment defining the southern limits of the Burt Plain for a distance of over 120 km (Fig. I.1-2). The contiguous basement terrain is drained northward by the Dashwood, Arumbera and Anburla creeks and a number of minor streams including the Charley, Halleem and Clarke creeks, all of which are lost in the Burt Plain. The southern limit of Narwietooma coincides approximately with the watershed between north and south-bound drainage. The latter includes the Breaden, Ormiston, Redbank, and Crawford creeks which drain into the Davenport creek at the upper reaches of the Finke River system. The western part of GLEN HELEN consists of low rises and isolated hills straddling the Dashwood and Derwent creeks east and north of Haast Bluff ridge.

The country includes a number of cattle stations, i.e. Hamilton Downs, Anburla, Milton Park, Narwietooma and Glen Helen, and the eastern part of the Papunya and Haast Bluff. aboriginal reserve. Major access routes include the Tanami road (Alice Springs to Yuendumu), the Alice Springs-Glen Helen tourist camp road, proceeding to Haast Bluff, a track connecting these two roads through Glen Helen station along the Dashwood creek, and a network of graded station tracks leading to wells. The hilly terrain south and east of Mt Zeil is inaccessible by vehicle, except for a bulldozed track along Haleem creek leading to Teapot soak.

[2] Aims and methods of investigation

Previous geological work in ANBURLA, NARWIETOOMA and GLEN HELEN (1:100 000) included limited aerial photographic reconnaissance in conjunction with the mapping of the HERMANNSBURG (1:250 000) Sheet (Quinlan and Forman, 1968) and photogeological mapping accompanied by limited helicopter traversing by Hunting Geology and Geophysics Pty Ltd (unpubl.). The HERMANNSBURG (1:100 000) Sheet has been mapped by Marjoribanks (1975) and isotopic age determinations for some of the rocks in this area reported by Marjoribanks and Black (1974) and Black et al. (1983). McDONNELL RANGES (1:100 000) has been mapped by Offe (1983). NAPPERBY (1:250 000) to the north has been mapped by Wells and Moss (in press) and Stewart et al. (1980). The area under consideration has little known economic mineralisation, although shows of allanite, copper, nickel, silver, lead and zinc have been prospected (Northern Territory Geological Survey, unpublished reports).

The present survey constituted a part of a semi-detailed mapping program of the Arunta Block. In particular this work is concerned with the relations between the Redbank-Mt Zeil thrust zone (RTZ) and the associated metamorphic and igneous rocks. Principal questions in this regard are: (1) the origin of the Mt Hay mafic granulites; (2) nature of metamorphic and anatectic processes which gave rise to the felsic to intermediate granulite phases; (3) vertical crustal compositional and metamorphic zonation in central Australia; (4) age relations between the RTZ and associated rock units.

Field traverses in the area were carried out during 1974, 1975 and 1979, totalling 7 months by AYG and 2 weeks by R.D. Shaw and L.A. Offe. Structural and petrographic data were plotted on 1:30 000 colour aerial photographs flown in 1973, using an RC9 camera at 14 500'. Owing to the compositional heterogeneity of individual outcrops, i.e. complex mesoscopic lithological banding, the terrain is more amenable to detailed

local studies than to regional mapping. Map-scale lithological units are commonly difficult to define, except for overall changes in the proportion of rock types and/or the state of deformation of the rocks. For this reason, few confident map-scale lithological boundaries could be defined. The 1:100 000 map thus consists of the following elements: (1) local structural data; (2) local petrographic data including abbreviated rock type and mineral names; (3) photointerpreted structure and rock unit boundaries. The significance of photo interpreted boundaries is not always apparent, namely variations in surface texture and vegetation patterns can not always be correlated with lithological variations. Furthermore, the charting of fault and shear zones may be complicated by widespread deformation throughout the terrain and the absence of stratigraphic marker units. Structural data such as foliation, banding, lineation and minor fold orientations were recorded in most stations. However, detailed structural analysis, including collection of oriented samples, was outside the scope of this survey.

Owing to the fine grained nature and therefore uncertain field identification of granulites, specimens from most stations were subjected to petrographic study. The rock type and mineral assemblage information is entered onto the 1:100 000 map in abbreviated form. Some specimens were further studied by electron microprobe, using the TPD energy dispersive system at the Research School of Earth Science, Australian National University, following the method of Reed and Ware (1975). The data were stored on flexible disc by the HP9825B desktop calculator using storage/retrieval programs written for this purpose (Glikson and Owen, 1982). Classification of pyroxenes and amphiboles has been carried out using computer programs by the above authors.

The present record is concerned with the principal stratigraphic and petrographic features of the terrain. The

second part of this study concerned with the geochemistry of granulites and gneisses is currently underway and will be reported separately.

FIGURE CAPTIONS FOR SECTION I

I.1 - LANDSAT imagery of part of the HERMANNSBURG 1:250 000 Sheet area. For explanation of morphological and geological features refer to Fig I.2

I.2 - (a) A Geological sketch map of the HERMANNSBURG 1:250 000 sheet outlining the southern and eastern limits of Fig. 1.I. (b) A schematic NS cross section across the terrain framed in Fig. 1.2 (a), showing the principal geological units and their interpreted field relations.

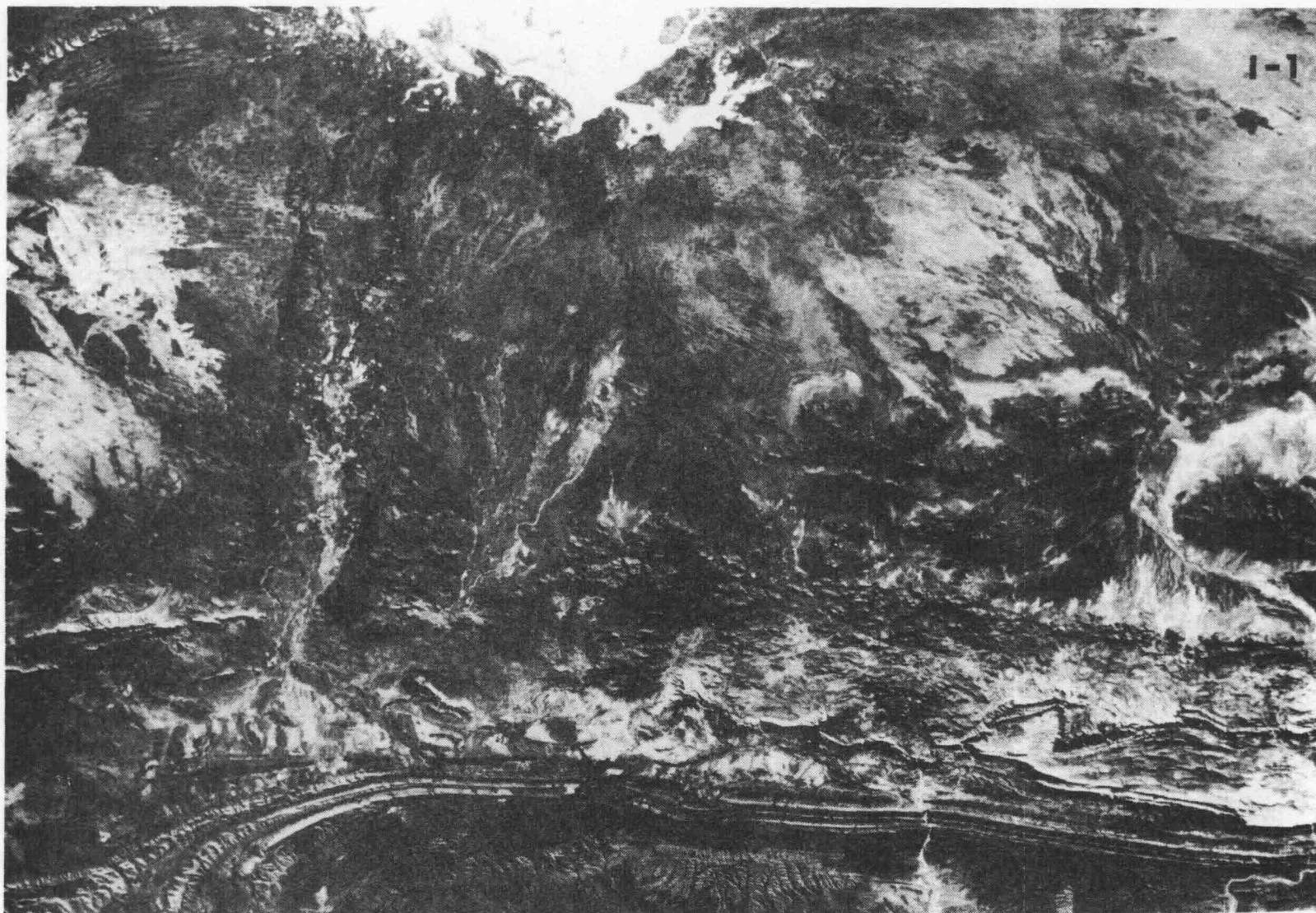
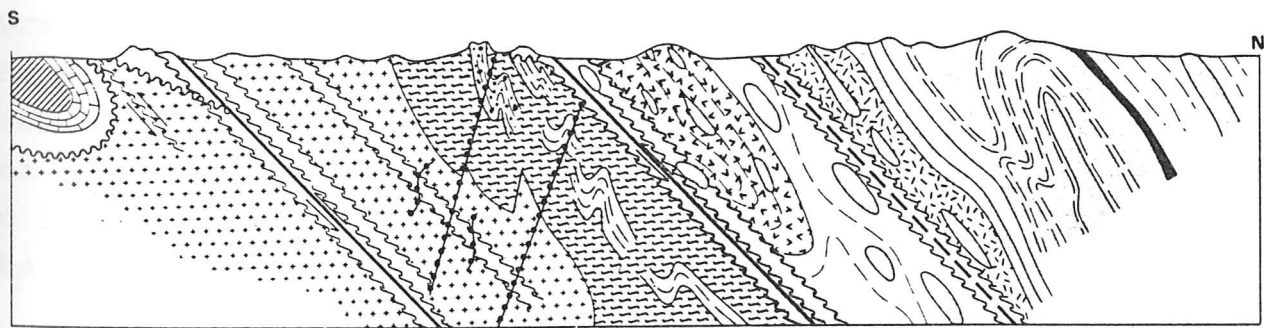
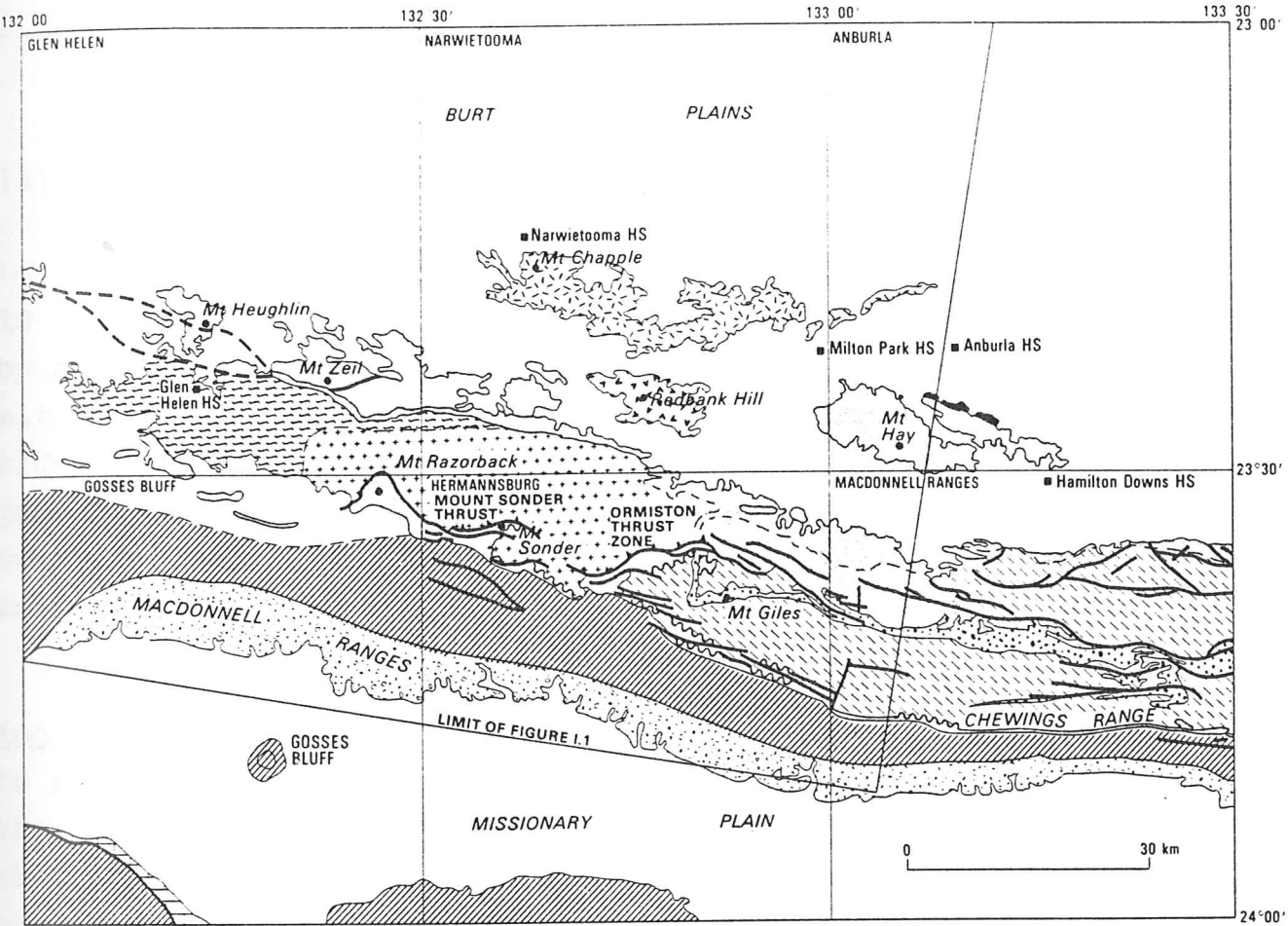


Fig. 1.2



16/F53-13

- | | | | | | |
|--------------------------------|----------------|--------------------------|----------------|---|----------------|
| Mount Hay basic granulite | } 2.0-1.5 B.Y. | Chewings Range Group | } 2.0-1.5 B.Y. | Redbank-Mount Zeil ca. 1.0 B.Y. thrust zone | } ca. 0.8 B.Y. |
| Mount Hay anorthosite | | Chewings Range quartzite | | Heavitree quartzite | |
| Mount Chapple granulite | | Teapot granite | | Bitter Springs limestone | |
| Mount Zeil granulite | | Dashwood migmatite | | Macdonnell Range Series | |
| Redbank porphyroblastic gneiss | | Derwent paragneiss | | Brewer conglomerate ca.0.3 B.Y. | |
| | | Migmatite | | | |

II. THE NORTHERN GRANULITE BLOCK

[1] Mt Hay Mafic Granulite-Anorthosite Belt

The Mt Hay ridge forms a discrete 100 degrees trending 30 x 10 km large topographic feature including a principal ridge capped by Mt Hay (1249 m) which consists of mafic granulites with anorthositic and intermediate to felsic gneiss stringers, and a lower ridge to the N and E made of anorthosite and of interlayered mafic granulite-anorthosite. The two ridges are separated by a narrow valley and are surrounded by a wide pediment conspicuous on space imagery (Fig. I.1).

The dominant structural grain outlined by compositional banding and by weak gneissosity is WNW (Fig. II. 2a). Marked deviations to northerly trends occur in the western and eastern extremities of the ridge. Banding and foliation dip steeply more commonly north than south. Flexures are mainly related to folding along steep east plunging axes delineated by a penetrative lineation system pitching 50-90° ESE (Fig. II. 2b). A large steeply plunging anti-form dominates the structure of the Mt Hay ridge in its eastern part and another antiform is outlined in the northern ridge. In some areas marked changes in trend are not obviously related to folding and may reflect fault dislocations, where fault traces are difficult to identify due to the uniformity of juxtaposed granulites, e.g. in the western part of the Mt Hay ridge.

The mafic granulites are of dark brown to black colour and of massive aspect in outcrop, the brown colour arising by weathering of plagioclase. The rocks consist of fine to medium grained granoblastic assemblages of plagioclase, clinopyroxene, orthopyroxene (often as small porphyroblasts), amphibole, biotite, ilmenite and magnetite. Calc-granulites contain scapolite, sphene, garnet and calcite along with cpx, opx, amph, highly calcic plg, and trace ilmenite and magnetite. A millimetre-scale and wider feldspar banding and feldspar-quartz

banding are common on microscopic, hand-specimen and outcrop scales (Fig. II.1). Generally the thicker the band the more likely it is to include K-feldspar and quartz. Principal mafic phases in these bands are opx, amph and biot, cpx is rare or absent. Feldspathic bands and stringers commonly form neosome fractions which parallel or engulf bands and lenses of mafic granulite, resulting in places in agmatitic and migmatitic structures (Fig. II.1a,b). The felsic units occur as continuous subparallel bands or streaks, discontinuous intrusive tongues (Fig. II.1c) glomeroblastic lenses and small porphyroblasts concentrated along foliations in the mafic granulites. It is the felsic fraction which manifests the structural lineation, forming parallel sets of small felsic pods on intersecting outcrop surfaces (Fig. II.1d). In places feldspathic material forms more than 50 percent of the rock, engulfing relic bands and pods of mafic granulite. A complete gradation exists between feldspar-rich bands consisting of the same phases as the associated mafic granulites and feldspar-rich bands consisting of almandine garnet, K-feldspar, plg and quartz, with biot, amph and opx as possible components. Sillimanite-garnet gneiss bands occur locally. Compositional banding and gneissosity are mostly parallel. Locally cataclastic and mylonitic to ultramylonitic bands occur, the latter consisting of rounded phenocrysts of garnet, feldspar and quartz and minor biotite set in a clouded siliceous matrix. The Mt Hay suite includes K-feldspar-quartz tourmaline pegmatites which often cut across the metamorphic foliation. The mineral compositions of selected granulites and gneisses are tabulated in Table II.1, and selected chemical indices are given for pyroxene, amphibole, biotite and garnet in Tables II.2-5.

The mafic granulites comprise two-pyroxene types, opx-bearing types, and cpx-bearing calc-granulites. The latter commonly include accessory scapolite and sphene. Two pyroxene granulites are represented by S36, consisting of a f.g. granoblastic assemblage of salite ($Mg' = 67-69$; $Wo:En:Fs = 46.36:17$), hypersthene ($Mg' = 52-56$), minor Ti-rich biotite

($X_{Ti}=0.11$) and ilmenite (Fig.II.1e). Plagioclase-banded opx-bearing mafic granulites are represented by S37. In this rock amphibole (potassian ferroan pargasite $Mg' = 48$; $K_2O = 2.3-2.5\%$) is an important component and is replaced by hypersthene ($Mg' = 50-51$) - notably more ferroan than the opx of two-pyroxene granulites. The feldspar-rich bands contain labradorite (An54), porphyroblastic K-feldspar of small 2V (ca 30°) and quartz. Ilmenite is a common trace component. Biotite replacement of pyx is associated with deformation of the porphyroblasts. The f.g. matrix contains zoned bytownite (An77-72), salite ($Mg' = 77.7$; Wo:En Fs = 47:40:12), and texturally young biotite ($Mg' = 63-66$) developed at the expense of pyroxene and ilmenite.

Granulites of anorthositic composition are finely interspersed with mafic granulites of the Mt Hay suite. Sample S45 contains aligned m.g. to c.g. subhedral porphyroblasts of hypersthene ($Mg' = 62.6$), partly replaced by biotite along cleavage planes, and often surrounded by finer grained aggregates of granoblastic amphibole (titanian ferroan pargasite; $Mg' = 57-62$), salite ($Mg' = 76.3$; Wo:En:Fes = 47:39:12) labradorite (An63-67), magnetite and ilmenite.

Sphene and scapolite bearing cpx-calc-granulites are represented by samples S53, S55 and S56. (Fig.II.1f). In S55 scapolite (Meionite; $Ca' = 78$) occurs as c.g. poikiloblasts which engulf amphibole (ferroan pargasite; $Mg' = 50$), salite ($Mg' = 81-82$), accessory garnet, sphene, calcite, ilmenite and magnetite. S53 is a sphene-bearing cpx-plg granulite, sphene occurring as bands of anhedral grains within granoblastic aggregate of f.g. salite ($Mg' = 60-62$; Wo:En:Fes = 49:31:19) and S57. S52 includes opx and amphibole rich bands and gnt-biotite-feldspar-quartz bands. The latter consist of m.g. anhedral porphyroblasts of Ca-poor ($X_{Ca} = 0.09$) almandine - rich garnet ($X_{Fe} = 0.58$), biotite ($Mg' = 70$), K-feldspar, plagioclase (An85) and quartz. Garnet commonly replaces biotite. The hypersthene ($Mg'=60-63$) and amphibole (Mg-

-hornblende; $Mg' = 64-67$) bearing bands contain little biotite and are devoid of garnet. Boundaries between bands are often sharp. Accessory ilmenite and magnetite are common. The garnet of S57, a felsic biotite-garnet gneiss band in the granulites, is more calciferous and ferroan ($X_{Ca} = 0.215$; $X_{Fe} = 0.686$), approximating andradite composition. Mylonitic zones occur within the Mt Hay suite: S30 consists of rounded microphenocrysts of Ca-poor iron-rich garnet ($X_{Ca} = 0.05$; $X_{Fe} = 0.647$) with inclusions of biotite ($Mg' = 63-66$), rounded microphenocrysts of bytownite (An 77-80) and quartz set in a clouded siliceous ultramylonitic matrix showing flow deformation.

Anorthosites and interbanded mafic granulites which occur in the northern ridge of the Mt Hay massif form light brown massive to layered outcrops which are of light colour compared to the mafic granulites (Fig. II.2-3). This outcrop pattern reflects the weathering-prone nature of calcic plagioclase. Amphibole and/or orthopyroxene-bearing bands, laminae, aggregates and clots impart a finely banded or mottled appearance to the rocks (Fig. II.3). The anorthosites consist of calcic plagioclase (mostly bytownite), amphibole (Magnesian hornblende), and/or hypersthene. No microscopic igneous texture is identified. Cross-lamination of probable deformational origin is discerned in places. The rocks are represented by samples S28 and S48. S28 consists of m.g. twinned anhedral bytownite (An73-78), pale green amphibole (Mg-hornblende, $Mg' = 70.6$) partly replaced by hypersthene ($Mg' = 62-63$). The ferro-magnesian minerals occur as elongated aggregates and bands which outline regular to patchy compositional banding. S48 is a well banded rock containing both cpx (salite, $Mg' = 78$; Wo:En:Fs = 47:40:11) and opx (hypersthene, $Mg' = 65$). The pyroxenes replace amphibole (titanian Mg-hornblende, $Mg' = 71$; TiO₂=1.3%). Plagioclase may show normal zonation in the range An63-An55. Significantly the anorthosites show little or no migmatization and intrusion by felsic bands.

[2] Mount Chapple Intermediate Granulite belt

The Mt Chapple granulites form a elongated narrow ridge which, including an eastermost chain of hills, runs for about 55 km east-west (Fig. I.1-2). The ridge is peaked at its westernmost extremity by Mt Chapple (1275 m). The widest and narrowest north-south sections through the range are 7 km and 1 km, respectively. The complex is predominantly made of granulites of intermediate to felsic composition, including abundant relic mafic granulites. Much of this suite is similar to the intermediate to felsic bands and layers in the Mt Hay basic granulite complex (Fig.II.1). Some of the intermediate to mafic granulites of the Mt Chapple suite contain garnet coexisting with opx and cpx. The granulites and associated granulite facies gneisses form massive to foliated and lineated dark brown to orange colour outcrops. Intruded into the granulites are stocks, pods and veins of granitic gneiss which stand out by their light colour and bouldery exfoliated and jointed nature. Structural trends outlined by the compositional banding and gneissosity mostly vary between WNW and EW (Fig. II.4a). Foliations dip mostly northward in the western part of the range and are variable in the eastern part. Foliation and compositional banding are mostly parallel. Penetrative lineation sets, expressed as feldspar-quartz rodding on foliation planes plunge steeply eastward (Fig. II.4b), corresponding to the axes of reclined isoclinal folds. Jointing is oriented at high angles to the metamorphic banding, i.e. at mainly longitudinal strikes.

The intermediate to felsic granulites are either uniformly fine to medium grained or, more commonly, feldspar-quartz glomeroblastic or hypersthene porphyroblastic. Plagioclase and hypersthene megacrysts impart a spotty brown weathered aspect to rock surfaces. Bands, lenses, enclaves and fragments of mafic granulite abound in the felsic to intermediate granulites, resulting in agmatite-like structures

(Fig. II.1). Mineral assemblages in these rocks contain some or all of opx, cpx, amphibole, biotite, garnet, plagioclase, Kfeldspar and quartz as chief constituents. Common accessories are magnetite, ilmenite, sphene, zircon, and rutile. The more felsic rocks contain fine to coarse grained porphyroblastic Kfeldspar, often displaying low 2V angles (ca 30°) suggestive of ?sanidine. Rapakivi textures are observed. Garnet, amphibole, biotite or hypersthene may dominate individual compositional bands within these rocks. Near-monomineralic compositional banding of feldspar and quartz occur where shearing and cataclasis are intense. Garnet-sillimanite gneisses are present as a relatively minor component. Small bodies of flow banded Porphyroblastic augen gneisses are represented by sample S117. It contains lenticular porphyroblasts of K-feldspar (2V of ca 30°) set in f.g. banded matrix including bands of K-feldspar, plagioclase and quartz and bands consisting of garnet poikiloblasts replacing foliated biotite. Accessory minerals in the felsic gneisses include apatite, zircon, allanite, rutile, iron oxide and amphibole. Other examples are samples S145 and S168. Components of the mafic bands are amphibole, hypersthene, clinopyroxene, plagioclase, apatite, ilmenite and iron oxide. A boundary between a biot-amph-cpx-opx-plg mafic granulite and opx-cpx-amph-plg-qz gneiss is shown in samples S128 (see also sample S137). Metamorphic segregation of feldspathic and quartzose bands is shown by S120. The mafic granulites are devoid of igneous or sedimentary texture. They may occur as bands within felsic granulite, as in sample S119. In this rock the mafic band consists of f.g. anhedral amphibole, hypersthene cpx, late-stage aligned biotite and plagioclase. However early stage mica is also recognised in some rocks, e.g. yellow phlogopite replaced by amphibole and pyroxene in S125. Most mafic granulites contain both opx and cpx, though many contain exclusively opx (S140). Examples of mafic granulites of the first type are samples S118, S132, and S133, which are pyribolites containing two pyroxenes and amphibole. The proportion of amphibole and biotite in mafic and intermediate granulites varies widely. Ilmenite and magnetite

are common accessories. Plagioclase is commonly weakly normally zoned. Commonly mafic granulites show segregation banding of ferromagnesian minerals from feldspar and quartz (S121) (Fig.II.1g). Many mafic granulites contain microphenocrysts of hypersthene which may be partly replaced by microcrystalline amphibole along cleavage planes (S124, S126, S190). A complete gradation exists between mafic and felsic granulites. S122 is an example of an intermediate granulite; it consists of elongated segregations of cpx, opx, amph and iron oxide, interspersed with plagioclase and quartz. Some granulites display a mottled texture, with elongated ferromagnesian components set in a plagioclase dominated matrix (S138).

Garnet is an important constituent of intermediate, and in some instances mafic, granulites. It is texturally younger than both amphibole and biotite (S123). Garnet may be the chief ferromagnesian phase in some granulites and gneisses (S127) (Fig.II.1h) along with amphibole (S207), opx (S147) and/or cpx (S167, S187, S188, S189, S193, S194, S215). It invariably constitutes^t the texturally youngest phase, except for rare retrogressive replacement by secondary biotite along cracks (S171). Garnet commonly develops at the expense of, and forms corona around, opaque iron oxide (S131, S187) (Fig.II.1i). Garnet is also commonly present in felsic gneisses, including mica-quartz-feldspar aggregates (S130), where it may be accompanied by sillimanite (S205) (Fig. II.1y) and minor spinel (S135). Plagioclase is mainly intermediate (andesine) in the felsic gneisses and calcic (labradorite) in the mafic granulites. It commonly contains graphic quartz inclusions.

Two samples of garnet-two pyroxene granulite (S188, S194) and one of garnet-hypersthene granulite (S187) from Mt Chapple were studied by electron probe. The garnets in these rocks are rich in the almandine molecule ($X_{Fe} = 0.58-0.60$), consistent with their occurrence as corona around ilmenite, and have approximately equal X_{Mg} and X_{Ca} values of 0.18-0.20. Coexisting pyroxenes include salite compositions ($Mg' = 65-70$)

similar to those of two pyroxene granulites from Mt Hay, and relatively ferroan hypersthene compositions ($Mg' = 53-55$). Accessory biotites are somewhat ferroan ($Mg' = 54-56$). The amphibole of S188 is a potassian magnesian hastingsite ($Mg' = 47.3$; $Ca:Mg:Fe = 30:24:47$; $K_2O = 2.38\%$). Plagioclase is of labradorite (An 57-59) composition and in some cases (S187) includes coexisting labradorite (An 58) and andesine (An 49).

Two samples of garnet-sillimanite gneiss from Mt Chapple (S135, S205) contain Ca-poor ($X_{Ca} = 0.02-0.03$) almandine-rich ($X_{Fe} = 0.601-0.845$) garnet of varying X_{Mg} and X_{Mn} components (Table II.5). The coexisting plagioclase of S135 is sodic oligoclase (An11). X_K values ($K/(K+Na+Ca)$) of associated K-feldspars are in the range of 0.87 and upward.

Relatively few of the observed Mt Chapple granulites display cataclasis (S182) or mylonitisation (S192). Planar segregation of quartz and feldspar related to deformation may be well developed (S216). Metamorphic retrogression is likewise rare, including weak alteration of garnet by biotite and pyroxene by amphibole.

[3] Redbank Hill Porphyroblastic Gneiss-Granulite belt

Redbank Hill is located about midway between the Mt Chapple ridge to the north and the Redbank-Mt Zeil thrust fault scarp to the south, forming a WNW-elongated hill about 16 x 6 km. The terrain consists typically of very coarse grained feldspar-blastic augen gneisses intruding and containing enclaves and xenoliths of, mafic to felsic granulites (Fig. II.5). Medium grained banded to laminated gneiss-granulite units are also common. The strike of metamorphic banding and foliation varies principally between EW and ENE, dips being near vertical (Fig. II.6). A northeastward pitching lineation set defines the axes of tight mesoscopic folds. Joints strike mainly longitudinally,

are well defined in the felsic porphyroblastic gneisses but are less pronounced in mafic granulites. Morphological patterns vary from bouldery to exfoliated light orange coloured outcrops of gneisses to massive dark grey and brown colour of intermediate to mafic granulites. Porphyroblastic gneisses contain rapakivi textured feldspars up to about 10 cm long, deformed and flattened porphyroblasts of K-feldspar, and glomeroblasts of feldspar and quartz embedded in felsic to intermediate gneissic or granulitic matrix. The porphyroblastic, glomeroblastic and even-grained gneisses intrude and contain abundant enclaves, xenoliths and bands of granulite (Fig.II.5 e-h). Where mafic granulites form detached bands, lenses, fragments, digested relics and streaked schlieren in the gneiss, a complete gradation exists from agmatite to nebulitic gneiss. Biotite and amphibole-rich mafic gneiss engulf xenoliths of two-pyroxene mafic granulite. Deformation of porphyroblastic and glomeroblastic gneisses has in places resulted in secondary flattening (Fig.II.5b,d). Moon tail-like shapes of glomeroblasts in places suggests syndeformational rotation (Fig. II.5a). The growth of porphyroblasts of feldspar within mafic to intermediate granulites, mainly along planar discontinuities, could have resulted from synmetamorphic migration of felsic neosome magma fractions.

Mineral assemblages of the porphyroblastic and glomeroblastic gneisses include chiefly garnet, amphibole, biotite, plagioclase, K-feldspar and quartz. Little or no orthopyroxene occurs in these rocks, as distinct from opx-bearing felsic gneiss fractions in the Mt Chapple and Mt Hay belts. The fine to medium grained intermediate to mafic granulites consist of orthopyroxene, clinopyroxene, amphibole, biotite, plagioclase, minor ilmenite and magnetite, and occasionally garnet. Intermediate to felsic granulites may contain garnet, orthopyroxene, biotite, amphibole, plagioclase, K-feldspar and quartz. Garnet-sillimanite gneisses occur locally (S232, S247). Cataclastic to mylonitic gneisses juxtaposed with shear zones

consist of deformed, recrystallised and clouded derivatives of the above rock types (Section V1). The common relic porphyroblastic phases in the mylonites are garnet, K-feldspar and quartz.

Sample S227 is a glomeroblastic Gnt-Biot-Amph-Plg-Qz augen gneiss typical of felsic components of Redbank Hill. Lenticular shaped aggregates of m.g. quartz and andesine (An42-45) are set in a f.g. clouded matrix which includes flakes of amphibole (potassian ferroan pargasite, $Mg' = 39$) and biotite ($Mg' = 42-45$). F.g. to m.g. anhedral to subhedral poikiloblasts of almandine-rich garnet (Ca:Mg:Fe = 22:12:65) with inclusions of quartz and biotite, and less commonly of amphibole, are common. Sample S241B includes a quartz-bearing Gnt-Opx-Amph-Biot-Plg band of m.g. granulite bordering a f.g. Gnt-Opx-Amph-Plg mafic granulite. Ilmenite is widely disseminated. Poorly defined augen of quartz and andesine (An 40-41) are set in fine grained granoblastic assemblages of plagioclase, ferroan hypersthene ($Mg' = 51-52$), and amphibole (potassian ferroan pargasite ($Mg' = 47-49$)). Poikiloblasts of almandine garnet (Ca:Mg:Fe = 19:17:65) are clearly younger than, and include inclusions of, biotite, amphibole and ilmenite. Sample S239 is an even grained granoblastic assemblage of Opx, Biot, Amph and Plg (Fig.II.5i) . Biotite is texturally younger than both amphibole and hypersthene, while the latter phases appear to be in equilibrium with each other. The Opx is hypersthene ($Mg' = 65$). Amphibole ranges from potassian pargasitic hornblende ($Mg' = 68-72$) to potassian edentitic hornblende ($Mg' = 77-78$). Biotite is of a pale brown magnesian variety ($Mg' = 70$). Plagioclase is normally zoned from bytownite (An75) to labradorite (An67). Cpx-bearing mafic granulites are represented by S228. The rock consists of microphenocrysts of hypersthene ($Mg' = 60-62$) set in a granoblastic matrix of salite (Wo:En:Fs = 46:37:15), labradorite (An60-61), olive green amphibole (pargasitic hornblende; $Mg' = 66$), potassium silicic edenite ($Mg' = 73.6$), biotite (texturally younger than other ferromagnesian phases), and minor ilmenite. The boundaries

between mafic and felsic bands are commonly sharp, e.g. the boundary between f.g. Gnt-Cpx-Amph-Plg mafic band and a felsic quartz-rich band in sample S353.

Cataclastic deformation, particularly of felsic gneisses, is common at Redbank Hill. Examples are samples S355, a deformed Gnt-Amph-Feld-Qz gneiss which displays mechanical granulation of feldspar and recrystallized quartz mosaics, and S386, displaying cataclastic rounding of grains. Some deformed quartzofeldspathic gneisses show a well pronounced segregation of monomineralic quartz and feldspar bands, cf. S581A and S518B. An incipient development of such deformational segregation is displayed by S516. Narrow shear zones are exemplified by S354, a Biot-Amph-Cpx-Opx-Plg granulite cut by a laminated quartz-saussurite shear (Fig.11.5n). A wide deformed zone occurs along part of the northern flank of Redbank Hill. Samples S365 and S366 include relic grains of amphibole, garnet and feldspar in a flow-textured matrix of elongated quartz aggregates and saussurite (Fig. 11.5m). Mylonites occur within this zone, cf. S513 and S518, consisting of relic fragments of feldspar set in laminated matrix which consists of micro-crystalline quartz bands and clouded K-feldspar-rich bands.

The order of crystallisation in the felsic to intermediate gneisses is commonly amphibole, pyroxene, biotite, and garnet as in sample S358 (Fig.II.5k). The development of glomeroblastic lenses of quartz and feldspar involves segregation around these augen of mafic mantles containing biotite, amphibole, garnet, apatite and sphene (S361B)(Fig.II.5l) Synmetamorphic porphyroblasis is indicated by occurrence of relic foliation within the glomeroblasts, while concomitant or younger deformation is suggested by rotation and flattening of these augen and the development of 'Moontail' structures (Fig. II.5a). In the mafic granulites biotite is the texturally younger phase. It is little deformed relative to other ferromagnesian minerals, cf. samples S368 and S370, which suggests post-tectonic growth (Fig.II.5y). Amphibole is either

older than, or appears to be in equilibrium with, pyroxene. These relations are consistent with the occurrence of biotite in distinct clusters in some rocks, suggestive of its late stage introduction.

Of the numerous enclaves of mafic granulite, generally more abundant toward the southern part of Redbank Hill, the most conspicuous enclave forms a morphologically well pronounced dark hill about 700 m in diameter about 3 km NE of Narwietooma bore no. 6 (Fig. II.5e). Mineral assemblages include opx, cpx, biot, amph, plg, and in some instances minor quartz and/or garnet. The mafic body is intruded by porphyroblastic and glomeroblastic gneiss and cataclastic gneiss consisting of gnt, biot, amph, plg, K-feld and quartz. The enclave constitutes a large mafic granulite relic, rather than an intrusion for which it may be mistaken by its massive and little deformed nature relative to the banded gneisses.

[4] Mount Zeil Felsic-Intermediate Granulite Belt

A WNW trending belt of granulite facies gneisses straddles the northernmost part of the basement terrain between south of Redbank Hill in the east and Dashwood creek in the west (Fig. I.1-2). This belt is confined between the Redbank-Mt Zeil Thrust Zone (RTZ) to the south and the Burt Plain to the north, constituting a 40 km long and up to 10 km wide zone whose principal topographic feature is Mt Zeil (1511 m). Further west, between the Dashwood and Derwent creeks, and west of the latter, discontinuous outcrops of granulites are widespread, including Mt Heughlin where the northern branch of the RTZ can be traced, separating granulites to the north from banded gneiss, migmatite and granite to the south.

The Mt Zeil granulites are predominantly of felsic to intermediate composition. Mafic granulites occur along the northern margin of the belt, but the mafic/felsic rock ratio is less than in the Mt Chapple range. Porphyroblastic gneisses are common; however, very coarse grained glomeroblastic gneisses of the Redbank Hill type are rare. Owing to the juxtaposition of the Mt Zeil granulite belt with the RTZ, cataclastic gneiss zones and mylonites are common and increase in frequency southward. Structural orientations in the granulites are markedly affected by the thrust fault, in whose proximity penetrative fracture sets and joints dip northward parallel to the thrust. The dominant trend of gneissosity is WNW (Fig. II.8a). With increasing distance from the fault northward, broad flexures are defined, the folding being controlled by steep eastward pitching fold axes defined by lineation as at Mt Chapple and Redbank Hill (Fig. II 8b). Felsic gneisses away from the thrust zones display strong jointing striking at high angles to the foliation. In outcrop, felsic to intermediate granulite facies gneisses display banded, and less commonly migmatitic, structures, engulfing palaeosome intermediate to mafic units (Fig. II.7-h). Chief mineral constituents of the felsic to intermediate gneisses include garnet, biotite, amphibole, orthopyroxene and less commonly clinopyroxene, plagioclase, K-feldspar and quartz. Sillimanite-garnet-biotite gneisses are present. Chief minerals of mafic enclaves include biotite, amphibole, orthopyroxene, clinopyroxene and plagioclase. Mafic granulites occur as bands, lenses, blocks or fragments within more felsic gneisses (Fig. II.7b-c).

Granulites of the type locality at Mt Zeil consist of predominantly f.g. weakly to well banded assemblages dominated by plagioclase (including antiperthite), microcline, quartz, biotite and iron oxide, with or without amphibole, orthopyroxene and/or garnet, and accessory epidote and apatite , cf. S697B, 698, 806C, 807B). Garnet is the youngest phase, replacing biotite, which in turn is younger than and replaces hypersthene and amphibole. Hypersthene is younger than amphibole. Garnet

is partly retrogressed by chlorite developed along cracks. Biotite and iron oxide are commonly associated with each other. Glomeroblastic quartzofeldspathic augen are common. Compositional banding involves segregation of ferromagnesian mineral dominated bands and quartz-feldspar rich bands; occasionally almost monomineralic bands occur. Biotite may be weakly aligned in the more gneissic rocks, outlining a weak foliation, but may be randomly oriented in the granoblastic assemblages. Mafic components of the Mt Zeil granulites occur as isolated bands and/or lenses (Fig. II.7c,d,g,h) consisting of granoblastic assemblages of amph, opx and/or cpx, calcic plg and iron oxide. Pyroxene tends to form discontinuous rims replacing amphibole. Biotite and quartz are possible minor constituents. Coarse grained Opx-Amph-Plg granulites occur and are represented by S598. The orthopyroxene may show alteration to secondary amphibole along cleavages. A complete compositional spectrum exists between felsic and mafic end members of the granulite suite. Intermediate types commonly contain abundant garnet and may include antiperthite, but generally have little or no K-feldspar (S703B, S704).

Owing to their proximity to the Redbank-Mt Zeil thrust zone, granulites and gneisses of the Mt Zeil suite commonly display a wide variety of quartz recrystallisation textures. Polygonization proceeded hand in hand with fracturing and mechanical rounding of relic phenocrysts of garnet and feldspar. Cataclastic gneisses may contain little deformed resistant relics of garnet set in penetratively foliated quartz-biotite matrix (S799B). End products of this process are represented by cataclasites consisting of elongated blebs of quartz interspersed with biotite, epidote and garnet (S800B, S803), and by mylonites consisting of well rounded anhedral porphyroblasts of quartz, antiperthite, epidote and garnet set in flow textured cryptocrystalline clouded saussurite-sericite-quartz matrix (S800A, S802).

[5] Mineral Compositions

Electron probe analyses were carried out on mineral assemblages of 36 samples. The data for selected samples are tabulated in Table II.1 (in microfiche). Selected compositional indices for pyroxenes, amphiboles, biotites, garnets and coexisting plagioclase feldspars are given in Table II.2-5, and plotted on the ACF diagrams (Fig. II.9).

A. PYROXENES

Plots on the Di-En-Fs-Hd diagram (Fig.II.10) indicate differences between pyroxenes associated with different assemblages. Salites of two-pyroxene mafic granulites have somewhat higher Di/Hd ratios and are slightly less Ca-rich than salites of calc-granulites. The field of salites of garnet-bearing two-pyroxene granulites (Mt Chapple) overlaps between the two groups. The cpx of some calc-granulites (S55, S56) has relatively high Jadeite (1.3) and tschermakite (3.5, 4.8) components, high Na₂O (0.31%) and Al₂O₃ (2.87%, 3.45%) contents. The Cpx of garnet granulites are likewise high in the tschermak molecule (4.0, 4.4). Hypersthene compositions of the above groups overlap, though those of some cpx-free hypersthene granulites (S37, Mg' = 50.4) and garnet-pyroxene granulites are relatively ferroan (Mg' = 52.8, 53.9, 54.8).

B. AMPHIBOLES

The compositions of amphiboles are given in Table II.3 and on the Ed-Tr-Ts-Pg diagram (Fig. II.11). The bulk of the data plot in the pargasite-rich field, corresponding to moderately high [Na + K]_A values. However, amphiboles of anorthosites are low alkali [Na + K]_A = 0.29, 0.27) Mg-hornblende (Mg' = 71) characterised by relatively low Al₂O₃

(8.72, 9.35) and K₂O (0.40, 0.45%). The minor amphibole components of two pyroxene mafic granulites and of hypersthene granulites overlap in composition, including potassian, ferroan and titanian pargasites and pargasitic hornblendes. Similar rock types may contain amphiboles of contrasting compositions, e.g. calc granulites contain high alumina (14.08%) ferroan pargasite (S55) and low alumina (7.47%) low [Na+K]_A = 0.16 actinolitic hornblende. Pargasites of Redbank Hill gneisses (S227, S241B) are more alkali rich, of potassian ferroan composition (Mg' = 39.7, 47.4; [Na+K]_A = 0.73, 0.80). Some of these gneisses contain a compositional range, e.g. S239 includes pargasitic and edenitic hornblende. Sample S228 contains an aluminous (Al₂O₃ = 11.22%) pargasitic hornblende and a younger (retrograde) potassium silicic edenite (Al₂O₃ = 5.83%). Amphiboles of the Derwent Paragneiss and Dashwood Migmatite (Section IV) include a wide compositional range, some being of low alumina actinolitic composition, i.e. S834 contains both potassian Mg-hastingsitic hornblende (Al₂O₃ = 11.0%; [Na₂O + K₂O]_A = 0.58), and potassian actinolite in felsic bands (Al₂O₃ = 2.29%; [Na+K]_A = 0.03), reflecting the generally lower metamorphic grade of these rocks.

C. BIOTITES

The Mg' numbers and X_{Ti} values (Ti/Ti+Mg+Fe) of biotites are listed in Table II.4. Biotites associated with mafic granulites are titanian and have Mg values in the 55-75 range, while those associated with felsic gneisses have lesser X_{Ti} values and are typically ferroan, i.e. S57 (Mg' = 33.3), S227 (Mg' = 44.3). The biotites of garnet-pyroxene granulites (Mg' = 53.9, 55.7) are of intermediate compositions. The biotite of a garnetiferous mylonite (S30) is magnesian (Mg' = 65.7) and thus probably of unequilibrated relic composition. Biotites of granites, migmatites and paragneisses of the southern block (Section IV) are typically ferroan (Mg' = 27-54) and of low X_{Ti} values mainly in the range of 0.04-0.06, and thus useful for distinctions from granulite-facies biotites.

D. GARNETS

The Ca:Mg:Fe, X_{Mg} , X_{Fe} , X_{Ca} and X_{Mn} values of garnets are given in Table II.5. Garnets of the Mt Chapple garnet-pyroxene granulites have a high almandine component ($X_{Fe} = 0.6$) and similar pyrope and grossular components ($X_{Ca} = 0.19$). Garnets of Redbank Hill gneisses are of similar composition, although of somewhat higher X_{Fe} and lower X_{Mg} values. Garnets of Mt Hay felsic gneiss/granulite and mylonite show a wide compositional range, some characterised by a very low grossular component ($X_{Ca} = 0.091, 0.049$). Garnets of garnet-sillimanite gneisses have typically low X_{Ca} values of about 0.02-0.04 and variable X_{Fe} , X_{Mg} and X_{Mn} . A grossular-rich garnet ($X_{Ca} = 0.696$) was analysed in a gneiss from the Derwent Paragneisses.

E. PLAGIOCLASE

Plagioclase compositions are given in table II.2,3 and 5. Anorthosites show ranges of An 56-78, two-pyroxene mafic granulite - An 58-77, garnet-pyroxene granulites - An 57-59, calc-granulites - An 82-93, felsic intermediate gneisses An 54-86, Redbank Hill gneiss - An 40-43, and Derwent Paragneisses An 32-36. The occurrence of wide compositional ranges in felsic to intermediate gneiss bands probably reflects retention of metastable calcic plagioclase relics derived from granulite mafic granulites. The high An levels in the bytownite-anorthite range in calc-granulites is in accord with the high CaO levels in these rocks.

Bulk rock chemistry control of the various mineral compositions is suggested with regard to the few available analyses (Table III.1), as follows: Broadly sympathetic relations exist between the X_{Ca} values (100 CaO/CaO+Na₂O) of the rocks and the An contents of the plagioclase feldspars (Fig.II.12b,c). Likewise, broadly positive relations appear to

hold between the bulk rock Mg' value and the Mg' values of their contained amphiboles and biotites (Fig. II.12b,c) but not with their contained pyroxenes (Fig.II.12d), although the sample population may not be sufficiently large to corroborate the bulk rock chemistry control. Sympathetic correlation appears to exist between the Mg' values of orthopyroxenes and clinopyroxenes, cpx being consistently higher by about 12 units than in the coexisting opx (Fig.II.12e). Broadly sympathetic relations pertain between the Mg' values of amphiboles and coexisting pyroxenes, and near linear relations between the Mg' of biotites and pyroxenes.

Comparisons between plagioclase An values and the Al₂O₃ contents of coexisting amphiboles, usually positively related upon prograde metamorphism (Winkler, 1967), does not reveal sympathetic relations, although some amphiboles of the Derwent Paragneiss have significantly lower Al₂O₃ than in granulites, reflecting their lower metamorphic grade. Nor does the An level in plagioclase relate positively to Mg' values in coexisting ferromagnesian phases.

Phase relations between different mineral assemblages are portrayed in the ACF diagrams (Figs. II.9 and IV.3). The diagrams reflect the contrasting garnet compositions in garnet-pyroxene granulites, garnet-sillimanite gneisses and Derwent Paragneiss, and broad overlaps in the chemistry of pyroxenes and biotites. The variations are consistent with aspects of whole rock chemical distinctions.

[6] Precursors of the granulites

The lack of preservation of any primary igneous or sedimentary structures and textures in granulites and granulite facies gneisses of the Mt Hay, Mt Chapple, Redbank Hill and Mt Zeil belts renders the identification of their original character a subject for geochemical evidence and for indirect consideration. The chemistry of the granulites is at present under study and will be discussed elsewhere (Glikson, in prep.). On the basis of present evidence, in considering the origin of the Mt

Hay mafic granulites, the following features are pertinent:

(1) The mafic granulites are mostly fine grained uniformly granoblastic rocks. Layering is mainly related to variations in the mafic minerals/plagioclase ratio. No inherited rhythmic banding or cyclicity are observed. Whereas it is possible that the banding could be inherited from igneous layering, remobilisation of the feldspar-rich fractions has resulted in obliteration of primary magmatic banding.

(2) The mafic granulites are intercalated with recrystallised anorthosites and plagioclase-rich intermediate granulites.

(3) No sedimentary units have been confidently identified within the Mt Hay belt.

It is possible that the felsic gneiss bands and lenses intruded into the granulites were derived from anatectically mobilised sedimentary materials. Likewise, the scapolite-sphene carbonate bearing mafic granulites may represent metamorphosed calc-silicates. However, carbonate segregations may also be trapped and metamorphosed within basic intrusions. Minor garnet-sillimanite gneiss occurrences at Mt Hay may represent either metamorphosed pelitic sediments or metamorphosed sheared (mica-enriched) gneisses. An alternative view of the felsic

phases is to regard them as derived by partial melting of mafic granulites. If so, this process is unlikely to have taken place in situ, since no residual ultramafic selvages juxtaposed with felsic-mafic rock boundaries have been observed. The progression from thin plagioclase dominated bands to thicker K-feldspar and quartz dominated bands suggests fractional crystallisation concomitant with magmatic segregation, although this conclusion awaits confirmation by further geochemical data. Owing to their association with anorthosites, generally typical of deep seated crustal zones, it will be suggested that the Mt Hay granulites could represent an uplifted infracrustal basic segment.

The Mt Chapple, Redbank Hill and Mt Zeil granulites have significantly higher ratios of intermediate to mafic granulites than the Mt Hay belt. However, inspite of the abundance of intermediate and felsic components, no relic identifiable sedimentary materials such as quartzite, calc-silicate, or banded iron formation typical of Proterozoic terrains were observed. The minor garnet-sillimanite gneisses occurring in these areas are of equivocal significance. These rocks may be interpreted as aluminous metasediments or, alternatively, in terms of metamorphism of altered micaceous bands developed in orthogneisses upon metamorphic differentiation and segregation banding. It is possible that these complexes constitute remobilised derivatives of feldspathic sediments or lavas containing basic igneous units, whereby the original textures were totally obliterated. Alternatively, they may represent progressive segregation of intermediate and felsic magmas arising by anatexis in deeper crustal regions and intruding higher level mafic granulites. If so, the progression from mafic to intermediate and felsic granulites shown in the Mt Hay-Mt Chapple-Redbank Hill-Mt Zeil belts, in this order, may reflect progressive segregation of intermediate to felsic magmatic components upwards in the crust. The very coarse grained glomeroblastic and porphyroblastic gneisses of Redbank Hill may indicate high stress environment under which the felsic

magmas were crystallised and metamorphosed in this area conceivably signifying a precursor stage of the Redbank-Mt Zeil thrust zone.

FIGURE CAPTIONS FOR SECTION II

II.1 - Mt Hay and Mt Chapple outcrops and microphotographs

- (A) Isoclinal folding of stromatic structures in mafic granulites, including cm-scale plagioclase-dominated bands injected along foliation planes. Pen-13 cm.
- (B) Agmatitic structures in mafic granulites, consisting of plagioclase-rich veins intruded mostly at subconcordant angles to the dominant foliation trend. Hammer - 30 cm.
- (C) Plagioclase-rich gneiss lense in mafic granulite, showing opx-amph-biot-plg gneiss intruding and containing relics of fine grained two-pyroxene mafic granulite. Notebook-16 cm long.
- (D) Stromatic banded plagioclase gneiss and glomeroblasts and porphyroblasts of plagioclase and microcline in mafic granulite. Notebook - 16 cm long.
- (E) S36 - biot-opx-cpx-plg-ilmenite mafic granulite; Mt Hay. Texturally late biotite replacing cpx; 32 x 12; PPL.
- (F) S54-Sphene-opx-cpx-plg-calc granulite, Mt Hay; 8 x 12; PPL
- (G) S121 - biot-amph-opx-cpx-plg granulite, Mt Chapple. Texturally late biotite replacing pyroxene; 24 x 12; PPL
- (H) S127 - garnet-biot-amph-plg-qz gneiss, Mt Chapple; garnet replacing biotite replacing amphibole; 17x12; PPL
- (I) S187 - garnet-opx-plg-ilmenite granulite; Mt Chapple; garnet corona around ilmenite, cpx replacing amphibole; 10 x 12; PPL
- (J) - S205 - garnet-sillimanite-biotite-feldspar-quartz gneiss; 6.3 x 12; PPL .CP5

II.2

- (A) contoured poles to 54 measured foliations of Mt Hay granulites and gneisses (lower hemisphere stereographic projection).
- (B) contoured projections of 27 measured lineations of Mt Hay

granulites and gneisses (lower hemisphere stereographic projection).

II.3

- (A) and (B) finely banded hornblende-opx anorthosite. Hammer - 30 cm long.
- (C) spotted anorthosites, showing clots of amphibole in a plagioclase-rich matrix.
- (D) layered anorthosites, showing well laminated amphibole-rich bands alternating with plagioclase rich bands. Pen - 13 cm.

II.4

- (A) contoured poles to 53 measured foliations of Mt Chapple granulites and gneisses.
- (B) Contoured projections of 15 measured lineations of Mt Chapple granulites and gneiss.

II.5 - Redbank Hill outcrops and microphotographs

- (A) Deformed glomeroblastic gneiss, showing lenses and rounded porphyroblasts of microcline set in foliated matrix (gnt-biot-amph). The hammer rests on a mafic granulite
- (B) interbanded felsic and mafic glomeroblastic zones. Note the deformed shapes of some porphyroblasts.
- (C) glomeroblastic mafic garnet-biotite-hornblende gneiss including relic bands and fragments of mafic granulite
- (D) deformed glomeroblastic felsic gneiss.
- (E) a body of homogeneous two-pyroxene mafic granulite ca 1.5x0.5 km large on the southwestern flank of Redbank Hill. The benches are separated by thin zones of intrusive glomeroblastic gneiss.
- (F) intercalated bands of basic granulite and intrusive felsic gneiss
- (G) a relic layer of mafic granulite within intermediate to felsic gneiss.

- (H) agmatitic structures consisting of fragments of mafic granulite intruded by biot-amph-plg-qz gneiss
- (I) S239 - biot-amph-cpx-plg gneiss; biotite replacing cpx replacing amphibole; 27 x 12; PPL
- (J) S368 - biot-amph-opx-cpx-plg granulite; texturally late biotite; 32 x 12; PPL
- (K) S358 - gnt-biot-amph-opx-cpx-plg granulite; garnet replacing biotite replacing pyroxene replacing amphibole; 6.3 x 12; PPL
- (L) S361B - garnet-biotite-amphibole mafic band in gneiss; 23 x 12; PPL
- (M) S365 - rounded relic porphyroblast of amphibole in quartz ribboned mylonite; 32 x 12; PPL
- (N) S354 - micromylonite zone in biot-amph-opx-cpx-plg granulite; 6.3 x 12; PPL .CP5

II.6

- (A) contoured stereographic plots of 33 poles to foliations of gneisses and granulites, Redbank Hill.
- (B) contoured stereographic projections of 8 lineations, Redbank Hill

II.7 - Mt Zeil granulite/gneiss outcrops

- (A) gneiss-injected mafic granulites
- (B) finely interbanded mafic-felsic granulites
- (C) a lense of mafic granulite within felsic granulite-facies gneiss
- (D) fragments of mafic granulite within intermediate to mafic opx-biot-amph gneiss
- (E) tightly folded migmatites, including xenoliths and bands of amphibolite.
- (F) folded migmatites, including biotite-rich units.
- (G and H) xenoliths of amphibolite in banded gneiss/migmatite

II.8

- (A) Contoured stereographic plots of poles to 39 measured foliations, Mt Zeil granulite belt.
- (B) Contoured stereographic projections of 11 lineations, Mt Zeil granulite belt.

II.9 ACF plots of mineral assemblages from Mt Hay, Mt Chapple and Redbank Hill. Open circles denotes whole rock composition.

II.10 Pyroxene compositional fields according to the Di-Hd-En-Fs tetrahedron.

II.11 amphibole compositional fields according to the Ed-Pg-Tr-Ts tetrahedron (Leake, 1968)

II.12 Mineral phase-whole rock chemical relations

- (a) plagioclase (An) VS $100\text{Ca}/(\text{Ca}+\text{Na})$ bulk rock
- (b) Mg' amphibole VS Mg' bulk rock
- (c) Mg' biotite VS Mg' bulk rock
- (d) Mg' pyroxene VS Mg' bulk rock
- (e) Mg' cpx VS Mg' opx

Fig. 11.1

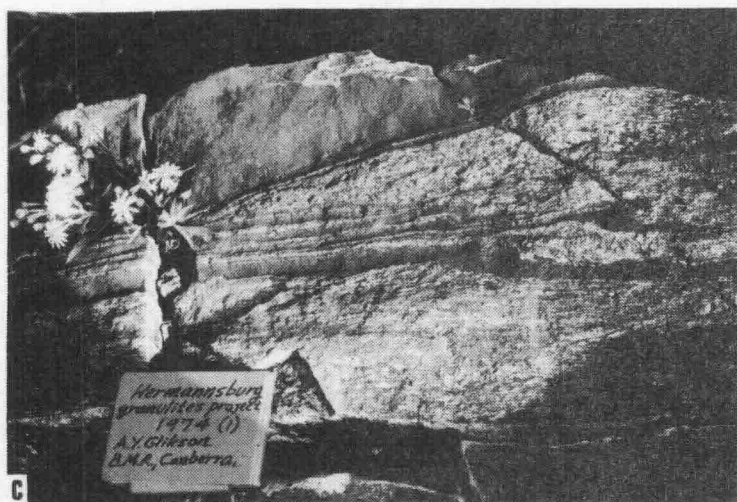
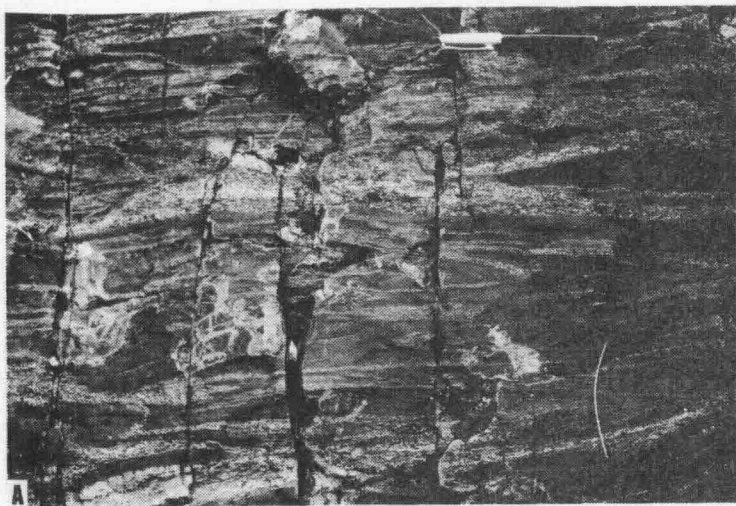


Fig II · 1(2)

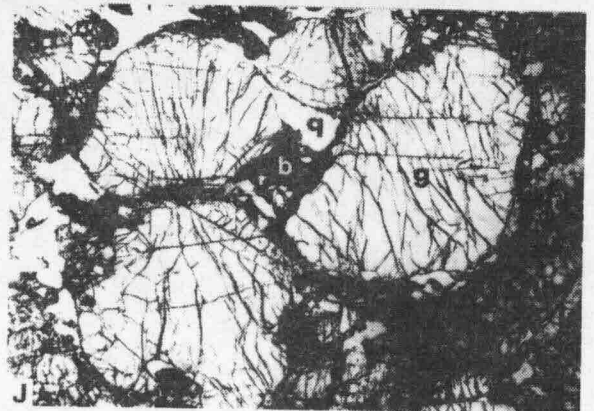
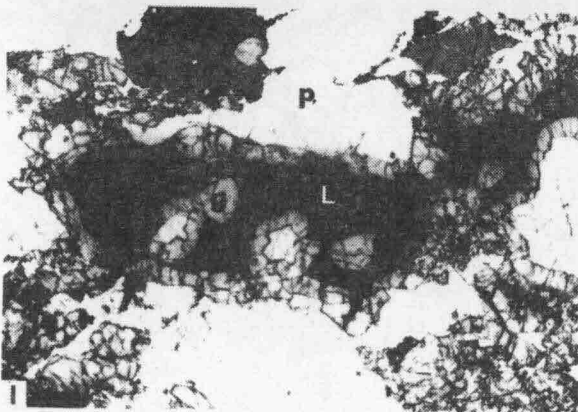
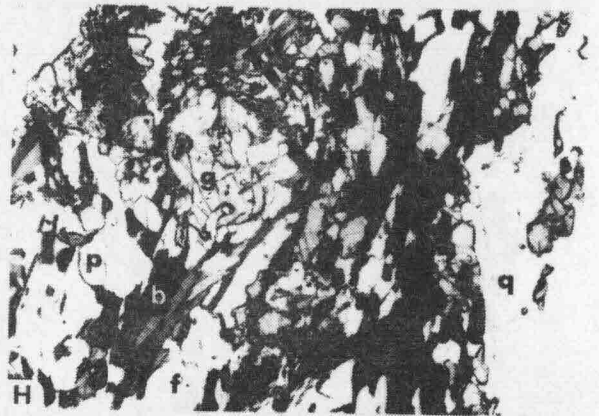
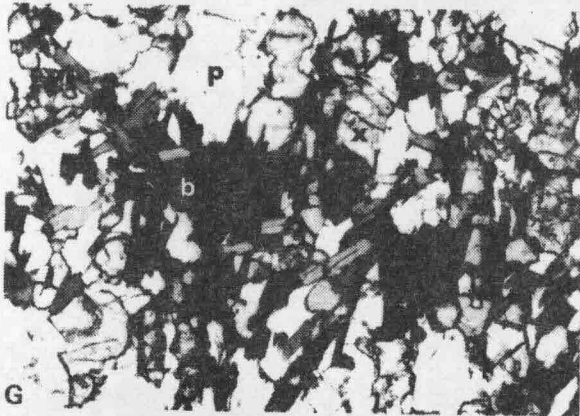
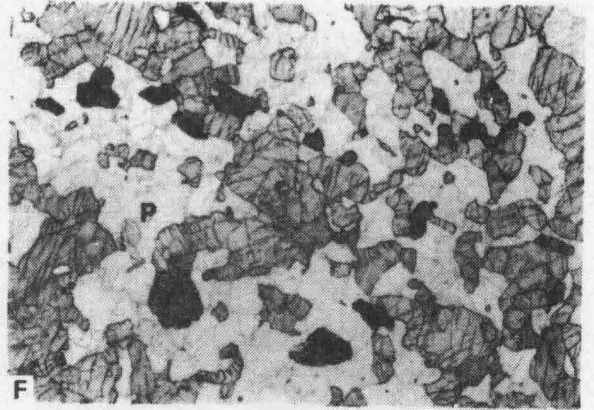
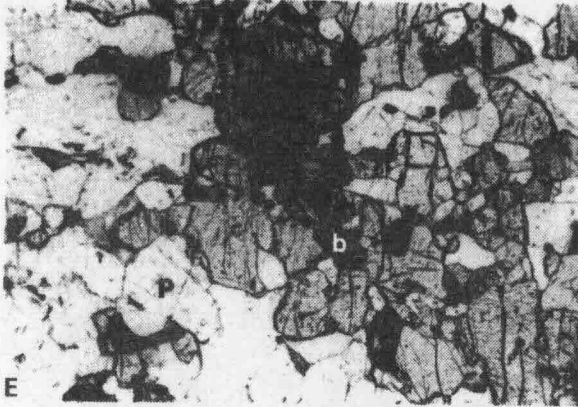
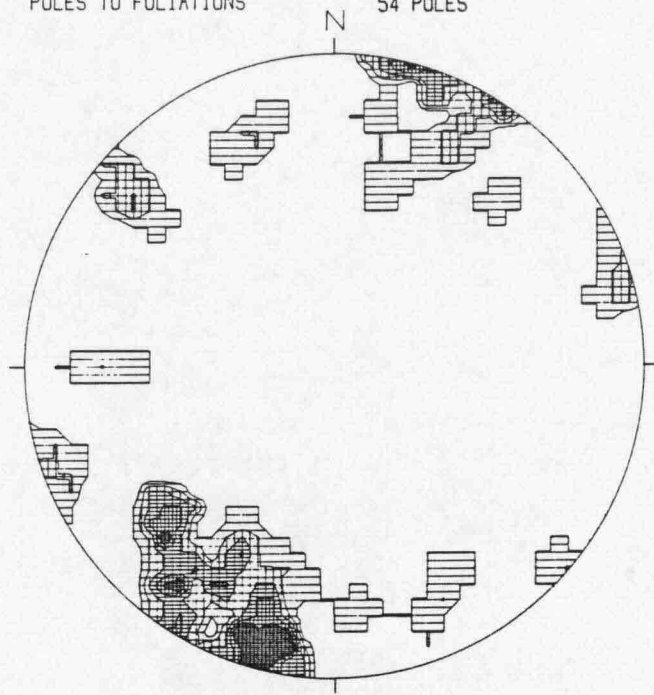
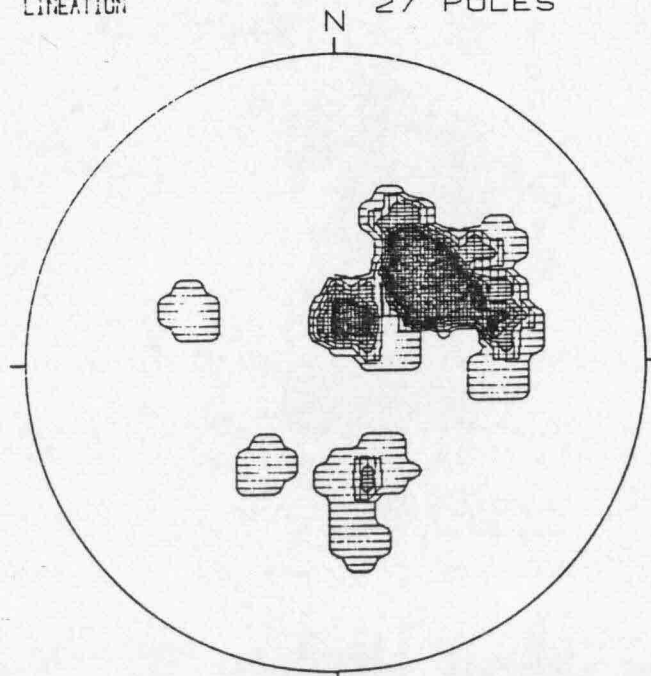


Fig. II.2

MOUNT HAY GRANULITES
POLES TO FOLIATIONS 54 POLES



MOUNT HAY GRANULITES
LINEATION 27 POLES



2-4% 4-6% 6-8% 8-10% >10%

Fig. 11.3

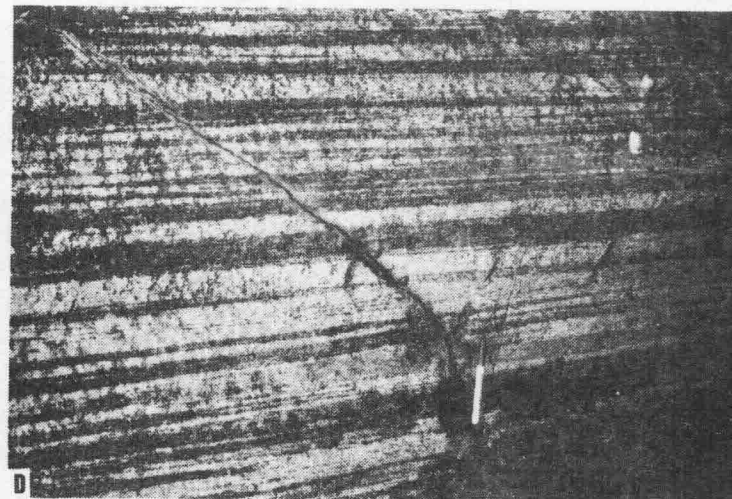
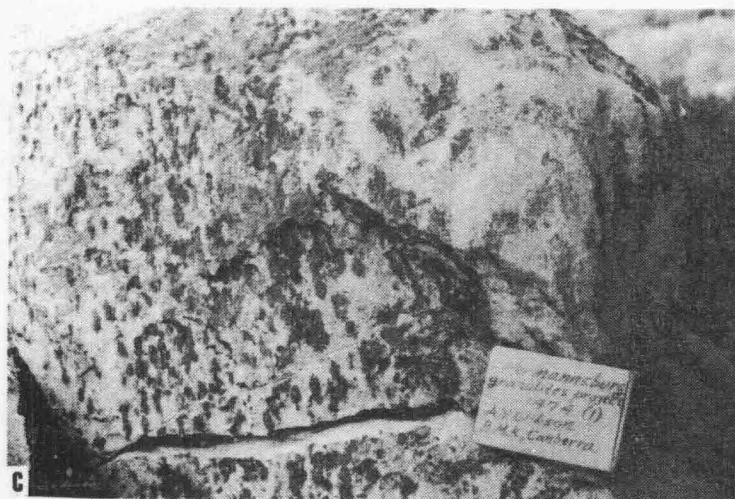
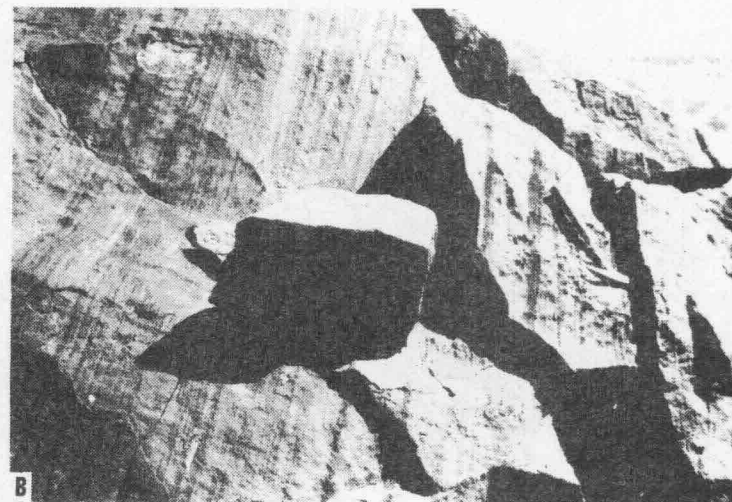
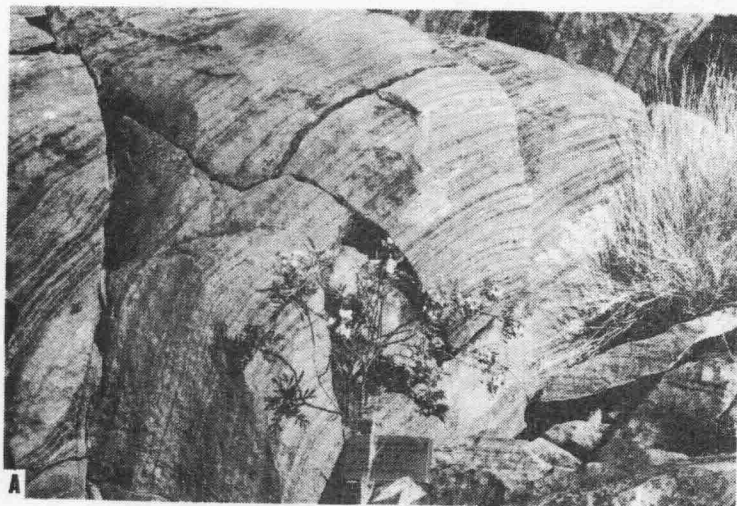
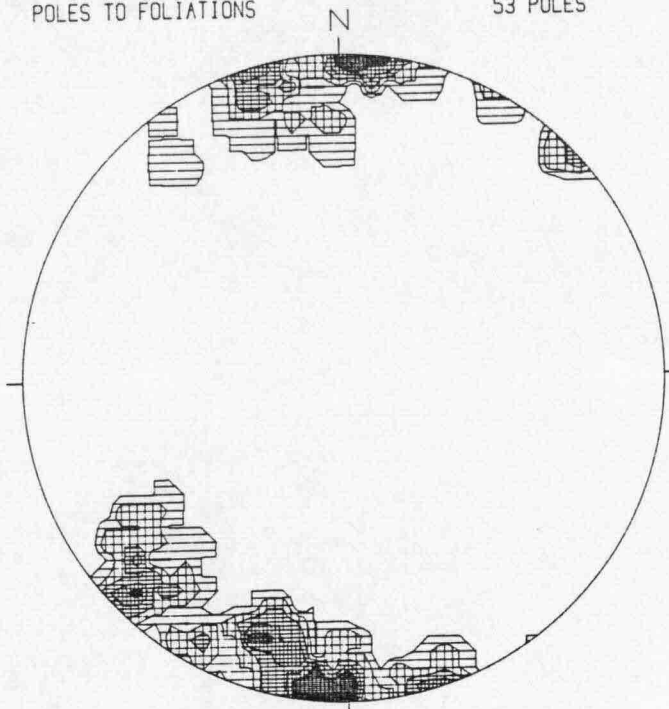
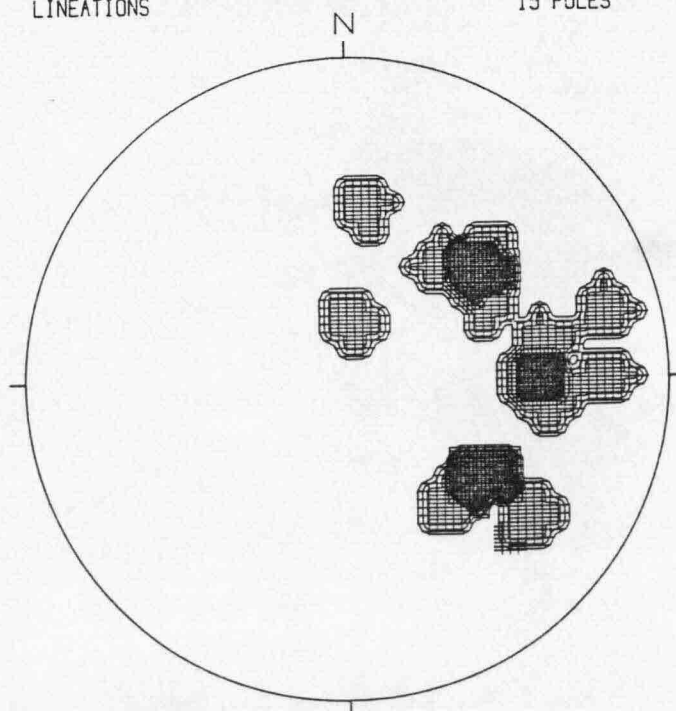


Fig. II.4 MOUNT CHAPPLE GRANULITES
POLES TO FOLIATIONS 53 POLES



MOUNT CHAPPLE GRANULITES
LINEATIONS 15 POLES








 2-4%	 4-6%	 6-8%	 8-10%	 >10%
--	--	--	--	--

Fig. 11.5

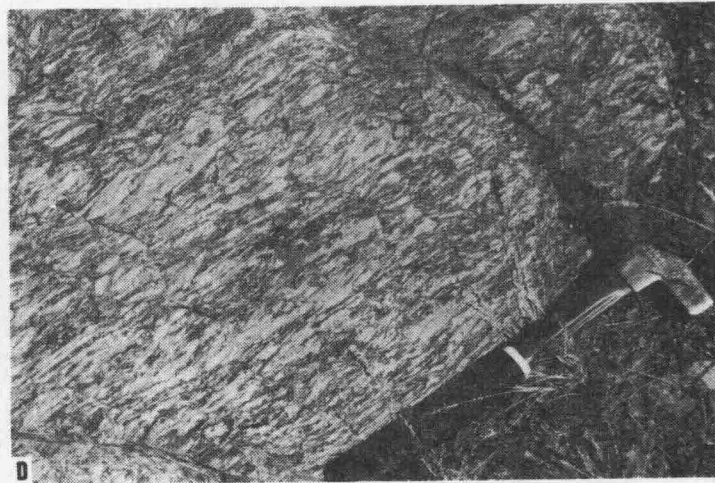
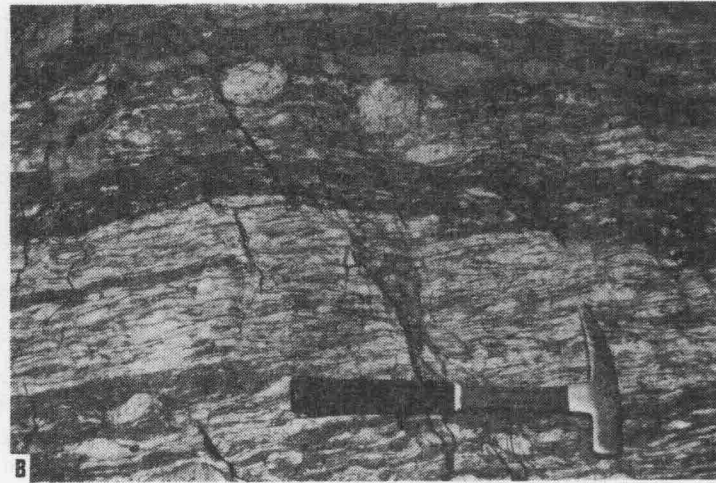
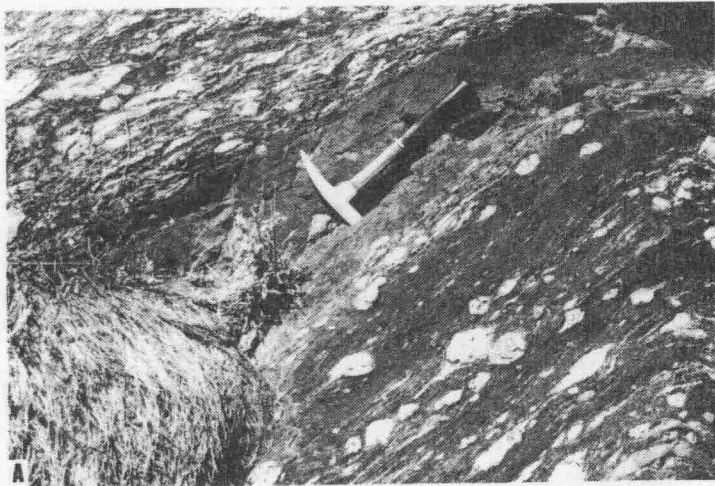


Fig. 11.5 2

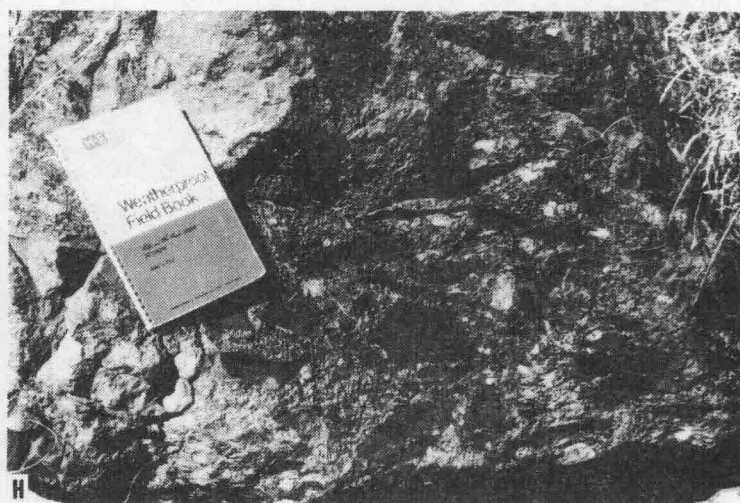
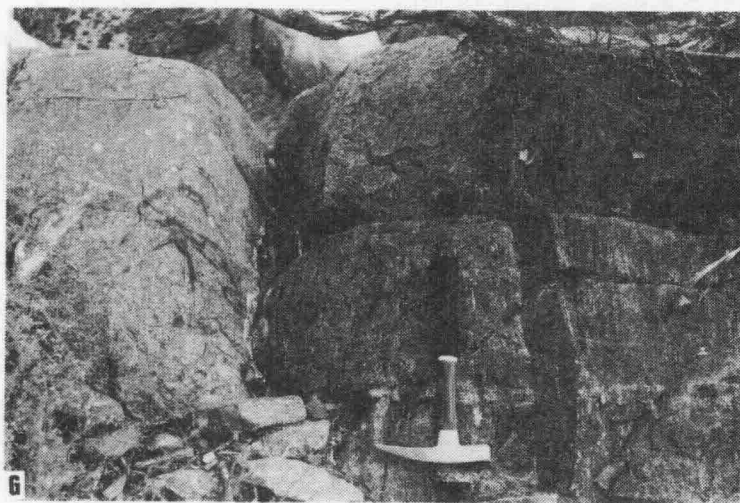
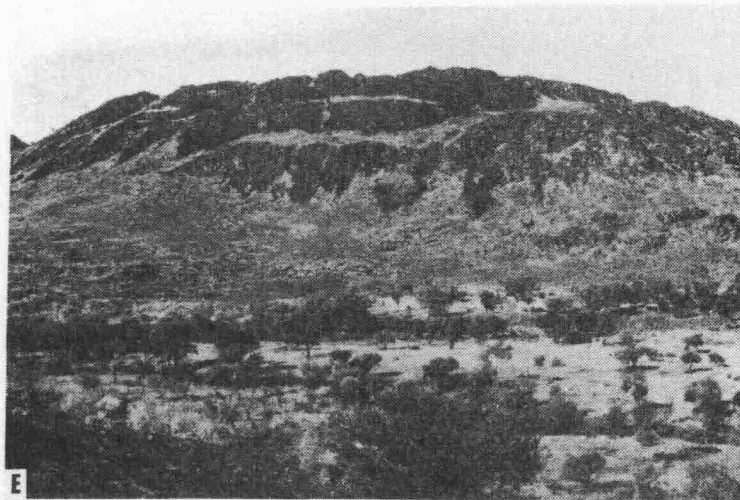


Fig II · 5(3)

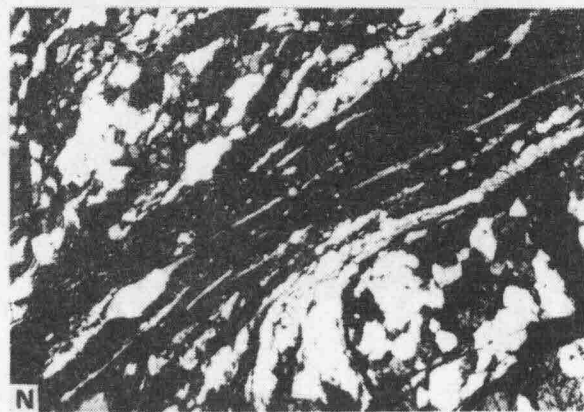
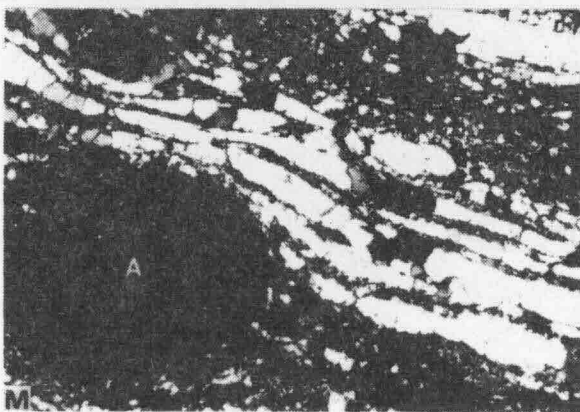
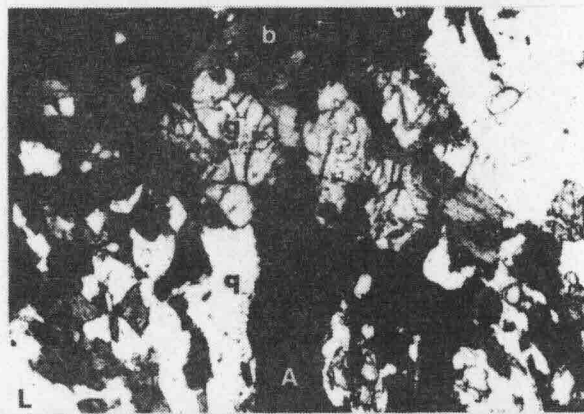
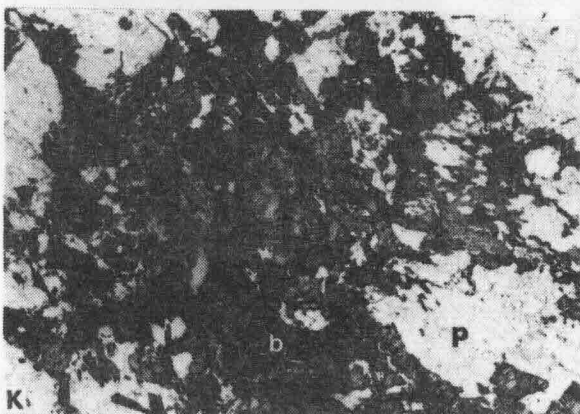
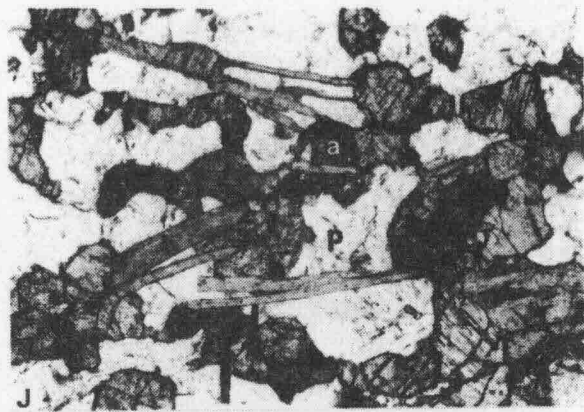
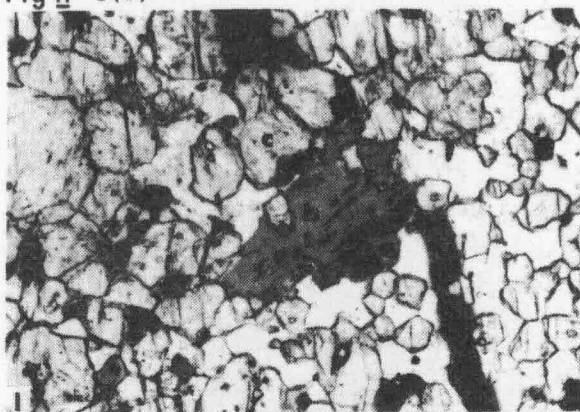
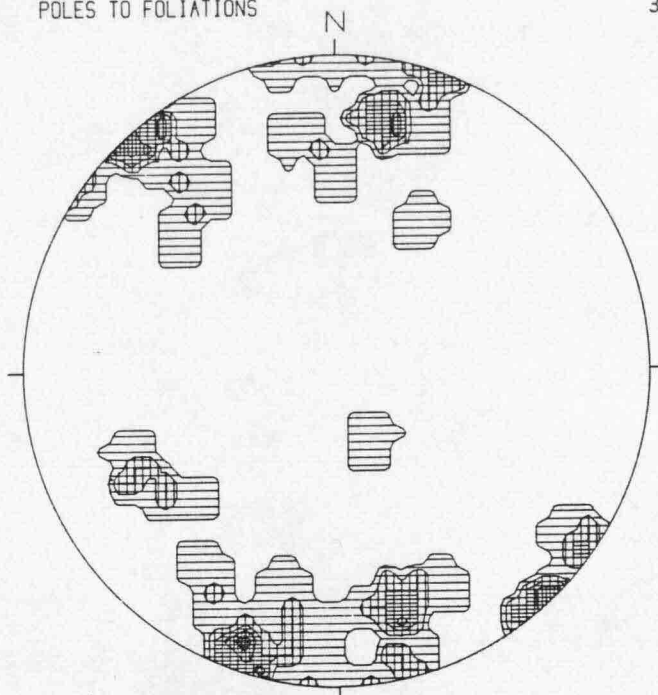
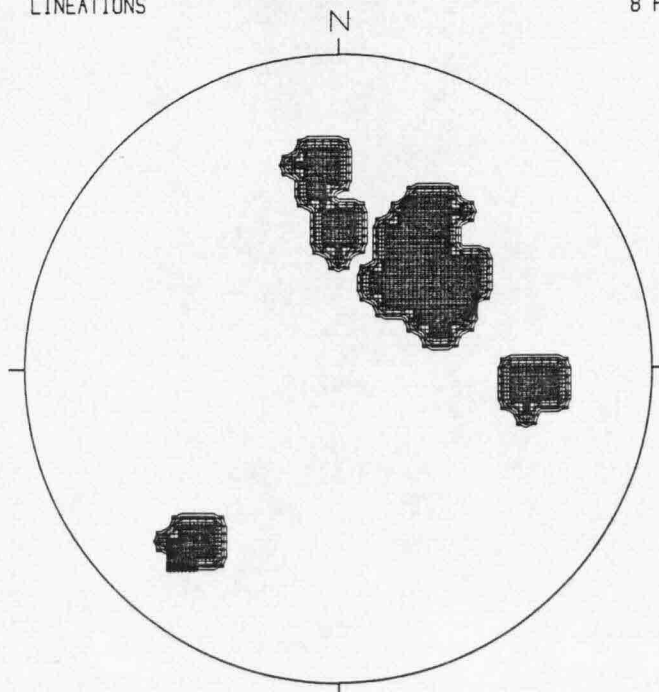


Fig. 11.6

REDBANK HILL GNEISS-GRANULITES
POLES TO FOLIATIONS 33 POLES



REDBANK HILL GNEISS-GRANULITES
LINEATIONS 8 POLES



2-4% 4-6% 6-8% 8-10% >10%

Fig. 11.7a

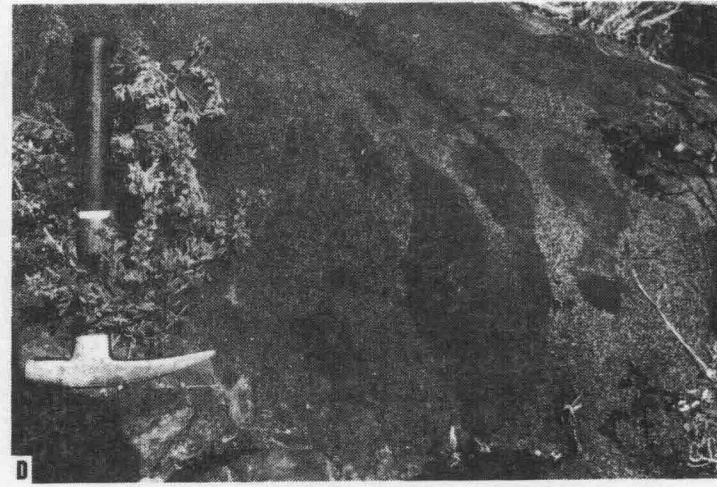
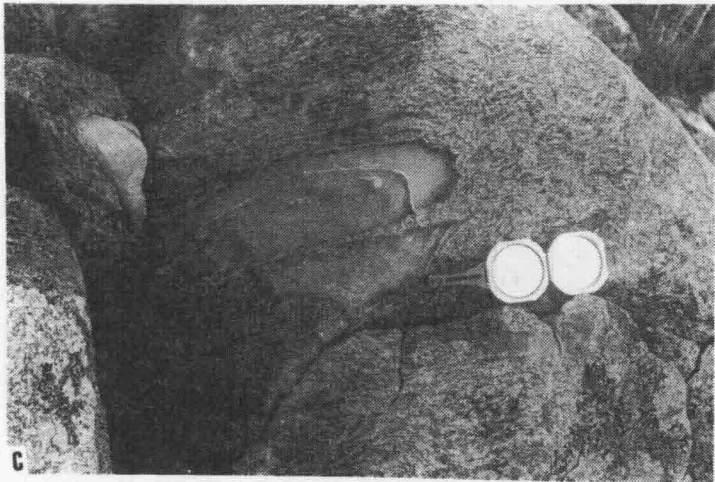
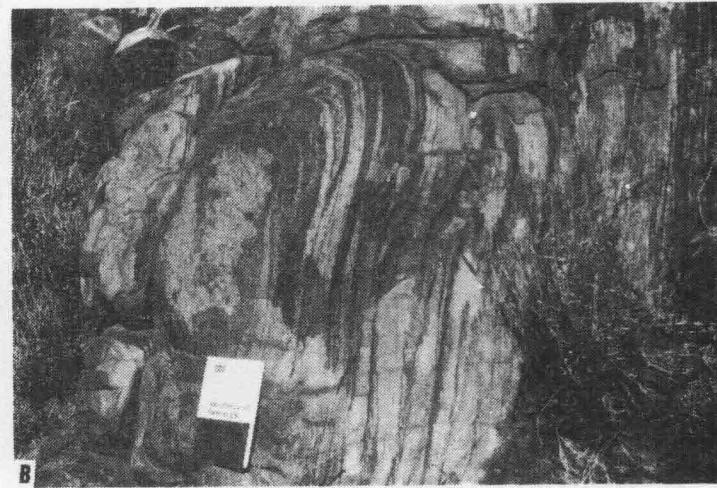
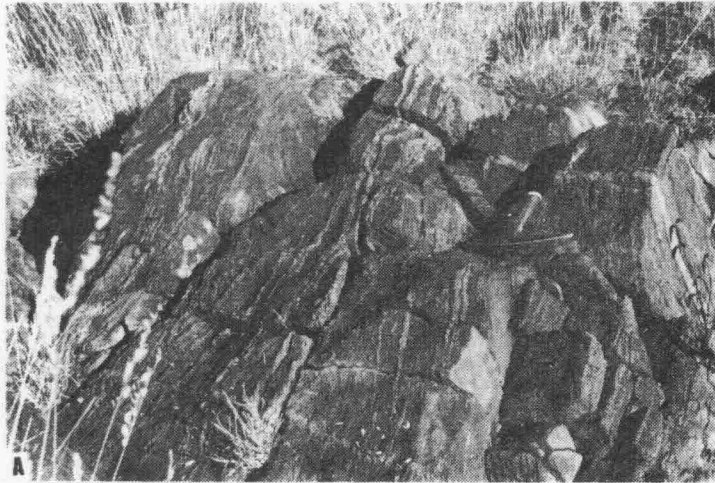


Fig. 11.7b

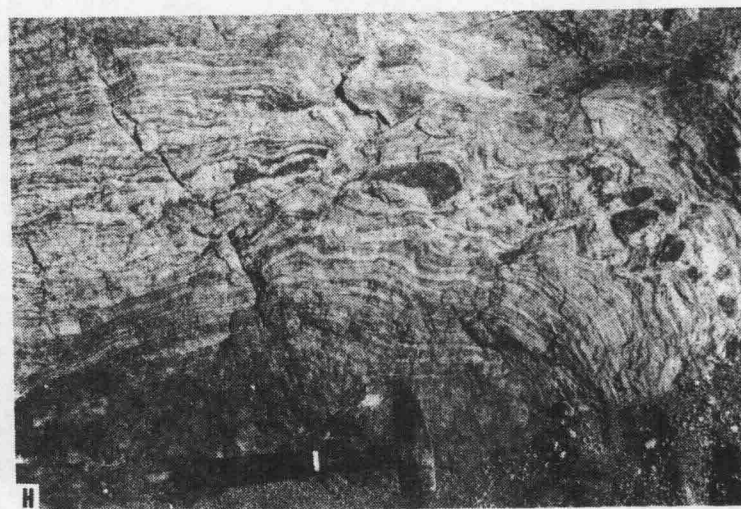
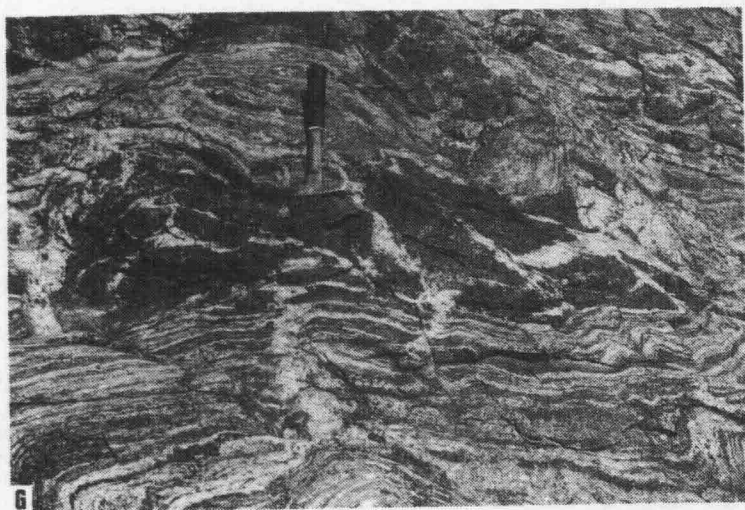
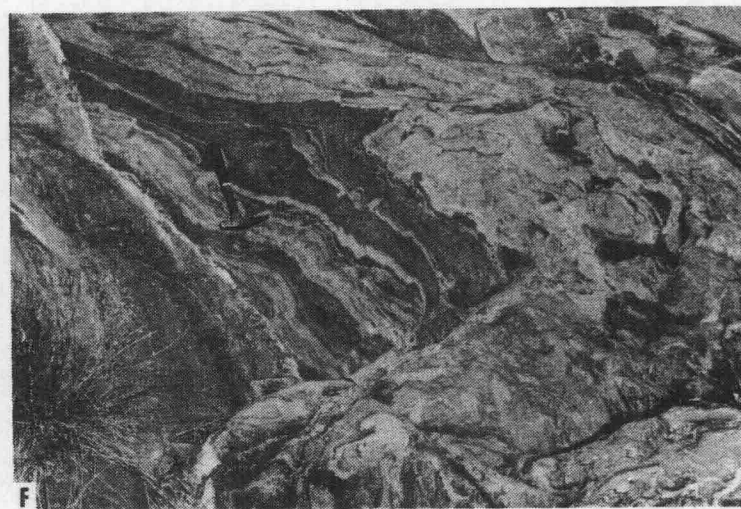
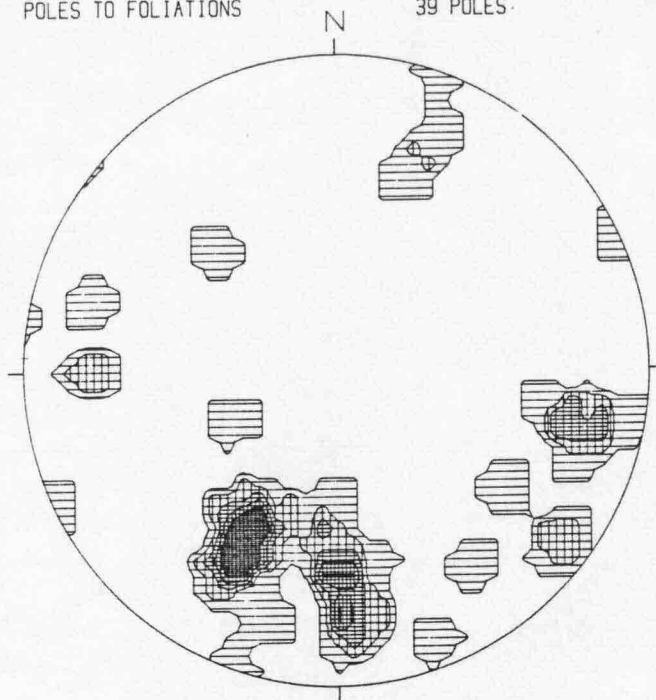
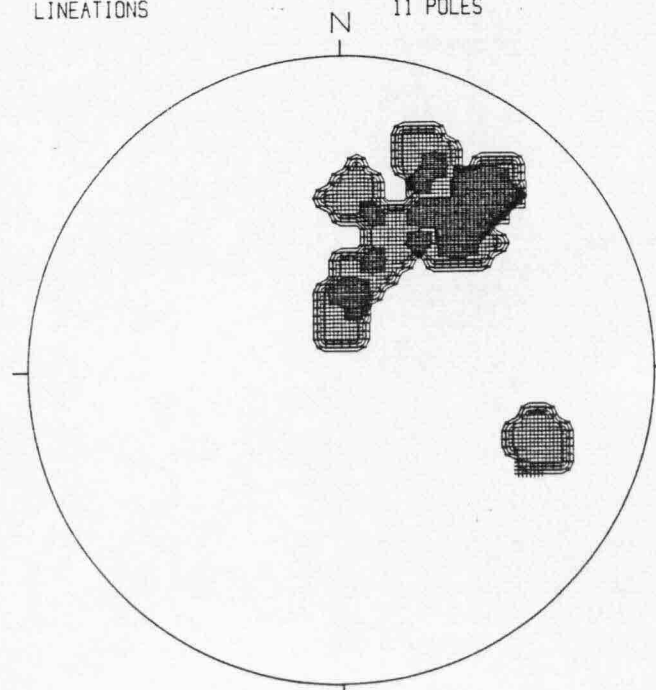


Fig. 11.8

MOUNT ZEIL GRANULITES
POLES TO FOLIATIONS 39 POLES.

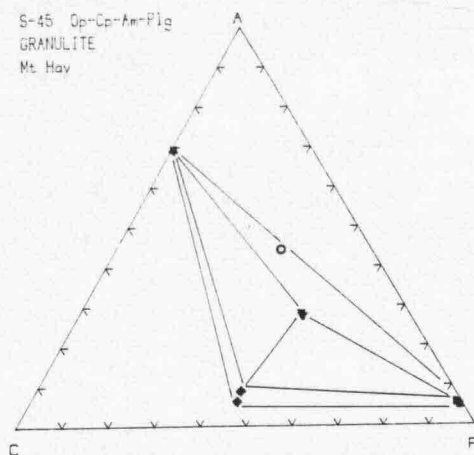


MOUNT ZEIL GRANULITES
LINEATIONS 11 POLES



2-4% 4-6% 6-8% 8-10% >10%

S-45 Op-Cp-Am-Plg
GRANULITE
Mt Hay



S-36 Bi-Op-Cp-Plg
BASIC GRANULITE
Mt HAY

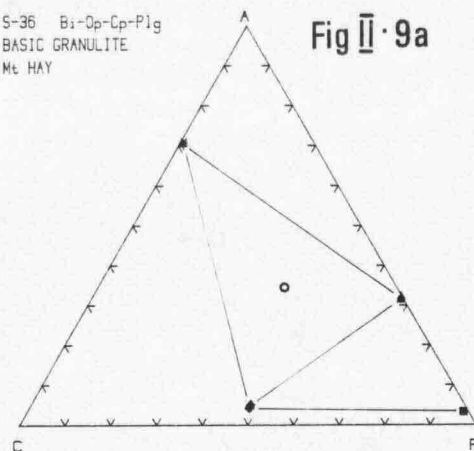
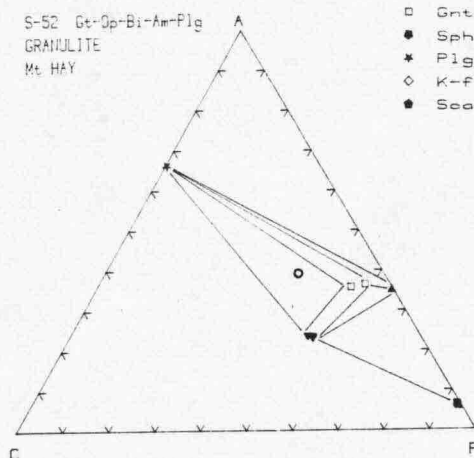


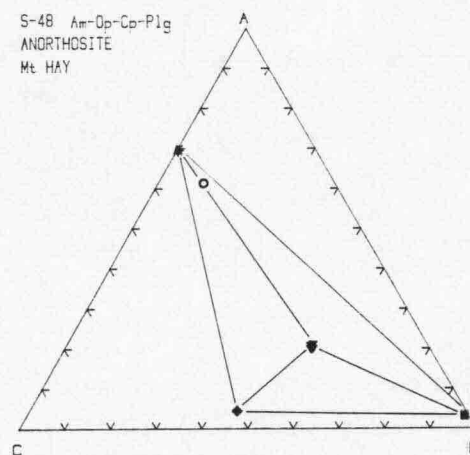
Fig II · 9a

S-52 Gt-Op-Bi-Am-Plg
GRANULITE
Mt HAY

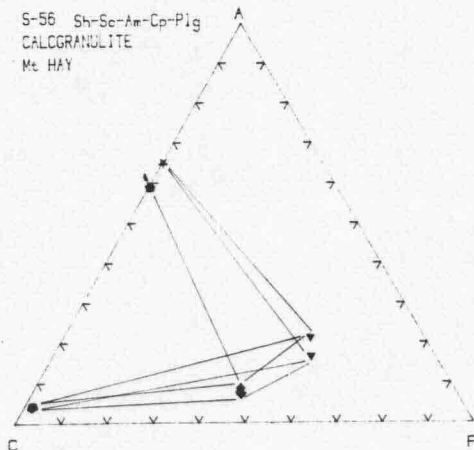


- Opx
- ◆ Cpx
- ▼ Amph
- ▲ Biot
- Gnt
- Sphene
- * Plg
- ◇ K-feldspar
- Scapolite

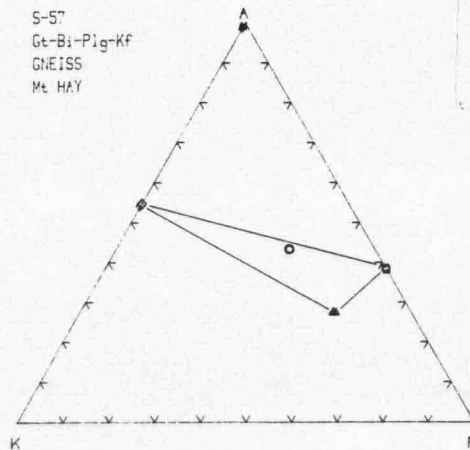
S-48 Am-Op-Cp-Plg
ANORTHOSITE
Mt HAY



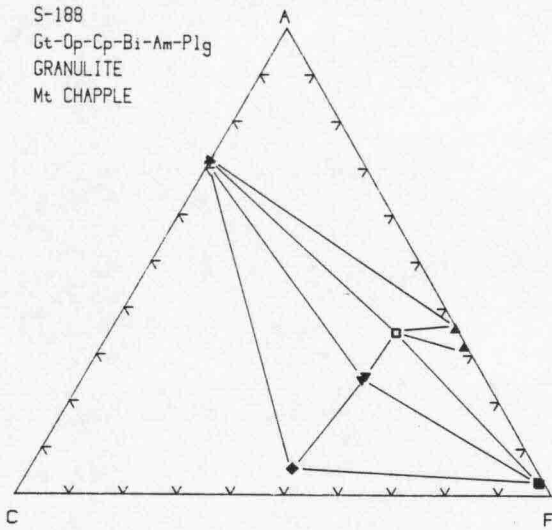
S-56 Sh-Sc-Am-Cp-Plg
CALCGRANULITE
Mt HAY



S-57
Gt-Bi-Plg-Kf
GNEISS
Mt HAY

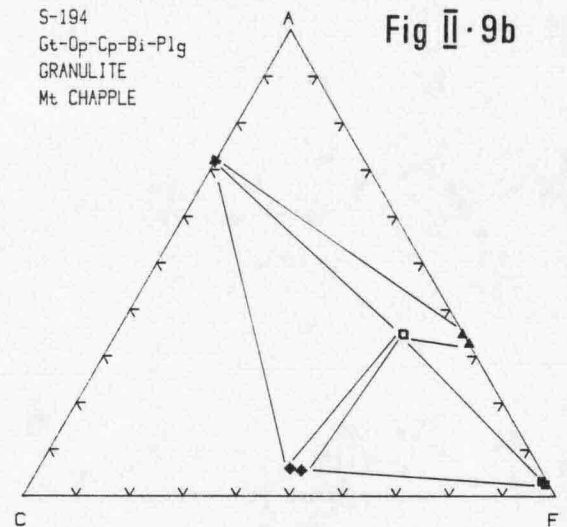


S-188
Gt-Op-Cp-Bi-Am-Plg
GRANULITE
Mt CHAPPLE

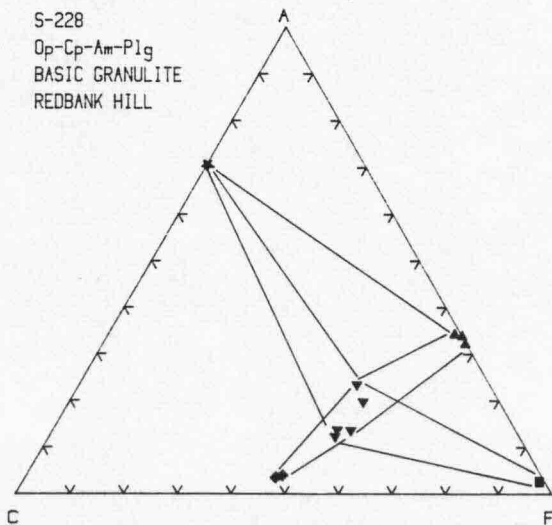


S-194
Gt-Op-Cp-Bi-Plg
GRANULITE
Mt CHAPPLE

Fig II-9b



S-228
Op-Cp-Am-Plg
BASIC GRANULITE
REDBANK HILL



S-241B
Gt-Bi-Hb-Op-Plg
PORPHYROBLASTIC
GNEISS
REDBANK HILL

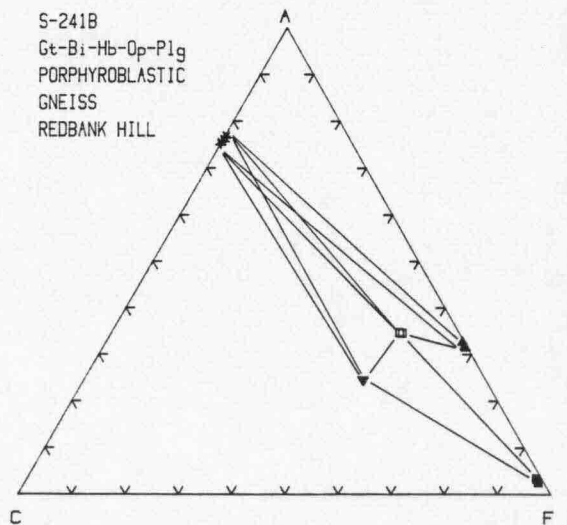


Fig II·10

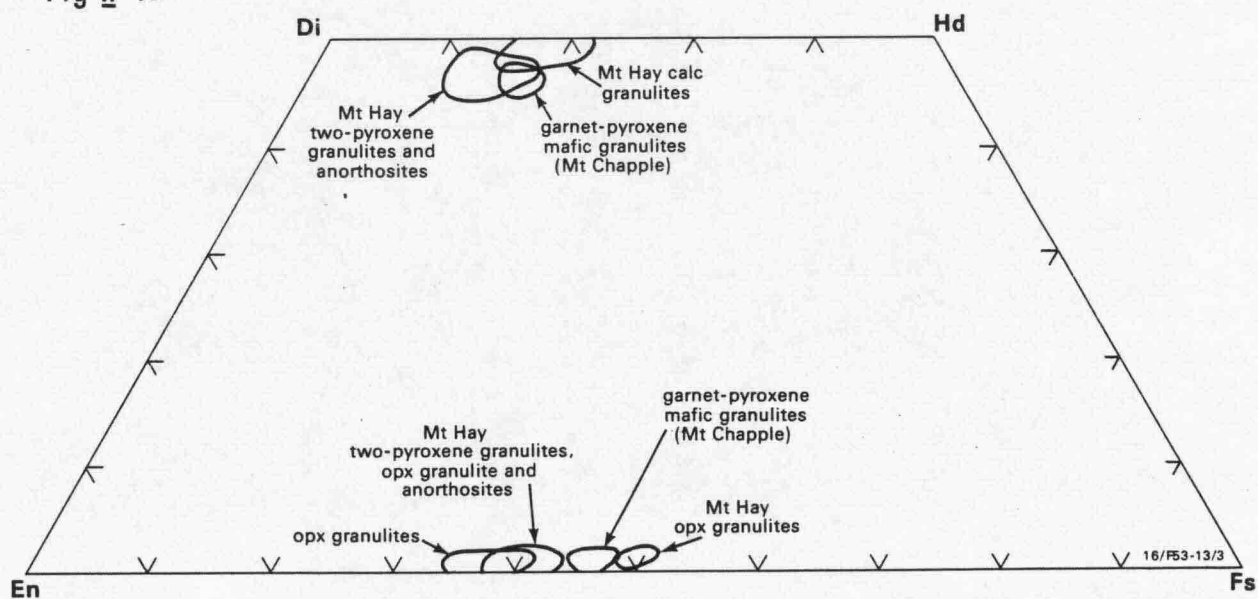


Fig II. 11

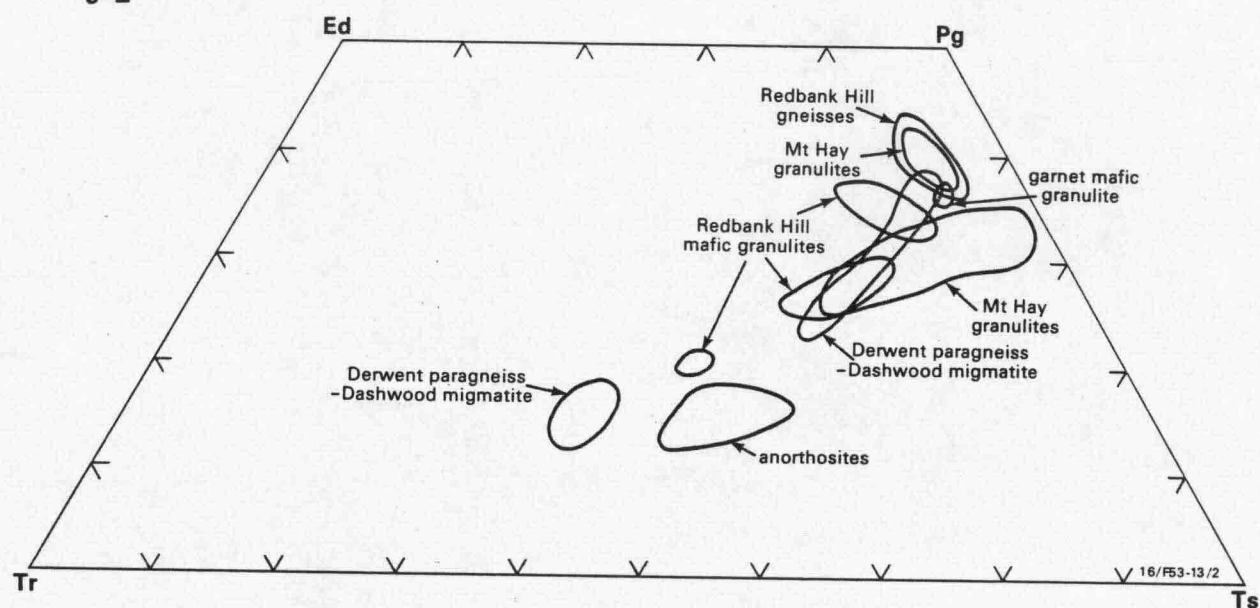


Fig II-12

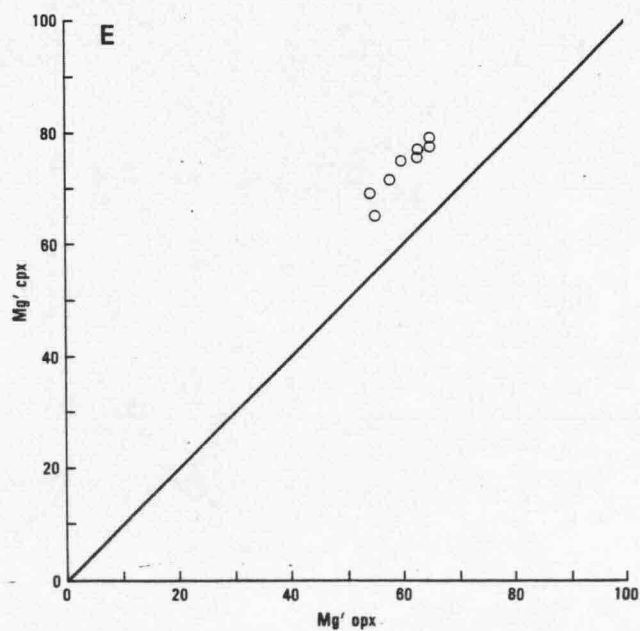
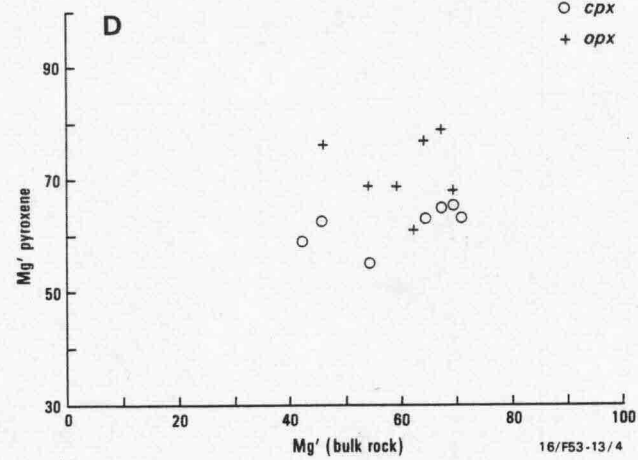
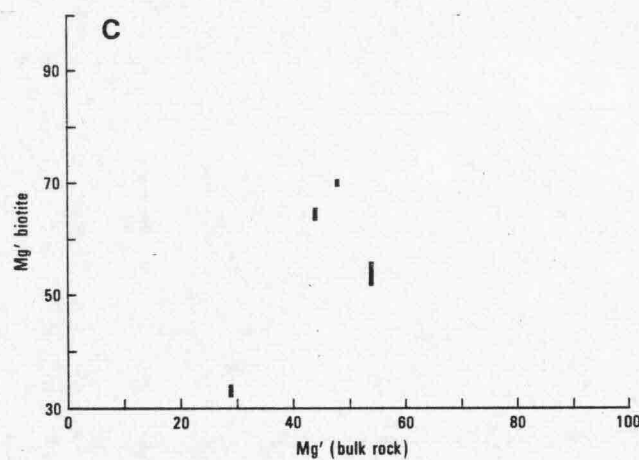
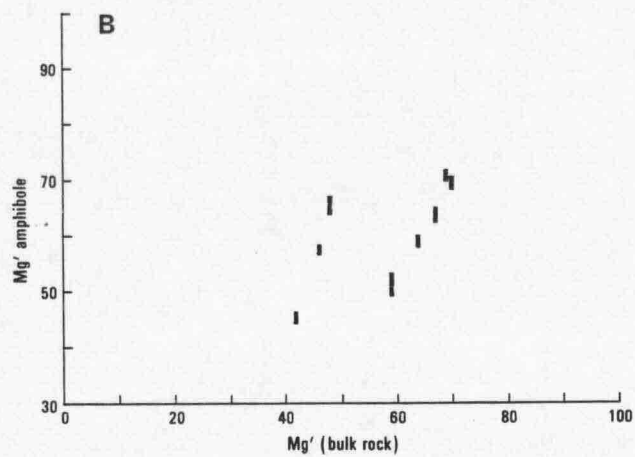
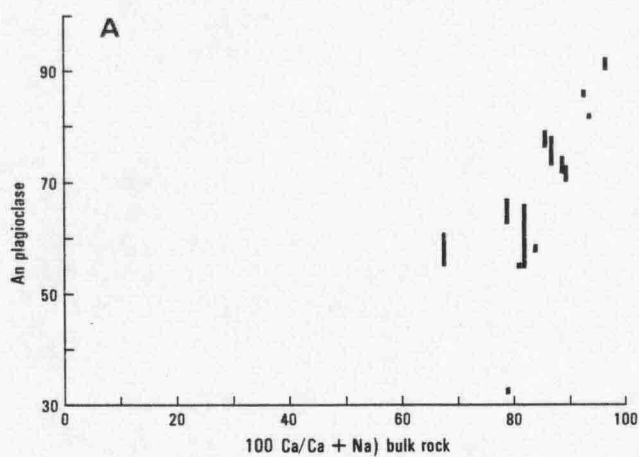


Table II.5 - Compositional indices of pyroxenes

		clinopyroxenes						orthopyroxenes						Coexisting plagioclase
Sample No.	Rock type	Classification	Mg ¹	Wo : En : Fs	Ac : Jd :		Al ₂ O ₃ ^{2,3}	Classification	Mg ¹	Wo : En : Fs	Ac : Jd :		Al ₂ O ₃ ^{2,3}	An
					Ts : Wo : En : Fs :	Ts : Wo : En : Fs :								
Mt Bay	836	BiOpCpPL basic granulite	salite	68.9	46 : 36 : 17	0.8 : 0.3 2.6 : 44.5 36.8 : 15.1	2.01	hypersthene	54.7	1 : 53 : 45	0 : 0 : 1.2 : 0.4 53.7 : 44.7	1.61	58-61	
	842	BiOpCpPL basic granulite	salite	77.7	47 : 40 : 12	0.9 : 0.9 : 2.9 : 44.7 : 41.0 : 9.6	2.15	Mg-hypersthene	65.8	1 : 64 : 34	0 : 0 : 1.8 : 0 65.7 : 32.5	1.43	72-77	
	845	AmOpCpPL granulite (intermediate)	salite	76.3	47 : 39 : 12	0.4 : 1.3 : 3.0 : 45 : 39.8 : 10.6	2.92	hypersthene	62.6	0 : 61 : 37	0 : 0 : 0.7 : 0 62.9 : 36.3	2.35	63-67	
	837	OpAmPL granulite						hypersthene	50.4	1 : 49 : 49	0 : 0 : 1.3 : 0 50.4 : 48.3	1.94	54-55	
	852	GtOpAmBi felsic granulite						hypersthene	63.1	0 : 62 : 36	0 : 0 : 0.7 : 0 63.6 : 35.7	3.04	85-86	
	828	OpAmPL anorthosite						hypersthene	62.8	0 : 61 : 37	0 : 0 : 0.8 : 0 62.3 : 36.9	1.25	73-78	
	848	AmOpCpPL anorthosite	salite	78.2	47 : 40 : 11	0.9 : 0.2 : 2.8 : 45.5 : 40.9 : 9.6	2.10	Mg-hypersthene	65.3	0 : 64 : 34	0 : 0 : 0.7 : 0 65.3 : 34.1	1.57	56-63	
	853	OpSpPL calcgranulite	salite	61.2	49 : 31 : 19	0.7 : 0.1 : 2.4 : 46.9 : 31.0 : 19.0	1.18							90-93
	855	ScAmOpPL calcgranulite	salite	68.9	48 : 34 : 16	1.3 : 1.3 : 3.5 : 45.5 : 35.1 : 13.3	2.87							82
	856	ScSpAmOp calcgranulite	salite	60.5	48 : 30 : 20	1.3 : 1.3 : 4.8 : 44.8 : 30.9 : 17.0	3.46							91-92
Mt Chappelle	8188	GtOpCpBiAmPL granulite	salite	65.2	46 : 35 : 18	0.8 : 0.8 : 4.4 : 42.8 35.9 : 15.3	2.77	hypersthene	54.8	1 : 53 : 45	0 : 0 : 1.1 : 0 : 56.3 : 42.6	1.44	57-59	
	8194	GtOpCpBiPL granulite	salite	69.3	46 : 36 : 16	0.7 : 0.7 4.0 : 43.6 : 37.2 : 13.8	2.90	hypersthene	53.9	0 : 53 : 46	0 : 0 : 0.7 : 0 55.6 : 43.7	1.27	57-58	
	8187							hypersthene	52.8	1 : 51 : 46	0 : 0 : 1.2 : 0 : 54.1 : 44.7	1.49	57	
Redbank Hill	8241B	GtBiAmOpPL gneiss						hypersthene	51.9	1 : 51 : 47	0 : 0 : 1.1 : 0 : 51.9 : 47	1.27	40-44	
	8239	BiAmOpPL granulite						hypersthene	64.9	0 : 63 : 35	0 : 0 : 0.8 : 0 : 65.2 : 34	1.77	67-76	
	8228	BiAmOpCp basic granulite	salite	55.1	46 : 39 : 13	0.7 : 0.1 2.5 : 44.3 40.2 : 12.1	1.88	hypersthene	60.1	1 : 59 : 39	0 : 0 : 1.0 : 0.1 : 59.6 : 39.3	1.18	61	

Table II.6 - Compositional indices of amphiboles

Sample No.	Rock type	amphibole classification (Leake, 1978)	100Mg/(Mg + Fe)	Ca : Mg : Fe	(Na + K) _A	TiO ₂ %	K ₂ O%	Al ₂ O ₃ %	Coexisting Plagioclase
Mt Hay	S28 OpAmPL anorthosite	Mg - hornblende	70.6	31 : 40 : 29	0.19	0.19	0.40	8.72	73-78
	S48 AmOpCpPL anorthosite	titanian Mg - hornblende	71.0	32 : 39 : 29	0.27	1.31	0.45	9.35	56-63
	S55 ScAmCpPL calcgranulite	ferroan pargasite	51.1	32 : 25 : 43	0.63	1.63	1.12	14.08	82
	S56 AcSpAmCpPL calcgranulite	actinolitic hornblende	63.1	32 : 33 : 34	0.16	0.29	0.25	7.47	91-92
	S37 OpAmPL granulite	potassian ferroan pargasite	48.7	31 : 24 : 45	0.81	1.88	2.34	12.34	54-55
	S45 AmOpCpPL basic granulite	titanian ferroan pargasite	61.6	32 : 32 : 36	0.78	2.61	1.94	14.45	63-67
	S52 GtOpAmBiPL granulite	Mg hornblende	67.2	32 : 36 : 32	0.41	0.79	0.92	10.80	85-86
Mt. Chapple	S188 GtOpCpBiAmPL granulite	potassian Magnesian hastingsite	47.3	30 : 24 : 47	0.75	1.51	2.38	13.48	57-59
	S227 GtBiAmPLQz gneiss	potassian ferroan pargasite	29.7	29 : 19 : 52	0.73	2.04	1.87	12.50	43
	S241B GtBiAmOpPLQz gneiss	potassian ferroan pargasite	47.4	30 : 23 : 46	0.80	2.13	2.22	12.53	40-44
Redbank Hill	S239 BiAmOpPL granulite	potassian pargasitic hornblende	72.5	34 : 39 : 27	0.59	1.47	1.07	10.72	67-76
	S239 BiAmOpPL granulite	potassian edenitic hornblende	77.2	34 : 43 : 23	0.52	1.75	1.06	10.89	67-76
	S228 BiAmOpCpPL basic granulite	pargasitic hornblende	66.0	32 : 35 : 32	0.52	1.73	1.16	11.22	61
	S228 BiAmOpCpPL basic granulite	potassium silicic edenite (Siper 23(0,04) = 7.53)	73.6	39 : 37 : 24	0.86	1.66	3.18	5.83	61
	S790 BiAm enclave in mimatite	subsilicic Mg - hornblende	70.5	32 : 39 : 29	0.26	-	0.57	7.83	
Dahwood Kigmatite	S830A GtBiAmPL gneiss	potassian arfredsonite	32.5	31 : 15 : 55	0.75	1.21	1.90	10.42	36 ; rim 33
	S827B AmPL amphibolite	Mg hastingsitic hornblende	58.8	31 : 31 : 39	0.54	0.82	0.97	11.56	45
	S834A BiAmPL amphibolite	potassian Mg - hasengsitic hornblende	47.7	30 : 24 : 46	0.58	1.30	1.27	11.00	32-33
	S834B felsic band in amphibolite	potassian actinolite	79.7	32 : 47 : 21	0.03	0.15	0.18	2.29	33-36

Table II.7 - Compositional indices of biotites

Samples	Rock Type	Mg ¹	X _{Ti}
Mt Hay	S36 BiOpCpPL basic granulite	55.9	0.11
	S42 BiOpCpPL basic granulite	64.7	0.12
	S52 GtOpAmBiPL felsic granulite	70.7	0.07
	S57 GtBiKfPLQz gneiss	33.3	0.095
	S30 GtBiPLQz mylonite	65.7	0.074
Mt Chapple	S188 GtOpCpBiAmPL granulite	53.9	0.098
	S194 GtOpCpBiPL granulite	55.7	0.098
Redbank Hill	S227 GtBiAmPLQz gneiss	44.3	0.099
	S241B GtBiAmOpPLQz gneiss	55.8	0.113
	S239 BiAmOpPL granulite	70.5	0.099
	S228 BiAmOpCp basic granulite	65.9	0.106
Mt Zeil	S376 GtSlBiKfPL gneiss	55.3	0.068
Teapot Granite	S537 BiKfPL granite	27.7	0.046
	S538 BiKfPLEpSp granite	32.8	0.053
Dashwood Migmatite	S789 BiMuEpPL gneiss	36.4	0.049
	S790 BiAm	68.7	0.016
Derwent Paragneiss	S830A GtBiAmPL gneiss	44.4	0.065
	S834A BiAmPL amphibolite	54.0	0.039
	S834B felsic band in amphibolite	51.3	0.057

Table II. 8- Compositional indices of garnets

	Sample No.	Rock name	Ca : Mg : Fe	X _{Mg}	X _{Fe}	X _{Ca}	X _M	Coexisting Plagioclase An
Mt Hay	S52	GtOpAmBiPL granulite	9 : 32 : 59	0.311	0.580	0.091	0.017	86
	S57	GtBiKfPLQz gneiss	22 : 7 : 71	0.069	0.686	0.215	0.030	33
	S30	GtBiPLQz mylonite	5 : 29 : 66	0.291	0.647	0.049	0.013	77-80
Mt Chapple	S187	GtOpPL gneiss	19 : 19 : 62	0.188	0.604	0.189	0.019	58
	S188	GtOpCpBiAmPL granulite	20 : 20 : 59	0.199	0.579	0.199	0.023	59
	S194	GtOpCpBiPL granulite	20 : 19 : 61	0.183	0.591	0.188	0.038	57
Redbank Hill	S227	GtBiAmPL gneiss	22 : 12 : 65	0.120	0.636	0.218	0.027	43
	S241B	GtBiAmOpPL gneiss	19 : 17 : 65	0.164	0.636	0.183	0.017	40
garnet-sillimanite gneisses	S51	GtSlPLKfQz gneiss	2 : 9 : 88	0.089	0.839	0.024	0.048	10
	S135	GtSlPLKfQz gneiss	2 : 9 : 89	0.085	0.845	0.022	0.047	11
	S205	GtSlKfQz gneiss	3 : 37 : 60	0.365	0.601	0.030	0.004	
	S376	GtSlBiKf gneiss	4 : 19 : 78	0.187	0.768	0.035	0.010	48
	S232	GtSlBiKf gneiss	3 : 39 : 59	0.384	0.584	0.027	0.005	
Dashwood-Derwent Section	S830A	GtBiAmPL gneiss	70 : 1 : 30	-	0.296	0.696	0.003	35; rim 33.5

III. GEOCHEMISTRY OF Mt HAY GRANULITES/GNEISSES

A reconnaissance geochemical study of Mt Hay granulites and gneisses was conducted on a suite consisting of 3 basic granulites, 3 anorthosites, 2 calc granulites, one felsic granulite, 2 garnet-bearing gneisses and one mylonite. The rocks were analysed at the BMR laboratories for major elements Ba, Rb, Sr, Pb, Th, U, Zr, Nb, Y, La, Ce, Nd, Sc, V, Cr, Ni, Cu, Zn, and Ga using XRF and atomic absorption spectroscopy (Table III. 1). The aim of this work is to investigate the nature of protoliths of the metamorphic rocks, discern the effects of metamorphism on their primary compositions, and assess the possibility of further geochemical studies of the granulites, currently in progress.

[1] Basic Granulites

Two samples of basic granulite (S43, S83) are characterised by high CaO (ca 12.5%), somewhat low FeO (total Fe as FeO) (ca 8.5%), low TiO₂ (ca 0.4%) and low K₂O (less than 0.1%). Trace element characteristics of the two samples are in accord with their major element features, i.e. alkali elements (K, Rb), incompatible elements (P, Zr, Nb, Y, Ce, La), and siderophile elements (Ti, V, Cr, Cu, Zn) compare with or are more depleted than midocean ridge basalts (MORB) (Figs. III.1a; III.2a). Sr abundances in these samples can be high, in accord with the high CaO. The chemistry of the two depleted basic granulites suggests transitional characteristics between residual high-Mg compositions and anorthositic compositions. On the other hand, the third basic granulite sample S36 has high Pb, Rb, Ba, Nb, K, La, Ce and Y as compared to MORB (Fig. III.1a).

In view of the total absence of primary igneous structures or textures in the granulites, it is necessary to examine the possibility of a sedimentary derivation. Given parental

shale-dolomite mixtures it is possible to derive metamorphic assemblages whose composition would in certain respects resemble those of basic igneous rocks (e.g. Walker et al., 1960).

Table III.2 presents average shale and CO₂-free average dolomite compositions (Knutson et al., 1983), shale:dolomite mixtures of 5:1 and 4:1 ratios, and the average of 3 basic granulites and 2 calc-granulites from Mt Hay. The 5:1 mixture ratio yields SiO₂ level commensurate with the granulites; however, Al₂O₃, FeO total, and MgO in the sedimentary mixture are lower, while the K₂O value is significantly higher, than in the granulites. The alumina discrepancy can be accounted for if more aluminous pelitic end members with ca 20% Al₂O₃ are invoked. The K₂O excess may be accounted for if the alkali elements were largely lost upon high grade metamorphism. However, the discrepancies in MgO and FeO are more difficult to reconcile with sedimentary compositions, unless metamorphism of ferromagnesian (basic rock-derived) greywackes is suggested. However thick uniform sequences of basic greywackes have not been observed in less metamorphosed parts of the Arunta Block. Also, the very low Zr, Nb, Y and REE abundances in the granulites militate against derivation from pelitic sediments, which are generally rich in these components. It is noted that the relatively immobile LIL elements were unlikely to have been significantly depleted upon metamorphism. Little or no primary compositional layering such as would be expected in paragneiss and metasedimentary granulite successions was observed. The minor occurrences of calc-granulites (see below) may represent calcareous concretions/segrations within basic igneous bodies. The minor occurrences of sillimanite-garnet gneisses may be interpreted in terms of metamorphic segregation banding, producing aluminous and quartzofeldspathic bands, as suggested above.

The depletion of some basic granulites in the incompatible elements by factors of up to 10 can be only partly accounted for by metamorphic dehydration and/or anatexis processes as has

been invoked in connection with granulite facies terrains (Lambert and Heier, 1968; Sighinolfi, 1969; Sheraton, 1970; Tarney and Windley, 1977). Thus, whereas alkali elements, U and Th are thought to be readily redistributed, the REE, Y, Zr and Nb are considered to be relatively immobile upon alteration (e.g. Smith and Smith, 1976; Floyd and Winchester, 1978; Glikson, 1979). Comparisons with basic granulites from other granulite terrains suggest that some of the Mt Hay granulites are significantly depleted in LIL elements. This observation, as well as the intercalated anorthosites, suggest one of two possibilities: (1) The basic granulite-anorthosite unit includes metamorphosed cumulates of a layered intrusion. (2) The basic granulite-anorthosite units include residues of a partially molten deep-seated infracrustal mafic layer. Both models account for the intense depletion in LIL elements. Model (1) is supported by the occurrence of anorthositic units but is not favoured by the absence of pyroxenitic to peridotitic compositions and the absence of igneous layering within the basic granulites, although such layering could have been partly obliterated by deformation and recrystallisation. It is evident that these models are not mutually exclusive, namely, the Mt Hay Complex may represent a deep-seated differentiated basic intrusion. Model (1) remains a possibility, while model (2) has particular attraction in view of considerations in chapter VI.

[2] Anorthosites

Two types of anorthosites are discerned: type A represented by samples S28 and S48 has very high Al_2O_3 (27-29%), CaO (ca 14%) and Mg' values (Ca 70). Type B, represented by sample S45, has significantly lower Al_2O_3 , CaO and Mg' values ($Mg' = 45.7$), and has high TiO_2 (1.99%) and relatively high V (431 ppm), Cu (32 ppm) and Zn (52 ppm) levels: The latter features are principally attributable to the important role of ilmenite and magnetite in S45, as shown by probe analyses (Table III.1). No positive correlation appears to hold between Sr and

Ca. Ni is higher and Cr is lower in the Ti-Fe rich anorthosite than in the magnesian anorthosites, suggesting contrasted behaviour of these elements. As in the depleted basic granulites, LIL elements are very low in the anorthosites, e.g. in S28: K₂O = 0.11%; P₂O₅ = 0.03%; Ba = 23 ppm; Zr = 3 ppm; Nb = 1 ppm; Y = 1 ppm; La and Ce are below detection limits. Particularly P, Zr, Ti and Y are low, whereas alkalis are normal by comparison with the MORB field (Fig. II.1b). Such low abundances of LIL elements in feldspar dominated rocks support a view of the basic granulite-anorthosite units as depleted cumulates and/or residues of infracrustal melting.

The observation that the anorthosites are not generally intruded by felsic gneiss or granulite bands (section II.1) suggests they either: (1) postdate the basic granulites; (2) occurred originally below the zone of anatexis, or (3) were not subjected to partial melting, unlike the basic granulites. If the third interpretation is correct, the composition of the anorthosites may have been less modified secondarily than those of the basic granulites, and the strongly incompatible element depleted nature of the anorthosites is likely to be of primary igneous significance.

[3] calc-granulites

The occurrence of calc-granulites within the Mt Hay complex is in apparent contradiction to the otherwise igneous nature of this block (sections III.1 and 2). The two analysed calc-granulites include a sphene-clinopyroxene rock (S53) and scapolite (meionite)-amphibole-clinopyroxene rock (S55). Both samples are characterised by Mg values of about 60 (similar to the basic granulites), high CaO (ca 22% and 18%, respectively) and very low Na₂O. These account for the highly calcic composition of their probed plagioclase feldspars (An₉₀ and An₈₂) and their highly calcic scapolite (Ca' = 77-79). The calc granulites are not as strongly depleted in LIL elements as

depleted basic granulites, although they still have significantly lower abundances than basic igneous rocks in general, i.e. Zr = 40, 57 ppm; Y = 27, 22 ppm. Alkali element abundances vary widely between the two samples (i.e. K₂O = 0.02, 0.31) and are markedly lower than would be expected in any sedimentary clay-rich mixture. Levels of less mobile LIL elements (P, Zr, Ti, Y) are similar to MORB while alkalis may be higher (Fig. III.1c). Trace ferromagnesian elements, Ni, Cr, Sc and V show a wide variation between the samples, generally corresponding to the MORB field (Fig. II.2c).

A comparison between the calc-granulites and average sedimentary compositions (Table III.2) indicates that a 4:1 shale:dolomite mixture is consistent with the SiO₂, Al₂O₃, FeO(total), MgO and Na₂O abundances in the calc-granulites, but is lower in CaO by a factor of near 20. Whereas K and related elements may well have been lost on high grade metamorphism, the excess CaO in the rocks may be interpreted in terms of original abundance of carbonate and subsequent synmagmatic loss of CO₂ during granulite facies metamorphism.

[4] felsic granulite/gneiss units

Intermediate to felsic bands, tongues and veins of gneiss and granulite occur throughout the basic granulites, although they are near-absent in the anorthosite units. The analysed samples include Opx-Amph-Plg granulite (S71), Opx-Gnt-Amph-Biot-Plg-Qz gneiss (S52), Gnt-Biot-Kf-Plg-Qz gneiss (S57) and Gnt-Biot-Plg-Qz mylonite (S30). It is important to test whether sequential element variations commensurate with magmatic differentiation pertain to these rocks. Plots of the basic to felsic compositions on Harker diagrams indicate strong negative correlations for CaO-SiO₂ and MgO-SiO₂ (Fig. III.3), suggesting liquid-residue (restite) equilibration and separation in terms of White and Chappell's (1977) model. Derivation of the felsic magma by partial melting of the basic granulites and the

entrainment of refractory residue (restite) is thus likely. The S-I indices ($Al/Na+K+Ca$) (Chappell and White, 1974) are below 1.1, suggesting igneous rather than sedimentary precursors for the intermediate-felsic bands. The gneisses are only slightly corundum normative. The mylonite sample (S30) is an exception, with $SI = 1.29$ and $C = 3.57$.

K/Rb ratios of the gneisses (200-600) correspond to average to intermediate igneous compositions, militating against selective expulsion of Rb relative to K. The Rb/Sr ratio correlates positively, and Ba correlates inconsistently, with K₂O. The LIL element characteristics of the analyses are compared to Turekian and Wedepohl's (1961) average high-Ca and Low-Ca granites on mantle normalised plots (Figs. III.1d). Owing to their intermediate composition some of the gneisses are low in LIL elements (Pb, Rb, Ba, Th, Nb, K, La, Ce) relative to average granites. The less mobile LIL elements (P, Zr, Ti, Y) fall within the low to high-Ca granite range. The basicity of the gneisses is also displayed on siderophile-refractory elements chondrite normalised plots (Fig. III.2d), where Ni, Cr, Zn, Fe, Mg, Mn, Cu, V, Ca and Ti are high relative to average granites. The more fractionated felsic granulite S71 and mylonite S30 have K, Ba, Sr and Zr levels consistent with average granites. Like the gneisses, these rocks still has high ferromagnesian element Cr, Fe, Mg, Mn, Cu, V levels relative to average granites.

The origin of the intermediate to felsic components of the Mt Hay belt can be interpreted in terms of either allochthonous intrusion by granitic melts derived from lower crustal levels or, alternatively, partial melting of the basic granulites themselves. The latter possibility appears to be supported by the following:

- (1) The residual high-Mg and LIL-depleted composition of some of the basic granulites.

(2) The intricate geometrical relations between the felsic bands, tongues and veins and the basic granulites, including "blind" felsic stringers (Fig. II.1).

(3) The markedly dehydrated state of the basic granulites, which include only minor amounts of amphibole and/or biotite, indicate the loss of a hydrous phase, probably upon anatexis.

Notwithstanding these points, the Mt Hay suite is not regarded as an anatectic source zone for the felsic magmas, mainly due to the relative scarcity of ultramafic residues. The source of these magmas must have been located yet further deeper in the crust.

FIGURE CAPTIONS FOR SECTION III

- III.1 - mantle-normalised plots of LIL elements (Pb, Rb, Ba, Th, U, Nb, K, La, Ce, Sr, P, Zr, Ti, Y) for Mt Hay rocks
- (a) basic granulites
 - (b) anorthosites
 - (c) calcgranulites
 - (d) intermediate-felsic gneiss/granulite, compared to field of Mid Ocean Ridge Basalts (MORB) (LIL-depleted to LIL-enriched) and to average high-Ca and low-Ca granite (Turekian and Wedepohl, 1961)
- III.2 - chondrite normalized plots of ferromagnesian and refractory lithophile elements (arranged in order of increasing MORB/Chondrite ratio) for Mt Hay rocks.
- (a) basic granulites
 - (b) anorthosites
 - (c) calcgranulites
 - (d) intermediate-felsic gneiss/granulite, compared to the field of MORB and to high-Ca and low-Ca granites (Turekian and Wedepohl, 1961).
- III.3 - CaO-SiO_2 and MgO-SiO_2 plots of Mt Hay basic granulites, felsic gneiss and mylonite samples.

Fig. III.1a - Mt HAY BELT: BASIC GRANULITES

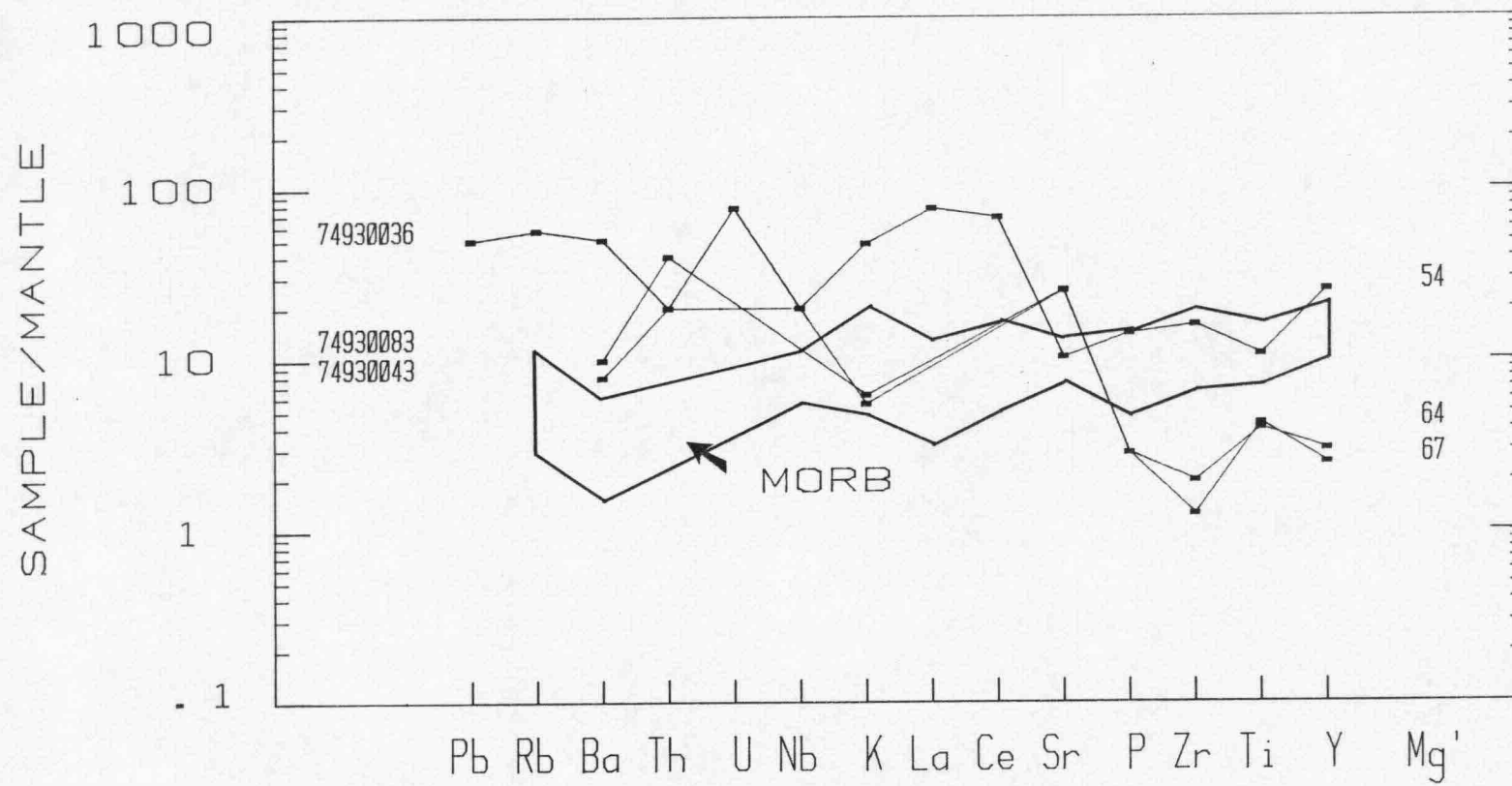


Fig. III.1b - Mt HAY BELT: ANORTHOSITES

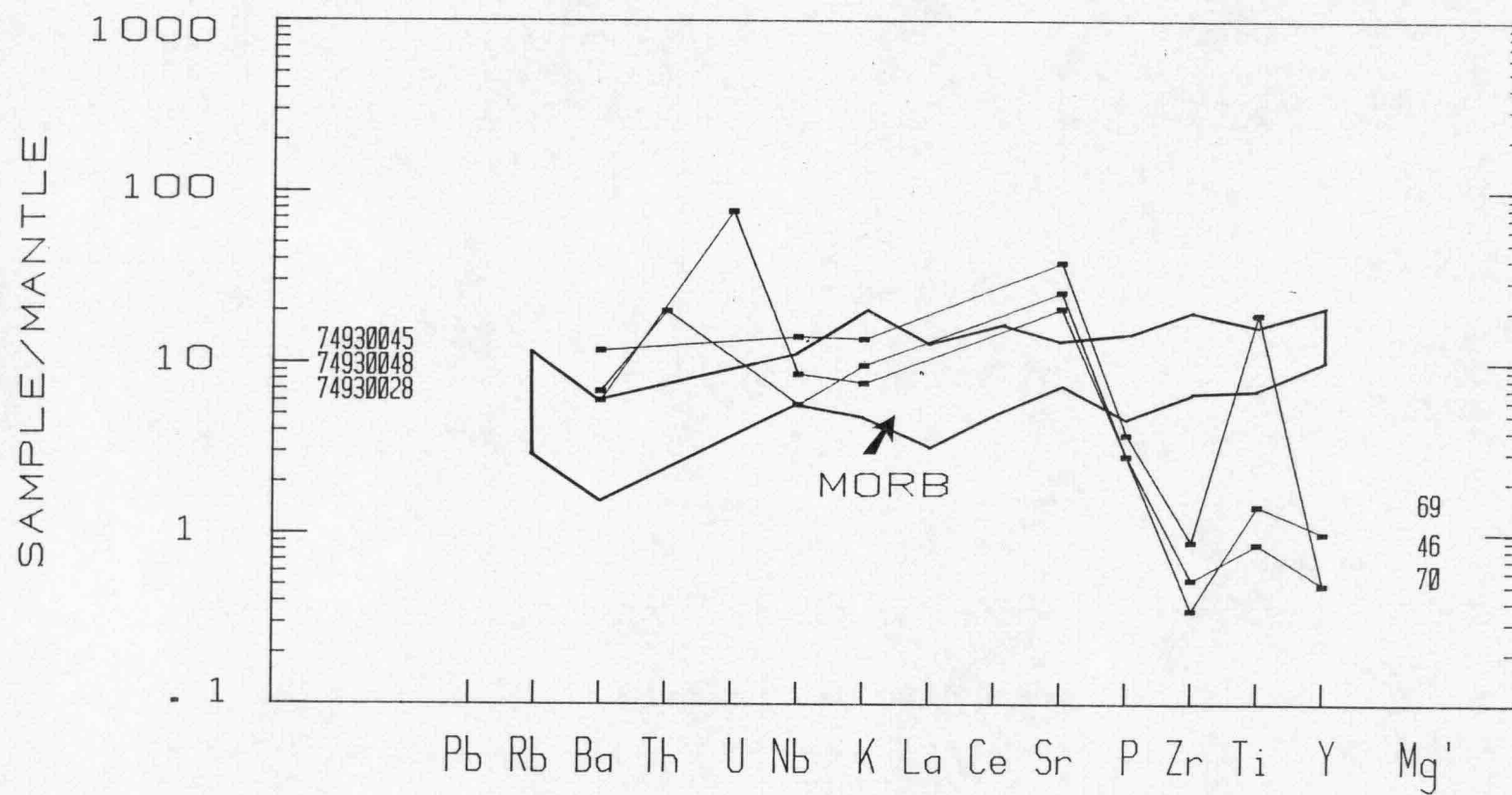


Fig. III.1c - Mt HAY BELT: CALC-GRANULITES

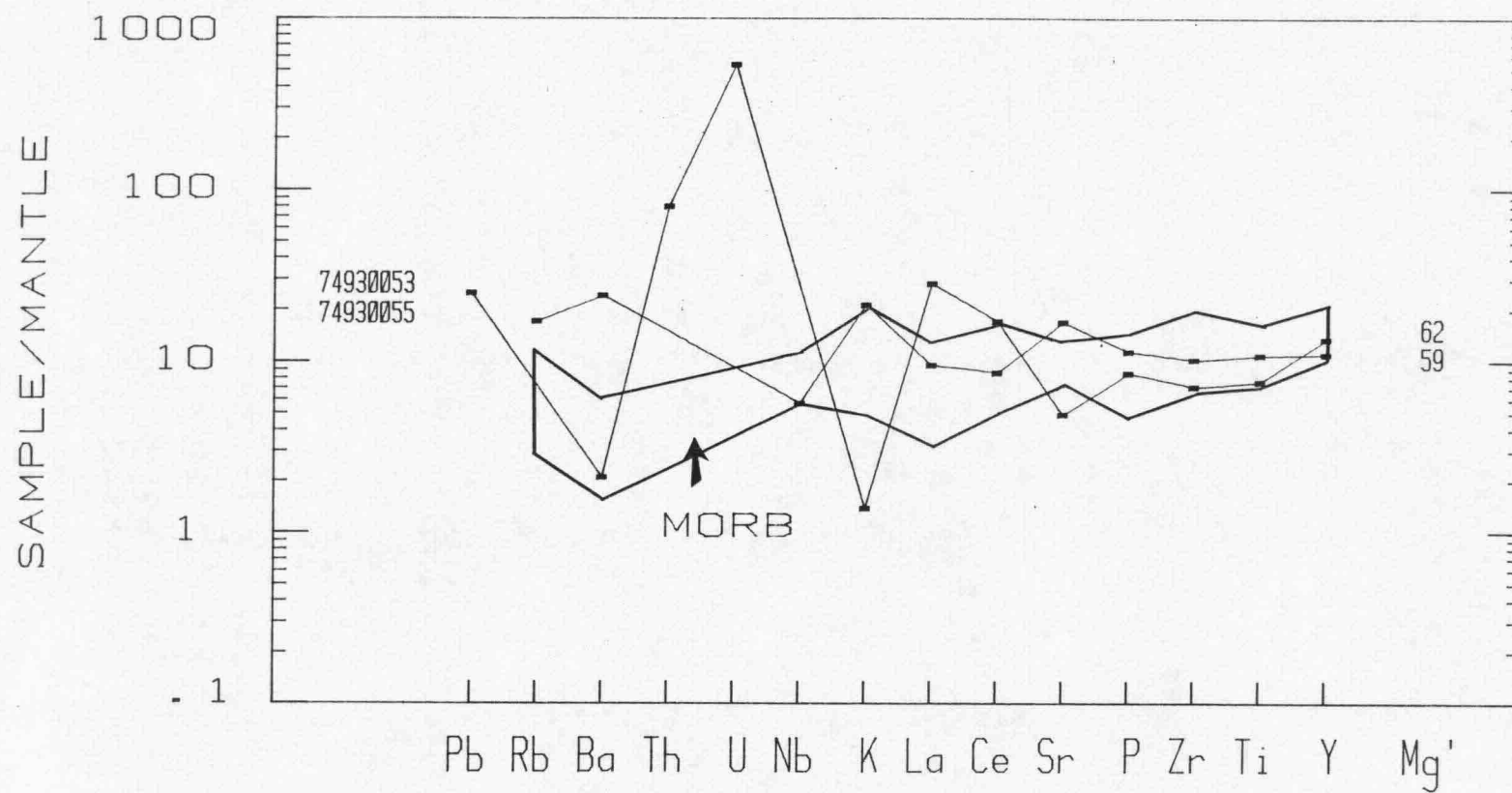


Fig. III.1d - Mt HAY BELT: INTERMEDIATE-FELSIC GNEISS/GRANULITE

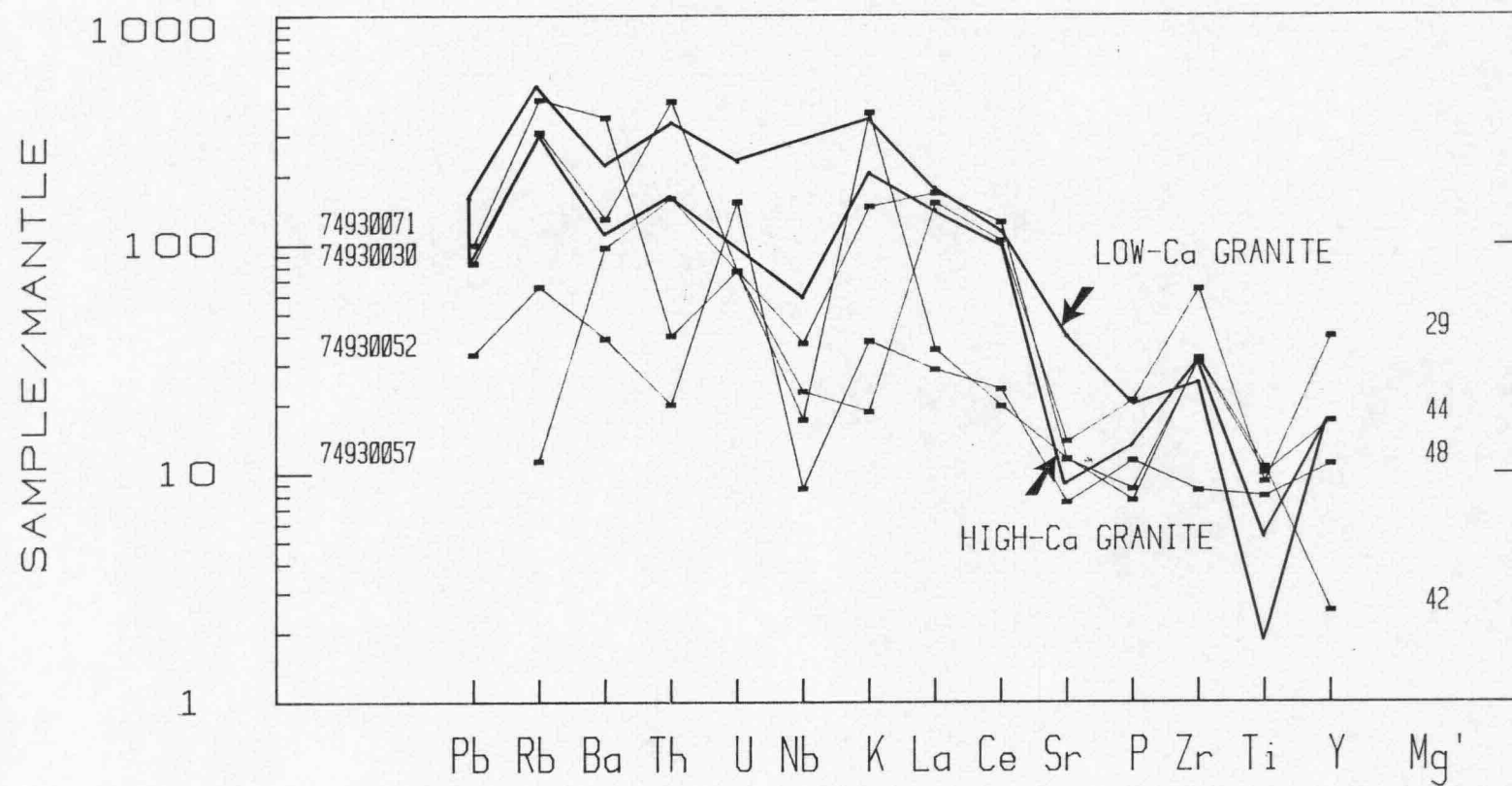


Fig. III.2a - Mt HAY BELT: BASIC GRANULITES

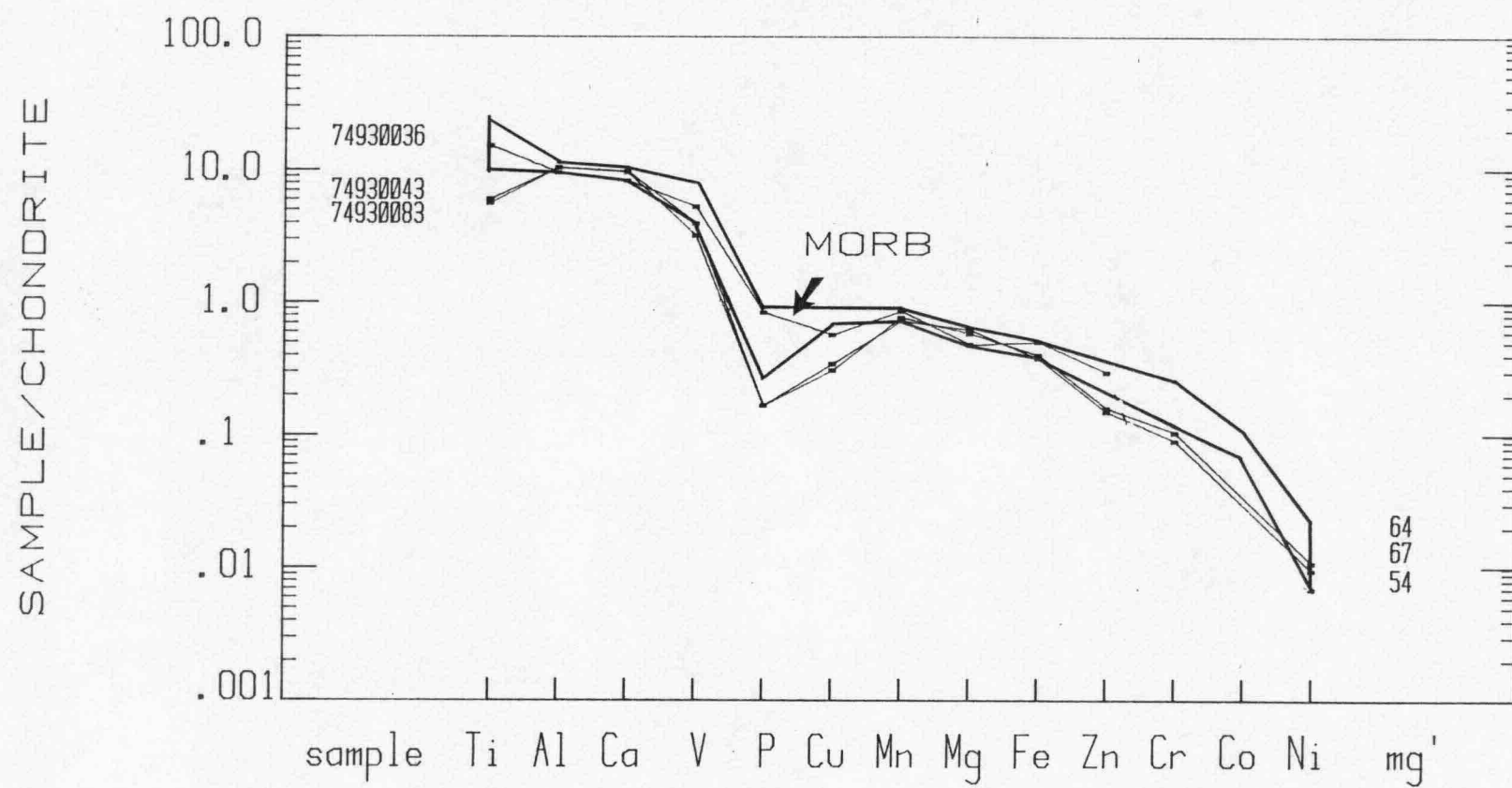


Fig. III.2b - Mt HAY BELT: ANORTHOSITES

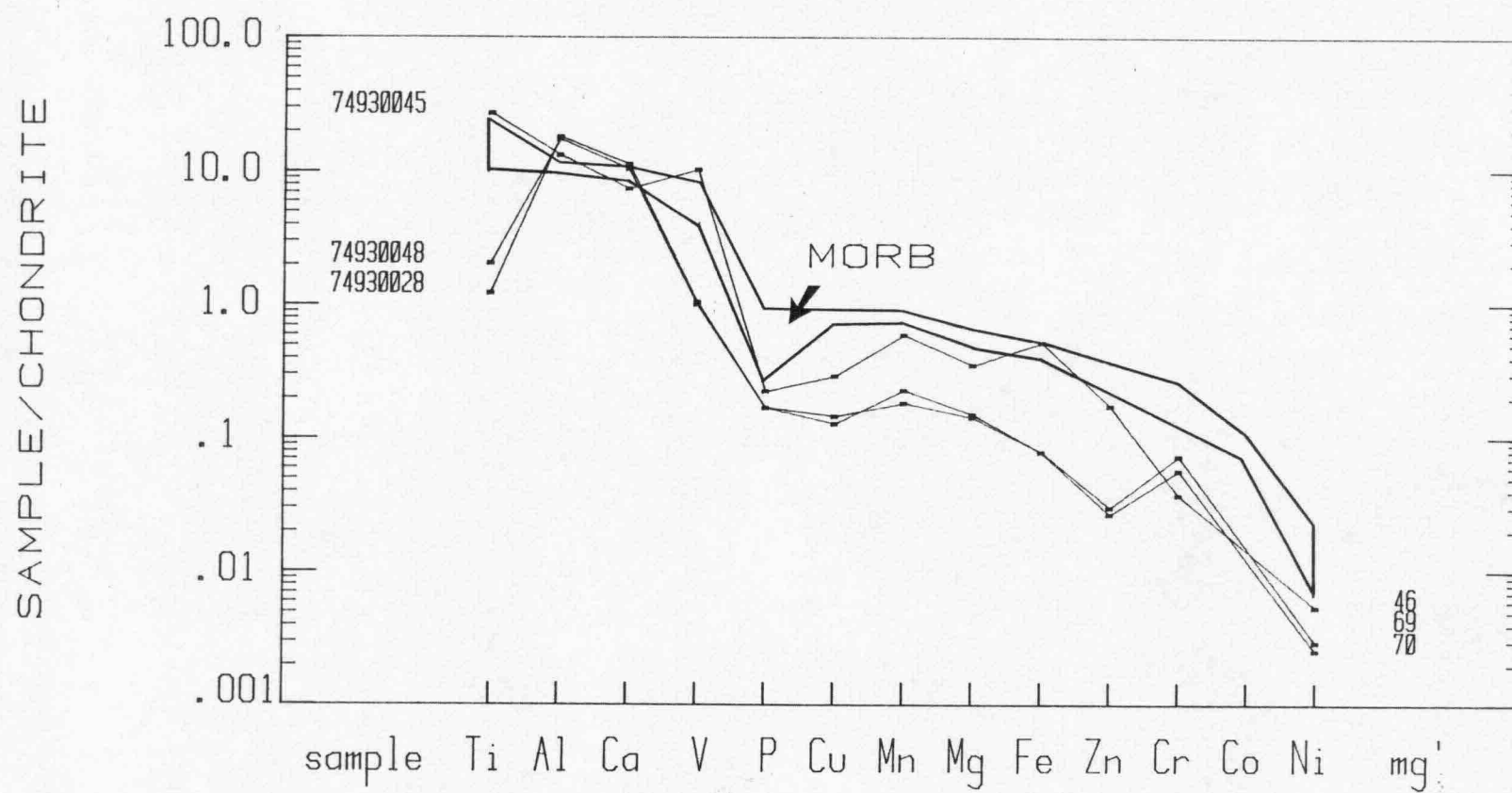


Fig. III.2c - Mt HAY BELT: CALC-GRANULITES

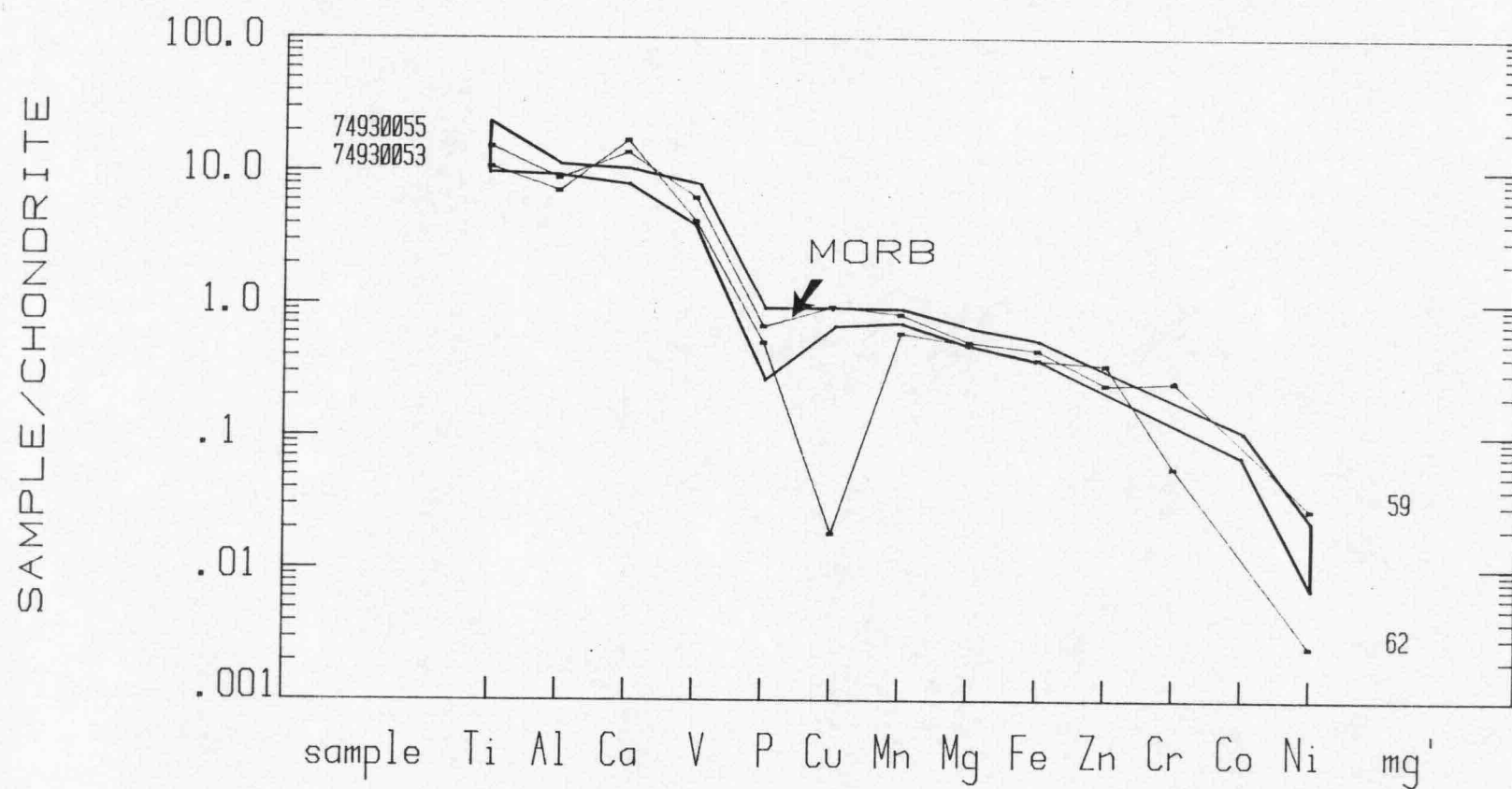


Fig. III.2d - Mt HAY BELT: INTERMDIATE-FELSIC GNEISS/GRANULITE

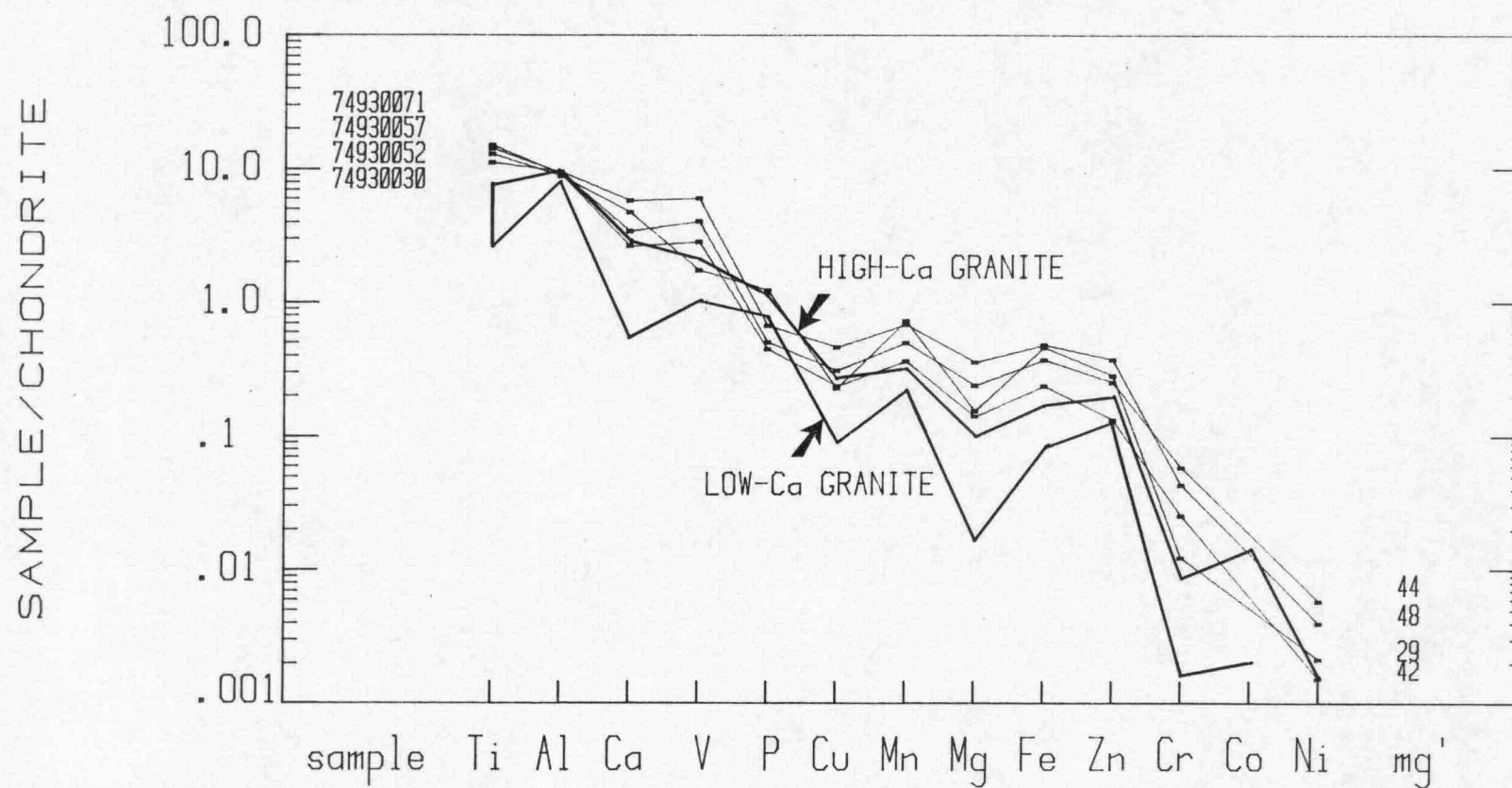


Fig III-3a

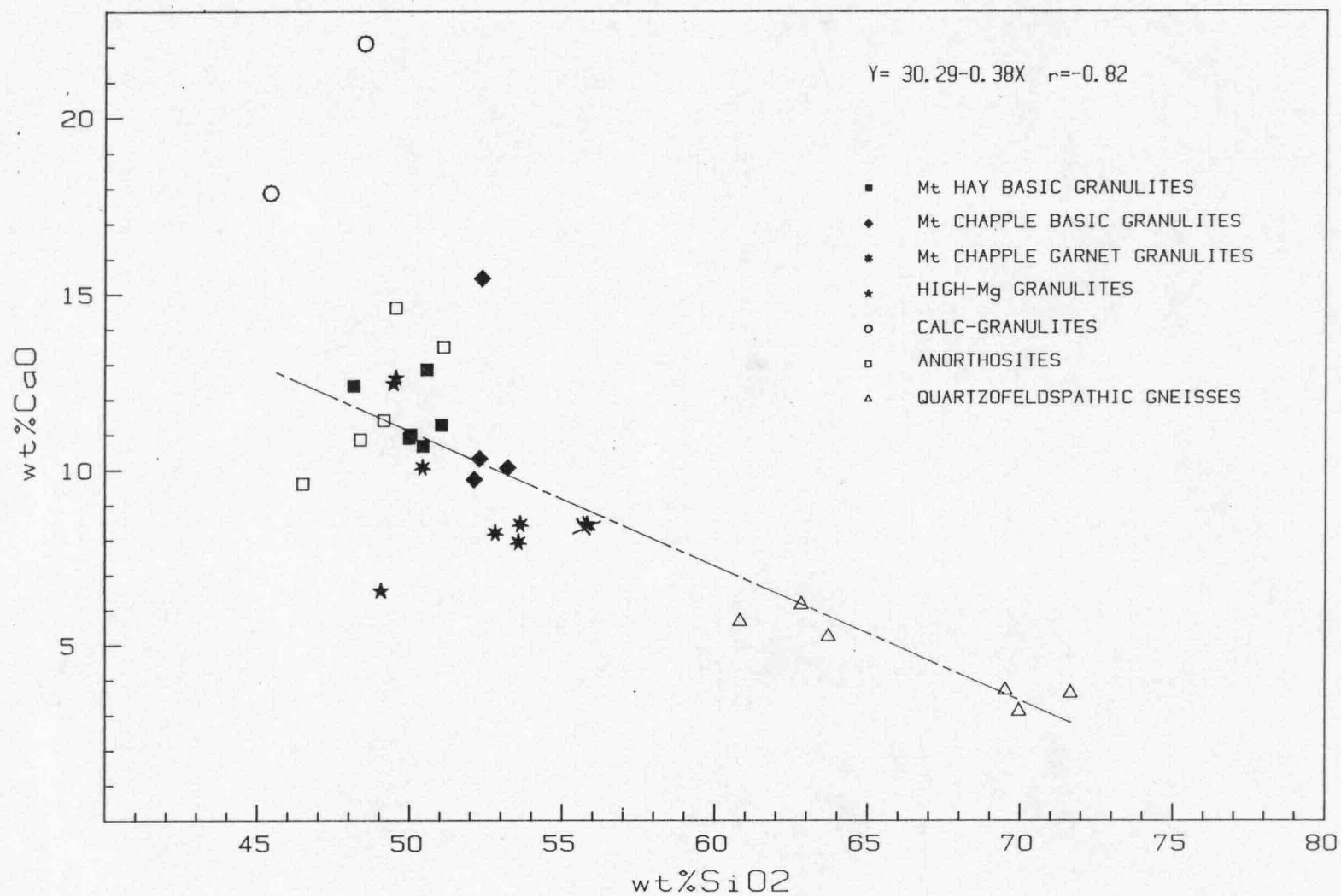


Fig III 3b

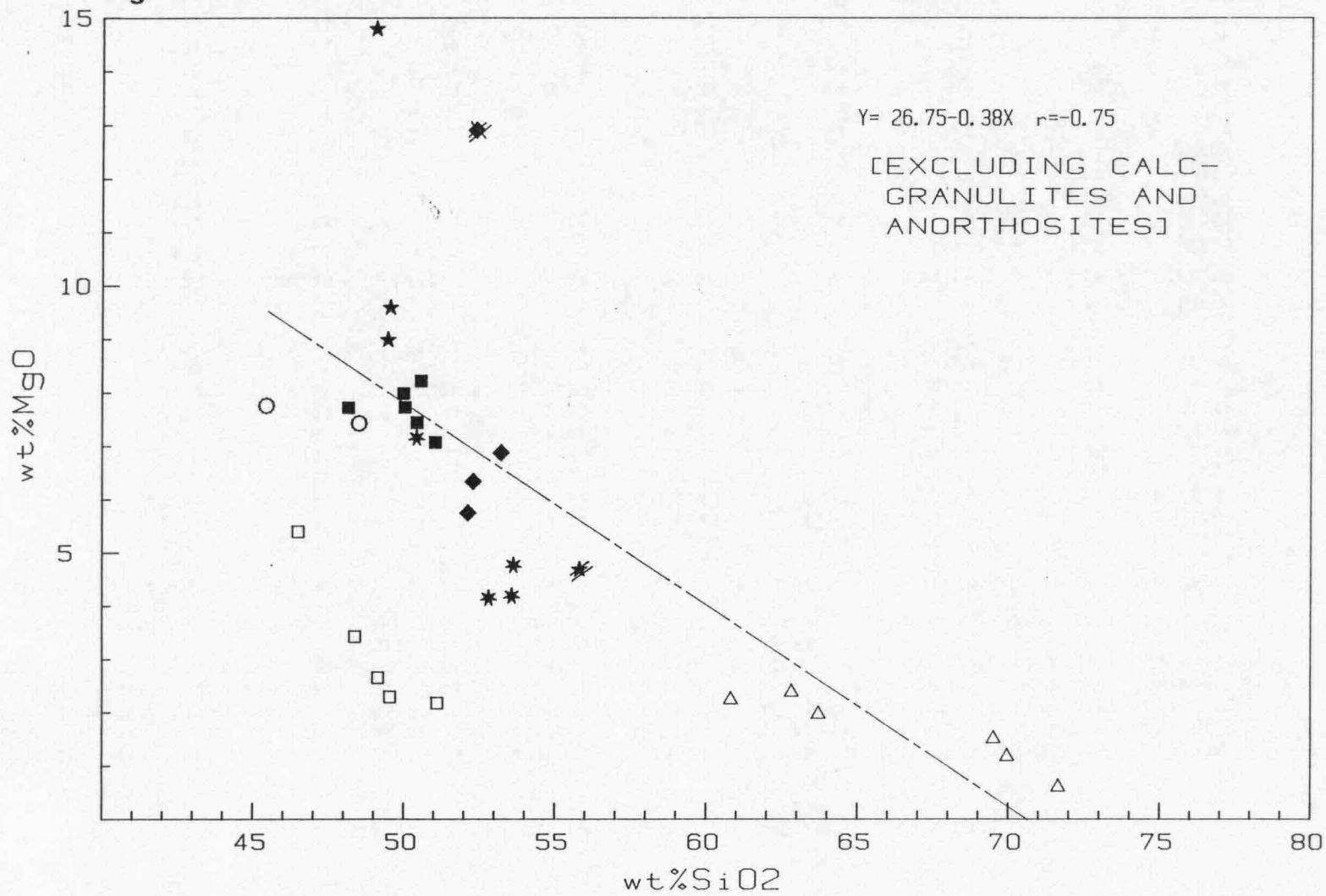


TABLE III-1 - CHEMICAL DATA FOR THE Mt HAY MAFIC GRANULITE-ANORTHOSITE COMPLEX

SAMPLE NUMBER	74930028	74930030	74930036	74930043	74930045	74930048	74930052	74930053	74930055	74930057
FORMATION	Mt HAY	Mt HAY	Mt HAY	Mt HAY	Mt HAY	Mt HAY	Mt HAY	Mt HAY	Mt HAY	Mt HAY
ROCK TYPE	GRANULITES	GRANULITES	GRANULITES	GRANULITES	GRANULITES	GRANULITES	GRANULITES	GRANULITES	GRANULITES	GRANULITES
	OpHbPlg	GntBtPlQz	BiOpCpPlg	HbOpCpPl	HbOpCpPl	HbOpCpPl	GntOpHbBi	SpCpPlg	SchbCpPl	GntBikfPl
	anorth.	qzmylonite	B.Granul	B.Granul	anorth.	anorth.	PlgQz	calc gran	calc gran	Qz gneiss
1:100 000 SHEET	ANBURLA	ANBURLA	ANBURLA	ANBURLA	ANBURLA	ANBURLA	ANBURLA	ANBURLA	ANBURLA	ANBURLA
SiO ₂	49.54	63.59	50.43	49.54	46.49	51.11	57.53	48.50	45.43	62.82
TiO ₂	0.09	1.04	1.11	0.44	1.99	0.15	0.82	0.79	1.12	0.95
Al ₂ O ₃	29.06	14.87	15.23	16.66	21.14	27.80	15.23	11.37	14.16	14.14
Fe ₂ O ₃	0.31	1.27	1.41	1.37	4.52	0.26	4.10	0.65	2.33	4.64
FeO	1.44	7.08	9.88	7.12	7.36	1.49	6.97	7.60	7.58	6.04
MnO	0.05	0.11	0.19	0.16	0.13	0.04	0.15	0.13	0.18	0.16
MgO	2.30	3.68	7.44	9.59	5.40	2.18	5.49	7.43	7.76	2.38
CaO	14.62	4.44	10.68	12.61	9.61	13.50	7.49	22.09	17.88	6.15
Na ₂ O	2.12	0.72	2.02	1.51	2.57	2.88	0.57	0.54	1.16	1.58
K ₂ O	0.11	2.12	0.69	0.08	0.20	0.14	0.55	0.02	0.31	0.27
P ₂ O ₅	0.03	0.09	0.15	0.03	0.04	0.03	0.12	0.09	0.12	0.22
H ₂ O ⁺	0.40	1.22	0.96	1.01	0.79	0.37	0.80	0.75	2.17	0.71
H ₂ O ⁻										
CO ₂										
TOTAL	100.07	100.23	100.19	100.12	100.24	99.95	99.82	99.96	100.20	100.06
Mg NUMBER	70.5	44.4	54.3	67.2	45.7	69.3	47.9	61.8	58.8	29.3
Ba	23	492	191	30	45	26	148	8	92	371
Rb		108	20				23		6	4
Sr	228	126	114	277	424	283	82	54	187	152
Pb		10	6				4	3		
Th		21	1	1		1	1	4		8
U	1	1	1				2	7		1
Zr	3	174	89	7	5	2	47	40	57	360
Nb	3	13	7	7	5	2	3		2	8
Y	1	34	51	5	1	2	22	27	22	80
La		53	24				9	9	3	48
Ce		102	55				19	14	7	85
Sc	13	21	36	31	15	12	37	31	39	24
V	44	170	221	165	431	42	252	175	263	73
Cr	138	142	36	220	90	177	105	138	610	30
Co										
Ni	25	57	68	93	53	29	39	25	271	21
Cu	14	34	63	38	32	16	51	2	103	25
Zn	8	76	89	45	52	9	112	102	73	85
Ga	16	18	18	15	21	18	16	12	12	20
S			31				10	9	6	47

TABLE III-1 (cont)

SAMPLE NUMBER	74930071	74930083
FORMATION	Mt HAY	Mt HAY
ROCK TYPE	GRANULITES	GRANULITES
	OpHbPlg	HbOpCpPl
	granulite	B.Granul depleted
1:100 000 SHEET	ANBURLA	ANBURLA
SiO ₂	65.53	49.46
TiO ₂	1.10	0.41
Al ₂ O ₃	14.60	16.65
Fe ₂ O ₃	1.37	1.92
FeO	4.03	7.12
MnO	0.08	0.17
MgO	2.16	8.99
CaO	3.43	12.45
Na ₂ O	1.64	1.58
K ₂ O	5.43	0.09
P ₂ O ₅	0.08	0.03
H ₂ O+	0.50	1.13
H ₂ O-		
CO ₂		
TOTAL	99.95	100.00
Mg NUMBER	42.2	64.4
Ba	1359	38
Rb	150	
Sr	127	280
Pb	12	
Th	2	2
U	1	
Zr	179	11
Nb	6	
Y	5	6
La	11	
Ce	16	
Sc	9	29
V	119	134
Cr	62	254
Co		
Ni	15	106
Cu	26	34
Zn	40	48
Ga	13	15
S	6	

TABLE 111. 2 - MAJOR ELEMENTS COMPARISONS BETWEEN MT HAY GRANULITES
AND AVERAGE SEDIMENTARY COMPOSITIONS

	(1)	(2)	A	B	C	D
SiO ₂	49.81	46.96	58.10	9.38	50.0	48.3
TiO ₂	0.65	0.95	0.65	0.12	0.56	0.54
Al ₂ O ₃	16.18	12.76	15.40	1.42	13.1	12.6
FeO total	9.45	8.82	6.10	7.62	6.3	6.4
MgO	8.67	7.59	2.44	27.4	6.6	7.4
CaO	11.91	19.98	3.11	45.6	10.2	11.6
Na ₂ O	1.70	0.85	1.30	0.14	1.1	1.07
K ₂ O	0.29	0.16	3.24	0.44	2.8	2.7

(1) Average of 3 Mt Hay basic granulites (samples S36,S43,S83)

(2) Average of 2 Mt Hay calc-granulites (samples S53,S55)

A - Average shale (Knutson et al., 1983)

B - Average dolomite (CO₂ face) Mt Gunson (Knutson et al., 1983)

C - Shale: dolomite 5:1 mixture

D - Shale: dolomite 4:1 mixture

IV. THE SOUTHERN MIGMATITE/GNEISS/GRANITE BLOCK

[1] Derwent Paragneiss

This unit consists of well layered and banded amphibolite facies metasediments and possibly metavolcanics, including quartzofeldspathic gneisses (meta-arenites and/or meta-rhyolite and para- and/or orthoamphibolites cut by abundant migmatites. Calc-silicates, metapelites and quartzites are common in GLEN HELEN. A correlation between the banded gneisses considered here and paragneisses of the Chewings Range Group (CRG) in the HERMANNSTADT 1:100 000 Sheet (Marjoribanks, 1975) is based on the intrusive relations between the Teapot Granite and related migmatites and the CRG. However, along the Chewings Range this group consists of a higher proportion of pelitic schist, semipelitic gneiss and quartzite - the latter forming the backbone of the range (Fig. I.1-2). In the area under consideration the paragneisses are best exposed in the southwestern part of GLEN HELEN south of the Redbank-Mt Zeil thrust zone (RTZ) west of Derwent Creek. The banded gneisses are progressively migmatized eastward between the Derwent and Dashwood creeks, grading into the Dashwood Migmatites. The distinction between the m.g. banded quartzofeldspathic paragneisses, their migmatized equivalents and intrusive gneiss fractions is not straight forward. This results in a difficulty in estimating the proportion of paragneiss relics within the migmatites.

Outcrops of Derwent Paragneiss are typically banded, as seen on aerial photographs, particularly in the Haast Bluff area where the gneisses are overlain unconformably by Heavitree Quartzite. Banding becomes progressively contorted and discontinuous upon migmatization. distinction between remobilised meta-arenite paragneiss and intrusive gneiss fractions is difficult or impossible. The quartzofeldspathic

gneisses consist principally of garnet, biotite, muscovite, plagioclase, K-feldspar and quartz. Sheared epidotised, cataclastic to mylonitic derivatives are common, displaying recrystallised quartz-feldspar mosaics. Porphyroblastic gneisses are locally present (Fig.IV.1) but are less common than in granulite facies gneisses north of the Redbank thrust zone. The amphibolites are well banded on a fine scale (Fig. IV.1a), including palaeosome amphibole-rich bands and migmatitic neosome bands, commonly displaying tight isoclinal folding. Typically, these rocks are pervasively intruded by amphibole-feldspar pegmatites. Calc-silicates are rare, and where observed form deep brown weathered surfaces. These rocks may include amphibole, clinopyroxene, epidote, sphene, calcite, scapolite, garnet, plagioclase, K-feldspar and quartz. Pelitic gneisses comprise sillimanite, garnet, biotite, plagioclase, K-feldspar and quartz. Heavily migmatised discernible relics of paragneisses occur as enclaves, streaks and wisps of amphibolite and biotite engulfed by leucosome mobilizate (Fig. IV-1c,d).

The amphibolites are represented by samples S827B and S834A, consisting of f.g. amphibole (Mg-hastingsitic hornblende ($Mg' = 59$) hornblende ($Mg' = 47$)). The amphibole in the latter sample is partly replaced by biotite ($Mg' = 54-58$), being typically the youngest phases in these rocks. Plagioclase compositions for the above samples are An45 and An33, respectively, and may be clear or saussuritised. Granoblastic textures prevail. No relic igneous texture has been discerned. Epidote, tremolite and chlorite are common accessory minerals. Felsic bands interlayered with the amphibolite are f.g to m.g. granoblastic, showing weak biotite foliation and containing augen of K-feldspar and quartz (S834B). Mafic components in these bands include amphibole (potassian actinolite, $Mg' = 80$) and biotite ($Mg' = 51-53$) which is more ferroan than in the juxtaposed amphibolite band. Felsic components include clouded andesine (An33-36), microperthitic K-feldspar and quartz. Quartz mosaics display intricately sutured grain boundaries, while individual grains show undulose extinction. Garnet-bearing

felsic bands occur, e.g. S830A - granoblastic Gnt-Biot-Amph-Plg gneiss which includes thin amphibole-biotite lamella. The garnet is an andradite (FeO=13%; CaO=23%) the biotite is iron-rich ($Mg' = 44-49$), the amphibole is potassian arfvedsonite ($Mg' = 32-40$) and the plagioclase is andesine (An33-35). Relatively pure quartzofeldspathic rocks, possible meta-arenite are represented by sample S778, which consists of granoblastic clouded plagioclase, K-feldspar and quartz. Common accessories are epidote, apatite, sphene, zircon, allanite and iron-oxide. Complete transitions exist from amphibolites through intermediate compositions (e.g. 831A) to felsic bands, suggesting original variations of calcareous and arenaceous bands. A distinction between paragneisses and orthogneisses within this sequence is difficult. Pure pelitic metasediments and calcareous metasediments are rare. Impure calcareous arenite compositions are suggested for assemblages dominated by intermediate plagioclase, epidote/saussurite, sphene, biotite, K-feldspar and quartz. Assemblages dominated by K-feldspar and epidote (S826D) may represent metamorphosed calcareous shales. Quartzose siltstones are represented by biotite-quartz schists (S718B) which contain accessory apatite, garnet, sphene and iron oxide. Thus, varying mixtures of arenitic, argillitic and calcareous components are represented by quartz, biotite and amphibole, respectively.

[2] Dashwood Migmatites

South of the Redbank-MtZeil thrust zone (RTZ) the terrain between Mt Zeil and Derwent creek is mostly occupied by quartzofeldspathic migmatites and banded gneisses containing abundant relics of Derwent Paragneiss, including amphibolites. Owing to the position of the Dashwood Migmatites between the RTZ to the north and the Mt Sonder-Mt Razorback thrust to the south the rocks are generally intensely deformed, exhibiting cataclastic textures. This is also the case with the Teapot Granite, which forms the core of the migmatitic zone (Fig.1.2).

Between Dashwood and Derwent creeks the migmatites grade imperceptibly westward into the banded gneisses of the Derwent Paragneiss. A migmatite front is difficult to delineate due to the widespread allochthonous intrusion of neosome mobilizate fractions into the paragneisses away from the main migmatite terrain. Type outcrops of Dashwood Migmatites occur along Dashwood Creek south and along a west-flowing creek east of Glen Helen homestead (Fig.IV.1). The migmatites contain high proportions of felsic mobilizate. The rocks are folded at random orientations, no consistent axial trends being evident, which suggests primary magmatic flow-folding under static conditions rather than post-consolidation deformation. Mineral assemblages of the felsic migmatites consist chiefly of biotite, plagioclase, K-feldspar and quartz. Cataclastic and mylonitized derivatives are characterized by epidote and sericite. Mafic xenoliths and schlieren to nebulitic palaeosome phases consist of amphibole and/or biotite; generally the smaller the size of the mafic enclave the smaller the proportion of amphibole to biotite. The latter is the principal ferromagnesian phase in mafic schlieren and nebulites. The migmatites are transected by numerous veins and dykes of fine grained granite and pegmatite.

Samples of migmatite and gneiss commonly display quartz recrystallisation and feldspar clouding related to their proximity to fault and shear zones. An example of an altered migmatite is S789 - a Biot-Mu-Ep-Plg gneiss, the sodic plagioclase (An₄₋₁₈) being sericitised and saussuritised. Quartz occurs as f.g. mosaics interspersed with sericite. Clots of biotite and epidote replace original ferromagnesian phases. Sample S788 is a least-altered gneiss showing relatively little disturbed m.g. anhedral to subhedral equigranular microcline and clouded plagioclase. Finer grained constituents include partly recrystallised quartz and biotite, epidote and muscovite. At the more advanced deformational stages schistose rocks are formed, for example sample S7 sericite-biotite-quartz schist containing few relic feldspar grains and representing the end product of alteration of gneiss.

Biotite-amphibole xenoliths are represented by sample S790. The rock consists of Mg-rich biotite ($Mg' = 68-69$) and amphibole (subsilic Mg-Hornblende; $Mg' = 70$) in apparent textural equilibrium, suggesting concomitant crystallisation.

[3] Teapot Granite

This body occupies an area approximately 200 km^2 large within the southeastern and southwestern parts of GLEN HELEN and NARWIETOOMA, respectively, and extends southward into HERMANNsburg (1:100 000). To the north the granite is bounded by migmatites akin to the Dashwood Migmatites and by the Redbank-Mt Zeil thrust zone. To the west the Teapot granite grades into the Dashwood Migmatites. Thus this intrusion forms the core of a wide migmatite aureole which intrudes the Derwent Paragneiss in the west and the Chewings Range Group in the east (Marjoribanks, 1975). The granite is penetratively sheared along E-W faults which run parallel to the RTZ and Mt Sonder-Mt Razorback thrusts (Fig. I. 1,2). Where least sheared, the granite forms large red to brown exfoliated domes (Fig. IV.2a). Typically, latitudinal shear zones and meridional joint systems dissect the granite terrain into rectangular land forms. This morphology, as well as the dolerite dyke swarm which intrudes the granite along E-W fractures, serve to distinguish this terrain from migmatite and gneiss terrains.

The Teapot Granite is commonly porphyritic, occasionally displaying flow banding outlined by oriented plagioclase prisms (Fig. III.2b). The granite includes xenoliths of banded biotite-rich gneiss and migmatite (Fig. IV.2c), indicating emplacement subsequent to migmatization. Sheared equivalents of the granite contain abundant sericite and epidote, and are particularly well developed along the Mt Sonder-Mt Razorback thrust fault, where cataclastic granites and phyllonites abound. Microscopically all samples of the Teapot Granite examined show some degree of deformation/recrystallisation. Sample S838 represents a sample of a least-deformed granitoid. It consists

of c.g. euhedral clouded prisms of plagioclase, m.g. anhedral microcline, mosaics of f.g. quartz, biotite-epidote clots and minor muscovite. No primary unrecrystallized quartz grains are seen. The complete recrystallization of quartz and rounding of feldspar grains constitute manifestation of penetrative deformation. An increase in cataclasis is reflected by further comminution of quartz and biotite, resulting in foliated microcrystalline aggregates outlining flow texture around relic grains of feldspar (S902,S904). Equigranular recrystallized textures may ensue (cf. S905), although foliated sericite-quartz schists may be more common.

[4] Basic Intrusions

Low grade to unmetamorphosed basic intrusions, as contrasted with high grade metamorphosed mafic granulites and amphibolites, have only been recorded south of the Redbank-Mount Zeil thrust zone (RTZ). Basic bodies south of this lineament are classified here in terms of three groups: (1) deformed partly amphibolitized gabbro stocks south of Mt Zeil; (2) deformed and altered basic dykes; (3) little deformed and little altered basic dykes.

A. GABBRO STOCKS SOUTH OF MT ZEIL

West of Mt Zeil and south of the RTZ (about $23^{\circ}24': 132^{\circ}21'$), covering an area about 10 x 2 km, are a number of small bodies of altered gabbro, dolerite and incorporated basic dykes cropping out sporadically within envelopes of leucocratic K-feldspar rich gneiss and biotite gneiss (Fig. V1). Three clusters of basic intrusions are outlined, each contained within its own gneiss envelope. The two western clusters outline a folded sill-like body about 100-300 m thick. The eastern body is the largest and has a thick gneiss mantle,

including a 2.5 km long eastern tongue which parallels the RTZ fault to the north. Foliation within the gneiss envelope is concentrically concordant with the gabbro bodies.

Some of the gabbro samples retain primary opx, cpx and plg, whereas other rocks are extensively amphibolitized. Sample S785 consists of poikilitic amphibole pseudomorphs after pyroxene, containing inclusions of mic. quartz, normally zoned prisms of plagioclase (An72) ,partly clouded by clinozoisite/saussurite and sericite, and texturally transgressive clots of biotite which replace amphibole. Amphibole is partly altered by chlorite. Apatite and opaque oxides are minor accessories. Recrystallised amphibolites represent comminution of grain size. Sample S812 is an amphibole-plagioclase-quartz rock with accessory epidote, apatite and opaque oxide, including relic tremolite replaced by hornblende. Sample S811A is a deformed ultramafic amphibolite, including less than 20 percent plagioclase, and comprising streaks of talc. Some rocks display strong biotitisation, cf S311B where late-stage biotite which includes exsolved opaque oxides replaces amphibole. The amphibole replaces poikilitic tremolite. Other components of this rock are labradorite (An60), epidote, clinozoisite, apatite, and quartz. Unmetamorphosed or little metamorphosed gabbro contain opx with lamellar texture, cpx partly replaced by amphibole and fresh plagioclase.

A likely interpretation of the leucocratic gneiss-biotite gneiss selvages around the metagabbro bodies is suggested in terms of local anatexis and remobilisation of the country rocks induced by excess heat of the intrusions. If so, biotite-rich zones within the gneiss mantle may represent partial assimilation of the gabbro by felsic partial melts. This model is consistent with the concentric banding of the gneiss around the gabbro outcrops, suggesting they postdate regional foliations within the Dashwood Migmatites. The juxtaposition of a mantle gneiss tongue with the Redbank-Mt Zeil thrust could suggest a pre-fault age; however, no cataclastic textures

attributable to the thrusting have been detected in these rocks. Alternatively, the intrusion of the gneiss was controlled and delimited by the overthrust block of Mt Zeil granulites. The mineral replacement sequence: pyroxene-tremolite-hornblende-biotite suggests greenschist facies metamorphism of the gabbro, or late to post-magmatic autometamorphism. Whether the metamorphism has predated the RTZ, occurred contemporaneously with thrusting due to associated heating, or represents autometamorphism remains an open question.

[b] BASIC DYKES

Dolerite dykes are widespread within the Teapot granite, where they intrude mainly along EW fractures. Deformed basic dykes occur in the marginal western portion of the granite and in the Dashwood migmatites to the west, where the trend of the dykes is often NW. Small dykes also intrude Derwent Paragneiss west of the Derwent Creek. No low grade or unmetamorphosed dykes have been observed in the high grade terrains north of the Redbank-Mt Zeil Thrust Zone, nor have any been seen to intersect this fault or the Mt Sonder-Mt Razorback thrust fault, or the unconformity as the base of the Heavitree Quartzite. These relations suggest that either the dykes predate the thrusting, or that their intrusion was controlled by joint systems mainly confined to the granites. While most dykes are little deformed, mild flexures in places (cf. $23^{\circ}29':132^{\circ}19'$) suggests that latest stages of deformation and fault-reactivation have post-dated dyke intrusion. The possibility that more than one dyke phase exists remains open.

Sample S591 is an olivine dolerite from a dyke intruded^d into the Teapot Granite. It consists of m.g. fractured clouded olivine, subophitic clinopyroxene, and labradorite (An58), accompanied by accessory alteration products. Chlorite forms rims around olivine, actinolite rims cpx and biotite rims opaque oxides. Sample S590A is a f.g. olivine dolerite with ophitic to

subophitic cpx and slender needles of labradorite (An68), in mic. chlorite-epidote matrix in which palimpsest subophitic pyroxene is outlined by brown cryptocrystalline alteration products and microcrystalline opaque oxides. Sample S266G is from a basaltic dyke intruded into a sliver of calcsilicates correlated with the Derwent Paragneiss. It consists of f.g. intergranular cpx and labradorite (An57), chlorite-altered pseudomorphs of olivine and/or pyroxene, opaque oxide and microcrystalline to cryptocrystalline chlorite and actinolite which cloud the pyroxene.

[5] Heavitree Quartzite

The area includes few outcrops of the Heavitree Quartzite the basal unit of the late Proterozoic to Devonian Amadeus Basin sequence (Wells et al., 1970), as follows: (1) Ridge-forming quartzite unconformably overlying Derwent Para gneiss along the Haast Bluff ridge west of Derwent Creek; (2) outcrops striking NW to EW along southwestern GLEN HELEN. Owing to poor outcrop, the relations between these and the basement are not clear; (3) An isolated outcrop of quartzite juxtaposed with, and located immediately north of, the Redbank-Mt Zeil thrust zone about $132^{\circ}01':23^{\circ}16'$ (section V.4). Immediately south of GLEN HELEN and NARWIETOOMA major ridge forming outcrops of Heavitree Quartzite form Mt Razorback and Mt Sonder, where the sediments are overthrust by heavily cataclastically deformed Teapot Granite. At Ormiston Pound the Heavitree Quartzite is about 230 m thick and consists of the following lithologies, from base to top (Marjoribanks, 1975):

- 0 - 35 m: quartzitic grit, pebbly layers, thin siltstone at base
- 35 - 180 m: massive f.g. commonly cross bedded orthoquartzite.
- 180 - 190 m: pebbly sandstone.
- 190 - 230 m: massive f.g. orthoquartzite with occasional shale partings.

FIGURE CAPTIONS FOR SECTION IV

IV.1 - Derwent Migmatite and Dashwood Paragneiss.

- (A) isoclinally folded foliated amphibolites (Derwent Paragneiss) injected lit par lit by granite bands
- (B) porphyroblastic gneiss (Derwent Paragneiss)
- (C) biotite-amphibole foliations within migmatite (Dashwood Migmatite)
- (D) bands of amphibolite within migmatite (Dashwood Migmatite)

IV.2 - Teapot Granite

- (A) exfoliated bouldery outcrops of Teapot Granite
- (B) flow-textured microcline phenocrysts, Teapot Granite
- (C) enclave of foliated biotite gneiss within the Teapot Granite

IV.3 - ACF ternary plot of mineral assemblages from the Derwent Paragneiss

Fig. IV.1

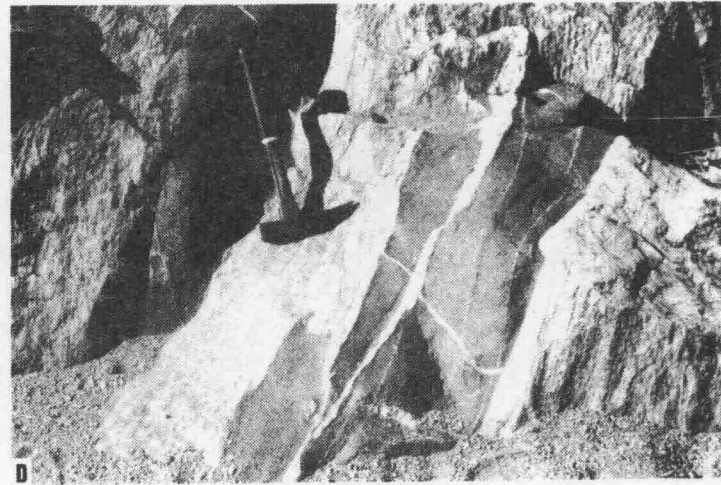
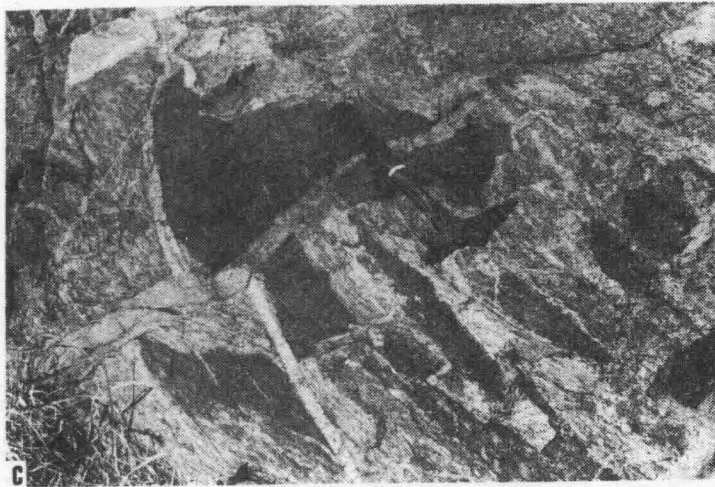
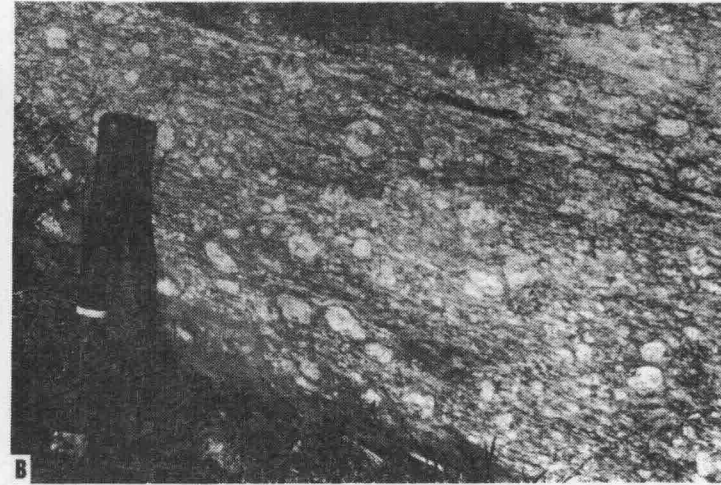
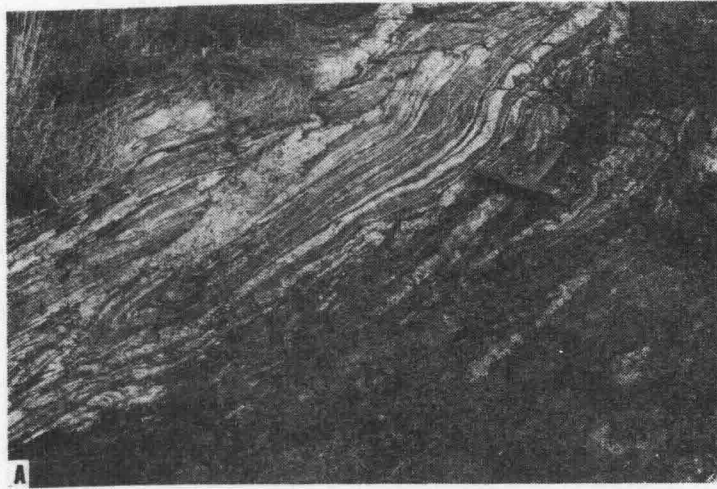


Fig. IV.2

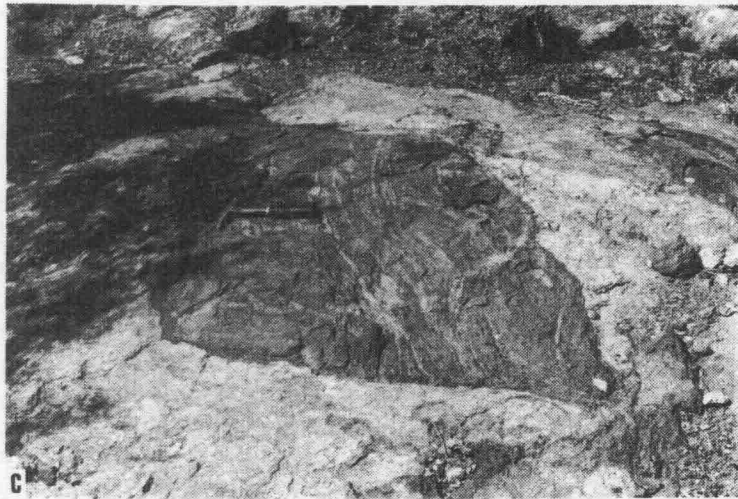
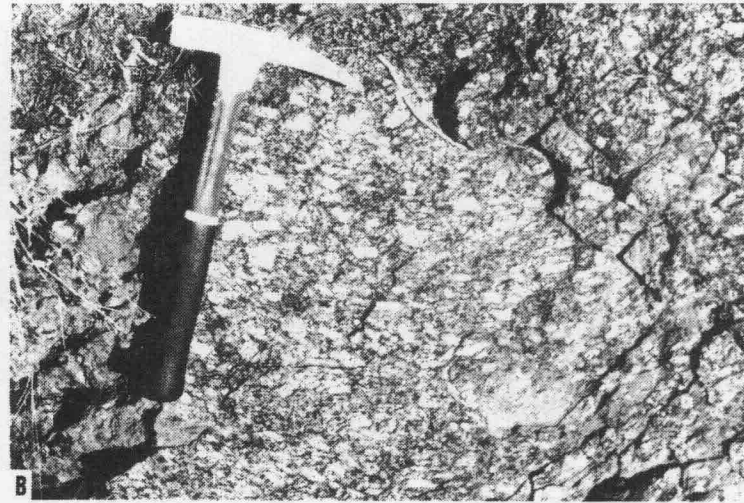
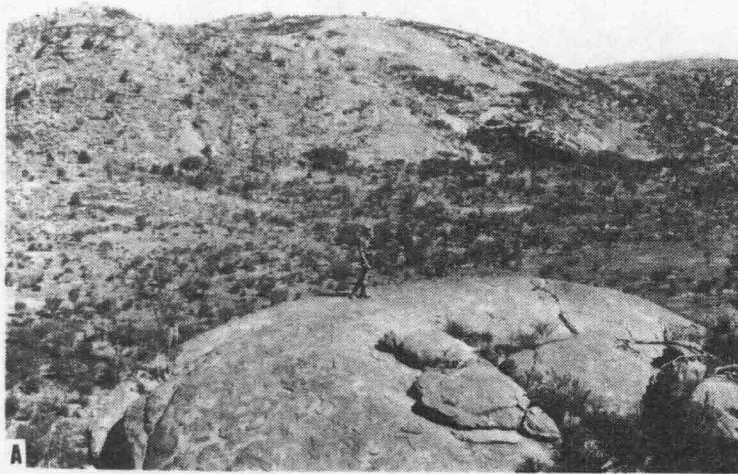
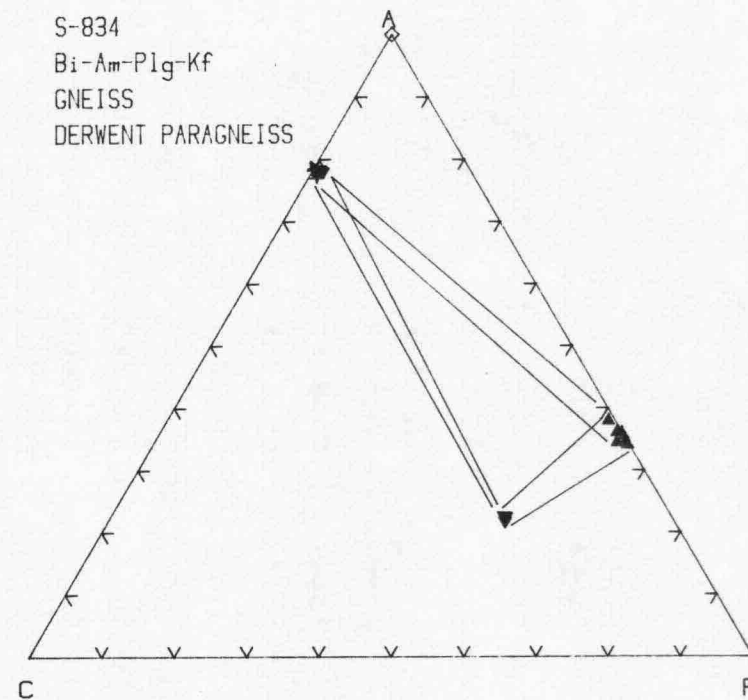
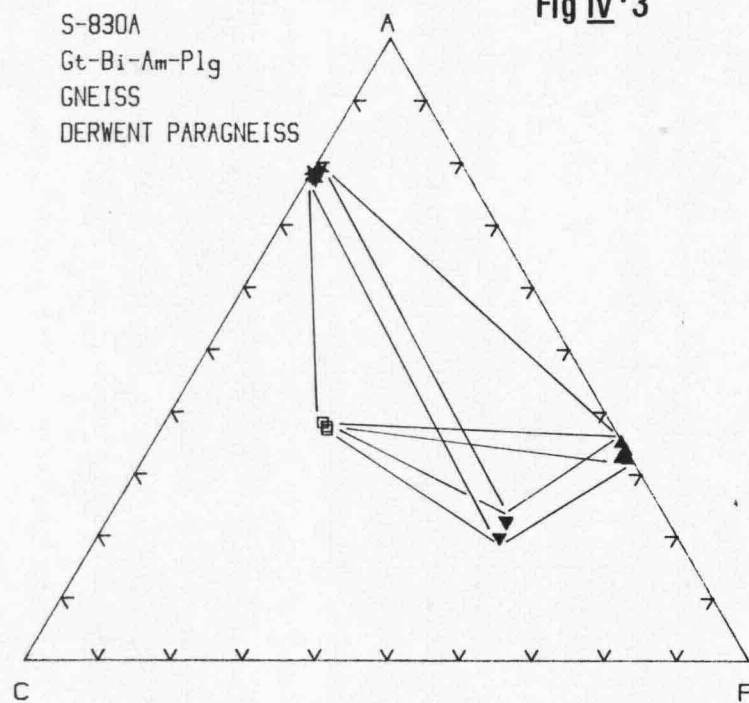


Fig IV·3



V. REDBANK-MOUNT ZEIL THRUST ZONE

[1] General Outline

Granulite facies rocks of the Mt Hay, Mt Chapple, Redbank Hill and Mt Zeil belts, described above, are separated from the Dashwood Migmatites, Teapot Granite and Derwent Paragneiss by a major deformed zone - denoted Redbank-Mt Zeil thrust zone (RTZ). This ^{uc} structural lineament consists of interlayered cataclastic gneiss, flaser gneiss, phyllonites, mylonites and ultramylonites.

Foliations dip northwards at shallow (ca 30° to steeper angles). In the southernmost central part of NARWIETOOMA and in McDONNELL RANGES, the RTZ strikes WNW, constituting the northern margins of an exposed basement plateau north of the Chewings Range (Fig. I.1-2). The termination of outcrop along this lineament results from the greater erodibility of the heavily sheared rocks. From about longitude 132°43' (south of Redbank Hill) westward the RTZ enters into the ranges east of Mt Zeil, forming a boundary between northward dipping granulites to the north and a deformed migmatite/gneiss terrain to the south. The width of the RTZ in this sector is difficult to estimate, since cataclasis is identified both within the thrust zone and in adjacent terrains. In addition, fault splays which branch off the main thrust render discrimination between the principal and subsidiary faults difficult in places. Thus, the migmatite/granite terrain between the RTZ and the Mt Sonder- Mt Razorback thrust fault is extensively deformed and faulted, as manifested by widespread cataclasis. Generally the RTZ narrows westward from the Redbank Hill area, from a width of approximately 2 km to a few hundred metres in the Mt Zeil area. The southern cliff face of the Mt Zeil range and lower cliffs east of this area result from the erosion of soft deformed zones capped by resistant granulites, resulting in northward dipping questa morphology reflecting thrust slices.

Major bifurcations of the RTZ occur east ($132^{\circ}27'$) and west ($132^{\circ}19'$) of Mt Zeil. In the latter instance the northern fault branch reappears at Mt Heughlin where a narrow zone of mylonite crops out high on the southern escarpment (Fig. V1). The southern fault branch can be intermittently traced in the north of Glen Helen homestead area where it consists of phyllonites, but is more difficult to trace further west. In this and other areas the most reliable criterion for identification of the RTZ is a sharp change from granulite-facies gneisses to the north to amphibolite facies paragneisses and migmatites to the south. Using this criterion it is clear that west of Mt Zeil the principal thrust fault is represented by the southern branch, since the terrain between the two fault branches includes granulites and granulite-facies gneisses. Another criterion is furnished by the air-borne radiometric map (Fig. VII.1) which displays a contrast between the K-U-Th-poor granulites and K-U-Th-rich granite/migmatite terrain. According to this criterion the northern branch is important. The two fault branches may merge about longitude $132^{\circ}03'E$, where granulites which surround downfaulted slivers of quartzite are juxtaposed with Derwent Paragneiss west of Derwent Creek.

To an extent the problem in identifying the RTZ trace results from variations in the deformational facies along this lineament. In the east the zone is mainly expressed by cataclastic and flaser gneisses, including abundant mylonitic and phyllonitic units. In the Mt Zeil area, where the thrust zone is narrowest (Fig. V1), mylonites and phyllonites are dominant. West of Mt Zeil and in the Dashwood Creek area phyllonites are widespread. West of Dashwood Creek the RTZ is difficult to trace, though the sporadic occurrence of phyllonites and mylonites in this area suggests its proximity.

Well exposed sections across the RTZ occur about longitudes $132^{\circ}32' - 132^{\circ}40'$ (SW of Redbank Hill), on Dashwood Creek between Glen Helen homestead and Mt Heughlin, and

along the southern escarpment of the Mt Zeil ridge ($132^{\circ}19'$ - $132^{\circ}25'$). In the following two of these sections are individually described.

[2] The RTZ SW of Redbank Hill

Granulites exposed about 1500 m north of the RTZ in this area disclose little or no effects of deformation, cf. S560 - a felsic Gnt-Cp-Am-Biot-Plg granulite showing neither cataclasis nor clouding. However, a few hundred metres from the deformed zone a Gnt-Biot-Am-Kfeld-Plg-Qz granulite displays recrystallised quartz aggregates and biotite folia delineating flaser texture. Progressive cataclasis within the shear zone is represented, for example, by sample S566A, a moderately deformed Biot-Plg-Kfeld-Qz (+/-sphen, apatite, opaque oxide) gneiss showing extensive recrystallisation of mic quartz interspersed with little deformed f.g. feldspar and foliated biotite. A coarse grained cataclasite is represented by S567A - a sphen rich Amph-Biot-Plg-Kfeld-Qz (Fig.V3a). Advanced development of flaser texture is shown by samples S563, S568A, B, biotite envelopes being well defined around quartzofeldspathic lenses (Fig.V3b). An intermediate stage between flaser gneiss and a biotite-quartz-albite schist is represented by sample S569. The cataclastic gneisses alternate intimately with zones of mylonite and ultramylonite and with phyllonites (Fig.V.2). Advanced deformation is represented by f.g. biotite-epidote-quartz schists (S566C), the epidote being texturally younger than, and replaces, biotite. Accessory ilmenite is replaced by sphen. Ultramylonites consist of microcrystalline strongly aligned sericite-quartz aggregates including microporphyroblasts of epidote (S566B). Relic grains of feldspar display crushed, embayed and recrystallised features, undulose extinction and deformation cracks (cf. S567B) microcrystalline quartz in cataclasites and mylonites often occurs in ribboned aggregates (S562B) (Fig.V.3c). The RTZ in this area includes sillimanite-garnetbiotite-quartz schists, cf. S376 (Fig.V3h) , S570,

containing accessory opaque oxide and tourmaline. The garnet and sillimanite clearly predate the superposed cataclasis, as shown by rotation and corrosion of the crystals.

Relics of little deformed granulites are common within the RTZ. The largest is a well preserved enclave of mafic granulite about 800x600 metres large forming a prominent dark hill. Samples S374A, S378A,B, S379A,B and S574A derived from this body consist of fresh poikiloblasts of hypersthene (pink-green) with inclusions of amph and plg, xenoblastic cpx containing similar inclusions, granoblastic labradorite, minor opaque oxide and texturally young biotite (Fig. V.3e). Except for minor fracturing and crystal bending these rocks display surprisingly little evidence of their incorporation within a major thrust zone. In other areas smaller pods of mafic granulite show considerable deformation and retrogression. An example is S562D which consists of f.g. granulated amphibole and strongly foliated mic. biotite which form replacement envelopes around amphibole (Fig. V.3f). Other components of the rock are mic quartz/feldspar mosaics, epidote and sphene. Upon advanced shearing amphibole is completely replaced by biotite, resulting in biotite-epidote-quartz schist (S566C)(Fig. V.3g). Intense deformation along the margin of the resistant enclave of granulite is represented by mylonites (S574B) and flaser gneiss (S377B).

West of the mafic granulite enclave is a thick belt of phyllonites and mylonites. A sample of phyllonite (S572) consists of a mic assemblage of moderately well agligned muscovite, clusters of epidote, quartz mosaics and accessory opaque oxide (Fig. V.3d). A sample of mylonite (S573) consists of mechanically granulated relic fragments of feldspar and garnet set in flow-textured matrix consisting of mic biotite and ribboned quartz. Epidote, muscovite, apatite and opaque oxide are accessory components. An incipient development of sericite schist from recrystallised comminuted felsic gneiss is

represented by S562A, whereby oriented flakes of muscovite and granular epidote developed within an aggregate of granulated f.g. K-feldspar, plagioclase and mic quartz mosaics.

Toward the southern part of the deformed zone felsic augen gneisses and their deformed equivalents represent material derived from the migmatite/gneiss terrain of the southern block. Augen gneiss (S564) consist of composite c.g. porphyroblasts of plagioclase/microcline containing inclusions of quartz, set in m.g. matrix of foliated biotite, feldspar and quartz, accessory apatite and iron oxide. Another example is a banded biotite gneiss (S566A) which contains sphene-biotite-iron oxide clots. Moderate cataclasis of this rock is represented by quartz recrystallisation to form mic anhedral mosaics.

[3] The RTZ in the Mt Zeil area

Where the Redbank-Mt Zeil thrust zone occurs at the base of the Mt Zeil escarpment, the fault separates felsic granulites and granulite facies gneisses on the north from banded biotite gneiss/migmatite to the south. The latter incorporate three large bodies of amphibolitized gabbro enveloped by K-feldspar rich felsic gneiss (Section IV.4a). In this area the thrust fault occurs as a narrow (<300 m) zone of mylonite, ultramylonite and deformed cataclastic gneiss. The thrust zone contains relics of little-deformed amphibolite to granulite facies gneiss.

Sample S781 is a sphene and ilmenite bearing Biot-Amph-Plg-Qz mafic gneiss forming a least-deformed relic within the thrust zone. Sample S784, an Opx-Gnt-Biot gneiss, shows fracturing and clouding associated with deformation. The feldspars are intersected by several sets of penetrative cracks, display undulose strain extinction, and may be physically bent. Quartz is recrystallised into mic aggregates. The rock is

transected by microjoints coated by crypt. clouding. Progressive deformation resulting in S782. The rock consists of corroded and fractured partly clouded f.g. K-feldspar and plagioclase set in a flow matrix of strongly ribboned mic. quartz, aggregates, of crypt. quartz and sericite. Progressive grain comminution results in ultramylonites, cf. S783A, which consists of relics of corroded f.g. microcline and plagioclase enveloped by muscovite and set in a matrix of mic. quartz, albite, poorly aligned biotite and accessory epidote, apatite and iron oxide. A more strongly biotite-foliated epidote-rich ultramylonite is represented by sample S783B.

A section through the principal southern sector of the RTZ southeast of Mt Zeil ($132^{\circ}25'$: $23^{\circ}25'$) has encountered the following rock types, from S to N:

S897 - Chloritoid-biotite-chlorite-muscovite phyllonite. Anhedral prismatic f.g. chloritoid parallels or intersects the foliation defined by mica, and is clearly the youngest phase in the rock. Quartz forms mic. embayed aggregates.

S896 - Banded epidote-quartz rock. Recrystallised euhedral and ribboned quartz aggregates are principal components, and are accompanied by relics of corroded and clouded plagioclase and accessory biotite, chlorite and iron oxide.

S895 - Muscovite-biotite-chlorite phyllonite, including relic corroded and clouded feldspars.

S894 - Ultramylonite, consisting of well-rounded relics of f.g. plagioclase and amphibole (less than 10% of the rock) set in strongly laminated crypt clouded matrix.

S893 - Mylonite, consisting of an assemblage of mic. biotite, quartz, albite and epidote, including relic grains of plagioclase and lenses of felsic gneiss.

S892 - Cataclastic Opx-Amph-Biot-Plg (antiperthite)-Qz banded intermediate granulite. The rock shows undulose extinction, clouding of feldspar, strain-recrystallisation of quartz resulting in mic embayed aggregates.

S891 - Ribboned-quartz mylonite, containing well rounded f.g. feldspar grains and minor amphibole set in strongly undulately laminated ribboned aggregates of mic quartz alternating with clouded flow matrix.

S888 - Opx-Amph-Biot-Plg intermediate granulite, with minor garnet, apatite and iron oxide, biotite being the youngest phase

S889 - Cataclastic Gnt-Opx-Cpx-Amph-Biot-Plg-Qz displaying extensive strain recrystallisation of quartz, feldspar clouding, and alteration of pyroxene to biotite and chlorite.

A section through the northern branch of the RTZ in the area east of Mt Zeil ($132^{\circ}26':23^{\circ}23'$) encounters the following rock types from S to N:

S881 - Porphyroblastic garnet gneiss containing c.g. augen of K-feldspar and m.g. anhedral garnet set in a f.g. biotite-poor quartz-feldspar aggregate. Deformation is reflected by quartz recrystallisation and feldspar clouding.

S879 - Banded Gnt-Cpx-Amph-Biot-Qz gneiss, with minor apatite, allanite, rutile and iron oxide. Garnet replaces biotite and iron oxide. Little deformation is discernible.

S878 - Cataclastic banded felsic garnet-biotite gneiss, showing extensive recrystallisation of quartz and undulose extinction in feldspar.

S882 - Cataclastic quartz-feldspar gneiss, including minor Gnt and Cpx, and intersected by flow-structured ultramylonitic shears which include small augen of comminuted feldspar.

S883 - Banded Amph-Biot-Plg-Qz gneiss with minor garnet, apatite and zircon, displaying undulose extinction and feldspar clouding, quartz recrystallisation and bending of grains.

S884 - F.g. Biot-Cpx-Amph-Plg mafic granulite, showing no superposed deformation. Biotite is the latest phase, replacing amphibole.

S885 - Gnt-Amph-Biot-Plg-Qz felsic gneiss. Minor cataclasis is represented by biotite coated fractures.

[4] Age Relationships of the RTZ

Marjoribanks and Black (1974) and Marjoribanks (1975) consider the Redbank-Mt Zeil Thrust Zone (RTZ) to have predated the 1053 ± 50 m.y. (Rb-Sr TR) age of Ormiston Zone migmatites and the 893 ± 97 m.y. (Rb-Sr TR-feldspar) age of porphyroblastic gneiss from Redbank Hill. This view is related to the correlation proposed by these authors between migmatites south and north of the RTZ and the classification of the southern part of Redbank Hill as an integral part of the deformed zone. In the present survey, however, it was observed that mylonite, cataclasites and phyllonites of the RTZ invariably transgress all other lithological units and are nowhere effected by younger migmatization. Relics of both the northern granulite terrains and the southern gneiss-migmatite terrain abound within the RTZ. No confident correlations can be made between felsic gneiss/migmatite units which occur north and south of the RTZ. In so far as the ca 1.0-0.9 b.y. Rb-Sr ages cited above represent igneous events they define maximum ages for the thrusting. However, since it is likely that deformation along the RTZ was associated with thermal activity and resetting of Rb-Sr ages, the ca 1.0-0.9 b.y. ages may actually reflect such thermal effects related to the development of the thrust zone, while the migmatites and gneisses may be significantly older. The preexistence of an antecedent phase of the RTZ

lineament is possible, and could account for the development of coarse grained augen and porphyroblasts at Redbank Hill. Such a view hinges on an interpretation of these gneisses as high grade metamorphosed blastomylonites, conceivably representative of high-strain root zones of an early shear zone.

A minimum age for vertical movements along the RTZ west of Derwent Creek is furnished by outcrops of Heavitree Quartzite south and probably north of the fault about $132^{\circ}01'$: $23^{\circ}16'$. In this area a narrow 1500 m long NS trending sliver of quartzite striking at 320° occurs within mafic granulites and gneisses north of the thrust fault. The quartzite-granulite contacts are faulted. Preservation of relic bedding in the quartzites suggests it may be derived from the Heavitree Quartzite rather than an older metamorphosed quartzite. If so, the structural position of this quartzite slice relative to the basal unconformity of the Heavitree Quartzite in the Haast Bluff range south of the RTZ would place limits on vertical fault movements in post-Heavitree Quartzite times. This sedimentary unit probably postdates the Stuart Dyke swarm, dated as 897 ± 9 m.y. (Rb-Sr TR-mineral age; Black et al., 1983), which intrudes neither the Heavitree Quartzite nor the RTZ. However, the little deformed state of these dykes (section IV.4b) suggests they postdate major movements along the thrust fault. It follows, tentatively, that only limited reactivation of the RTZ occurred in the area south of Mt Zeil, where little deformed dykes are intruded into Dashwood Migmatite and Teapot Granite. Such a conclusion, however, is difficult to reconcile with (1) the major movements along the Mt Sonder-Mt Razorback thrust faults during ca 0.4 b.y. ago (Alice Springs Phase), and (2) the development of the early Carboniferous Brewer Conglomerate which contains very coarse grained detritus derived from the basement to the north (Fig. I.1-2), signifying major uplift. However, significantly the conglomerate is devoid of pebbles of granulites. This implies further uplift and erosion in yet younger times. Thus, from the evidence above, while the RTZ was

mainly active about 1.0-0.9 b.t ago, significant reactivations of some sectors during the Alice Springs Phase and younger times are probable.

FIGURE CAPTION FOR SECTION V

- V.1 - Aerial photograph of part of the Redbank-Mt Zeil thrust zone (RTZ) in the Mt Zeil area. Arrows define approximate limits of the fault zone. g-Gabbro intrusion; K-alkali feldspar-rich zones around gabbro; N-banded gneiss and migmatite; R-granulites;
- V.2 - Redbank-Mt Zeil thrust zone (RTZ) outcrops
- (a) banded mylonite (dark units) and cataclastic flaser gneiss (light coloured units)
 - (b) Relic rounded feldspar phenocrysts and glomeroblast in mylonite
 - (c) folded epidote-quartz mylonite (light coloured) and porphyroblastic mylonite (dark bands).
 - (d) folded mylonite including folded quartzose veins and segregations
- V.3 - RTZ microphotographs
- (A) S567A - Cataclastic sphene-amphibole-biot-Kfelds-plg-quartz gneiss showing deformed corroded fragments of feldspar in a flow matrix of foliated biotite and recrystallised quartz; about $132^{\circ}40'E23^{\circ}28'S$; 6.3 x12; CN.
 - (B) S568A - Cataclastic biot-amph-plg-feldspar-quartz flaser gneiss, showing corroded grains of feldspar in a flow matrix of foliated biotite and recrystallised quartz; about $132^{\circ}40'E-23^{\circ}28'S$; 6.3 x 12; CN
 - (C) S562B - Ribboned quartz mylonite; about $132^{\circ}40'E23^{\circ}28'S$; 13 x 12; CN.

- (D) S572 - epidote-muscovite-quartz mylonite within the RTZ, about $132^{\circ}40'E23^{\circ}28'S$; 13 x 12; CN
- (E) S378A - A relic body of mafic granulite within the RTZ $132^{\circ}40'E23^{\circ}28'S$; microphotograph showing fractured grains of opx with inclusions of amphibole, interspersed with plagioclase; 8 X12; PPL
- (F) S562D - sphene-bearing biotite-amphibole-plg-qz schist showing deformed fragments of amphibole in phyllonitic matrix about $132^{\circ}40'E23^{\circ}28'S$; 21 x 12; PPL.
- (G) S566C - epidote-biotite-plg-qz phyllonite; about $132^{\circ}40'E23^{\circ}28'S$; 16 x 12; PPL
- (H) S276 - garnet-sillimanite-biotite flaser gneiss; about $132^{\circ}40'E23^{\circ}28'S$; 6.3 x 12; PPL

Fig. V-1

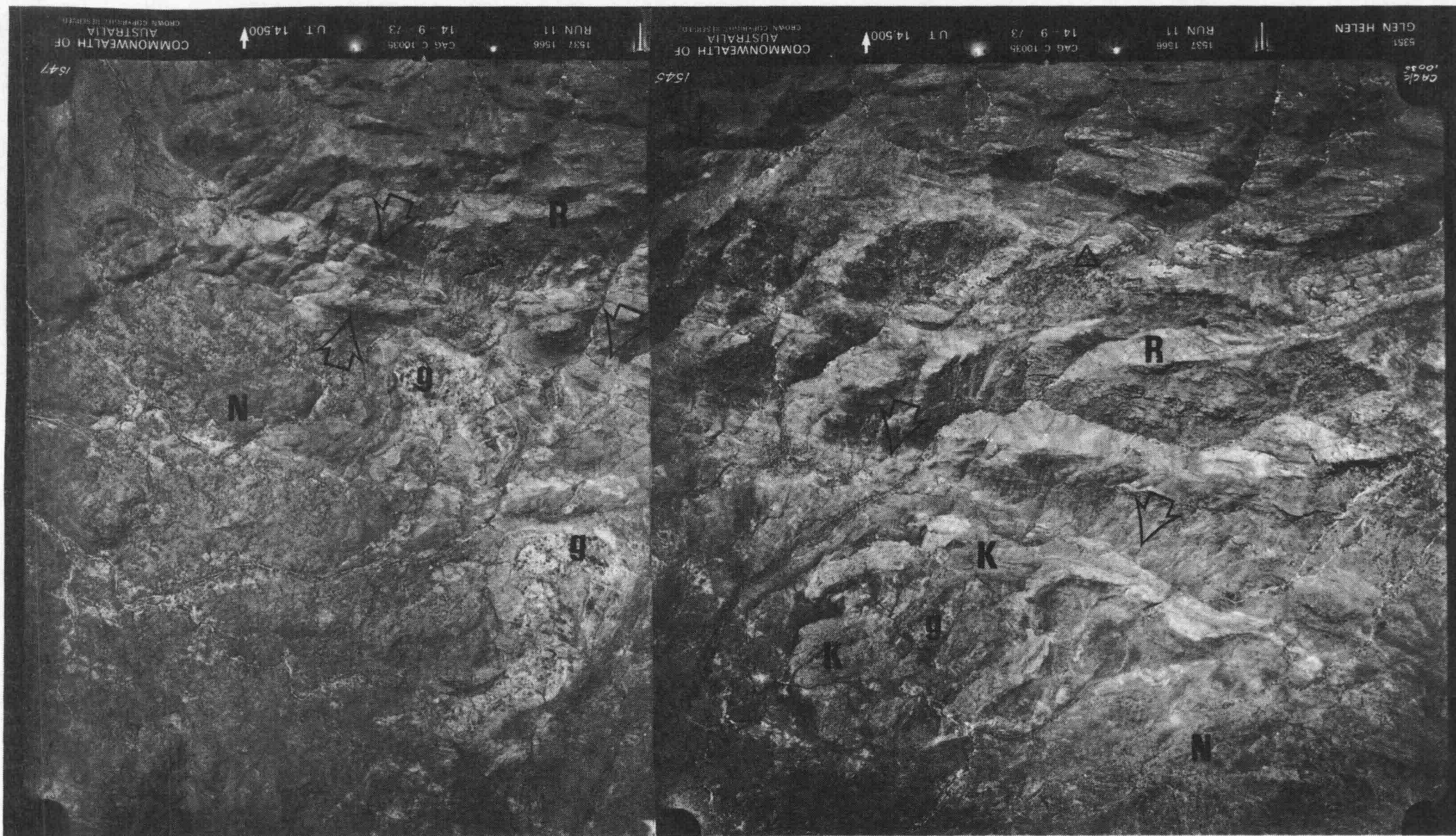


Fig. V.2

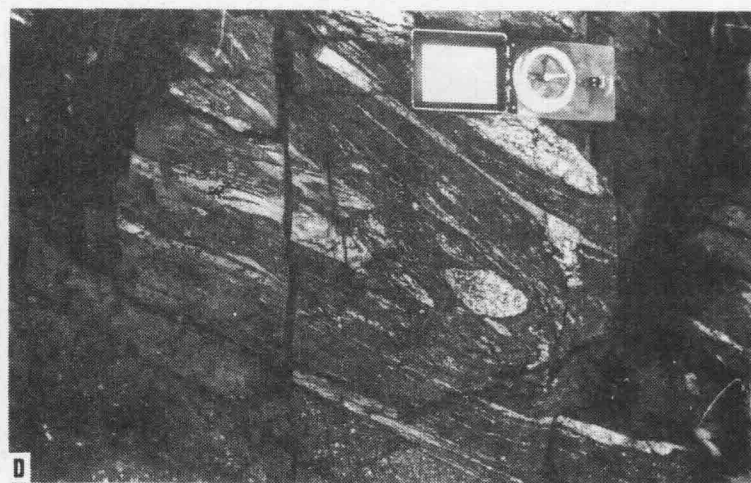
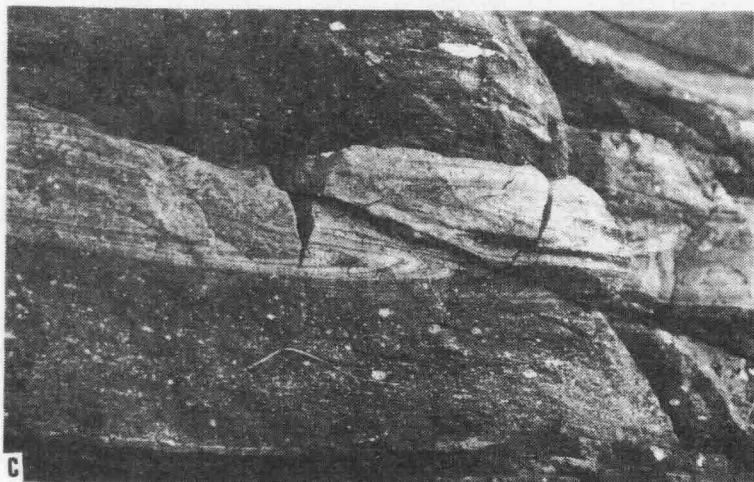
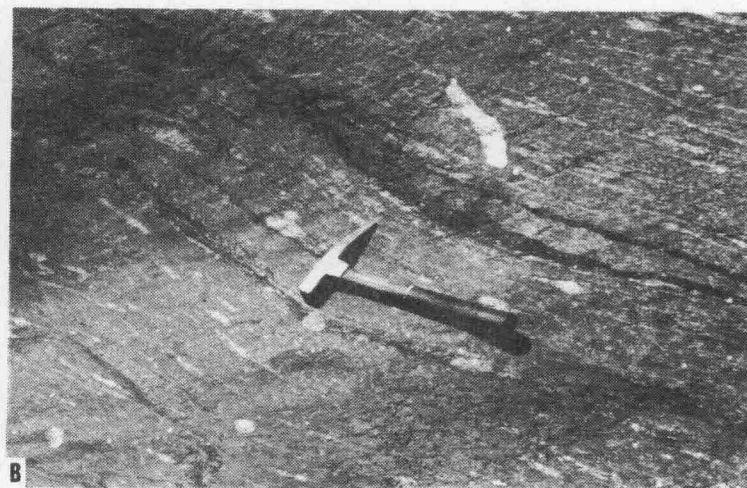
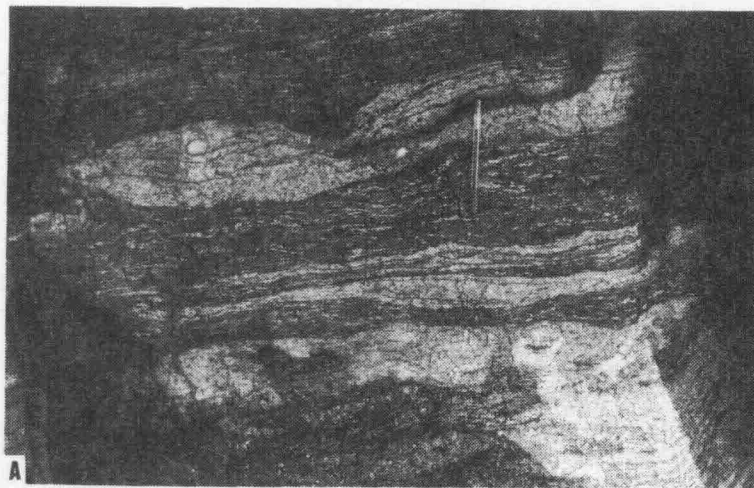
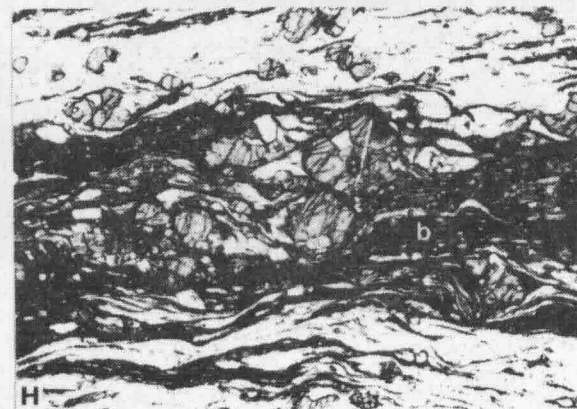
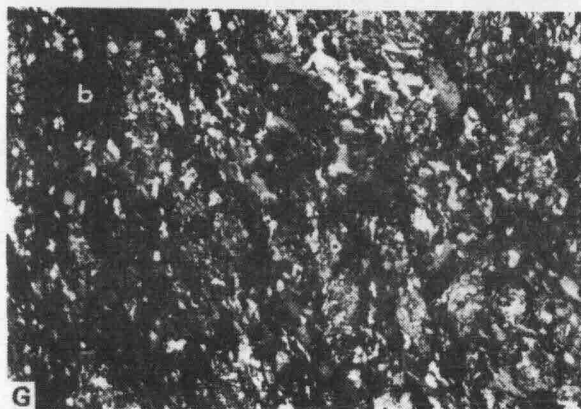
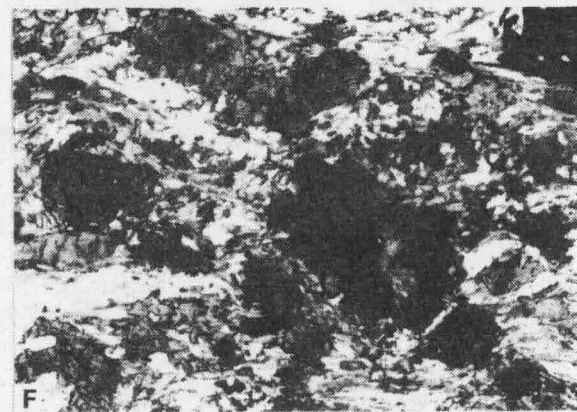
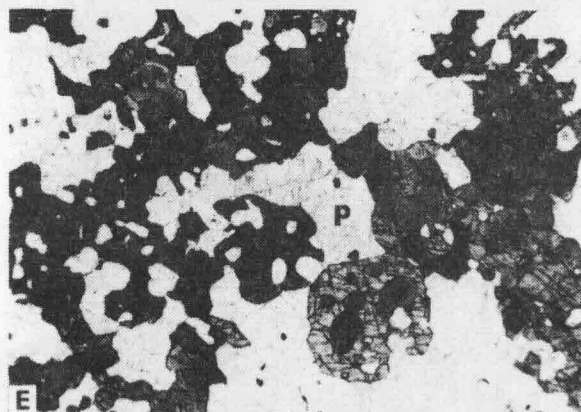
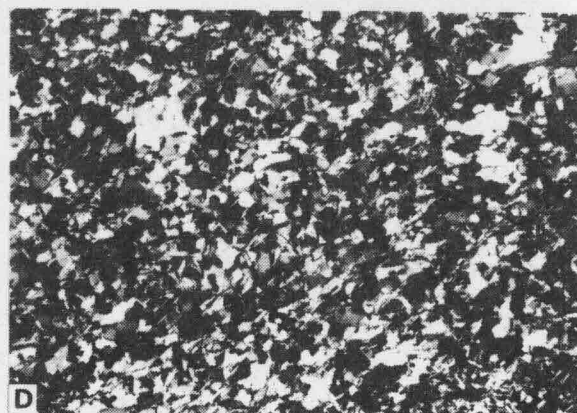
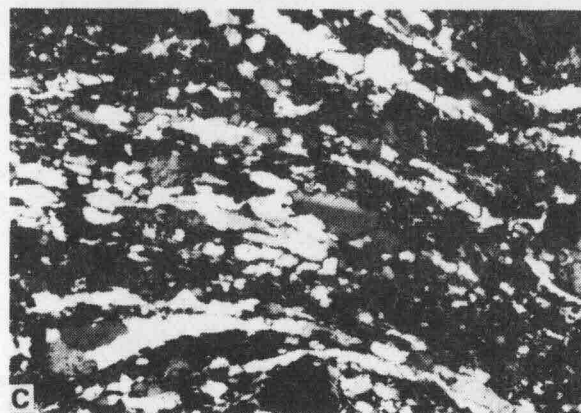
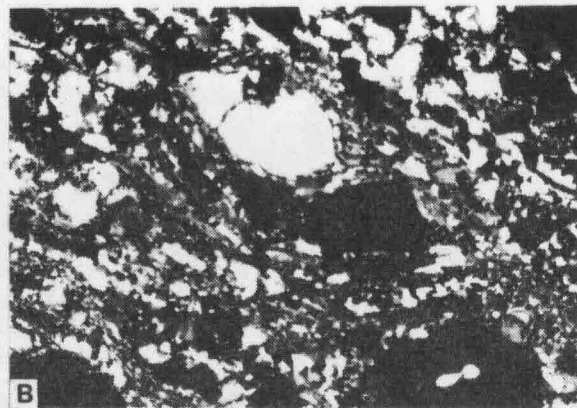
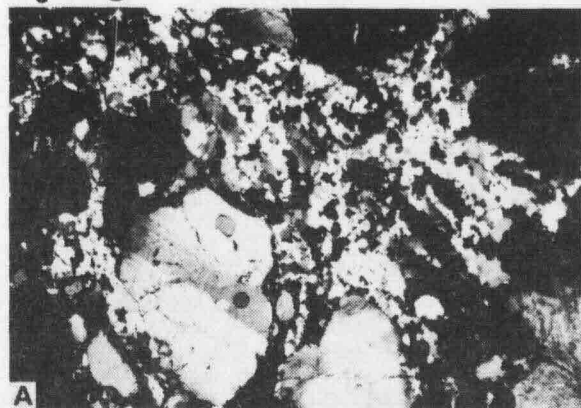


Fig V·3



VI. GEOTHERMOMETRY AND GEOBAROMETRY

Criteria for the selection of suitable mineral assemblages containing evidence for temperature-sensitive and pressure-sensitive cation exchange reactions include: (1) availability of well reversed experimental data and/or thermodynamic calibrations for these reactions in the literature; (2) textural and compositional evidence for equilibrium conditions, namely absence of obvious retrogression effects and/or marked chemical heterogeneity, and (3) compositional limits on the mineral phase in question, cf. effects of x_{Ca}^{gt} on An-Gnt-Sil geobarometry, of x_{Ca}^{gt} , x_{Mg}^{gt} , and x_{Ti}^{bi} , on gnt-bi geothermometry, or of x_{Na}^{cpx} on gt-cpx geothermometry (Essene, 1982). In the northern granulite block the observed mineral assemblages allow information on equilibria conditions associated with the following reactions:

[1] GEOTHERMOMETERS

[1]...1/3 pyrope + hedenbergite = 1/3 almandine + diopside
 temperature-sensitive partitioning $K_{D \text{ gnt-cpx Fe-Mg}}$ allows
 correlation with significant ΔH (enthalpy) and ΔS (entropy)
 changes and thus derivation of T for assumed P values at
 equilibrium conditions:

$$[2] \dots \Delta H^{\circ} - T\Delta S^{\circ} + (P-1)\Delta V^{\circ} + RT \ln K_D = 0$$

Experimental data for this reaction were reviewed by Saxena (1979), Dahl (1980) (based on linear regression) and Ellis and Green (1979). The latter conducted experiments at 24-30 kb taking into account the effects of x_{Fe}^{gt} on $K_{D \text{ gt-cpx Fe-Mg}}$

due to non-ideal Ca-Mg substitution.

[3]...alamandine + phlogopite = pyrope + annite

Co-existing garnet-biotite assemblages yield $K_D^{gt-bi}_{Fe-Mg}$ which allow P-T correlations for this temperature-sensitive reaction, given the experimental data presented by Ferry and Spear (1978) who used synthetic minerals. This calibration is considered suitable for garnets low in x_{Ca}^{gt} and x_{Mg}^{gt} and biotites low in x_{Ti}^{bi} . The application of this reaction is considered by Essene (1982) to be more suitable for assemblages formed under greenschist to amphibolite facies than under granulite facies as in the latter high-Ti biotites are common. The effect of Fe^{+3} on the P-T correlation is uncertain.

[4]...enstatite = clinoenstatite

The temperature dependence of $K_{D-Mg}^{cpx-opx}$ in co-existing orthopyroxenes and clinopyroxenes allowed by the diopside-enstatite miscibility gap indicated by Wood and Banno (1973) and Wells (1977), assuming ideal mixing and applying empirical correction for Fe, which yields T estimates within $\pm 70^\circ C$ from the experimental data (Wells, 1977). Difficulties with this thermometer arise from non-ideal mixing between Ca and Mn in the M site. Bohlen and Essene (1979) have found this T-estimate method imprecise and Harris et al. (1982) found the results vary in excess of $100^\circ C$ in charnockitic assemblages.

[5]...geikielite (Mg-ilmenite) + Ferrosilite = ilmenite + enstatite

[6]...geikielite + hedenbergite = ilmenite + diopside

The temperature-dependant $K_{D-Fe-Mg}^{cpx-il}$ co-efficients have been experimentally calibrated as a function of temperature and pressure by Bishop (1980), who showed the solid solutions

exhibit a significant departure from ideality. A good agreement was observed between experimental results and thermodynamic calculations in the opx-il system, and less so in the cpx-il system.

Miscibility relations in the system albite-Kfeldspar-anorthite were calibrated by many workers, and it has been shown that below 800°C little solid solution occurs between plagioclase and the alkali feldspars. Stormer (1965) calibrated the partitioning of albite between plagioclase and alkali feldspars, taking into account non-ideality and the effects of pressure, obtaining results in agreement with Seck's (1972) experimental data. Low temperature exsolution in feldspars may be a problem in applying the two-feldspar geothermometer, which can be overcome by defocused beam (averaging) electron probe analysis. In the present study temperatures are read directly from Stormer's (1965) albite partitioning graphs.

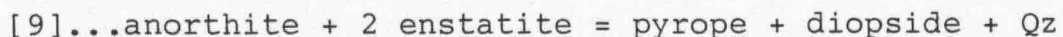
[2] GEOBAROMETERS

[7]...anorthite + enstatite = 1/3 grossular + 2/3 pyrope + Qz

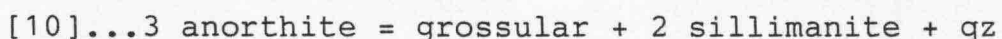
[8]... anorthite + diopside = 2/3 grossular + 1/3 pyrope + Qz

These pressure-sensitive reactions have been calibrated by Perkins and Newton (1981) from measured thermodynamic data, improving on earlier incomplete data sets. Calculations of activity coefficients of garnet take the symmetrical excess energy Margules parameters and effects of other components into account, K of reaction 7 being defined as replaced by $(a_{Ca}^{gt})(a_{Mg}^{gt})^2 / (a_{en}^{opx})(a_{an}^{plg})$ replaced by a_{di}^{cpx} for reaction 8. Pyroxene activities apply the two site approach of Wood and Banno (1973). Pressures obtained by this method are close to those derived by Hensen's (1981) two-pyroxene-garnet

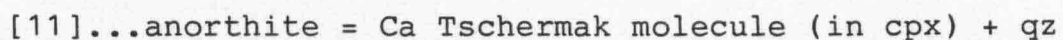
plagioclase-quartz barometer.



representing the pressure dependant transition from the low-pressure opx-plg subfacies to the high-pressure cpx-almandine subfacies. The presence of quartz as a product is important, as in undersaturated rocks the reaction occurs at lower pressures. Hensen (1981) calibrated the P-T curve of this reaction as a function of Mg/Fe and Ca/Na relations, K being the function of the activity ratio. In the present study the activities were calculated following the method by Perkins and Newton (1981) as suggested by Harris et al. (1982).



As the $K^{\text{an-gt}}_{\text{D:Ca}}$ is pressure-dependant (large V values) and is also affected by the almandine and pyrope activities in garnet. In this study the equilibrium constants derived by Ghent (1976) on the basis of the experimental study of pure phases were used in conjunction with activity coefficients of garnet calculated according to the method by Newton and Haselton (1981). Essene (1982) points to potential problems with this geobarometer, including the small fraction and thereby analytical uncertainty of $X^{\text{gt}}_{\text{Ca}}$, the uncertainties in activity coefficients of garnet and anorthite below 600° and the effects of andradite. However, he concludes it is one of the most reliable geobarometers available.



This reaction has been calibrated by Gasparik and Lindsay (1980). Difficulties arise due to the substitution of the Tschermak molecule $\text{CaAl}_2\text{SiO}_6$ by $\text{CaTiAl}_2\text{O}_6$ or CaFeSiAlO_6 . However, many granulite facies clinopyroxenes fall close to the diopside-hedenbergite join (Essene, 1982). Application of this barometer gives results which are somewhat

scattered as compared to other methods. Ellis (1980) recalibrated this reaction from thermodynamic data of Robie and Waldbaum (1968) and using K values $(X_{CT}^{cpx})/(X_{an}^{plg})$. Obtained pressures for clinopyroxenes with X_{CT}^{cpx} below 0.35 and neglect of non-ideality yield pressures low by Ca 1-2 kb compared to other P barometers.

Electron probe analyses used in calculating pressures and temperatures in the present study are listed in Table II.1. Ferrous/ferric iron distribution has been calculated on the basis of ideal formula numbers of oxygens for clinopyroxene, orthopyroxene and ilmenite, but not for gnt-bi pairs in view of the difficulties in assuming Fe^{+3}/Fe^{+2} partitioning in these minerals.

[3] MT HAY BELT

The common assemblage opx-cpx-plg (+/-biotite, amphibole, ilmenite) which dominates the Mt Hay granulites and abounds as relics in the Mt Chapple, Redbank Hill and Mt Zeil belts can be studied by reactions [4], [5], [6] and [11] above. Evidence for equilibrium in these assemblages includes: (1) compositional uniformity of the various phases, as evidenced by small standard deviations, and (2) the lack of clear replacement relations between phases, suggesting near equilibration. Evidence for reaction [11] requires the presence of quartz. Distribution of quartz in the basic granulites is uneven, and it is commonly concentrated in stringers and felsic feldspar-quartz bands, suggesting secondary remobilisation. Thus, it is not possible to determine whether the quartz is derived by reaction [11] or is introduced allochthonously. Temperature estimates for the basic granulites vary according to the reaction applied. The cpx-opx geothermometer (reaction 4) results in close clustering of the Mt Hay and Redbank Hill rocks in the 880-940°C range i.e. above the H_2O saturated gabbro solidus and below the dry gabbro solidus (Lambert and Wyllie, 1972) (Fig. VI.1). By

contrast, the pressure-dependant opx-il in the 650-750°C range and the cpx in the 540-700°C range for intermediate crustal P values. Re-equilibration of ilmenite during cooling is therefore evident. With the exception of two samples (S45, S237) the An-CaTs geobarometer (reaction 11) indicates very close clustering of the basic granulites, defining crustal pressures in the range 6.5-9.0 kb in a T range of 600-900°C. A well defined intersection between the cpx-opx and An-CaTs curves corresponds to $P = 6-6.7$ kb and $T = 880-930^{\circ}\text{C}$. If these parameters are accepted as minimum values for the metamorphism of the basic granulites, their location well above the wet gabbro solidus indicates that partial melting would have occurred provided PH_2O was high. The abundance of felsic to intermediate bands and stringers in the granulites and the occurrence of biotite and amphibole rich selvages along basic granulite-gneiss boundaries suggests anatexis has locally occurred. This conclusion accords with the strongly LIL-element depleted nature of some of the basic granulites (section III.1). Similarities between basic granulites of Mt Hay and relic basis granulites from Redbank Hill with respect to their mineralogy and thus PT parameters suggest possible derivation of the Redbank Hill bodies from more continuous basic bodies such as Mt Hay.

Felsic granulite stringer from Mt Hay is represented by sample S52, a Gt-Op-Hb-Bi-Plg-Qz' (+/-il, mt) granulite. The intersection between An-En-Gt-Qz geobarometer (reaction 7) and Bi-Gnt geothermometer (reaction 3) PT loci defines $T = 670^{\circ}\text{C}$ and $P = 5.9$ kb, lying on the wet gabbro solidus, in agreement with derivation by partial melting of hydrated granulites following peak metamorphic conditions (Fig. VI.2). A sample of Gnt-Si-Pl-Kf-Qz gneiss derived from a band intercalated with the granulites was studied, yielding an intersection about 580°C and 6.7 kb using the An-Gnt-Si-Qz geobarometer (reaction 10) and the two feldspars geothermometer values derived from Stormer (1965). This intersection plots within the kyanite field according to both Holdaway's (1971) and

Winkler's (1978) schemes, in contrast to the occurrence of sillimanite in the assemblage, and is thus unreliable. This could arise from re-equilibration of the two-feldspar thermometer and the low X_{Ca}^{gt} value of the garnet.

[4] MT CHAPPLE BELT

The occurrence of garnet-two pyroxene assemblages in the Mt Chapple belt, not observed at Mt Hay, enables the application of reactions [1], [7], [8] and [9] to their thermobarometry. In addition, the cpx-opx, opx-ilmenite, cpx-ilmenite, gnt-biotite and An-CaTschermak methods can be attempted, furnishing a means of evaluating the consistency of several geothermometers and geobarometers. Two samples have been studied:

S188 - Gnt-Op-Cp-Bi-Am-Pl-Qz granulite

S194 - Gnt-Op-Cp-Bi-Pl-Qz granulite

For petrographic description of these rocks refer to section II.2 .P-T plots according to the above schemes are presented in Fig. VI.3 and VI.4. As a reference point the intersections of PT loci for reaction [7] geobarometer and the cpx-gnt geothermometer according to Ellis and Green's (1979) geothermometer (reaction [1]) are taken as relatively reliable indicators in accord with the literature (Essense, 1982; Harris et al., 1982). For sample S188 this defines $T = 770^{\circ}C$ and $P = 8.1$ kb. For sample S194 this defines $T = 680^{\circ}C$ and $P = 7.3$ kb. Pressures according to either reaction [8] or Hensen's (1981) gnt-two pyroxene method (reaction [9]) are significantly lower, i.e. by 1-2 kb. Temperatures according to Saxena's (1979) and Dahl's (1980) gnt-cpx geothermometry are higher for S188 by 50-100 $^{\circ}C$ and similar or higher for S194. The cpx-opx thermometer yields only slightly higher (20-30 $^{\circ}C$) temperatures than the gnt-cpx method of Ellis and Green (1979). The

opx-ilmenite and cpx-ilmenite methods yield lower temperatures in this order. Thus, in so far as it is assumed that the geothermometers correspond to a single metamorphic episode, the equilibration sequence upon cooling progresses through reactions [4], [1], [3], [5], and [6] in this order. Alternatively, the error margins for these calibrations may mask the cooling sequence. The differences between temperatures yielded by the three cpx-gnt methods are within the errors indicated by their respective authors i.e. ± 40 C for Ellis and Green (1979), $\pm 30^{\circ}\text{C}$ for Saxena (1979) and $\pm 50^{\circ}\text{C}$ for Dahl (1980).

A sample of garnet-sillimanite gneiss (S135) collected from Mt Chapple belt allows comparisons between the PT value obtained by the above methods and those corresponding to reaction [10]. The PT conditions for these rocks can be further tested by the two-feldspar thermometer. The corresponding PT lines for equilibrium conditions of sillimanite-garnet gneiss sample S135, the two-feldspar thermometer defines a considerably lower temperature of ca 400°C , whose intersection with the PT line of reaction [10] would yield very low pressures. Thus, cooling re-equilibration of the feldspars is evident in these rocks.

As shown in figures VI.3 and VI.4 the intersections of PT loci for the more reliable geothermometers and geobarometers occur near or well above the H_2O saturated solidus of granite (Kerrick, 1972), tonalite (Lambert and Wyllie, 1974) and gabbro (Lambert and Wyllie, 1972). These relations, in analogy to those indicated by the Mt Hay mafic granulites, suggest that, under hydrous conditions, the Mt Chappel granulites were subjected to anatexis and palingenesis, in accord with field observations (sections II.1 and II.2).

[5] REDBANK HILL

Mafic granulite remnants display similar PT line intersections for the cpx-opx thermometer and An-CaTs barometer as the Mt Hay mafic granulites, namely between 6.4-7.8 kb and 900-920°C (Fig. VI.6). Likewise, the opx-il and cpx-il geothermometers yield progressively lower temperatures in the overall range of 850-550 °C. Temperature estimates for the porphyroblastic quartzofeldspathic gneisses are given by gnt-bi pairs in the general range of 600-700°C. The data can be interpreted in terms of a two-fold origin of the mafic granulites and the porphyroblastic gneisses, i.e. the former representing relics of Mt Hay type mafic granulites, and the latter products of later anatexis and metamorphism. Such dichotomy, however, implies little equilibration of the mafic granulites, and is subject to the uncertainties inherent in the thermometers. Sample S241B - a Gt-Bi-Am-Op-Plg-Qz gneiss allows both Gnt-Bi thermometry and Gt-Op-Plg barometry, yielding an intersection at 6.4 kb and 640°C. This point lies on the wet granite solidus of Kerrick (1972), and in the sillimanite field close to the boundary with the kyanite field. The somewhat high P/T ratio indicated by this intersection may support a possible development of the Redbank Hill porphyroblastic gneisses along an antecedent phase of the Redbank-Mt Zeil Thrust Zone.

[6] MT ZEIL BELT

Sample S376 - a Gt-Si-Bi-Kf-Plg-Qz gneiss derived from this belt allows Gnt-Plg barometry and Gnt-Bi thermometry. PT equilibrium loci for reaction [10] have low P/T ratios, and are intersected by the Gt-bi PT line at low pressures of about 1.5-2.5 kb at ca 600°C (Fig.VI.7), which is consistent with the temperature deduced from the two-feldspar geothermometer of Stormer (1965). Whereas sillimanite occurs in the rock, the intersection of PT lines occurs close to the andalusite field, suggesting low pressure equilibration. Alternatively, the assemblages may not signify equilibrium conditions, due to later recrystallisation.

[7] THE SOUTHERN BLOCK

Mineral assemblages observed in the Derwent Paragneiss, Dashwood Migmatite and Teapot Granite do not contain pyroxene and only rarely contain garnet or sillimanite. For this reason geobarometry is difficult to pursue, although further sampling may unravel suitable parageneses. Geothermometry can be conducted using the two-feldspar method (Stormer, 1965) and hornblende-plagioclase assemblages according to Spear (1980). The latter method depends on an estimate of Fe^{+3} in amphibole, which affects assignment of Na to the M4 site, to determine the K_D value $(X_{\text{Ca}}/X_{\text{Na}})\text{Plg}/(X_{\text{CaM4}}/X_{\text{Na}})\text{Am}$ and is thus uncertain. Temperature estimates based on coexisting Gnt-Biot in sample S830A was not possible due to the almost pure grossular composition of the garnet (CaO - 23-24%).

Two feldspar thermometry assuming 5 kb pressure suggests an equilibration temperature of 579°C for Bi-Plg-Kf-Qz

assemblage forming a felsic band in gneiss of Derwent Paragneiss temperature estimates for two samples of Teapot Granite are as follows:

S537 - Bi-Kf-Plg-Qz granite

core - ($X_{ab}^{Kf} = 0.048$; $X_{ab}^{Plg} = 0.67$) - ca 400°C

rim - ($X_{ab}^{Kf} = 0.017$; $X_{ab}^{Plg} = 0.68$) - 200-300°C

S538 - Bi-Kf-Plg-Ep-Sp-Qz granite

core - ($X_{ab}^{Kf} = 0.046$; $X_{ab}^{Plg} = 0.71$) - below 400°C

rim - ($X_{ab}^{Kf} = 0.051$; $X_{ab}^{Plg} = 0.69$) - below 400°C

It thus appears that the feldspars have re-equilibrated during cooling or upon retrograde metamorphism, and can not provide an indication for primary igneous temperatures of the Teapot Granite. This observation is consistent with the deformed and widely retrogressed nature of the Teapot Granite between the Redbank-Mt Zeil thrust zone and the Mt Sonder-Mt Razorback thrust fault. The lack of suitable geobarometers for samples collected from the southern block does not allow an estimate of the amount of vertical displacement along the Redbank-Mt Zeil thrust zone.

[8] IMPLICATIONS FOR GEOTHERMAL GRADIENTS

The P-T estimates discussed above allow an insight into the evolution of geothermal gradients in the northern granulite block. Application of reactions [4] and [11] to mafic granulites of Mt Hay outline a P-T intersection region corresponding to an average gradient range of 44-51°C/km. Lower geotherms are suggested by felsic to intermediate bands in the mafic granulites. The PT estimate for S52 - a Gnt-Opx-Am Bi-Plg-Qz felsic granulite - applying reactions [3] and [7], corresponds to an average gradient of 38°C/km. Garnetiferous granulites from Mt Chapple indicate an average geotherm of 32°C/km for sample S188 and 31°C/km for sample S194, applying reactions [1] (Ellis and Green, 1979) and [7] (Perkins and Newton, 1981). Garnet-sillimanite gneisses from Mt Chapple define lower gradients, i.e. 25-28°C/km for sample S51, applying reaction [10] (Newton and Hasleton, 1981) and the two-feldspar thermometer (Stormer, 1965). For Redbank Hill samples, mafic granulites define an average range of 39-47°C/km (according to reactions [4] and [11]) while porphyroblastic garnet-biotite gneiss (S241B) defines an average gradient of 33°C/km, using reactions [3] and [7]. A consistent trend thus appears to pertain, which involves a geothermal decline from the period during which the mineral assemblages of the mafic granulites equilibrated to the stage at which intermediate granulites of the Mt Chapple type and felsic-intermediate stringers within the Mt Hay mafic granulites equilibrated. Since the latter are likewise of granulite-facies mineralogy, it follows that granulite facies metamorphism has persisted before and during the migmatization/anatectic stage that produced the felsic magma. If so, the retention of higher PT mafic granulites alongside the felsic rocks suggests non-equilibration of the basic mineral assemblages upon the decline in pressure and temperature, possibly due ^{to} low diffusion rates related to their anhydrous non-reactive state. The differences of geothermal gradients between felsic-intermediate components

of the Mt Hay, Mt Chapple and Redbank Hill could be taken to imply a protracted or multiphase anatectic history of these bodies, i.e. separate igneous events pertaining to each of the units. However, pending detailed isotopic studies of these rocks such a conclusion remains unwarranted, particularly in view of the possible original location of these bodies at different crustal levels and the possible existence of major structural discontinuities between them.

It is instructive to compare the above PT estimates with those obtained in the Strangways Range granulites, approximately 80 km ENE of Mt Hay. Warren (1983) has identified nine stages in the evolution of this terrain, including (1) deposition of a bimodal volcanic suite and sediments; (2) migmatisation; (3) dry granulite facies metamorphism, where $P = 8 \pm 1$ kb and $T = 850-920^\circ\text{C}$ were estimated for the western area; (4) hydration represented by biotite/phlogopite; (5) isobaric cooling to normal gradients in the kyanite stability field; (6) development of kyanite ($T = 650-720^\circ\text{C}$ and $P = 7.5-8.7$ kb); (7) uplift and development of cordierite; (8) isobaric cooling and development of sillimanite and staurolite; (9) hydration/deformation and development of chlorite upon retrogression. The geothermal gradient estimated for stage (3) at about $35-38^\circ\text{C/Km}$ is similar to that of felsic granulite bands in the Mt Hay block. The gradient for stage (6) at about $25-32^\circ\text{C/km}$ is similar to that of garnet-sillimanite gneisses from Mt Chapple. Further isotopic and mineralogical studies are required to establish correlations between the two terrains.

FIGURE CAPTIONS FOR SECTION VI

Pressure-temperature equilibria loci calculated from mineral chemistry data for reactions denoted along the plotted PT loci. For explanation refer to text. Sample numbers are indicated along diagram margins. Solid symbols indicate intersections of PT loci of different reactions for the same samples

VI.1 basic granulites

VI.2 felsic gneiss/granulite, Mt Hay

VI.3 garnet-pyroxene granulite, S188, Mt Chapple

VI.4 garnet-pyroxene granulite, S194, Mt Chapple

VI.5 sillimanite-garnet gneisses, Mt Chapple

VI.6 Redbank Hill granulites and gneisses

VI.7 garnet-sillimanite gneiss, Mt Zeil belt

A - H₂O-saturated granite solidus (Kerrick, 1972)

B - H₂O-saturated tonalite solidus (Lambert and Wyllie, 1974)

C - H₂O-saturated gabbro solidus (Lambert and Wyllie, 1972)

D - dry gabbro solidus (Lambert and Wyllie, 1972)

E - Andalusite-sillimanite-kyanite trip le point (Holdaway, 1971)

F - andalusite-sillimanite-kyanite trip le point (Winkler 1979)

Fig. VI.1
BASIC GRANULITES

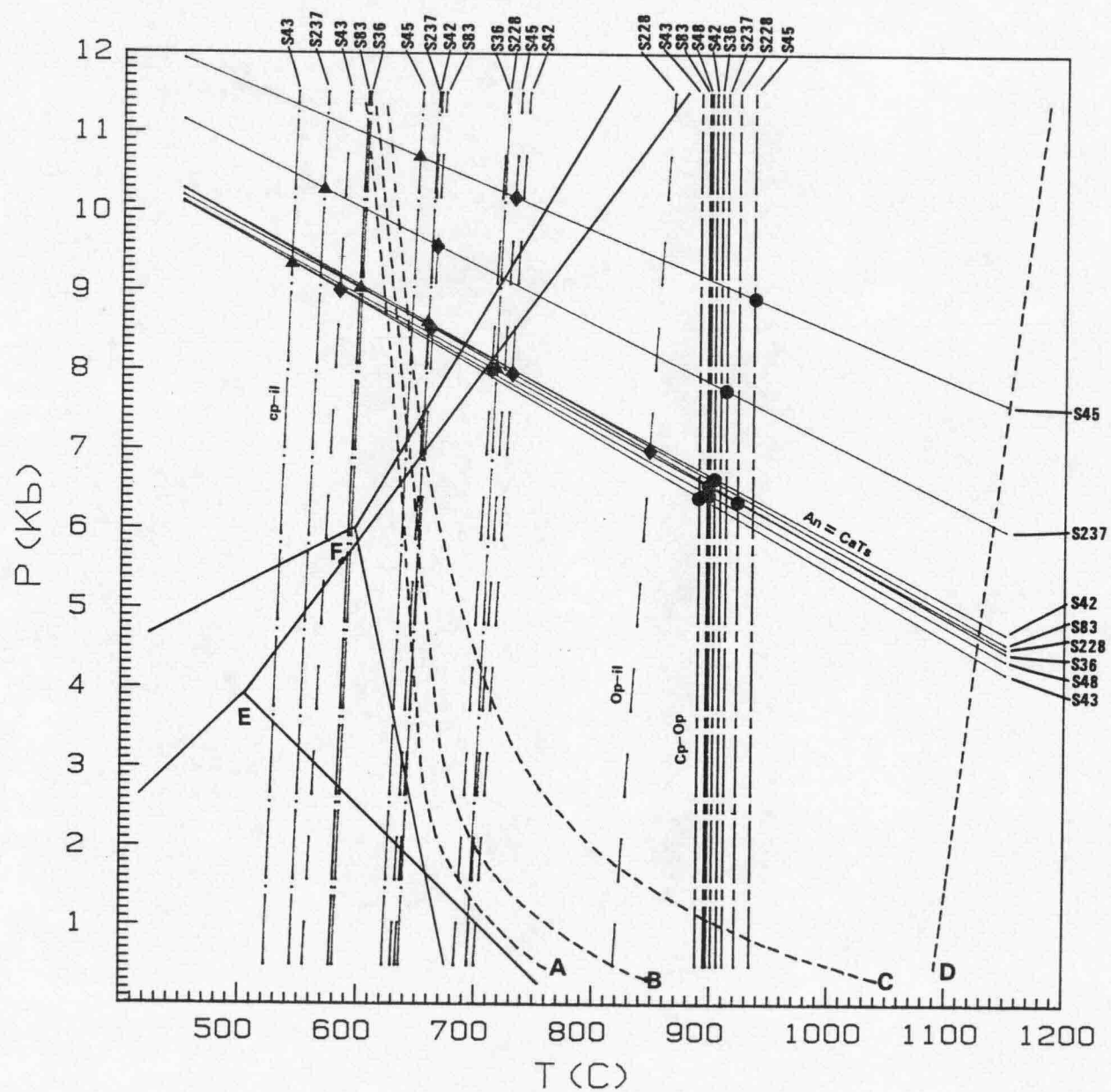


Fig. VI.2

FELSIC GNEISS/GRANULITE - Mt HAY

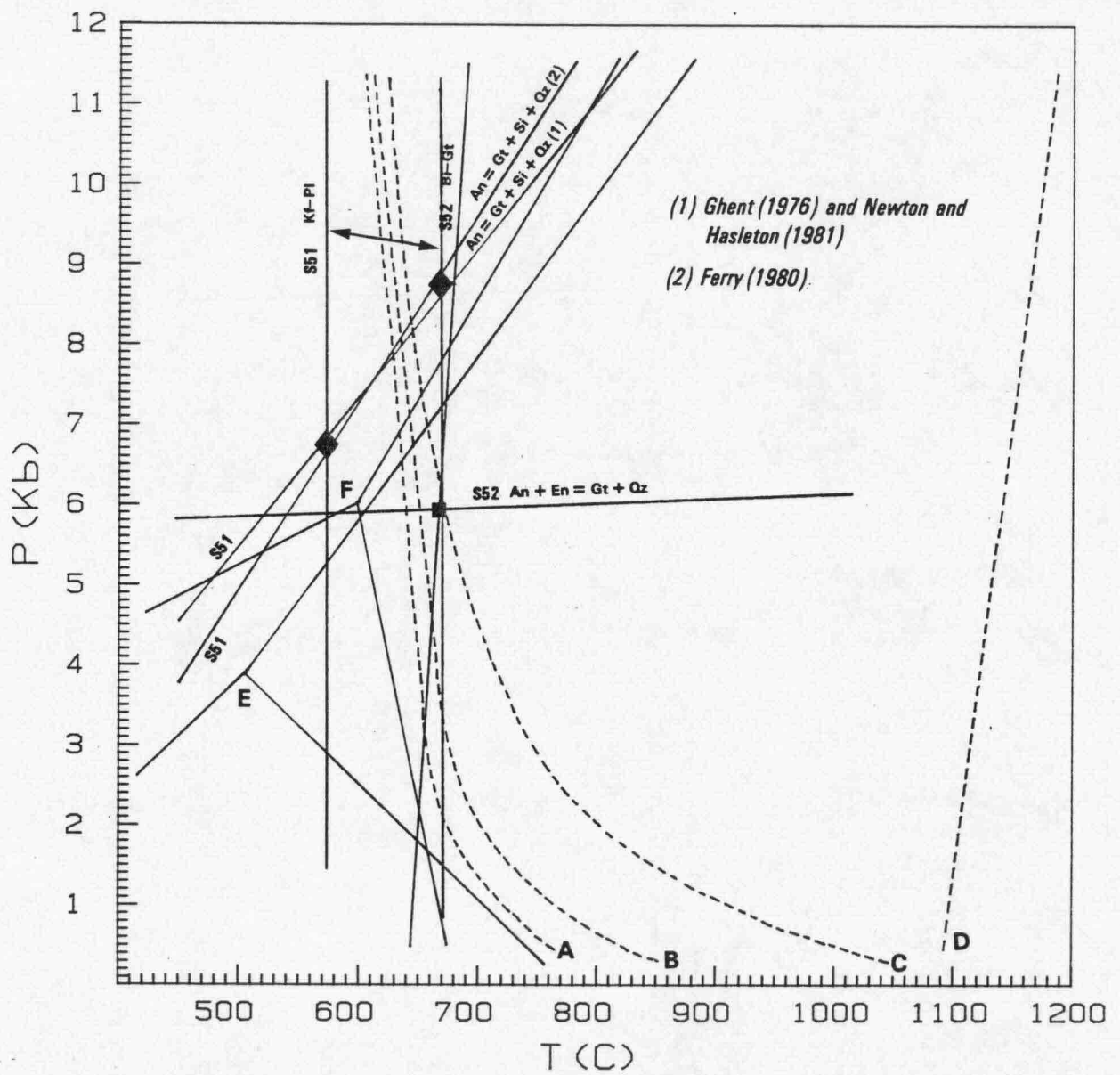


Fig. VI.3

S188 - Gt-Op-Cp-Bi-Am-Pl-Qz GRANULITE
Mt CHAPPLE

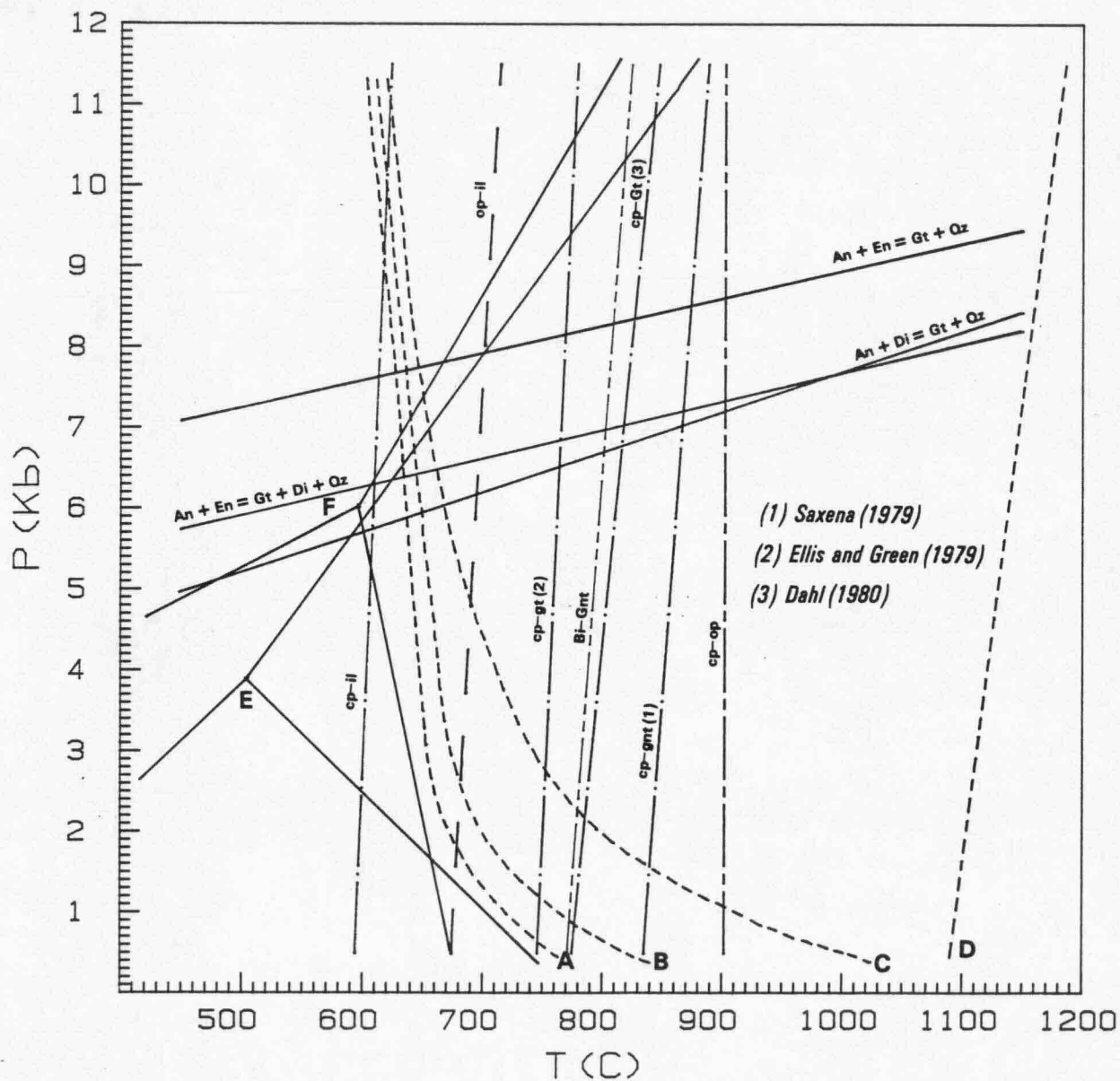


Fig. VI.4

S194 - Gt-Op-Cp-Bi-Pl-Qz GRANULITE
Mt CHAPPLE

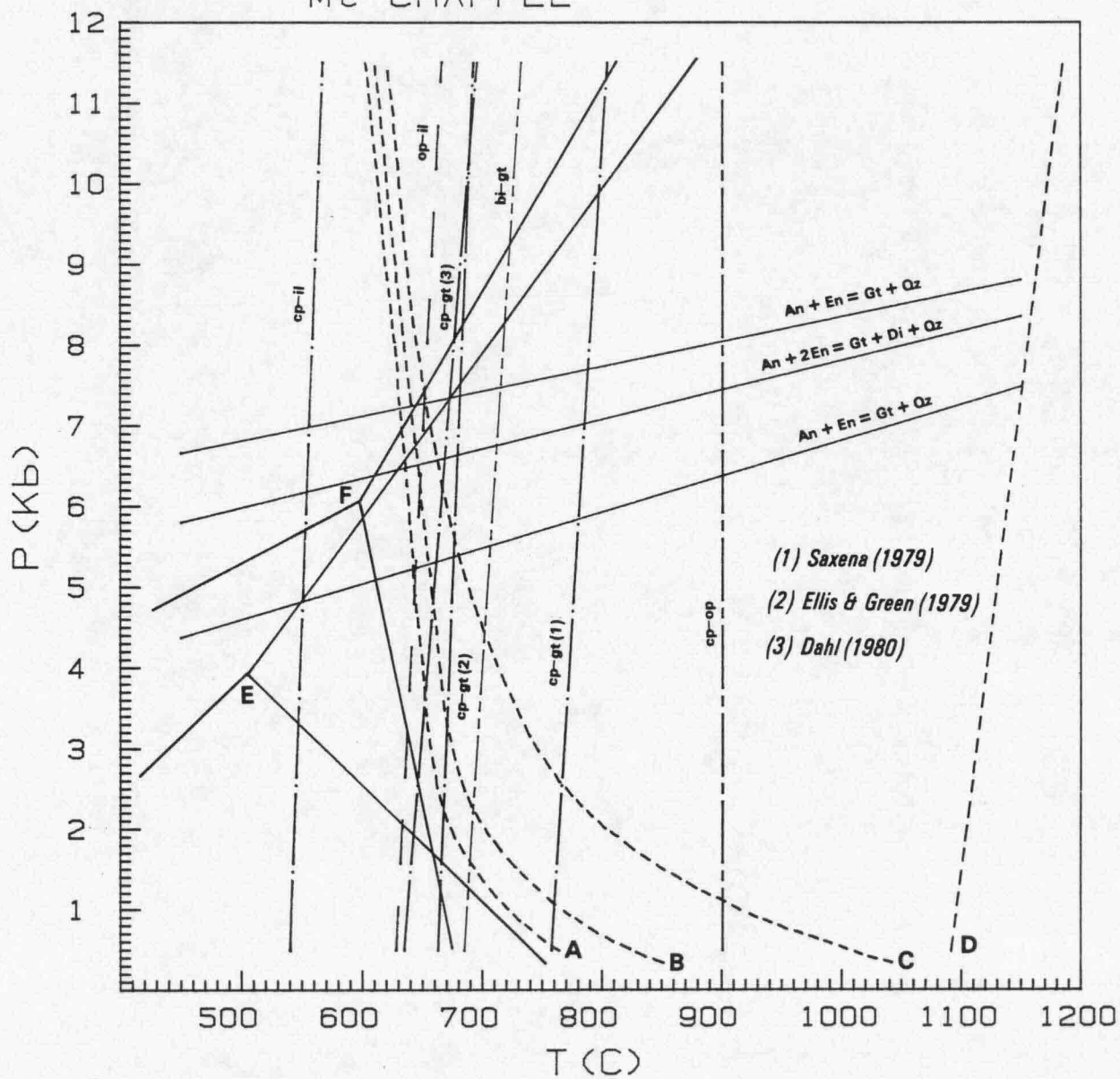


Fig. VI.5

Mt CHAPPLE BELT
SILLIMANITE-GARNET GNEISSES

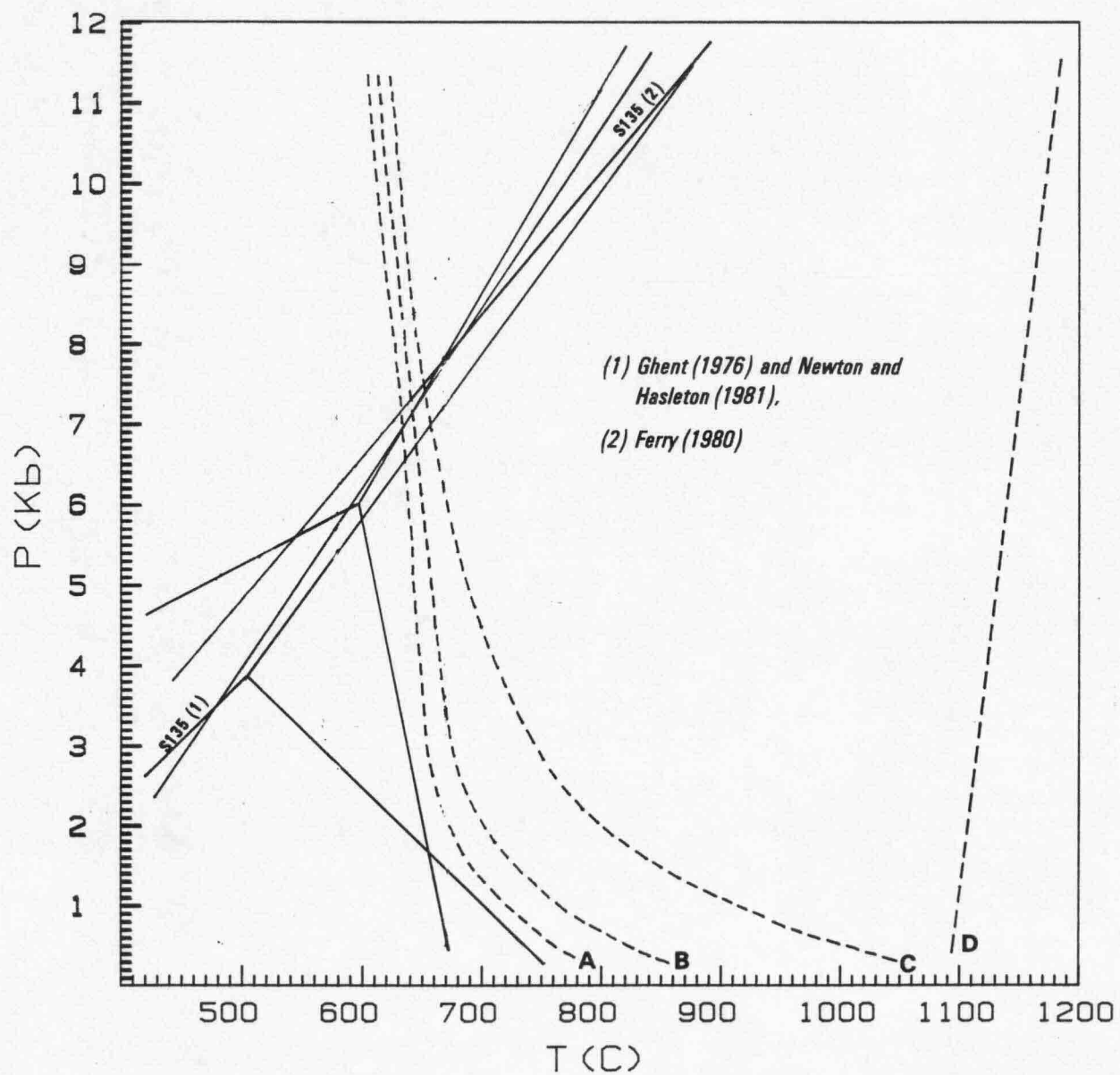


Fig. VI.6

REDBANK HILL GRANULITES & GNEISSES

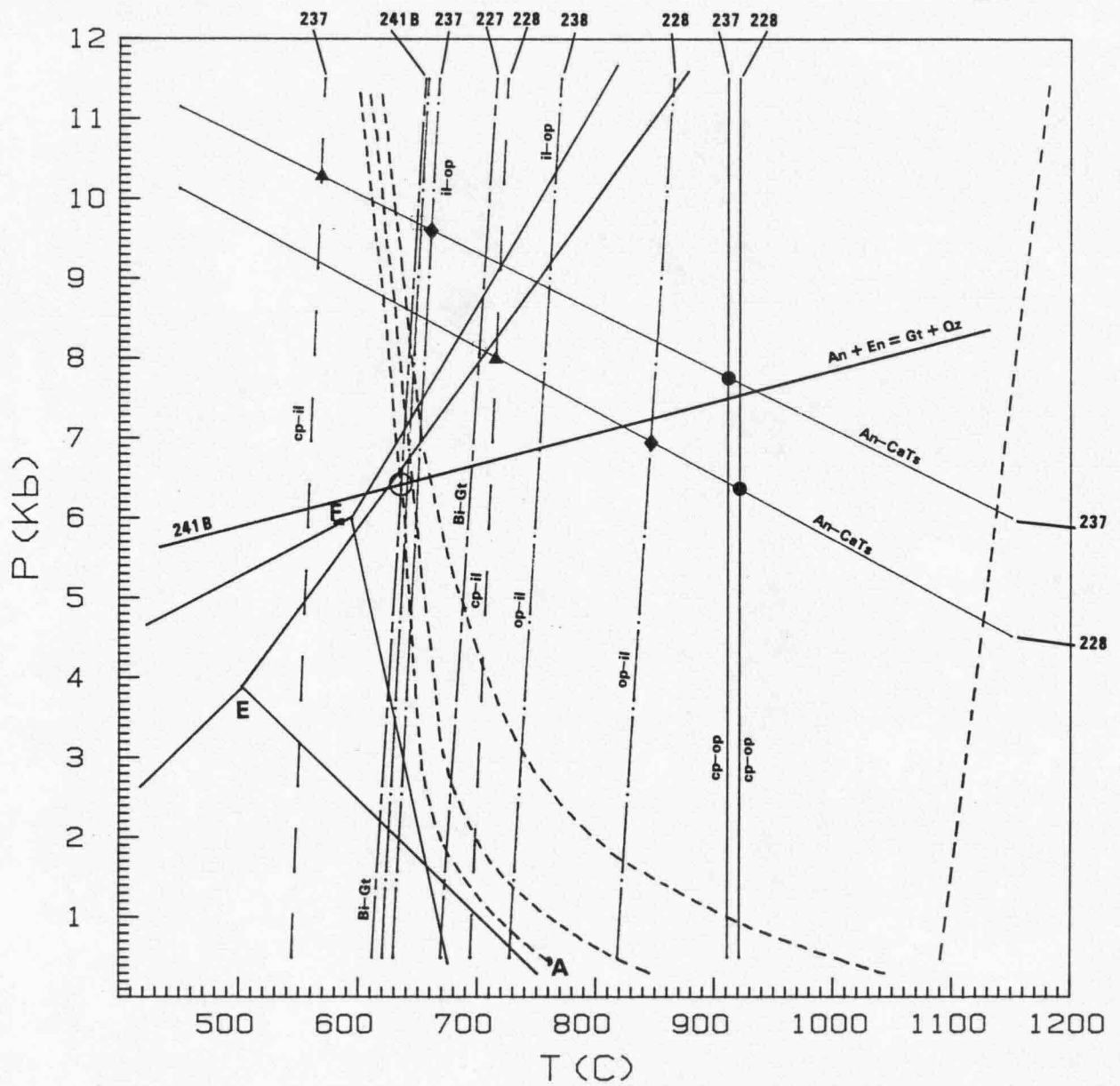
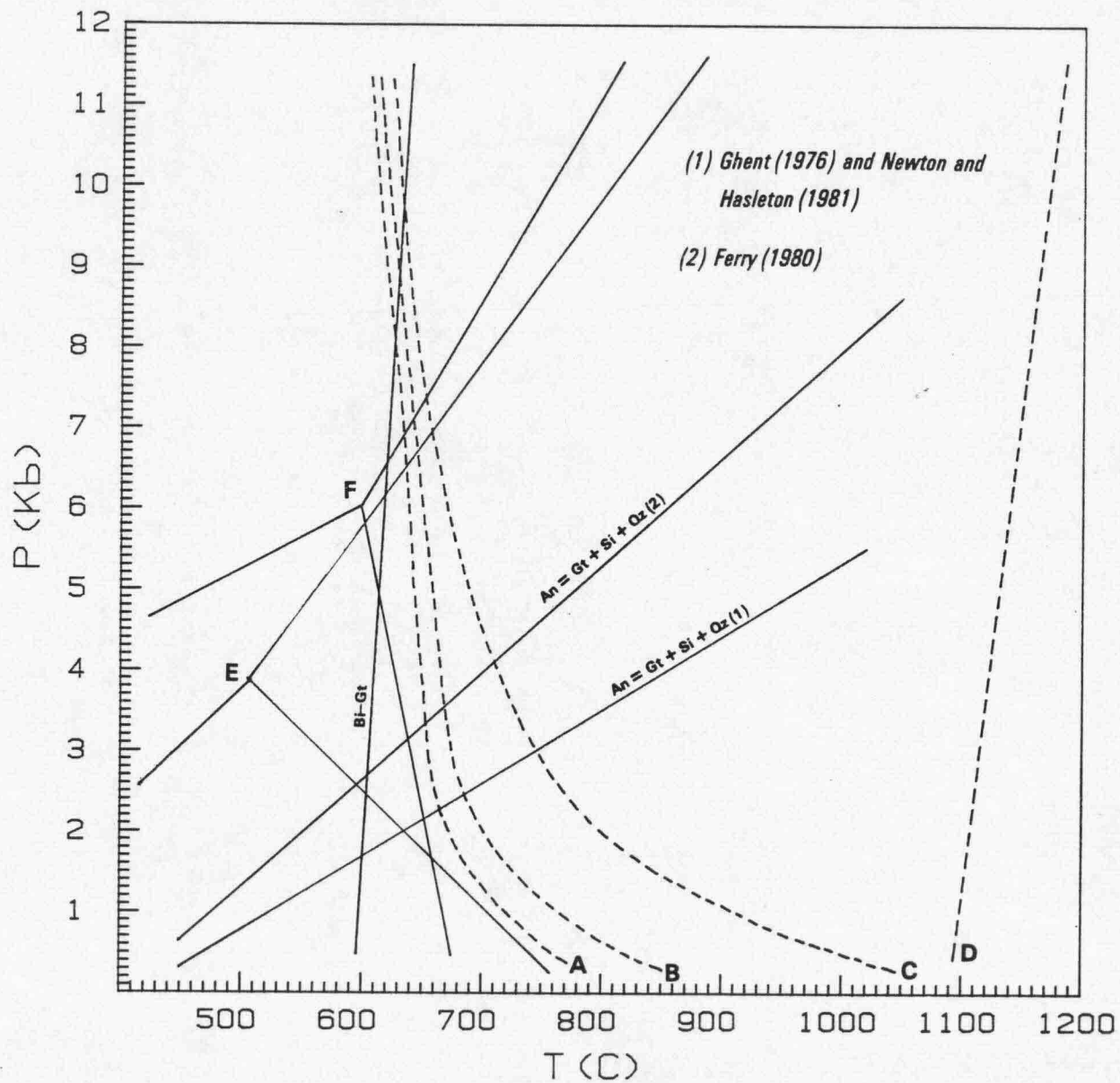


Fig. VI.7

S376 - Gt-Si-Bi-Kf-Pl-Qz GNEISS
Mt ZEIL BELT



VII. IMPLICATIONS TO CRUSTAL STRUCTURE AND EVOLUTION

[1] GEOPHYSICAL-GEOLOGICAL CORRELATIONS

Figure VII.1 displays airborne gamma-ray radiometric anomaly patterns for the northern part of HERMANNSBURG 1:250 000. The survey (BMR, 1976) has been flown along NS lines spaced 500 m apart at 100 m a.g.l. A ground total magnetic intensity and radiometric survey has been conducted by BMR in the MOUNT LIEBIG and MOUNT RENNIE 1:250 000 areas in the west, including collection of samples for magnetic susceptibility, remnant magnetisation and specific gravity tests (Mutton et al., 1983). Fig. VII.2 displays Bouguer gravity anomalies for the northern part HERMANNSBURG 1:250 000 (Lonsdale and Flavelle, 1963). Fig. VII.3 displays airborne magnetic anomalies for the area of interest flown by BMR (1976). Correlation between geological features and the radiometric data indicate the following principal features: (1) The principal granulite outcrops, including Mr Hay, Mt Chapple, Redbank Hill and the Mt Zeil belt north of the RedbankMt Zeil Thrust Zone (RTZ) are matched closely by low radiometric anomalies; (2) Total radiometric reading is inversely related to the basicity of the rocks, with negative anomalies over mafic granulites. Thus, circular negative anomalies of ca 20 c/s (count per second) occur over the mafic granulites of the Mt Hay block, 60-80 c/s over mafic to intermediate granulites of the Mt Chapple range, 80-100 c/s over intermediate to felsic granulites of the Redbank Hill block. The felsic Mt Zeil belt granulite and gneisses correspond to anomalies in the 120-200 c/s range and also include a number of small radiometric highs, representing K-enriched zones within the granulite facies gneisses; (3) The Redbank-Mt Zeil Thrust Zone (RTZ) stands up clearly on the radiometric map due to sharp contrast between contour levels generally below 200 over granulites to the north and generally

above 200 over migmatite, granite and gneiss to the south; (4) The southern block, including the Teapot Granite, Dashwood Migmatite and Derwent Paragneiss, includes numerous circular position anomalies up to 600 c/s and smaller intermediate negative anomalies. The anomalies are strongest over the Teapot Granite, well developed over the Dashwood Migmatites, and weaker over the Derwent Paragneiss. These variations, reflecting the K, U and Th levels in the rocks, are consistent with the observed petrographic and geochemical characteristics of these formations (sections II, III, IV). Furthermore, the radiometric map provides an effective means of estimating the relative abundance of K-rich and K-poor lithologies where close interbanding renders such distinctions difficult to achieve; (5) Anomaly patterns over the Burt Plain north of Mt Hay and Mt Chapple Ranges consist of numerous NS elongated lows about 100 or 120 c/s. These may reflect relatively mafic granulite rock bodies, as observed in isolated outcrops. Two positive anomalies (up to 300 c/s) coincide with isolated hills of orthopyroxene-bearing intermediate to felsic granulite and garnetiferous felsic gneiss $132^{\circ}48' - 132^{\circ}53'$; $23^{\circ}02' - 23^{\circ}08'$.

A comparison between the Bouguer gravity map (Fig. VII.2) and principal geological features indicates the following: (1) A major positive gravity anomaly of +50 mgl, the Papunya Gravity High, coinciding at its centre with the positive radiometric anomalies and isolated outcrops of intermediate orthopyroxene biotite granulites and garnet-biotite gneiss in the Burt Plain, ca 20 km N of the Mount Chapple ridge. (2) A steep gravity gradient of over 3 mgl/km from N to S, from a maximum of +50 mgl over the Burt Plain to a minimum of -120 mgl over the Teapot Granite. (3) The gravity contours and the Redbank - Mt Zeil thrust zone are near parallel between $132^{\circ}20' - 132^{\circ}45'$ where the trace of the RTZ almost coincides with the -105 mgl contour and intersect at low angles west of this area. It thus appears the gravity gradient may reflect the northward thickening of a dense granulite wedge thrust over the southern migmatite-gneiss-granite block. The coincidence of the centre

of the Papunya gravity high with a radiometric anomaly remains unexplained. The intermediate to felsic composition of isolated granulite outcrops in this area do not shed much light on the nature of these anomalies. However, the occurrence of localized positive anomalies under the Burt Plain and at the peripheries of the large granulite massifs (Fig. VII.1) suggests that K-rich rocks may perhaps be more common beneath the alluvial cover, a possibility consistent with the generally stronger weathering of K-feldspar-rich rocks.

Significant correlations are observed between the air-borne magnetic anomaly map (Fig. VII.3) and observed lithological and structural features (see Mutton et al., 1983). The granulites north of the RTZ are significantly more disturbed than the Teapot Granite and Dashwood Migmatite to the south, demarcating the thrust fault along most of its length (Fig. VII.3). The Derwent Paragneiss displays weakly disturbed patterns. The significance of the anomalies within the northern granulite block, however, is difficult to interpret. For example, major linear positive anomalies occur immediately north of the Mt Hay, Mt Chapple and Mt Zeil ridges, as compared to lower magnetic intensities over the exposed granulite massifs themselves. The anorthosite-basic granulite body of the northern Mt Hay ridge coincides with a strong positive anomaly (5961 nZ) whereas granulites of the southern Mt Hay ridge form a magnetically quiet zone. Well pronounced anomalies occur over the Burt Plain north of the Mt Chapple ridge. The factors underlying these features remain unclear.

[2] EVOLUTION OF THE NORTHERN GRANULITE BLOCK

Because of their separation by the Redbank-Mt Zeil thrust zone (RTZ), the temporal relations between the northern granulite block and the southern gneiss/migmatite/granite block can only be determined by isotopic methods. Primary spatial relations in the crust may be elucidated through thermobarometry, allowing an idea as to the depth at which the mineral assemblages^a equilibrated (section VI). Available geochronological data for the area concerned and adjacent terrains are tabulated in Table VII.1.

The oldest isotopic ages recorded in the Arunta Block are from banded mafic-felsic granulites in the Strangway Range, 80 km east and north of the Mt Hay-Mt Chapple belt. Windrim and McCulloch (1983) reported a Sm-Nd isochron age of 2015 ± 120 m.y. ($\text{ENd}^{(I)} = +1.4$) and a Rb-Sr isochron age of 2085 ± 175 m.y. ($R_i = 0.70249 \pm 0.00019$), representing isotopic homogenisation of felsic and mafic compositional bands. These could well be of primary late-igneous age. An alternative interpretation in terms of age resetting is less likely in view of the relative immobility of rare earth elements. In so far as similar primary ages may be assumed for the Mt Hay-Mt Chapple granulite belts, these relations suggest an anatectic/intrusive development of felsic neosome bands at a time isotopically indistinguishable from the basic igneous activity which gave rise to precursors of the metamorphosed mafic rocks. In the Strangways Range a supacrustal origin for the mafic rocks is suggested by the presence of metasedimentary and possibly metavolcanic matrix (Warren, 1983). However, in the Mt Hay-Mt Chapple belts similar age relations may also be consistent with a deep crustal origin of the basic rocks. Had precursors of the mafic granulites been of supacrustal nature, an isotopically significant time interval could perhaps be expected between magmatic activity, burial and regional metamorphism. In the Mt Hay-Mt Chapple belts deep crustal origin is favoured by (1) the associated anorthosites, typically rocks of deep level

emplacement; (2) the uncertainty whether supracrustal material exists in this terrain; (3) the large dimensions of the Papunya gravity anomaly, reflecting a three dimensional scale of the mafic granulite body akin to that of a major crustal uplift; (4) the dry nature of the Mt Hay granulites, i.e. the relatively minor role of amphibole and biotite.

The earliest recognizable deformation of the Mt Hay and Mt Chapple mafic granulites (D1) is reflected by lit-par-lit injection of felsic magma fractions. However, in so far as D1 elements may be masked by remobilisation of felsic neosome during D2, a distinction between the two phases is difficult. Typically, felsic bands and stringers are dominated by plagioclase, whereas wider bands and intermediate-scale granitoid bodies contain abundant Kfeldspar and quartz, indicating increased magmatic fractionation associated with magmatic segregation. Forceful injection intrusion was locally associated with folding and brecciation, producing migmatites and agmatites (Fig.II.1). The consequent compositional banding (S1) may have been superposed on primary igneous layering (S0) in the parental rocks, now undetectable except in anorthosites (Fig. II.3). No consistent folding orientation is discerned in these magmatic/anatectic flow folds (F1). It is possible that much of the flow folding was related to neosome remobilization during later high grade metamorphism, which would be expected to have reset Rb/Sr isotopic systems. Such resetting of Rb-Sr ages is reported from both the Strangways Range (1800 ± 25 m.y., $R_i = 0.70722$; Windrim and McCulloch, 1983) and from Mt Hay (1768 ± 20 m.y., $R_i = 0.7085$; 1728 ± 65 m.y., $R_i = 0.706$; Black et al., 1983). This event may either signify a temporally distinct high-grade metamorphic episode or, alternatively, represent the waning through uplift and cooling of long-term infracrustal metamorphism during 2.0-1.8 b.y. ago. The high R_i values are consistent with a metamorphic origin. The metamorphism was associated with development of S2 gneissosity and F2 isoclinal folding according to a steeply NE plunging axial lineation (L1) - representing the dominant

deformation (D2) within the northern granulite belts (Fig.V.1). A synmetamorphic nature of the penetrative gneissosity and lineation/folding is suggested by the control of crystallisation of the metamorphic minerals according to these fabrics. Remobilisation of neosome felsic phases and their emplacement as small granitoid bodies throughout the mafic to intermediate granulite terrain resulted in intrusion-related deformation which departs from the consistent tectonic fabric denoted above. Prograde metamorphism is represented by replacement reactions from amphibole to orthopyroxene or clinopyroxene, followed by late stage biotite, which in some instances is replaced by garnet. These relations suggest introduction of a K-bearing fluid phase toward the close of, or later than, the high grade metamorphic stage, probably about 1.8 b.y. ago. The observation that late-stage biotites are often little aligned suggests that this metasomatism occurred upon relaxation of regional stress. It is likely that introduction of K to the mafic granulites was associated with late-stage remobilization of felsic neosome phases.

It is possible that a protracted ca 200 m.y. long cooling period reflected by the Sm-Nd and Rb-Sr ages corresponds to the geothermal decline reflected by the Mt Hay granulites, i.e. from ca. 880-930°C for cpx-opx pairs to 650-750°C for opx-ilmenite pairs under 6.5 - 9.0 kb range (chapter VI.3). Toward the close of this period partial melting under high H₂O is indicated by felsic stringers in the Mt Hay granulites. Similar conclusions can be drawn from the Mt Chapple belt, where granulite facies metamorphism under 680-770°C and 8.1-7.3 kb was succeeded by anatexis conditions under lower temperature and higher partial H₂O pressures.

S2 foliation in the granulites are deflected by mostly northplunging flexures and open folds (F3) representing deformation (D3) probably of post - 1.8 b.y. age. These folds predate ductile deformation along the Redbank-Mt Zeil thrust zone (RTZ) (D4) and its associated fault splays and regional

cataclasis, as suggested by the superposition of drag folds (F4) in the vicinity of the thrust. The thrusting (D4) was associated with retrograde metamorphism resulting in cataclastic/mylonitic zones described in Chapter IV. The age of D4 is believed to correspond to a whole rock-mineral (K-feldspar) Rb-Sr age of 893 ± 97 m.y. ($R_i = 0.756 \pm 97$) reported by Black et al. (1983) for porphyroblastic gneiss at Redbank Hill just north of the Redbank-Mt Zeil thrust zone. In summary, the following deformational stages are tentatively suggested for the northern granulite belts:

D1 - Intrusion of lit-par-lit felsic magma into infracrustal basic rocks probably about 2.0 b.y. ago, producing lit-par-lit injection forming S1 banding and irregular F1 magmatic folding of S1 banding. The layering of the Mt Hay anorthosite is classified as S0 banding.

D2 - Granulite facies metamorphism, possibly continuous between 2.0-1.8 b.y., producing S2 gneissosity, L1 lineation defining F2 folding, and local migmatitic flow folding and agmatitic fragmentation resulting from remobilisation of felsic material and possible further anatexis of mafic granulites. Metamorphism and recrystallisation must have outlasted the emplacement of the felsic gneiss, since no clear magmatic texture is preserved in these rocks.

D3 - Open folding and flexure with steeply N-plunging axes (F3)

D4 - Thrusting, shearing and drag folding (F4) associated with the development of the Redbank-Mt Zeil thrust zone about 1.0 b.y. ago and probably also during the ca 0.4 b.y. Alice Springs Orogeny (Marjoribanks, 1975)

This structural sequence is similar to that described in the Strangeways Range granulites by Shaw and Langworthy (in prep.) as follows: F1 - mesoscopic intrafolial folds; F2 -

isoclinal folds of N-dipping E-striking axial planes; F3 - open folds of N-trending axes; F4 - open folds cutting across the F3 axial trends.

Marjoribanks (1975) suggested that felsic gneiss units at Mt Hay and Mt Chapple and porphyroblastic felsic gneiss at Redbank Hill can be correlated with migmatites of the Ormiston zone south of the Redbank-Mt Zeil thrust zone, and that granulite facies metamorphism was related to and concomitant with early thrusting. This interpretation is related to a view of the southeastern part of Redbank Hill as an integral part of the Redbank-Mt Zeil deformed zone. However, this concept is in disagreement with observations arising from the present survey:

(1) Redbank Hill constitutes an integral part of the granulite-facies terrain, as indicated by mineral assemblages (chapter II.3). There is little basis for distinguishing between amphibolite facies porphyroblastic felsic gneiss fractions which intrude the mafic and intermediate granulites at Redbank Hill and amphibolite to granulite facies porphyroblastic gneisses which pervade the Mt Hay, Mt Chapple and Mt Zeil granulite belts. The coarser grained development of feldspar-quartz glomeroblasts at Redbank Hill may be related to an origin under higher strain conditions, supported by the "moon-tail" type of augen deformation. Redbank Hill is intersected and bordered by a number of younger shears and faults marked by cataclasites and mylonites and clearly related to younger deformation (D4) along the Redbank-Mt Zeil thrust zone to the south.

(2) Rb-Sr isochron ages of Mt Hay banded mafic-felsic granulites at ca 1.8 b.y. are significantly older than Rb-Sr ages of southern block gneisses and migmatites (Potrock Gneiss, ca 1.6 b.y.; migmatite, ca 1.05 b.y.; Marjoribanks and Black, 1974). The ca 0.9 b.y. Rb-Sr whole rock-feldspar age of porphyroblastic gneiss at Redbank Hill (Black et al., 1983) may well reflect isotopic resetting related to the Redbank-Mt Zeil

thrusting. From available geochronological data the temporal relations between felsic gneisses in the northern and southern blocks remain unknown, nor can felsic gneiss or migmatites be traced between these blocks, since all units are sharply truncated by the thrust zone.

Pending U-Pb zircon and/or Sm-Nd age determinations in the southern migmatite-gneiss-granite terrain, two alternative interpretations of the northern granulite belts are possible: (1) the granulites are older than, and in some instances may have formed the basement for, the gneiss-migmatite-granite terrain, an interpretation favoured by Offe (1983); (2) the granulites represent deep crustal coeval root zones of the amphibolite facies gneiss-migmatite-granite terrain. The question will be discussed further below.

[3] EVOLUTION OF THE SOUTHERN GNEISS-MIGMATITE-GRANITE BLOCK

A detailed structural study of HERMANNSBURG (1:100 000) was conducted by Marjoribanks (1975), whose observations are in part also applicable to adjoining western parts of the southern block, including the Dashwood Migmatite and Derwent Paragneiss. This author has defined the following units:

(1) Chewings Range Zone (CRZ) - quartzofeldspathic gneiss, pelitic to semipelitic gneiss, quartzite.

(2) Ormiston Zone (OZ) - migmatized felsic gneiss, mica schist, quartzite, amphibolite and mylonitic rocks. At the core of the migmatites are a number of granitic bodies, the largest of which is the Teapot Granite. The Ormiston Zone migmatites are thought to represent granitized remnants of Chewings Range zone paragneisses.

Marjoribanks' (1975) classification is similar to that between the Derwent Paragneiss and the Dashwood Migmatite. Together, migmatites of the Ormiston Zone and Dashwood Migmatites form an aureole around the Teapot Granite and may be considered as the intrusive front of this pluton. If so, the lithological variations between the quartzite-pelite rich CRZ and the arenite-amphibolite rich Derwent Paragneiss may either represent lateral facies changes or different ages of these sequences. The minimum age of the CRZ is given by a total rock (TR) Rb-Sr isochron age of 1586 ± 69 m.y. ($R_i = 0.729$) of Potrock Gneiss (Marjoribanks and Black, 1974). The high R_i value indicates long crustal history and/or high Rb/Sr ratio of precursors of the gneiss. A TR-mineral Rb-Sr age for these rocks yields an age more similar to that of Ormiston Zone migmatites. The latter yield a TR-muscovite age of 1053 ± 50 m.y., considered by Marjoribanks and Black (1974) as representative of the migmatisation event. The migmatisation is thought by these authors to have postdated the onset of deformation along the Redbank-Mt Zeil thrust zone. Alternatively, the pervasive nature of migmatisation in the southern Block may have caused Rb-Sr age resetting in the contemporaneously metamorphosed Chewings Range Zone. In this case, the ca 1.6 b.y. age corresponds to migmatisation and regional metamorphism, whereas the ca 1.05 b.y. age is related to tectono-thermal effects induced by deformation along the Redbank-Mt Zeil thrust zone.

Structural elements in the Chewings Range Zone are in part correlatable with those in the Derwent Paragneiss. Marjoribanks (1975) distinguished the following deformation episodes:

D1 (Pre-Chewings Phase) - marked by rare F1 intrafolial folds which effect relic sedimentary layering (S1), and is mainly retained in pelitic and quartzitic units but not in felsic gneisses.

D2 (Chewings Phase) - marked by a strong S2 axial plane cleavage related to F2 folds. The schistosity transposes and partly obliterates the S1 layering. S2-S1 intersections (F2 fold axes) define L2 lineation.

D3 (Ormiston Phase) - local ENE-trending folds (F3) expressed as axial cleavage (S3) in quartzite in the Ormiston Pound area, and thought to originate by deflection induced by the Ormiston Pound granite and related migmatisation.

D4 (Mt Giles Phase) - major EW trending assymmetric open folds (F4) effecting the Chewings Range Quartzite but having little effect on gneisses to the north.

D5 (Alice Springs Phase) - uplift of the Arunta basement along the northern margin of the late Proterozoic to Devonian Amadeus Basin, represented by the Ormiston thrust, Mt Sonder-Mt Razorback thrusts, thrust-nappe structures in the Heavitree Quartzite, and probably reactivation of the Redbank Hill-Mt Zeil thrust. The involvement of Devonian sediments in the deformation and K/Ar ages of ca 0.4 b.y. (Black et al., 1983) define the age of these movements.

Owing to the paucity of pelitic schists and quartzites in the Derwent Paragneiss, older structural elements related to D1 are more difficult to identify than in the Chewings Range. However, finely banded amphibolites display magmatic flow folding, deformation associated with lit-par-lit injection, and refolded folds (Fig.IV.1a). Depending on whether migmatisation is attributable to D1 as in the northern granulite block, or to D3 as in the Chewings Range Zone, these refolded folds would be defined as F1-F3 or F3-F4, respectively. The mostly parallel orientation of lithological banding (S1) and gneissosity (S2) in the amphibolites, and the nonschistose nature of the rocks, renders difficult distinctions between F1 and F2 folds. In the terrain between the Redbank-Mt Zeil thrust zone and the

Mt Sonder-Mt Razorback thrust fault the gneiss, migmatite and granite of the southern block are transected by numerous EW trending cataclastic/mylonitic zones related to the thrusting.

The temporal/spatial correlation between the northern and the southern block across the RTZ remains uncertain and, pending further age determinations, is subject to indirect evidence. Had the migmatites of the Ormiston Zone and Dashwood Migmatite formed contemporaneously with the felsic gneiss and migmatite injected into the northern granulite block, the Sm-Nd and Rb-Sr ages reported from the Strangways Range by Windrim and McCulloch (1983) could suggest their origin by anatexis of mafic granulite about 2.0 b.y. ago. If so, the ca 1.6 b.y. age of the CRZ and 1.05 b.y. age of Ormiston Zone migmatites represent thermal age resetting, the latter age possibly reflecting the dynamothermal effects of Redbank-Mt Zeil thrust zone deformation. Alternatively, if the southern felsic igneous terrain is younger than the northern granulites, the existence of metamorphic discontinuities or unconformities, as well as retrograde metamorphic effects in the granulites, can be expected. To date little evidence for such relations can be offered, possibly with the exception of late biotite replacement relations in the granulites.

[4] SUMMARY AND CONCLUSIONS

The significance of the major Bouguer anomalies in central Australia is the subject of an on-going debate. Forman and Shaw (1973) and Mathur (1976) interpreted the Papunya gravity peak (+50 mg1) in terms of major upward dislocation of the Moho discontinuity, either through doming or thrusting. Anfiloff and Shaw (1973) modelled the gravity anomalies in terms of lateral intracrustal lithological and density heterogeneities, namely between dense granulite-dominated blocks and less dense granite and sediment-dominated blocks. Wellman (1978) calculated that the density contrasts may extend as deep as 20 km and below. Shaw et al. (in press) attribute the large gravity highs to basic igneous activity along the axis of an early Proterozoic ensialic rift zone. Currently seismic reflection studies are planned by BMR to throw light on deep crustal structure in the Arunta

The present study bears relevance to the above problem in documenting a well exposed wedge of granulites, south of the centre of the Papunya anomaly, thrust over a migmatite-gneiss-granite terrain along the Redbank-Mt Zeil thrust zone. The evolution of this terrain discussed above is summarised as follows:

(1) Emplacement of plutonic basic, high magnesian and anorthositic protoliths ca 2.0 b.y. ago. Strong depletion of some basic granulites in alkali elements (K, Rb, Ba), large ion lithophile elements (P, Zr, Nb, Y, Ce, La) and siderophile elements (Ti, V, Cr, Cu, Zn) favours a residual cumulate origin of some of these rocks.

(2) Granulite facies metamorphism and deformation, under pressures of 6-7kb and temperatures of ca. 900°C. Extensive synmetamorphic anatexis of basic rocks and consequent

lit-par-lit injection of gneiss and migmatite into basic granulites and segregation of larger granitic intrusions ca 1.8 b.y. ago.

Granulite facies metamorphism occurred under steep geothermal gradients of $40-50^{\circ}\text{C}/\text{km}$ while felsic igneous fractions were metamorphosed and equilibrated under generally lower gradients in the $30-40^{\circ}\text{C}/\text{km}$ range. Differentiated felsic fractions may have risen to higher crustal levels and may be represented by the granite-migmatite of the southern block (Teapot Granite, Dashwood Migmatite). Metasediments in that area (Derwent Paragneiss) may have originally overlain the basic granulites. Isotopic data are insufficient to ascertain these possibilities.

(3) Synmetamorphic hydration of granulites is represented by late biotite. Persistence of metamorphic conditions is represented by late garnet replacing biotite, possibly reflecting P change.

(4) Thermal events (Rb-Sr whole rock isochron) of ca 1.6 b.y. affected gneisses of the Southern block. It is not clear whether this represents felsic igneous activity or thermal imprint.

(5) Thermal resetting ca 1.0-0.9 b.y ago is interpreted in terms of initiation of the Redbank-Mt Zeil thrust zone (RTZ) and associated dynamothermal retrograde metamorphic effects on juxtaposed granulites and gneisses. The possibility of an earlier origin of the RTZ remains open.

(6) Repeated reactivation of the RTZ and uplift of the granulite terrain, particularly during the Alice Springs Orogeny ca 0.4 b.y. ago. If quartzite outcrops north of the RTZ are correlated with Heavitree Quartzite (ca 0.8 b.y.), the bulk of movement along the RTZ occur in post 0.8 b.y. times.

From Wellman's (1978) estimate of crustal density contrasts in central Australia, it may follow that the bulk of the crust underlying the basic granulites is of similar composition, which would support an origin of these rocks by plutonic emplacement rather than supracrustal extrusion over older sialic basement. Following this rationale further, the Mt Hay rocks may represent a segment of an infracrustal predominantly basic layer, a possibility supported by their LIL-depleted nature and by the association of anorthosites. The major Bouguer gravity anomalies in this part of the Arunta Block may thus be due to the uplift of a deep-seated subcrustal transition zone - an anatectic source of felsic magmas in the middle Proterozoic.

The distribution of lithologies in the southwestern Arunta Block can be interpreted in terms of a vertically zoned crustal model in which the ratio of felsic to mafic rocks increases upward. Thus, the Mt Hay, Mt Chapple, Redbank Hill and Mt Zeil belts could have originally occupied progressively shallower crustal levels, representing an anatectic mafic source and upward segregating granitic magmas. To extend this model further, the granite-orthogneiss-migmatite suite of the Southern Block could conceivably represent yet higher level and more differentiated magmas, intruding paragneisses representing supracrustal sediments originally representing uppermost crustal levels. Detailed isotopic studies of these terrains are required to examine this possibility.

FIGURE CAPTIONS FOR SECTION VII

- VII.1 - Radiometric anomaly map of the northern part of HERMANNSBURG 1:250 000 Sheet area (BMR, unpublished).
- VII.2 - Bouguer gravity anomaly map of the northern part of HERMANNSBURG 1:250 000 Sheet area (Lonsdale and Flavelle, 1963)
- VII.3 - Aeromagnetic anomaly map for the northern part of HERMANNSBURG 1:250 000 Sheet area
- VII.4 - (a) Contoured poles to 229 measured foliations in the ANBURLA, NARWIETOOMA and GLEN HELEN 1:100 000 Sheet areas.

(b) Contoured projections of 61 measured lineations in the ANBURLA, NARWIETOOMA and GLEN HELEN 1:100 000 sheet sheet areas

Fig. VII.1

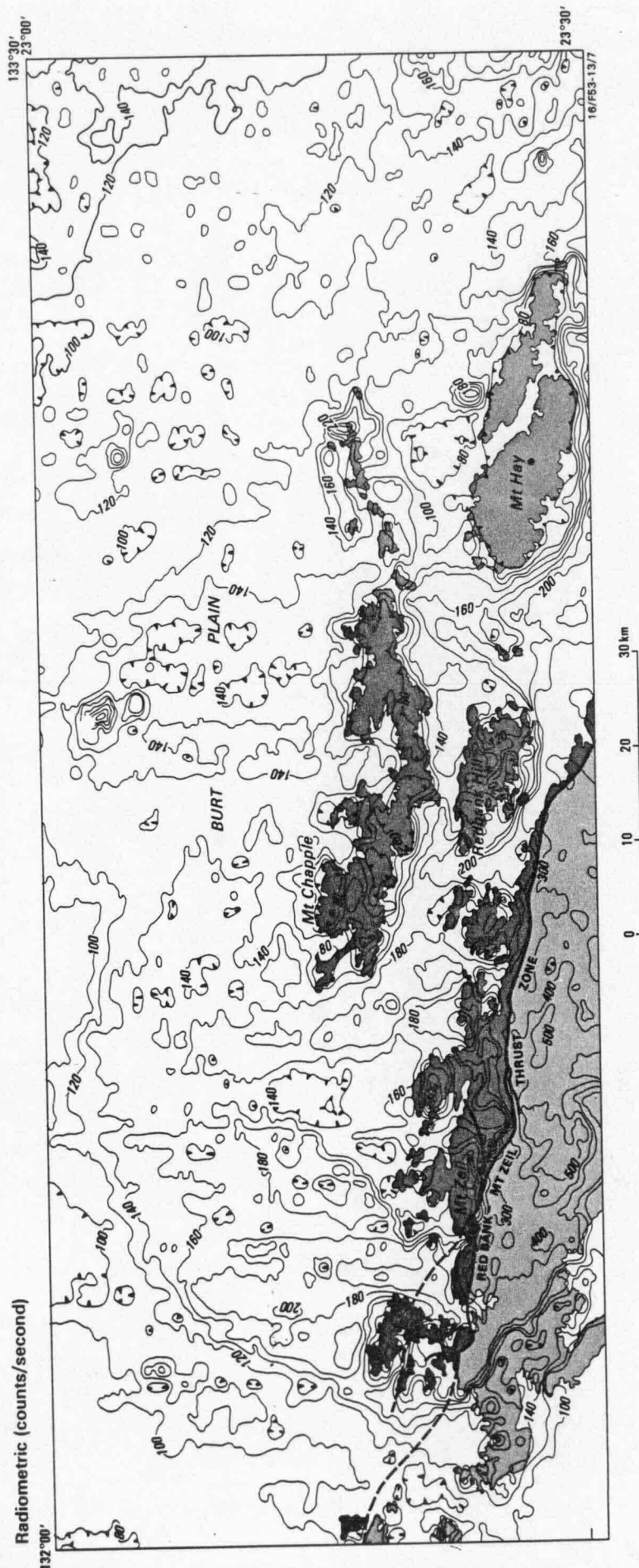


Fig. VII.2

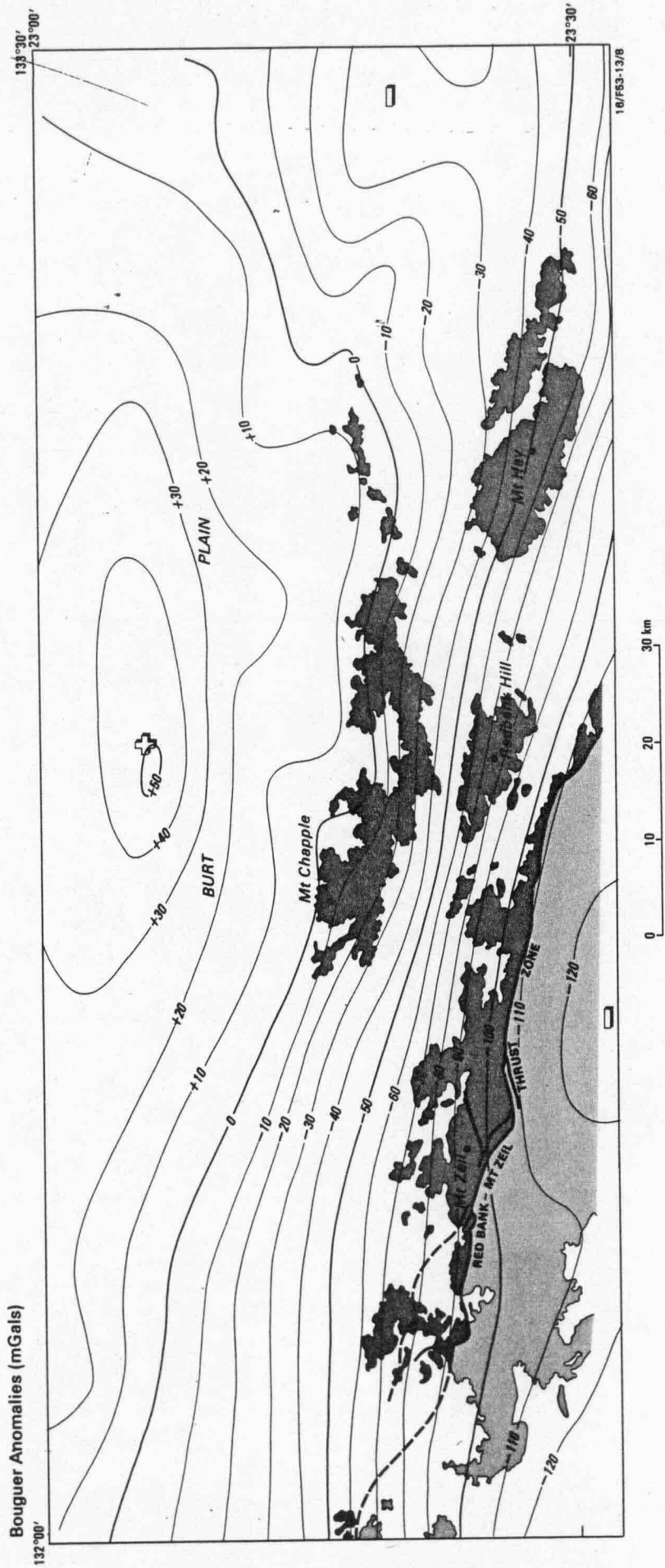


Fig. VII.3

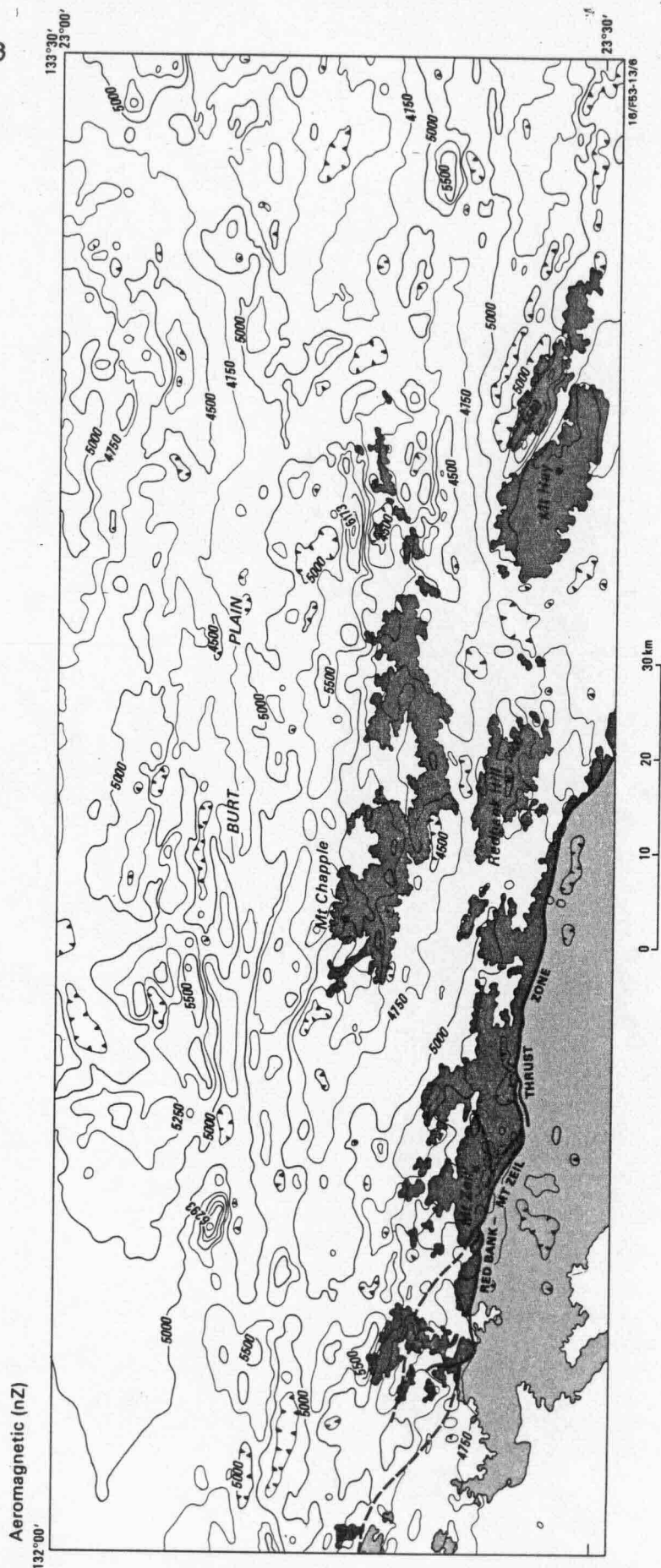


Fig. VII. 4a

POLES TO METAMORPHIC BANDING/GNEISSOSITY
ANBURLA, NARWIETOOMA & GLEN HELEN SHEET AREAS
229 POLES

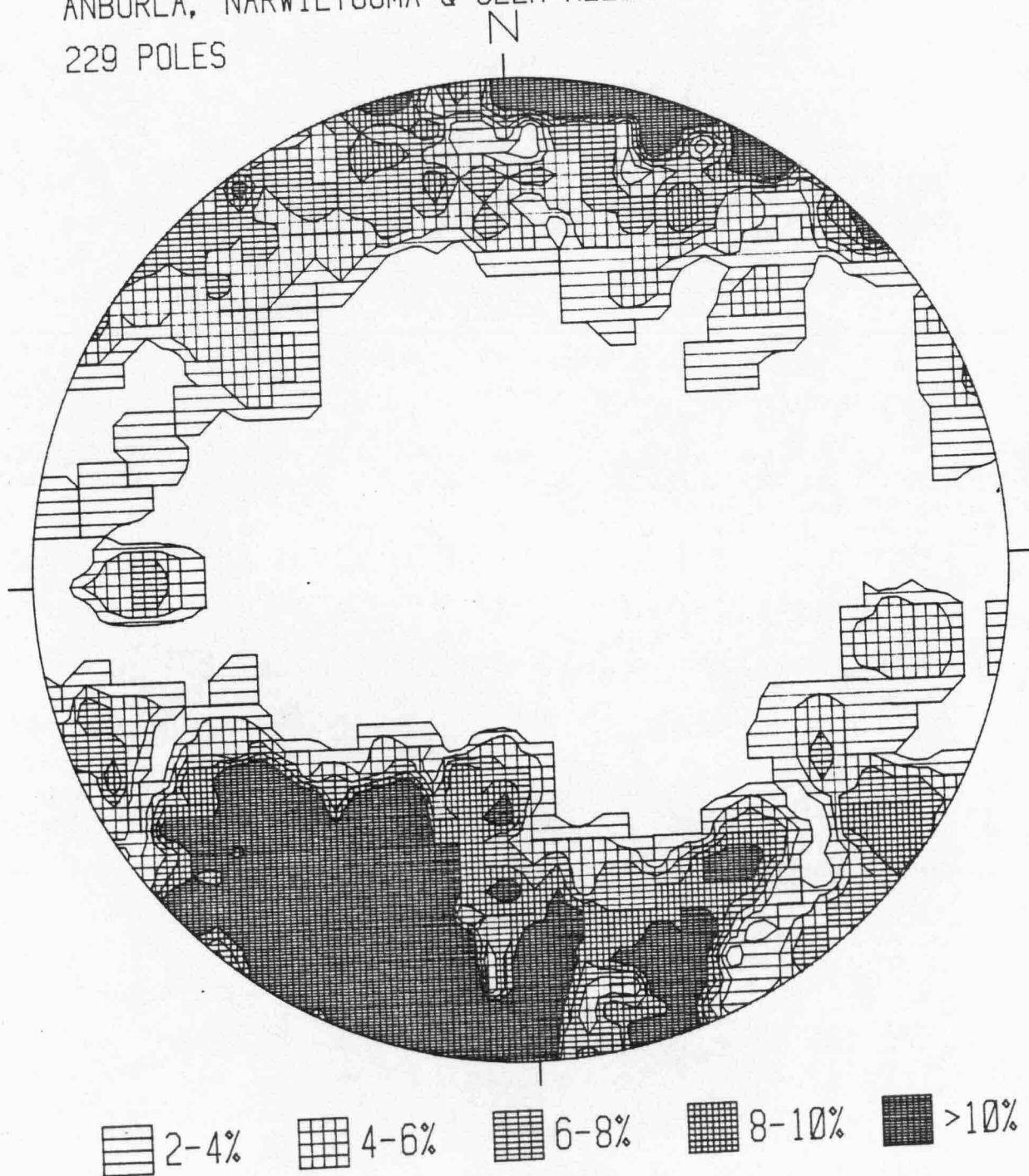


Fig. VII. 4(b)

LINEATIONS IN GRANULITES AND GNEISSES
ANBURLA, NARWIETOOMA & GLEN HELEN SHEET AREAS

61 POLES

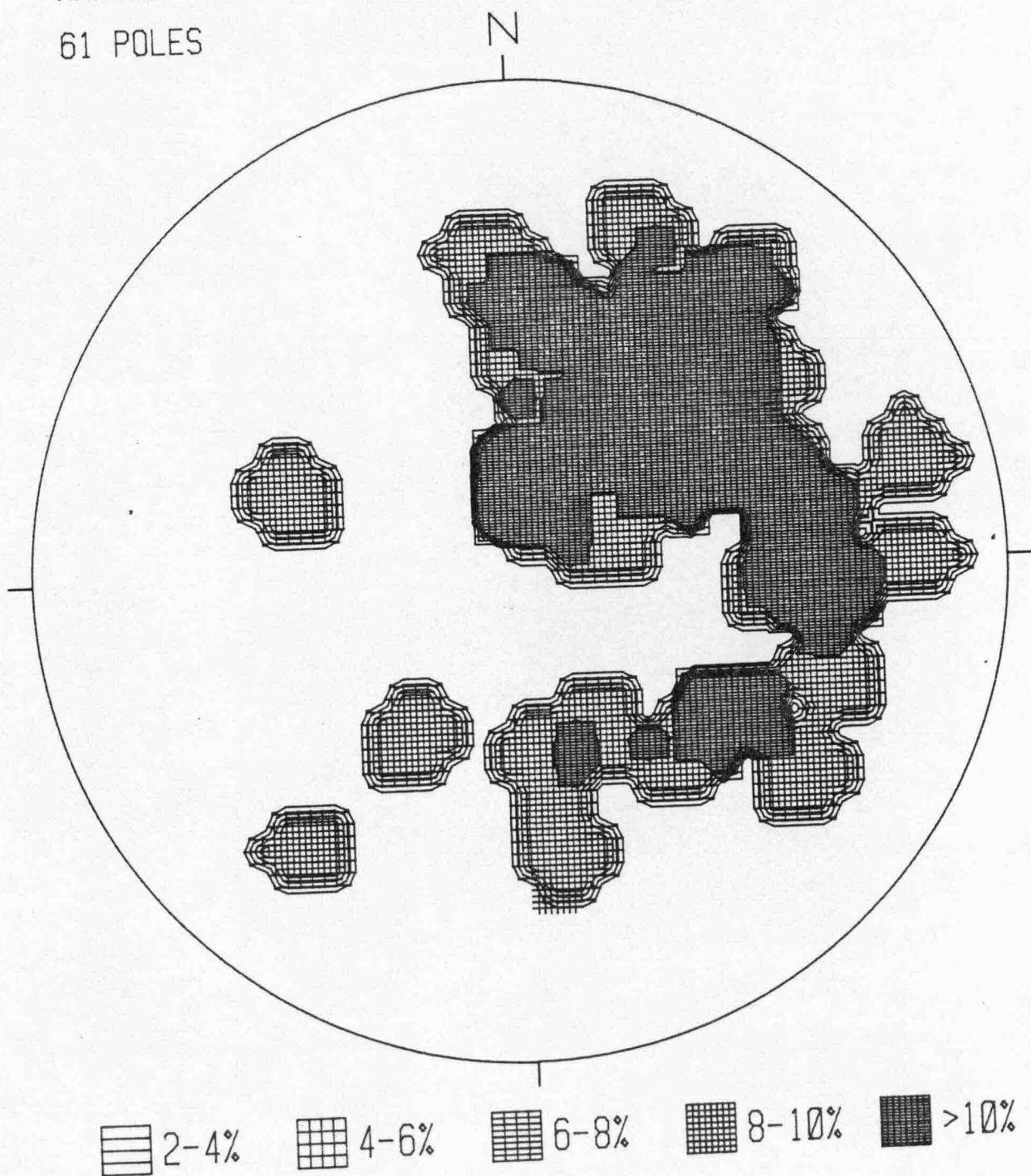


Table VII.1 Isotopic age data for the southwestern part of the Arunta Block and adjacent areas

Age	Initial Ratio	Method	Geological Unit	Locality	Reference
2015 [±] 120	ENd ^(I) = +1.4	Sm/Nd isochron	banded granulites	Strangeway Range	Windrim and McCulloch, 1983
2085 [±] 175	Ri=0.70249	Rb/Sr WR isochron	" "	" "	"
1800 [±] 25	Ri=0.70722	"	" "	"	"
1768 [±] 20	Ri=0.7085	"	" "	Mt Hay	Black et al., 1983
1728 [±] 65	Ri=0.706	"	" "	"	"
893 [±] 97	Ri=0.756	Rb-Sr WR-age feldspar	Porphyroblastic gneiss	Redbank Hill	"
1586 [±] 69	Ri=0.729	Rb-Sr WR isochron	Potrock gneiss	Chewings Range	Marjoribanks and Black, 1974
1053 [±] 50		Rb-Sr muscovite	migmatite	Ormiston zone	"
897 [±] 9		Rb-Sr WR-minerals	dolerite dyke	Stuart dyke swarm	Black et al., 1980

Acknowledgements

I thank G. Fruzzetti, D. Clarke and R. Thompson of the Northern Territory Geological Survey for their cooperation during the life of the project, R.D. Shaw, John Ferguson, R.G. Dodson, J.N. Casey and L.A. Offe for their field visits, D. Morrison for his invaluable assistance in the field and the laboratory, N. Ware for guidance with electron microprobe analyses, J. Pyke for the chemical analyses, and A.J. Stewart and J.W. Sheraton for their comments on the manuscript.

REFERENCES

Anfiloff, W. and Shaw, R.D., 1973 - The gravity effects of three large uplifted granulite blocks in separate Australian shield areas. Proc. Symp. Earth Gravity Field and secular variations in position, 273-289.

BISHOP, F.C., 1980 - The distribution of Fe and Mg between coexisting ilmenite and pyroxene, with application to geothermometry. Am.J.Sci. 280: 46-77

BLACK, L.P., SHAW, R.D. and OFFE, L.A., 1980 - The age of the Stuart dyke swarm and its bearing on the outset of late Precambrian sedimentation in Central Australia. J.Geol.Soc. Aust.27: 151-155

BLACK, L.P., SHAW, R.D. and STEWART, A.J., 1983 - Rb-Sr Geochronology of Proterozoic events in the Arunta inlier, central Australia. Bureau of Mineral Resources J. Aust. Geol. and Geophys. 8: 129-137

CHAPPELL, B.W., and WHITE, A.J.R., 1974 - Two contrasting granite types. Pacif. Geol. 8: 173-174

DAHL, P.S., 1980 - The thermal-compositional dependance of Fe-Mg distributions between coexisting garnets and pyroxenes: applications to geothermometry. AM. Miner. 65: 852-866

ELLIS, D.J. and GREEN, D.H., 1979 - An experimental study of the effect of Ca upon garnet-clinopyroxene Fe-Mg exchange equilibria: Contrib.Mineral.Petrol.71: 13-22

ELLIS, D.J., 1980 - Osumilite-sapphirine-quartz granulites from Enderby Land, Antarctica: P-T conditions of metamorphism, implications for garnet-cordierite equilibria and the evolution of the deep crust. Contr.Mineral.Petrol. 74: 201-210

ESSENE, E.J., 1982 - Geologic thermometry and barometry. In: Reviews in Mineralogy (P.H. Ribbe, ed.), Vol. 10, 153-196

FERRY, J.M., 1980 - The comparative study of geothermometers and

geobarometers of pelitic schists from south central Maine.

Am. Miner. 65: 720-732

FERRY, J.M., and SPEAR, F.S., 1978 - Calibration of Fe and Mg partitioning between biotite and garnet. Contr. Miner. Petrol. 66: 113-117

FLOYD, P.A. and WINCHESTER, J.A., 1978 - Indication and discrimination of altered and metamorphosed volcanic using immobile elements. Chem. Geol. 21: 291-306

FORMAN, D.J. and SHAW, R.D., 1973 - Deformation of crust and mantle in central Australia. Aust. Bur. Miner. Resour. Bull. 144

GANGULY, J., 1979 - Garnet and clinopyroxene solid solution and geothermometry based on Fe-Mg distribution coefficients. Geochim. Cosmochim. Acta 43: 1021-1029

GASPARIC, T. and LINDSLEY, D.H., 1980 - Phase equilibria at high pressures of pyroxenes containing monovalent and trivalent ions. In: Pyroxenes. (Prewitt, C.T., ed.) Reviews in Mineralogy 7: 309-340

GHENT, E.D., 1976 - Plagioclase-garnet- AlSi_2O_5 -quartz: a potential geobarometer-geothermometer. Am. Miner. 61: 710-714

GLIKSON, A.Y., 1979 - Siderophile and lithophile trace element evolution of the Archaean mantle. Bureau Mineral Resources J. Austr. Geol. Geophys. 4: 253-279

GLIKSON, A.Y. and OWEN, M., 1982 - HP9825A software system for electron probe data, major/trace and RE element geochemistry, magmatic fractionation models and Rb-Sr isotopic parameters. Bureau of Mineral Resources Record 1982/39

HENSEN, B., 1981 - The transition from pyroxene-granulite facies to garnet clinopyroxene facies: Experiments in the system $\text{CaO-MgO-Al}_2\text{O}_3\text{-SiO}_2$ Contrib. Miner. Petrol. 76: 234-242

HARRIS, N.B.W., HOLT, R.W. and DRURY, S.A., 1982 - Geobarometry, geothermometry and late Archaean geotherms from the granulite facies terrains of South India. J. Geol. 90: 509-527

HOLDAWAY, M.J., 1971 - Stability of andalusite and the aluminium silicate phase diagram. Am. J. Sci. 271: 97-131

KERRICK, D.M. 1972 - Experimental determination of muscovite + quartz stability with $\text{PH}_2\text{O} = \text{Ptotal}$. Am J. Sci. 272: 946-958

KNUTSON, J., DONNELLY, T.H., and TONKIN, D.G., 1983 - geochemical constraints on the genesis of copper mineralization in the Mt Gunson area, South Australia. Econ. Geol. 78: 250-274

LAMBERT, I.B., and HEIER, K.S., 1968 - Geochemical investigations of deep-seated rocks in the Australian shield. Lithos 1: 30-53

LAMBERT, I.B. and WYLLIE, P.J., 1972 - Melting of gabbro (quartz eclogite) with excess water to 35 kilobars with geological implications. J. Geol. 80: 693-708

LAMBERT, I.B. and WYLLIE, P.J., 1974 - Melting of tonalite and crystallization of andesite liquid with excess water to 30 kilobars. J. Geol. 82: 88-97

LONSDALE, G.F. and FLAVELLE, A.J., 1963 - Amadeus and South Canning Basins reconnaissance gravity survey using helicopters, N.T. and W.A., 1962. Bureau of Mineral Resources Record 1963/152

MARJORIBANKS, R.W., 1975 - The structural and metamorphic geology of the Ormiston area, central Australia. Bureau of Mineral Resources Record 1975/13

MARJORIBANKS, R.W. and BLACK, L.P., 1974 - The Geology and geochronology of the Arunta Complex north of Ormiston Gorge, Central Australia. J. Geol. Soc. Aust. 21: 291-299

MATHUR, S.P., 1976 - Relationship of Bouguer anomalies to crustal structure in southwestern and central Australia. Bureau Mineral Resources J. Aust. Geol. Geophys 1:177-186

MUTTON, A.J., SHAW, R.D. and WILKES, P.G., 1983 - Analyses of geological geophysical and physical property data from the southwest Arunta Block, N.T. Bureau Mineral Resources Record 1983/1

NEWTON, R.C. and HASELTON, H.J., 1981 - Thermodynamics of the garnet-plagioclase-Al₂O₅-quartz geobarometer. In: Thermodynamics of minerals and melts; Springer Verlag (Newton, R.C., Navrotsky, A. and Wood, B.J. eds.). New York, pp. 125-145

OFFE, L.A., 1983 - Geology of the MacDonnell Ranges 1:100 000 Sheet area, Northern Territory. Bureau of Mineral Resources Record 1983/4

QUINLAN, T. and FORMAN, D.J., 1968 - Hermannsburg, NT - 1:250 000 Geological Series. Bureau of Mineral Resources, Australia, Explanatory Notes SF/53-13

PERKINS, D. and NEWTON, R.C., 1981 - Charnockite geobarometers based on coexisting garnet-pyroxene-plagioclase-quartz. *Nature* 292: 144-146

REED, S.J.B. and WARE, N.G., 1975 - Quantitative electron probe analysis of silicates using energy dispersive X-ray spectrometry. *J. Petrol.* 16: 499-519

ROBIE, R.A., and WALDBAUM, D.R., 1968 - Thermodynamic properties of minerals and related substances at 298.15 K and one atmosphere pressure and at higher temperatures. *U.S. Geol. Surv. Bull.* 1259

SAXENA, S.K. 1979 - The origin of the Lewisian Gneisses of northwest Scotland, with particular reference to the Drumbeg Area, Sutherland. *Earth Planet. Sci. Lett.* 8: 301-310

SHAW, R.D. STEWART, A.J. and BLACK, L.P., 1984 - Tectonic history of the Arunta Block: A complex ensialic mobile belt in central Australia. *Aust. J. Earth Sci.* (in press)

STEWART, A.J., GLIKSON, A.Y., WARREN, R.G., and OFFE, L.A., 1980 - Geology of the North Arunta Block, N.T. Bureau of Mineral Resources Record 1980/63

STORMER, J.C., 1965 - A practical two-feldspar thermometer. *Am. Miner.* 60: 667-674

SECK, H.A., 1972 - The influence of pressure on the alkali feldspar solvus from peraluminous and persilicic materials. *Fortschr. Mineral.* 49: 31-49

SMITH, R.E. and SMITH, S.E., 1976 - Comments on the use of Ti, Zr, Y, Sr, K, P and Nb in classification of basaltic magmas. *Earth Planet. Sci. Lett.* 32: 114-120

TARNEY, J. and WINDLEY, B.F., 1977 - Chemistry, thermal gradients and evolution of the lower continental crust. J. Geol. Soc. London 134: 153-172

TUREKIAN, K.K. and WEDEPOHL, K.H., 1961 - Distribution of the elements in some units of the Earth's crust. Geol. Soc. Am. Bull. 72: 175

WALKER, K.R., JOPLIN, G.A., LOVERING, J.F. and GREEN, R., 1960 - Metamorphic and metasomatic convergence of basic igneous rocks and lime magnesia sediments of the Precambrian of north-western Queensland, J. Geol. Soc. Aust. 6: 149-178

WARREN, R.G., 1983 - Metamorphic and tectonic evolution of granulites, Arunta Block, central Australia. Nature 305: 300-303

WELLMAN, P., 1978 - Gravity evidence for abrupt changes in mean crustal density at the junction of Australian crustal blocks. BMR J Aust. Geol. Geophys. 3: 153-162

WELLS, A.T. and MOSS J., 1984 - Stratigraphy and structure of the Napperby Basin, N.T., Bureau Mineral Resources Bull. 212

WELLS, P.R.A., 1977 - Pyroxene thermometry in simple and complex systems. Contr. Mineral. Petrol. 62: 129-139

WHITE, A.J.R. and CHAPPELL, B.W., 1977 - Ultrametamorphism and granitoid genesis. Tectonophysics 43: 7-22

WINDRIM, D.P. and McCULLOCH, M.T., 1983 - Nd and Sr chronology of Strangways Range granulites: implications for crustal growth and reworking in the Proterozoic of central Australia (abstract). Proceedings 6th Aust. Geol. Convention, Canberra. 192-193

WINKLER, H.G.F., 1967 - Petrogenesis of Metamorphic Rocks.
 Springer-Verlag, New York

WOOD, B.J. and BANNO, S., 1973 - Garnet-orthopyroxene and
 orthopyroxene-clinopyroxene relationships in simple and
 complex systems. Contr. Mineral. Petrol. 42: 109-124

TABLE II-1[a] - Mt HAY MAFIC GRANULITE S-36

SAMPLE NUMBER	S-36	S-36	S-36	S-36	S-36
ROCK TYPE	BiCpCpPl	BiOpCpPl	BiOpCpPl	BiOpCpPl	BiOpCpPl
	B.GRANULIT	B.GRANULIT	B.GRANULIT	B.GRANULIT	B.GRANULIT
MINERAL DATA	OPX	CPX	ILMENITE	BIOTITE	PLG
GEOLOGICAL UNIT	Mt Hay	Mt Hay	Mt Hay	Mt Hay	rim/px
LOCALITY	ARUNTA	ARUNTA	ARUNTA	ARUNTA	Mt Hay
					ARUNTA
SiO ₂	51.12	51.75	0.20	36.02	52.92
TiO ₂		0.11	48.82	5.36	
Al ₂ O ₃	1.61	2.01	0.11	14.03	30.01
V ₂ O ₃		0.13	0.63	0.25	
Cr ₂ O ₃					
FeO[t]	27.33	10.20	48.14	17.37	0.27
MnO	0.58	0.21	0.29		
MgO	18.50	12.65	1.00	12.35	0.13
NiO					
CaO	0.56	22.52	0.07	0.10	12.30
Na ₂ O		0.29			4.29
K ₂ O				10.00	0.24
P ₂ O ₅					
Cl				0.19	
TOTAL	99.70	99.87	99.26	95.67	100.16
Si	1.959	1.949	0.005	5.479	9.577
Ti		0.003	0.943	0.613	
Al	0.073	0.089	0.003	2.516	6.403
V		0.004	0.013	0.031	
Cr					
Fe	0.876	0.321	1.034	2.210	0.041
Mn	0.019	0.007	0.006		
Mg	1.056	0.710	0.038	2.800	0.035
Ni					
Ca	0.023	0.909	0.002	0.016	2.385
Na		0.021			1.505
K				1.941	0.055
P					
OXYGENS,CATIONS	6.04	6.04	3.02	22.16	32.20
TOTAL CATIONS	4.006	4.013	2.044	15.606	20.001

TABLE II-1[b] - Mt HAY MAFIC GRANULITE S-42

SAMPLE NUMBER	S-42	S-42	S-42	S-42	S-42
ROCK TYPE	BiOpCpPl B.GRANULIT	BiOpCpPl B.GRANULIT	BiOpCpPl B.GRANULIT	BiOpCpPl B.GRANULIT	BiOpCpPl B.GRANULIT
MINERAL DATA	OPX	CPX	ILMENITE	BIOTITE	PLG
GEOLOGICAL UNIT	Mt Hay	Mt Hay	Mt Hay	Mt Hay	core
LOCALITY	ARUNTA	ARUNTA	ARUNTA	ARUNTA	Mt Hay ARUNTA
SiO ₂	52.32	51.88	0.30	36.52	49.60
TiO ₂	0.12	0.24	47.94	5.79	
Al ₂ O ₃	1.56	2.15	0.12	14.45	32.14
V ₂ O ₃			0.47	0.21	
Cr ₂ O ₃		0.15	0.38	0.25	
FeO[t]	21.62	7.31	48.63	14.02	
MnO	0.44	0.24	0.39		
MgO	23.01	14.32	1.76	14.40	0.11
NiO					
CaO	0.43	23.13		0.14	15.13
Na ₂ O		0.25			2.89
K ₂ O				10.23	0.14
P ₂ O ₅					
Cl					
TOTAL	99.50	99.67	99.99	96.01	100.01
Si	1.952	1.936	0.008	5.439	9.054
Ti	0.003	0.007	0.920	0.649	
Al	0.069	0.095	0.004	2.537	6.917
V			0.010	0.025	
Cr		0.004	0.008	0.029	
Fe	0.675	0.228	1.038	1.746	
Mn	0.014	0.008	0.008		
Mg	1.280	0.796	0.067	3.196	0.030
Ni					
Ca	0.017	0.925		0.022	2.959
Na		0.018			1.023
K				1.944	0.033
P					
OXYGENS.CATIONS	6.04	6.04	3.02	22.16	32.20
TOTAL CATIONS	4.010	4.017	2.063	15.587	20.016

TABLE II-1[c] - Mt HAY ANORTHOSITE S-28

SAMPLE NUMBER	S-28	S-28	S-28
ROCK TYPE	op/hb/plg	op/hb/plg	op/hb/plg
	ANORTHOSIT	ANORTHOSIT	ANORTHOSIT
MINERAL DATA	OPX	AMPH	PLG
GEOLOGICAL UNIT	Mt Hay	Mt Hay	Mt Hay
LOCALITY	ARUNTA	ARUNTA	ARUNTA
SiO ₂	52.34	47.77	49.20
TiO ₂		0.91	
Al ₂ O ₃	1.25	8.72	32.78
V ₂ O ₃			
Cr ₂ O ₃		0.23	
FeO[t]	23.10	11.07	
MnO	0.51	0.25	
MgO	21.87	14.93	
NiO			
CaO	0.39	11.65	15.28
Na ₂ O		1.05	2.75
K ₂ O		0.40	
P ₂ O ₅			
Cl			
TOTAL	99.46	96.98	100.01
Si	1.967	6.950	8.976
Ti		0.100	
Al	0.055	1.496	7.050
V			
Cr		0.026	
Fe	0.726	1.347	
Mn	0.016	0.031	
Mg	1.225	3.237	
Ni			
Ca	0.016	1.816	2.987
Na		0.296	0.973
K		0.074	
P			
OXYGENS.CATIONS	6.04	23.15	32.20
TOTAL CATIONS	4.005	15.373	19.986

TABLE II-1[d] - Mt HAY ANORTHOSITE S-48

SAMPLE NUMBER	S-48	S-48	S-48	S-48
ROCK TYPE	HbOpCpPl	HbOpCpPl	HbOpCpPl	HbOpCpPl
MINERAL DATA	BGRANULITE	BGRANULITE	BGRANULITE	BGRANULITE
	AMPH	OPX	CPX	PLG
GEOLOGICAL UNIT	Mt Hay	Mt Hay	Mt Hay	Mt Hay
LOCALITY	ARUNTA	ARUNTA	ARUNTA	ARUNTA
SiO ₂	47.12	52.23	52.22	51.30
TiO ₂	1.31			
Al ₂ O ₃	9.35	1.57	2.10	30.81
V ₂ O ₃				
Cr ₂ O ₃	0.35		0.14	
FeO[t]	10.65	21.66	7.04	
MnO		0.52	0.16	
MgO	14.61	22.89	14.18	0.19
NiO				
CaO	12.02	0.32	23.28	13.51
Na ₂ O	1.09		0.31	3.75
K ₂ O	0.45			0.18
P ₂ O ₅				
Cl	0.06			
TOTAL	97.01	99.19	99.43	99.74
Si	6.856	1.956	1.949	9.349
Ti	0.143			
Al	1.604	0.069	0.092	6.619
V				
Cr	0.040		0.004	
Fe	1.296	0.678	0.220	
Mn		0.016	0.005	
Mg	3.168	1.277	0.789	0.052
Ni				
Ca	1.874	0.013	0.931	2.638
Na	0.308		0.022	1.325
K	0.084			0.042
P				
OXYGENS.CATIONS	23.15	6.04	6.04	32.20
TOTAL CATIONS	15.373	4.009	4.012	20.025

TABLE II-1[e] - Mt HAY CALC GRANULITE S-53

SAMPLE NUMBER	S-53	S-53	S-53
ROCK TYPE	CpSpPl	CpSpPl	CpSpPl
MINERAL DATA	CPX	SPHENE	PLG
GEOLOGICAL UNIT	Mt Hay	Mt Hay	rim pyx
LOCALITY	ARUNTA	ARUNTA	Mt Hay ARUNTA
SiO ₂	51.65	29.53	44.53
TiO ₂		34.97	
Al ₂ O ₃	1.81	2.10	35.42
V ₂ O ₃			
Cr ₂ O ₃		0.15	
FeO[t]	12.06	0.50	0.22
MnO			
MgO	10.66		
NiO			
CaO	23.60	28.58	19.01
Na ₂ O	0.21		0.86
K ₂ O			
P ₂ O ₅			
Cl			
TOTAL	99.99	95.83	100.04
Si	1.962	4.029	8.233
Ti		3.588	
Al	0.081	0.338	7.720
V			
Cr		0.016	
Fe	0.383	0.057	0.034
Mn			
Mg	0.603		
Ni			
Ca	0.960	4.178	3.766
Na	0.015		0.308
K			
P			
OXYGENS.CATIONS	6.04	20.12	32.20
TOTAL CATIONS	4.004	12.206	20.061

TABLE II-1[f] - Mt HAY CALC GRANULITE S-55

SAMPLE NUMBER	S-55	S-55	S-55
ROCK TYPE	SchbCpPl	SchbCpPl	SchbCpPl
MINERAL DATA	CGRANULITE	CGRANULITE	CGRANULITE
GEOLOGICAL UNIT	AMPH4	CPX	SCAPOLITE
LOCALITY	core	MEIONITE	
	Mt Hay	Mt Hay	Mt Hay
	ARUNTA	ARUNTA	ARUNTA
SiO ₂	41.05	51.03	46.23
TiO ₂	1.63	0.24	
Al ₂ O ₃	14.08	2.87	29.36
V ₂ O ₃			
Cr ₂ O ₃		0.11	
FeO[t]	15.98	9.69	0.20
MnO	0.14	0.19	
MgO	9.37	12.06	0.19
NiO			
CaO	12.06	23.45	19.87
Na ₂ O	1.56	0.34	3.12
K ₂ O	1.12		0.11
P ₂ O ₅			
Cl			0.07
TOTAL	96.99	99.98	99.15
Si	6.210	1.922	6.557
Ti	0.185	0.007	
Al	2.511	0.127	4.909
V			
Cr		0.003	
Fe	2.022	0.305	0.024
Mn	0.018	0.006	
Mg	2.112	0.677	0.040
Ni			
Ca	1.955	0.946	3.020
Na	0.458	0.025	0.858
K	0.216		0.020
P			
OXYGENS.CATIONS	23.15	6.04	24.16
TOTAL CATIONS	15.687	4.018	15.428

TABLE II-1[g] - Mt HAY CALC GRANULITE S-56

SAMPLE NUMBER	S-56	S-56	S-56	S-56	S-56	S-56
ROCK TYPE	ScSpHbCp PlCaCGRAN	ScSpHbCp PlCaCGRAN	ScSpHbCp PlCaCGRAN	ScSpHbCp PlCaCGRAN	ScSpHbCp PlCaCGRAN	ScSpHbCp PlCaCGRAN
MINERAL DATA	SPHENE	SCAPOLITE MEIONITE	AMPH	CPX	ILMENITE	PLG
GEOLOGICAL UNIT	Mt Hay	Mt Hay	Mt Hay	Mt Hay	Mt Hay	Mt Hay
LOCALITY	ARUNTA	ARUNTA	ARUNTA	ARUNTA	ARUNTA	ARUNTA
SiO ₂	30.11	43.21	50.50	49.71	0.34	45.35
TiO ₂	37.21		0.29	0.37	52.16	
Al ₂ O ₃	1.27	29.17	7.47	3.45		35.22
V ₂ O ₃	0.23			0.11		
Cr ₂ O ₃	0.14		0.11	0.25		
FeO[t]	0.53	0.14	13.04	12.06	46.26	
MnO				0.18	0.82	
MgO			12.54	10.37	0.83	
NiO						
CaO	29.31	20.19	12.30	23.12	0.35	18.74
Na ₂ O		2.37	0.70	0.33		0.95
K ₂ O			0.25			
P ₂ O ₅	0.14					
Cl						
TOTAL	98.94	95.08	97.20	99.95	100.76	100.26
Si	3.987	6.399	7.333	1.896	0.008	8.341
Ti	3.706		0.032	0.011	0.980	
Al	0.198	5.093	1.279	0.155		7.637
V	0.024			0.003		
Cr	0.015		0.013	0.008		
Fe	0.059	0.017	1.584	0.385	0.966	
Mn				0.006	0.017	
Mg			2.714	0.590	0.031	
Ni						
Ca	4.159	3.204	1.914	0.945	0.009	3.693
Na		0.681	0.197	0.024		0.339
K			0.046			
P	0.016					
OXYGENS. CATIONS	20.12	24.16	23.15	6.04	3.02	32.20
TOTAL CATIONS	12.164	15.394	15.112	4.023	2.011	20.010

TABLE II-1[h] - Mt HAY GRANULITE S-37

SAMPLE NUMBER	S-37	S-37	S-37	S-37
ROCK TYPE	OpAmPl	OpAmPl	OpAmPl	OpAmPl
MINERAL DATA	GRANULITE	GRANULITE	GRANULITE	GRANULITE
	OPX	AMPH	ILMENITE	PLG
GEOLOGICAL UNIT	Mt Hay	Mt Hay	Mt Hay	Mt Hay
LOCALITY	ARUNTA	ARUNTA	ARUNTA	ARUNTA
SiO ₂	49.28	39.47	0.18	54.07
TiO ₂		1.88	49.79	
Al ₂ O ₃	1.94	12.34		28.92
V ₂ O ₃		0.12	0.48	
Cr ₂ O ₃				
FeO[t]	29.22	17.07	48.43	
MnO	0.67		0.68	
MgO	16.67	9.10		0.11
NiO				
CaO	0.60	11.74	0.26	11.12
Na ₂ O		1.23		5.08
K ₂ O		2.34	0.10	0.19
P ₂ O ₅				
Cl		0.54		
TOTAL	98.38	95.83	99.92	99.49
Si	1.939	6.182	0.005	9.808
Ti		0.221	0.958	
Al	0.090	2.279		6.185
V		0.015	0.010	
Cr				
Fe	0.962	2.236	1.036	
Mn	0.022		0.015	
Mg	0.978	2.124		0.030
Ni				
Ca	0.025	1.970	0.007	2.161
Na		0.374		1.787
K		0.468	0.003	0.044
P				
OXYGENS.CATIONS	6.04	23.15	3.02	32.20
TOTAL CATIONS	4.016	15.869	2.034	20.015

TABLE II-1[i] - Mt HAY INTERMDIATE GRANULITE S-45

SAMPLE NUMBER	S-45	S-45	S-45	S-45	S-45	S-45
ROCK TYPE	HbOpCpPl	HbOpCpPl	HbOpCpPl	HbOpCpPl	HbOpCpPl	HbOpCpPl
	BGRANULITE	BGRANULITE	BGRANULITE	BGRANULITE	BGRANULITE	BGRANULITE
MINERAL DATA	OPX	CPX	AMPH	MAGNETITE	ILMENITE	PLG
GEOLOGICAL UNIT	Mt Hay	Mt Hay	Mt Hay	Mt Hay	Mt Hay	Mt Hay
LOCALITY	ARUNTA	ARUNTA	ARUNTA	ARUNTA	ARUNTA	ARUNTA
SiO ₂	51.50	51.62	40.61	0.44	0.26	51.72
TiO ₂		0.11	2.61	0.57	48.77	
Al ₂ O ₃	2.35	2.92	14.45	0.89	0.31	30.73
V ₂ O ₃			0.16	1.63	0.57	
Cr ₂ O ₃				0.25		
FeO[t]	23.21	7.53	12.95	65.44	48.19	
MnO	0.39	0.18			0.37	
MgO	21.76	13.57	11.66	31.01	1.51	
NiO						
CaO	0.35	22.76	11.83		0.11	13.06
Na ₂ O		0.44	1.84			3.95
K ₂ O			1.94			0.18
P ₂ O ₅						
Cl						
TOTAL	99.56	99.13	98.05	100.23	100.09	99.64
Si	1.935	1.935	6.034	0.017	0.007	9.419
Ti		0.003	0.292	0.016	0.932	
Al	0.104	0.129	2.531	0.039	0.009	6.597
V			0.019	0.049	0.012	
Cr				0.007		
Fe	0.729	0.236	1.609	2.055	1.024	
Mn	0.012	0.006			0.008	
Mg	1.218	0.758	2.582	1.736	0.057	
Ni						
Ca	0.014	0.914	1.883		0.003	2.548
Na		0.032	0.530			1.395
K			0.368			0.042
P						
OXYGENS.CATIONS	6.04	6.04	23.15	4.03	3.02	32.20
TOTAL CATIONS	4.012	4.013	15.848	3.919	2.052	20.001

TABLE II-1[j] - Mt HAY FELSIC GRANULITE S-52

SAMPLE NUMBER	S-52	S-52	S-52	S-52	S-52	S-52
ROCK TYPE	GtOpHbBi	GtOpHbBi	GtOpHbBi	GtOpHbBi	GtOpHbBi	GtOpHbBi
MINERAL DATA	PlQzGRAN	PlQzGRAN	PlQzGRAN	PlQzGRAN	PlQzGRAN	PlQzGRAN
	GNT	OPX	AMPH	BIOTITE	ILMENITE	PLG
GEOLOGICAL UNIT	Mt Hay	Mt Hay	Mt Hay	Mt Hay	Mt Hay	Mt Hay
LOCALITY	ARUNTA	ARUNTA	ARUNTA	ARUNTA	ARUNTA	ARUNTA
SiO ₂	38.89	51.38	41.59	37.56	0.97	46.17
TiO ₂			0.79	3.45	47.06	
Al ₂ O ₃	22.24	3.04	10.80	15.42	0.44	34.16
V ₂ O ₃			0.12	0.15	0.42	
Cr ₂ O ₃					0.51	
FeO[t]	27.27	22.85	11.00	12.15	45.55	
MnO	0.80	0.32			0.45	
MgO	8.21	21.93	12.64	16.43	1.16	0.16
NiO						
CaO	3.33	0.34	11.15	0.17	0.21	17.19
Na ₂ O			1.08			1.54
K ₂ O			0.92	10.05	0.07	
P ₂ O ₅						
Cl						
TOTAL	100.74	99.86	90.09	95.38	96.84	99.22
Si	5.968	1.920	6.587	5.546	0.025	8.545
Ti			0.094	0.383	0.923	
Al	4.024	0.134	2.016	2.684	0.014	7.454
V			0.015	0.018	0.009	
Cr					0.011	
Fe	3.500	0.714	1.457	1.500	0.993	
Mn	0.104	0.010			0.010	
Mg	1.878	1.221	2.983	3.615	0.045	0.044
Ni						
Ca	0.548	0.014	1.892	0.027	0.006	3.409
Na			0.332			0.553
K			0.186	1.893	0.002	
P						
OXYGENS.CATIONS	24.16	6.04	23.15	22.16	3.02	32.20
TOTAL CATIONS	16.022	4.013	15.562	15.666	2.038	20.005

TABLE II-1[k] - Mt HAY GARNET-BIOTITE GNEISS S-57

SAMPLE NUMBER	S-57	S-57	S-57	S-57	S-57
ROCK TYPE	GtBikfPl	GtBikfPl	GtBikfPl	GtBikfPl	GtBikfPl
	QzGNEISS	QzGNEISS	QzGNEISS	QzGNEISS	QzGNEISS
MINERAL DATA	GNT	BIOTITE	ILMENITE	PLG	KFELD
GEOLOGICAL UNIT	Mt Hay	Mt Hay	Mt Hay	Mt Hay	Mt Hay
LOCALITY	ARUNTA	ARUNTA	ARUNTA	ARUNTA	ARUNTA
SiO ₂	36.90	35.05	0.77	59.92	64.51
TiO ₂		4.27	47.28		0.28
Al ₂ O ₃	20.22	15.34		25.47	18.69
V ₂ O ₃			0.37		
Cr ₂ O ₃					
FeO[t]	31.04	24.42	48.94		
MnO	1.30		0.26		
MgO	1.75	6.83			
NiO					
CaO	7.58	0.09		6.82	0.19
Na ₂ O		0.31	0.49	7.35	0.81
K ₂ O		9.62		0.21	15.52
P ₂ O ₅	0.10				
Cl		0.54		0.07	
TOTAL	98.95	96.47	98.11	99.84	100.00
Si	6.000	5.477	0.020	10.685	11.906
Ti		0.502	0.930		0.039
Al	3.876	2.826		5.355	4.067
V			0.008		
Cr					
Fe	4.221	3.191	1.070		
Mn	0.187		0.006		
Mg	0.424	1.591			
Ni					
Ca	1.321	0.015		1.303	0.038
Na		0.094	0.025	2.541	0.290
K		1.918		0.048	3.654
P	0.014				
OXYGENS.CATIONS	24.16	22.16	3.02	32.20	32.20
TOTAL CATIONS	16.043	15.614	2.059	19.932	19.994

TABLE II-1[1] - Mt HAY GARNET-SILLIMANITE GNEISS S-51

SAMPLE NUMBER	S-51	S-51	S-51	S-51
ROCK TYPE	GtSlPlKf	GtSlPlKf	GtSlPlKf	GtSlPlKf
MINERAL DATA	gneiss	gneiss	gneiss	gneiss
	GNT	SILL.	KFELD	PLG
GEOLOGICAL UNIT	Mt Hay	Mt Hay	Mt Hay	Mt Hay
LOCALITY	ARUNTA	ARUNTA	ARUNTA	ARUNTA
SiO ₂	36.57	37.32	65.50	65.77
TiO ₂				
Al ₂ O ₃	20.99	62.15	19.29	21.62
V ₂ O ₃				
Cr ₂ O ₃				
FeO[t]	37.12	0.52		
MnO	2.12			
MgO	2.21			
NiO				
CaO	0.82		0.54	2.03
Na ₂ O	0.17		4.48	10.29
K ₂ O			10.13	0.20
P ₂ O ₅				
Cl				0.10
TOTAL	100.00	99.99	99.94	100.01
Si	5.953	4.035	11.876	11.561
Ti				
Al	4.028	7.922	4.123	4.480
V				
Cr				
Fe	5.053	0.047		
Mn	0.292			
Mg	0.536			
Ni				
Ca	0.143		0.105	0.382
Na	0.054		1.575	3.507
K			2.343	0.045
P				
OXYGENS.CATIONS	24.16	20.12	32.20	32.20
TOTAL CATIONS	16.059	12.004	20.022	19.975

TABLE II-1 [m] - Mt HAY MYLONITE S-30

SAMPLE NUMBER	S-30	S-30	S-30
ROCK TYPE	GaBiPlgQz	GaBiPlgQz	GaBiPlgQz
MINERAL DATA	MYLONITE	MYLONITE	MYLONITE
	GNT	BIOTITE	PLG
GEOLOGICAL UNIT	Mt Hay	Mt Hay	Mt Hay
LOCALITY	ARUNTA	ARUNTA	ARUNTA
SiO ₂	37.91	34.14	48.44
TiO ₂		3.60	
Al ₂ O ₃	21.65	17.36	32.69
V ₂ O ₃			
Cr ₂ O ₃			
FeO[t]	30.21	13.80	
MnO	0.61		
MgO	7.62	14.86	
NiO			
CaO	1.78	0.61	16.37
Na ₂ O	0.20	0.85	2.32
K ₂ O		9.58	0.18
P ₂ O ₅			
Cl		0.19	
TOTAL	99.98	94.99	100.00
Si	5.933	5.156	8.878
Ti		0.409	
Al	3.995	3.091	7.064
V			
Cr			
Fe	3.954	1.743	
Mn	0.081		
Mg	1.777	3.345	
Ni			
Ca	0.299	0.099	3.215
Na	0.061	0.249	0.825
K		1.846	0.042
P			
OXYGENS.CATIONS	24.16	22.16	32.20
TOTAL CATIONS	16.100	15.938	20.024

TABLE II-2[a] - Mt CHAPPLE GNT-OPX GNEISS S-187

SAMPLE NUMBER	S-187	S-187	S-187	S-187
ROCK TYPE	GtOpPl	GtOpPl	GtOpPl	GtOpPl
	gneiss	gneiss	gneiss	gneiss
MINERAL DATA	GNT	OPX	ILMENITE	PLG rim
GEOLOGICAL UNIT	Mt Chapple	Mt Chapple	Mt Chapple	Mt Chapple
LOCALITY	ARUNTA	ARUNTA	ARUNTA	ARUNTA
SiO ₂	36.79	49.93	0.11	53.43
TiO ₂		0.16	48.27	
Al ₂ O ₃	21.06	1.49		29.99
V ₂ O ₃				
Cr ₂ O ₃			0.16	
FeO[t]	27.98	28.93	50.42	
MnO	0.87	0.23	0.23	
MgO	4.89	18.19	0.83	
NiO				
CaO	6.85	0.57		11.83
Na ₂ O				4.73
K ₂ O				0.16
P ₂ O ₅				
Cl				
TOTAL	98.44	99.50	100.02	100.14
Si	5.903	1.935	0.003	9.646
Ti		0.005	0.934	
Al	3.983	0.068		6.383
V				
Cr			0.003	
Fe	3.754	0.938	1.085	
Mn	0.118	0.008	0.005	
Mg	1.169	1.050	0.032	
Ni				
Ca	1.178	0.024		2.288
Na				1.656
K				0.037
P				
OXYGENS. CATIONS	24.16	6.04	3.02	32.20
TOTAL CATIONS	16.105	4.028	2.062	20.010

TABLE II-2(b) - Mt CHAPPLE GNT-OPX-CPX GRANULITE S-188

SAMPLE NUMBER	S-188	S-188	S-188	S-188	S-188	S-188	S-188
ROCK TYPE	GtOpCpBi	GtOpCpBi	GtOpCpBi	GtOpCpBi	GtOpCpBi	GtOpCpBi	GtOpCpBi
MINERAL DATA	AmPlgran	AmPlgran	AmPlgran	AmPlgran	AmPlgran	AmPlgran	AmPlgran
	CPX	OPX	GNT	BIOTITE	AMPH	ILMENITE	PLG
GEOLOGICAL UNIT	Mt Chapple	Mt Chapple	Mt Chapple	Mt Chapple	Mt Chapple	Mt Chapple	Mt Chapple
LOCALITY	ARUNTA	ARUNTA	ARUNTA	ARUNTA	ARUNTA	ARUNTA	ARUNTA
SiO ₂	50.79	50.70	37.32	35.64	39.35		53.02
TiO ₂				4.78	1.51	46.11	
Al ₂ O ₃	2.77	1.44	21.33	14.19	13.48	0.56	29.70
V ₂ O ₃				0.17		0.49	
Cr ₂ O ₃				0.41		0.16	
FeO[t]	11.63	28.20	27.23	18.31	18.35	48.77	
MnO		0.46	1.06			0.34	
MgO	12.23	19.15	5.25	12.00	9.26	1.00	
NiO							
CaO	22.38	0.52	7.30	0.29	11.68	0.14	11.91
Na ₂ O	0.20				1.18		4.58
K ₂ O				9.92	2.38		0.16
P ₂ O ₅							
Cl				0.18	0.39		
TOTAL	100.00	100.47	99.49	95.89	97.58	97.57	99.37
Si	1.921	1.937	5.905	5.442	6.069		9.647
Ti				0.549	0.175	0.914	
Al	0.124	0.065	3.979	2.554	2.451	0.017	6.371
V				0.021		0.010	
Cr				0.049		0.003	
Fe	0.368	0.901	3.603	2.338	2.367	1.075	
Mn		0.015	0.142			0.008	
Mg	0.690	1.091	1.238	2.731	2.128	0.039	
Ni							
Ca	0.907	0.021	1.238	0.047	1.930	0.004	2.322
Na	0.015				0.353		1.616
K				1.932	0.468		0.037
P							
OXYGENS, CATIONS	6.04	6.04	24.16	22.16	23.15	3.02	32.20
TOTAL CATIONS	4.025	4.030	16.105	15.663	15.941	2.070	19.993

TABLE II-2(c) - Mt CHAPPLE GNT-OPX-CPX GRANULITE S-194

SAMPLE NUMBER	S-194	S-194	S-194	S-194	S-194	S-194
ROCK TYPE	GtOpCpBi	GtOpCpBi	GtOpCpBi	GtOpCpBi	GtOpCpBi	GtOpCpBi
MINERAL DATA	Plgran	Plgran	Plgran	Plgran	Plgran	Plgran
	CPX	OPX	GNT	BIOTITE	ILMENITE	PLG
GEOLOGICAL UNIT	Mt Chapple	Mt Chapple	Mt Chapple	Mt Chapple	Mt Chapple	Mt Chapple
LOCALITY	ARUNTA	ARUNTA	ARUNTA	ARUNTA	ARUNTA	ARUNTA
SiO ₂	51.08	50.99	36.82	35.41	1.04	52.93
TiO ₂	0.19		0.11	4.72	43.91	
Al ₂ O ₃	2.90	1.27	20.98	14.33	3.03	29.74
V ₂ O ₃					0.42	
Cr ₂ O ₃					0.18	
FeO[t]	10.09	29.03	27.60	17.35	50.07	
MnO		0.37	1.76		0.28	
MgO	12.79	19.03	4.79	12.26	0.79	
NiO						
CaO	22.75	0.34	6.85		0.11	11.51
Na ₂ O	0.19					4.70
K ₂ O				10.13		0.19
P ₂ O ₅						
Cl			0.09	0.07		
TOTAL	99.99	101.03	99.00	94.27	99.83	99.07
Si	1.920	1.942	5.893	5.467	0.027	9.653
Ti	0.005		0.013	0.548	0.842	
Al	0.129	0.057	3.959	2.608	0.091	6.394
V					0.009	
Cr					0.004	
Fe	0.317	0.925	3.694	2.240	1.068	
Mn		0.012	0.239		0.006	
Mg	0.716	1.080	1.143	2.821	0.030	
Ni						
Ca	0.916	0.014	1.175		0.003	2.249
Na	0.014					1.662
K				1.995		0.044
P						
OXYGENS. CATIONS	6.04	6.04	24.16	22.16	3.02	32.20
TOTAL CATIONS	4.017	4.030	16.116	15.679	2.080	20.002

TABLE II-2[d] - Mt CHAPPLE GARNET-SILLIMANITE GNEISS S-135

SAMPLE NUMBER	S-135	S-135	S-135	S-135
ROCK TYPE	GtSiPlQz	GtSiPlQz	GtSiPlQz	GtSiPlQz
	Gneiss	Gneiss	Gneiss	Gneiss
MINERAL DATA	GNT	SILL.	PLG	KFELD
GEOLOGICAL UNIT	Mt Chapple	Mt Chapple	Mt Chapple	Mt Chapple
LOCALITY	ARUNTA	ARUNTA	ARUNTA	ARUNTA
SiO ₂	36.48	37.05	66.03	58.10
TiO ₂				
Al ₂ O ₃	20.91	62.51	22.58	26.78
V ₂ O ₃				
Cr ₂ O ₃				
FeO[t]	37.63	0.57		
MnO	2.07			
MgO	2.13			
NiO				
CaO	0.78		2.27	0.10
Na ₂ O			9.83	1.58
K ₂ O			0.15	13.44
P ₂ O ₅				
Cl			0.07	
TOTAL	100.00	100.13	100.93	100.00
Si	5.949	4.003	11.480	10.462
Ti				
Al	4.020	7.962	4.628	5.685
V				
Cr				
Fe	5.132	0.052		
Mn	0.286			
Mg	0.518			
Ni				
Ca	0.136		0.423	0.019
Na			3.314	4.693
K			0.033	0.363
P				
OXYGENS.CATIONS	24.16	20.12	32.20	32.20
TOTAL CATIONS	16.041	12.017	19.878	21.222

TABLE II-2[e] - Mt CHAPPLE GARNET-SILLIMANITE GNEISS S-205

SAMPLE NUMBER	S-205	S-205	S-205
ROCK TYPE	GtSlKf	GtSlKf	GtSlKf
	gneiss	gneiss	gneiss
MINERAL DATA	GNT	SILL.	KFELD
GEOLOGICAL UNIT	Mt Chapple	Mt Chapple	Mt Chapple
LOCALITY	ARUNTA	ARUNTA	ARUNTA
SiO ₂	38.03	36.76	64.27
TiO ₂			
Al ₂ O ₃	22.22	63.20	18.88
V ₂ O ₃			
Cr ₂ O ₃			
FeO[t]	28.66		0.17
MnO	0.20		
MgO	9.61		
NiO			
CaO	1.14		
Na ₂ O			0.58
K ₂ O			16.13
P ₂ O ₅			
Cl			
TOTAL	99.86	99.96	100.03
Si	5.887	3.968	11.894
Ti			
Al	4.055	8.043	4.119
V			
Cr			
Fe	3.710		0.026
Mn	0.026		
Mg	2.217		
Ni			
Ca	0.189		
Na			0.208
K			2.808
P			
OXYGENS.CATIONS	24.16	20.12	32.20
TOTAL CATIONS	16.084	12.011	20.055

TABLE II-3 [a] - REDBANK HILL PORPHYROBLASTIC GNT GNEISS S-227

SAMPLE NUMBER	S-227	S-227	S-227	S-227
ROCK TYPE	GtBiHbPl	GtBiHbPl	GtBiHbPl	GtBiHbPl
	QzGNEISS	QzGNEISS	QzGNEISS	QzGNEISS
MINERAL DATA	GNT	AMPH	BIOTITE	PLG
GEOLOGICAL UNIT	Redbank H.	Redbank H.	Redbank H.	Redbank H.
LOCALITY	ARUNTA	ARUNTA	ARUNTA	ARUNTA
SiO ₂	37.52	38.68	32.77	57.25
TiO ₂		2.04	4.42	
Al ₂ O ₃	21.13	12.50	13.97	26.67
V ₂ O ₃			0.12	
Cr ₂ O ₃				
FeO[t]	29.15	19.71	20.11	
MnO	1.21			
MgO	3.08	7.28	8.98	0.12
NiO				
CaO	7.80	11.24	1.07	8.45
Na ₂ O	0.16	1.41	0.28	6.43
K ₂ O		1.87	8.56	0.26
P ₂ O ₅			0.48	
Cl		0.63	0.42	
TOTAL	100.05	95.36	91.18	99.18
Si	5.967	6.158	5.335	10.333
Ti		0.244	0.541	
Al	3.962	2.346	2.681	5.675
V			0.016	
Cr				
Fe	3.877	2.624	2.738	
Mn	0.163			
Mg	0.730	1.727	2.179	0.032
Ni				
Ca	1.329	1.917	0.187	1.634
Na	0.049	0.435	0.088	2.250
K		0.380	1.778	0.060
P			0.066	
OXYGENS. CATIONS	24.16	23.15	22.16	32.20
TOTAL CATIONS	16.077	15.831	15.609	19.984

TABLE II-3 [b] - REDBANK HILL PORPHYROBLASTIC GNT GNEISS S-241B

SAMPLE NUMBER	S-241B	S-241B	S-241B	S-241B	S-241B	S-241B
ROCK TYPE	GtBiHbOp	GtBiHbOp	GtBiHbOp	GtBiHbOp	GtBiHbOp	GtBiHbOp
MINERAL DATA	PlQzGNEISS	PlQzGNEISS	PlQzGNEISS	PlQzGNEISS	PlQzGNEISS	PlQzGNEISS
	GNT	BIOTITE	AMPH	OPX	PLG	ILMENITE
GEOLOGICAL UNIT	Redbank H.	Redbank H.	Redbank H.	Redbank H.	Redbank H.	Redbank H.
LOCALITY	ARUNTA	ARUNTA	ARUNTA	ARUNTA	ARUNTA	ARUNTA
SiO ₂	37.54	35.55	40.35	50.89	57.57	0.30
TiO ₂		5.54	2.13			49.17
Al ₂ O ₃	21.31	13.72	12.53	1.27	26.57	0.17
V ₂ O ₃		0.30				
Cr ₂ O ₃						
FeO[t]	29.48	17.23	17.81	29.32		48.34
MnO	0.76			0.29		0.20
MgO	4.28	12.21	9.00	17.73	0.09	0.72
NiO						
CaO	6.63	0.17	11.68	0.51	7.95	
Na ₂ O		0.18	1.48		6.70	
K ₂ O		9.29	2.22		0.31	
P ₂ O ₅						
Cl		0.40	0.54			
TOTAL	100.00	94.59	97.74	100.01	99.19	98.90
Si	5.945	5.471	6.198	1.960	10.380	0.008
Ti		0.641	0.246			0.952
Al	3.979	2.489	2.269	0.058	5.648	0.005
V		0.037				
Cr						
Fe	3.905	2.218	2.288	0.945		1.041
Mn	0.102			0.009		0.004
Mg	1.010	2.801	2.060	1.018	0.024	0.028
Ni						
Ca	1.125	0.028	1.922	0.021	1.536	
Na		0.054	0.441		2.342	
K		1.824	0.435		0.071	
P						
OXYGENS.CATIONS	24.16	22.16	23.15	6.04	32.20	3.02
TOTAL CATIONS	16.066	15.563	15.859	4.011	20.001	2.038

TABLE II-3[c] - REDBANK HILL GRANULITE S-239

SAMPLE NUMBER	S-239	S-239	S-239	S-239	S-239
ROCK TYPE	BiHbOpPl	BiHbOpPl	BiHbOpPl	BiHbOpPl	BiHbOpPl
MINERAL DATA	GRANULITE	GRANULITE	GRANULITE	GRANULITE	GRANULITE
	BIOTITE	AMPH	AMPH	OPX	PLG
GEOLOGICAL UNIT	Redbank H.	Redbank H.	Redbank H.	Redbank H.	Redbank H.
LOCALITY	ARUNTA	ARUNTA	ARUNTA	ARUNTA	ARUNTA
SiO ₂	36.94	40.26	44.57	52.60	50.12
TiO ₂	4.99	1.47	1.75		
Al ₂ O ₃	14.73	10.72	10.89	1.77	31.85
V ₂ O ₃		0.15			
Cr ₂ O ₃	0.78	1.00	0.69	0.14	
FeO[t]	12.00	8.80	8.13	22.14	0.36
MnO				0.40	
MgO	16.12	13.05	15.43	23.01	0.15
NiO					
CaO	0.09	11.21	12.16	0.37	14.34
Na ₂ O	0.14	1.22	1.43		3.18
K ₂ O	9.78	1.07	1.06		
P ₂ O ₅					
Cl	0.17	0.20	0.13		
TOTAL	95.74	89.15	96.24	100.43	100.00
Si	5.458	6.442	6.540	1.948	9.137
Ti	0.555	0.177	0.193		
Al	2.566	2.022	1.884	0.077	6.845
V		0.019			
Cr	0.091	0.126	0.080	0.004	
Fe	1.483	1.178	0.998	0.686	0.055
Mn				0.013	
Mg	3.550	3.112	3.374	1.270	0.041
Ni					
Ca	0.014	1.922	1.912	0.015	2.801
Na	0.040	0.379	0.407		1.124
K	1.844	0.218	0.198		
P					
OXYGENS.CATIONS	22.16	23.15	23.15	6.04	32.20
TOTAL CATIONS	15.601	15.595	15.586	4.013	20.003

TABLE II-3[d] - REDBANK HILL MAFIC GRANULITE S-228

SAMPLE NUMBER	S-228	S-228	S-228	S-228	S-228	S-228	S-228
ROCK TYPE	BiHbOpCp BGRANULITE	BiHbOpCp BGRANULITE	BiHbOpCp BGRANULITE	BiHbOpCp BGRANULITE	BiHbOpCp BGRANULITE	BiHbOpCp BGRANULITE	BiHbOpCp BGRANULITE
MINERAL DATA	BIOTITE	AMPH lightgreen	AMPH lightbrown	ILMENITE	OPX	CPX	PLG
GEOLOGICAL UNIT	Redbank H.	Redbank H.	Redbank H.	Redbank H.	Redbank H.	Redbank H.	Redbank H.
LOCALITY	ARUNTA	ARUNTA	ARUNTA	ARUNTA	ARUNTA	ARUNTA	ARUNTA
SiO ₂	36.56	43.68	49.67	2.04	51.39	52.35	52.97
TiO ₂	5.22	1.73	1.66	48.19		0.14	
Al ₂ O ₃	14.38	11.22	5.83	0.45	1.18	1.88	30.19
V ₂ O ₃	0.14	0.14		0.32			
Cr ₂ O ₃	0.17	0.33	0.39	0.28		0.14	
FeO[t]	13.53	11.85	8.71	44.62	24.34	8.31	
MnO				0.50	0.43	0.18	
MgO	14.67	12.93	13.64	1.99	20.57	14.05	
NiO							
CaO		11.91	14.10	0.10	0.49	22.73	12.62
Na ₂ O		1.37	0.21			0.22	4.36
K ₂ O	10.18	1.16	3.18				0.15
P ₂ O ₅							
Cl	0.15	0.19	0.09	0.10			
TOTAL	95.00	96.51	97.48	98.59	98.40	100.00	100.29
Si	5.492	6.508	7.251	0.051	1.967	1.951	9.567
Ti	0.590	0.194	0.182	0.915		0.004	
Al	2.547	1.971	1.003	0.013	0.053	0.083	6.428
V	0.017	0.017		0.006			
Cr	0.020	0.039	0.045	0.006		0.004	
Fe	1.700	1.477	1.063	0.942	0.779	0.259	
Mn				0.011	0.014	0.006	
Mg	3.284	2.871	2.967	0.075	1.173	0.780	
Ni							
Ca		1.901	2.205	0.003	0.020	0.908	2.442
Na		0.396	0.059			0.016	1.527
K	1.951	0.220	0.592				0.035
P							
OXYGENS. CATIONS	22.16	23.15	23.15	3.02	6.04	6.04	32.20
TOTAL CATIONS	15.601	15.594	15.367	2.022	4.006	4.011	19.999

TABLE II-4 - Mt ZEIL BELT GARNET-SILLIMANITE GNEISS S-376

SAMPLE NUMBER	S-376	S-376	S-376	S-376	S-376	S-376
ROCK TYPE	GtSlBikf	GtSlBikf	GtSlBikf	GtSlBikf	GtSlBikf	GtSlBikf
MINERAL DATA	Plgneiss	Plgneiss	Plgneiss	Plgneiss	Plgneiss	Plgneiss
	GNT	SILL.	BIOTITE	IIMENITE	PLG	KFELD
GEOLOGICAL UNIT	Zeil Belt	Zeil Belt	Zeil Belt	Zeil Belt	Zeil Belt	Zeil Belt
LOCALITY	ARUNTA	ARUNTA	ARUNTA	ARUNTA	ARUNTA	ARUNTA
SiO ₂	36.29	36.20	34.75		55.76	63.32
TiO ₂			3.15	51.33		
Al ₂ O ₃	22.13	63.80	17.82	0.17	28.87	19.07
V ₂ O ₃						
Cr ₂ O ₃						
FeO[t]	35.04		17.35	48.34		
MnO	0.44					
MgO	4.78		12.06	0.15		
NiO						
CaO	1.26					
Na ₂ O					9.51	
K ₂ O			10.19		5.79	1.62
P ₂ O ₅					0.08	14.55
Cl	0.06					
TOTAL	100.00	100.00	95.32	99.99	100.01	98.56
Si	5.812	3.909	5.282		10.000	11.834
Ti			0.360	0.980		
Al	4.178	8.122	3.193	0.005	6.104	4.202
V						
Cr						
Fe	4.693		2.206	1.026		
Mn	0.060					
Mg	1.141		2.732	0.006		
Ni						
Ca	0.216					
Na					1.828	
K					2.013	0.587
P			1.976		0.018	3.469
OXYGENS. CATIONS	24.16	20.12	22.16	3.02	32.20	32.20
TOTAL CATIONS	16.100	12.031	15.749	2.017	19.963	20.092

TABLE IV-1[a] - TEAPOT GRANITE SAMPLE S-537

SAMPLE NUMBER	S-537	S-537	S-537	S-537
ROCK TYPE	BiKfPl	BiKfPl	BiKfPl	BiKfPl
	granite	granite	granite	granite
MINERAL DATA	BIOTITE	MUSCOVITE	KFELD	PLG
GEOLOGICAL UNIT	Teapot G.	Teapot G.	Teapot G.	Teapot G.
LOCALITY	ARUNTA	ARUNTA	ARUNTA	ARUNTA
SiO ₂	34.74	46.24	64.44	59.79
TiO ₂	1.96	0.10		
Al ₂ O ₃	16.46	31.19	18.77	25.78
V ₂ O ₃				
Cr ₂ O ₃				
FeO[t]	26.34	5.00		
MnO	0.26			
MgO	5.65	1.06		
NiO				
CaO			0.29	6.79
Na ₂ O			0.53	7.65
K ₂ O	9.91	11.41	15.97	
P ₂ O ₅				
Cl	0.30			
TOTAL	95.62	95.00	100.00	100.01
Si	5.517	6.325	11.914	10.638
Ti	0.234	0.010		
Al	3.082	5.030	4.091	5.407
V				
Cr				
Fe	3.498	0.572		
Mn	0.035			
Mg	1.337	0.216		
Ni				
Ca			0.057	1.294
Na			0.190	2.639
K	2.008	1.991	3.767	
P				
OXYGENS.CATIONS	22.16	22.14	32.20	32.20
TOTAL CATIONS	15.711	14.144	20.019	19.978

TABLE IV-1[b] - TEAPOT GRANITE S-538

SAMPLE NUMBER	S-538	S-538	S-538	S-538	S-538	S-538
ROCK TYPE	BiKfPlEpSp	BiKfPlEpSp	BiKfPlEpSp	BiKfPlEpSp	BiKfPlEpSp	BiKfPlEpSp
MINERAL DATA	granite	granite	granite	granite	granite	granite
	BIOTITE	MUSCOVITE	EPIDOTE	SPHENE	PLG	KFELD
GEOLOGICAL UNIT	Teapot G.	Teapot G.	Teapot G.	Teapot G.	Teapot G.	Teapot G.
LOCALITY	ARUNTA	ARUNTA	ARUNTA	ARUNTA	ARUNTA	ARUNTA
SiO ₂	34.52	44.67	37.63	46.79	60.36	62.95
TiO ₂	2.31	0.35		19.48		
Al ₂ O ₃	15.91	30.29	24.71	6.90	25.10	18.51
V ₂ O ₃				0.16		
Cr ₂ O ₃						
FeO[t]	25.14	5.67	11.98	1.03		
MnO						
MgO	6.89	1.11				
NiO						
CaO			23.14	19.90	5.78	0.12
Na ₂ O				1.83	8.19	0.52
K ₂ O	10.10	11.06		0.07	0.13	16.14
P ₂ O ₅						
Cl	0.29					
TOTAL	95.16	93.15	97.46	96.16	99.77	98.24
Si	5.488	6.264	3.181	5.875	10.771	11.880
Ti	0.276	0.037		1.840		
Al	2.982	5.008	2.463	1.021	5.280	4.118
V				0.016		
Cr						
Fe	3.342	0.665	0.847	0.108		
Mn						
Mg	1.632	0.232				
Ni						
Ca			2.096	2.677	1.105	0.024
Na				0.446	2.834	0.190
K	2.048	1.979		0.011	0.030	3.886
P						
OXYGENS, CATIONS	22.16	22.14	13.08	20.12	32.20	32.20
TOTAL CATIONS	15.768	14.185	8.587	11.994	20.020	20.098

TABLE IV-2[a] - DASHWOOD MIGMATITE GNEISS S-789

SAMPLE NUMBER	S-789	S-789	S-789	S-789
ROCK TYPE	BiMuEpPl	BiMuEpPl	BiMuEpPl	BiMuEpPl
	GNEISS	GNEISS	GNEISS	GNEISS
MINERAL DATA	BIOTITE	MUSCOVITE	EPIDOTE	PLG
GEOLOGICAL UNIT	W.Dashwood	W.Dashwood	W.Dashwood	W.Dashwood
LOCALITY	ARUNTA	ARUNTA	ARUNTA	ARUNTA
SiO ₂	35.36	44.59	37.28	63.32
TiO ₂	2.11	0.34		
Al ₂ O ₃	17.00	28.99	22.93	22.59
V ₂ O ₃				
Cr ₂ O ₃				
FeO[t]	23.26	4.08	12.06	
MnO	0.19			
MgO	7.46	1.56		0.12
NiO				
CaO	0.09	0.10	22.81	3.64
Na ₂ O	0.23	0.26		9.11
K ₂ O	9.58	10.10		0.12
P ₂ O ₅		0.16		
Cl	0.12			0.06
TOTAL	95.40	90.18	95.08	98.96
Si	5.513	6.377	3.239	11.283
Ti	0.247	0.037		
Al	3.124	4.888	2.349	4.746
V				
Cr				
Fe	3.033	0.488	0.876	
Mn	0.025			
Mg	1.733	0.332		0.032
Ni				
Ca	0.015	0.015	2.123	0.695
Na	0.070	0.072		3.148
K	1.905	1.843		0.027
P		0.019		
OXYGENS.CATIONS	22.16	22.14	13.08	32.20
TOTAL CATIONS	15.665	14.071	8.587	19.931

TABLE IV-2[b] - DASHWOOD MIGMATITE - AMPHIBOLITE XENOLITH S-790

SAMPLE NUMBER	S-790	S-790
ROCK TYPE	BiHb	BiHb
MINERAL DATA	AMPHIBOLIT	AMPHIBOLIT
	BIOTITE	AMPH
GEOLOGICAL UNIT	W.Dashwood	W.Dashwood
LOCALITY	ARUNTA	ARUNTA
SiO ₂	39.69	49.25
TiO ₂	0.79	
Al ₂ O ₃	15.43	7.83
V ₂ O ₃		
Cr ₂ O ₃	0.16	0.11
FeO[t]	13.73	11.60
MnO	0.21	0.43
MgO	16.87	15.57
NiO		
CaO	0.18	12.53
Na ₂ O		0.84
K ₂ O	10.00	0.57
P ₂ O ₅		
Cl	0.14	
TOTAL	97.20	98.73
Si	5.767	7.064
Ti	0.086	
Al	2.643	1.324
V		
Cr	0.018	0.012
Fe	1.668	1.392
Mn	0.026	0.052
Mg	3.653	3.328
Ni		
Ca	0.028	1.926
Na		0.234
K	1.854	0.104
P		
OXYGENS.CATIONS	22.16	23.15
TOTAL CATIONS	15.743	15.436

TABLE IV-3[a] - DERWENT PARAGNEISS GNT-AMPH GNEISS S-830A

SAMPLE NUMBER	S-830A	S-830A	S-830A	S-830A
ROCK TYPE	GtBiHbPl	GtBiHbPl	GtBiHbPl	GtBiHbPl
MINERAL DATA	GNEISS	GNEISS	GNEISS	GNEISS
	GNT	BIOTITE	AMPH	PLG
GEOLOGICAL UNIT	W.Dashwood	W.Dashwood	W.Dashwood	W.Dashwood
LOCALITY	ARUNTA	ARUNTA	ARUNTA	ARUNTA
SiO ₂	38.53	35.60	38.48	59.29
TiO ₂	0.21	3.00	1.21	
Al ₂ O ₃	23.35	15.12	10.42	25.65
V ₂ O ₃			0.15	
Cr ₂ O ₃	0.16		0.18	
FeO[t]	13.21	21.62	23.07	
MnO	0.13	0.36	0.58	
MgO	0.13	9.68	6.24	0.17
NiO				
CaO	24.27	0.30	12.95	7.22
Na ₂ O			0.37	7.39
K ₂ O		9.51	1.90	0.28
P ₂ O ₅				
Cl		0.22	0.43	
TOTAL	99.99	95.41	95.98	100.00
Si	5.920	5.529	6.227	10.583
Ti	0.024	0.350	0.147	
Al	4.229	2.768	1.988	5.398
V			0.019	
Cr	0.019		0.023	
Fe	1.697	2.808	3.122	
Mn	0.017	0.047	0.080	
Mg	0.030	2.241	1.505	0.045
Ni				
Ca	3.995	0.050	2.245	1.381
Na			0.116	2.558
K		1.884	0.392	0.064
P				
OXYGENS.CATIONS	24.16	22.16	23.15	32.20
TOTAL CATIONS	15.931	15.677	15.864	20.029

TABLE IV-3 [b] - DERWENT PARAGNEISS - AMPHIBOLITE S-827B

SAMPLE NUMBER	S-827B	S-827B
ROCK TYPE	HbP1	HbP1
MINERAL DATA	AMPHIBOLIT	AMPHIBOLIT
GEOLOGICAL UNIT	AMPH	PLG
LOCALITY	core	core
	W.Dashwood	W.Dashwood
	ARUNTA	ARUNTA
SiO ₂	42.82	55.79
TiO ₂	0.82	
Al ₂ O ₃	11.56	27.45
V ₂ O ₃		
Cr ₂ O ₃		
FeO[t]	14.86	
MnO		
MgO	11.90	0.10
NiO		
CaO	11.82	8.99
Na ₂ O	1.50	6.19
K ₂ O	0.97	0.09
P ₂ O ₅		
Cl	0.36	
TOTAL	96.61	98.61
Si	6.470	10.146
Ti	0.093	
Al	2.059	5.885
V		
Cr		
Fe	1.878	
Mn		
Mg	2.680	0.027
Ni		
Ca	1.914	1.752
Na	0.439	2.183
K	0.187	0.021
P		
OXYGENS, CATIONS	23.15	32.20
TOTAL CATIONS	15.720	20.014

TABLE IV-3[c] - DERWENT PARAGNEISS - AMPHIBOLITE S-834A

SAMPLE NUMBER	S-834A	S-834A	S-834A
ROCK TYPE	BiHbP1	BiHbP1	BiHbP1
MINERAL DATA	AMPHIBOLIT	AMPHIBOLIT	AMPHIBOLIT
	BIOTITE	AMPH	PLG
GEOLOGICAL UNIT	W.Dashwood	W.Dashwood	W.Dashwood
LOCALITY	ARUNTA	ARUNTA	ARUNTA
SiO ₂	36.19	41.62	59.59
TiO ₂	1.76	1.30	
Al ₂ O ₃	15.68	11.00	25.88
V ₂ O ₃			
Cr ₂ O ₃		0.16	
FeO[t]	17.92	18.37	0.21
MnO	0.21	0.25	
MgO	11.82	9.39	0.16
NiO			
CaO	0.19	11.85	6.84
Na ₂ O	0.34	1.23	7.59
K ₂ O	8.98	1.27	0.07
P ₂ O ₅			
Cl	0.19	0.09	0.07
TOTAL	93.28	96.53	100.41
Si	5.615	6.420	10.588
Ti	0.205	0.151	
Al	2.868	2.000	5.421
V			
Cr		0.020	
Fe	2.325	2.370	0.031
Mn	0.028	0.033	
Mg	2.733	2.159	0.042
Ni			
Ca	0.032	1.959	1.302
Na	0.102	0.368	2.615
K	1.778	0.250	0.016
P			
OXYGENS. CATIONS	22.16	23.15	32.20
TOTAL CATIONS	15.686	15.730	20.015

TABLE IV-3 [d] - DERWENT PARAGNEISS - FELSIC BAND IN AMPHIBOLITE S-834B

SAMPLE NUMBER	S-834B	S-834B	S-834B	S-834B
ROCK TYPE	BiPlkf	BiPlkf	BiPlkf	BiPlkf
MINERAL DATA	FELSICBAND	FELSICBAND	FELSICBAND	FELSICBAND
	BIOTITE	TREMOLITE	PLG	KFELD
GEOLOGICAL UNIT	W. Dashwood	W. Dashwood	W. Dashwood	W. Dashwood
LOCALITY	ARUNTA	ARUNTA	ARUNTA	ARUNTA
SiO ₂	36.65	56.32	59.23	64.32
TiO ₂	2.66	0.15		0.13
Al ₂ O ₃	15.91	2.29	25.75	18.92
V ₂ O ₃				
Cr ₂ O ₃		0.48		
FeO[t]	19.35	7.57	0.20	
MnO		0.27		
MgO	11.43	16.64	0.15	
NiO				
CaO	0.12	11.24	7.21	
Na ₂ O		0.39	7.15	1.49
K ₂ O	9.71	0.18	0.30	14.45
P ₂ O ₅				
Cl		0.30		
TOTAL	95.83	95.83	99.99	99.31
Si	5.562	8.027	10.575	11.900
Ti	0.304	0.016		0.018
Al	2.846	0.385	5.420	4.127
V				
Cr		0.054		
Fe	2.456	0.902	0.030	
Mn		0.033		
Mg	2.585	3.534	0.040	
Ni				
Ca	0.020	1.716	1.379	
Na		0.108	2.475	0.535
K	1.880	0.033	0.068	3.411
P				
OXYGENS. CATIONS	22.16	23.15	32.20	32.20
TOTAL CATIONS	15.653	14.808	19.987	19.991

The map is a geological survey of the Keweenaw Peninsula, divided into six quadrants by a grid. The quadrants are labeled as follows:

- Top Left:** GLEN HELEN (100 000)
- Top Middle:** KEWEENAW (100 000)
- Top Right:** MASONVILLE (100 000)
- Middle Left:** GLEN HELEN (100 000)
- Middle Middle:** KEWEENAW (100 000)
- Middle Right:** MASONVILLE (100 000)
- Bottom Left:** GLEN HELEN (100 000)
- Bottom Middle:** KEWEENAW (100 000)
- Bottom Right:** MASONVILLE (100 000)

The map shows various geological features, including the Keweenaw Peninsula, the Mazonville Ranges, and the Mazonville Plain. Key locations marked include Glen Helen, Keweenaw, and Mazonville. The map includes a scale bar and a north arrow.

[illegible]

A map of the Northern Territory of Australia. A line representing a road or route starts at Darwin on the left and extends eastwards. Along this route, several points are marked with small circles. One of these points is labeled 'ALICE SPRINGS'. The map is titled 'MAP LOCALITY' at the top and 'NORTHERN TERRITORY' in the center. A legend at the bottom right shows a solid black line and a dashed line, with 'ALICE SPRINGS' written next to the solid line.

UNIVERSAL GRID DIFFERENCE

GRID ZONE DESIGNATION
123
1000 METRE SQUARE IDENTIFICATION

GROUPS THE SMALLER SQUARES into four grid numbers: these are the **GRID ZONE IDENTIFICATION** numbers. **ONLY THE LARGER SQUARES** of the grid number example.

TO GIVE A STANDARD REFERENCE ON THIS SHEET TO MEASURE US METHODS

SAMPLE POINT: 0.000000

1. Read the **VERTICAL** "1000 metre square" in which the point lies.
2. Read the **HORIZONTAL** "1000 metre square" in which the point lies.
3. Estimate tenths from grid line to point or between squares.
4. Locate four **ADJACENT** squares.
5. Read **BIGLER** point and read **LARGER** "square" in which the point lies.
6. Estimate **1000 metre** on the line itself.
7. Estimate tenths from grid line to point.

SAMPLE DIFFERENCE


8. Reporting based on **1000 metres** in any direction, prefix Grid Zone Designation, as: **123 1000 000000**


From standard lines are 1000 metre squares Australian Map Grid, Zone 52.

Grid values are shown in full only on the **1000 metre** square.

Figure 1 consists of four panels (A, B, C, D) showing geologic cross-sections of the Redbank-Mount Zeil Thrust. Each panel includes a vertical scale on the left (0 to 1000 feet) and a horizontal scale at the top (stations 1 to 10). The cross-sections show various geological units, including the Redbank-Mount Zeil Thrust, the Redbank-Mount Zeil Thrust, and the Redbank-Mount Zeil Thrust. The units are labeled with their respective names and are shown in different colors and patterns. The cross-sections also show the locations of various faults and folds, including the Redbank-Mount Zeil Thrust and the Redbank-Mount Zeil Thrust. The cross-sections are labeled with their respective names and are shown in different colors and patterns.

[illegible]


PRELIMINARY EDITION
AUGUST 1983
SUBJECT TO AMENDMENT



© Commonwealth of Australia 1983
Permits reproducing in perpetuity of this map may reproduce
it for their own use or for that of their staff, but not
for any other purpose except with the written permission
of the Director. MAP. P.5. Ser 378. Customs Code. ACT 2001

GLEN HELEN, NARIWETOOMA, ANBURULA